

**Arabidopsis AMP-activated protein kinases in
proteasomal complexes and their role in cell signalling**

**Inaugural-Dissertation
zur
Erlangung des Doktorgrades
der Mathematisch-Naturwissenschaftlichen Fakultät
der Universität zu Köln**

vorgelegt von

Mihály Horváth

aus Budapest

KÖLN 2007

*Berichterstatter: Prof. Dr. George Coupland
Prof. Dr. Ingo Flügge
Prof.Dr. Karin Schnetz*

Tag der mündlichen Prüfung: 17. 01. 2007

CONTENTS

1. INTRODUCTION	1
1.1. NUTRIENT AVAILABILITY AND PLANT GROWTH CONTROL	1
1.2. GLUCOSE REGULATED MECHANISMS IN YEAST	2
1.2.1. Snf1 (Sucrose non-fermenting 1).....	3
1.2.2. Nomenclature of the Snf1-related protein kinases.....	4
1.2.3. Structure of the AMP-activated protein kinases	4
1.2.4. Relatives of AMPKs	5
1.3. REGULATION OF AMPKS.....	5
1.3.1. Domain structure of the catalytic subunit.....	7
1.4. THE ROLE OF BETA SUBUNITS IN REGULATION	8
1.4.1. Subcellular localization.....	8
1.4.2. Substrate definition	9
1.5. GLUCOSE SIGNALING IN YEAST.....	10
1.5.1. Snf1 is a central regulator in yeast glucose signaling	12
1.5.2. Snf1 and controlled protein degradation.....	12
1.6. SNF1-RELATED KINASES IN PLANTS AND THEIR ATYPICAL SUBUNITS.....	14
1.6.1. Physiological roles of SnRK1 kinases in plants.....	14
1.6.2. Involvement of SnRK1 kinases in plant sugar signaling	17
1.6.3. Conserved and divergent elements in yeast and <i>Arabidopsis</i> glucose signal perception.....	18
1.6.4. Sugar response mutants and developmental impact of sugar signaling	19
1.7. SUGAR SIGNALING AND PROTEIN DEGRADATION	22
1.7.1. Conserved mechanisms suggest involvement of SnRK1 kinases in sugar dependent proteolysis 23	
1.8. AIMS OF THE PRESENT WORK.....	23
2. MATERIALS AND METHODS.....	25
2.1. MATERIALS	25
2.1.1. Chemicals and laboratory supplies	25
2.1.1.1. General chemicals.....	25
2.1.1.2. Enzymes.....	26
2.1.1.3. Culture media and hormones	26
2.1.1.4. Antibiotics.....	27
2.1.1.5. Chromatography resins	27
2.1.1.6. Antibodies.....	27
2.1.1.7. Radiochemicals	27
2.1.2. Bacterial strains.....	28
2.1.2.1. E.coli strains.....	28
2.1.2.2. Agrobacterium strains.....	28
2.1.3. Plasmid vectors and constructs	28
2.1.3.1. Plasmid vectors	28
2.1.3.2. Plasmid constructs	28
2.1.4. Plant material	29
2.1.4.1. <i>Arabidopsis thaliana</i> wild type and mutant lines	29
2.1.4.2. <i>Arabidopsis</i> cell suspension cultures	30
2.1.5. <i>Arabidopsis</i> cDNA libraries.....	30
2.1.6. Oligonucleotides	30
2.1.6.1. Oligonucleotides for cloning.....	30
2.1.6.2. Oligonucleotides for sequencing.....	32
2.1.6.3. Oligonucleotides for site-directed mutagenesis	32
2.1.6.4. Oligonucleotides for T-DNA insertion mutant screens and RT-PCR.....	32
2.2. GROWTH MEDIA AND STOCK SOLUTIONS.....	33
2.2.1. Stock solutions.....	33
2.2.1.1. Antibiotics.....	33
2.2.1.2. Plant hormones	33
2.2.1.3. Protease inhibitors.....	34
2.2.1.4. Other stock solutions.....	34

2.2.2.	Culture media.....	34
2.2.2.1.	LB medium	34
2.2.2.2.	YEB medium	34
2.2.2.3.	Culture medium for root-derived dark grown Arabidopsis cell suspension culture	35
2.2.2.4.	Culture medium for leaf-derived light-grown green (photosynthetic) Arabidopsis cell suspension culture	35
2.2.2.5.	Culture medium for Arabidopsis seedlings.....	35
2.3.	METHODS	36
2.3.1.	DNA methods	36
2.3.1.1.	Precipitation of DNA with ethanol or isopropanol	36
2.3.1.2.	Plasmid DNA miniprep (Alkaline lysis method).....	36
2.3.1.3.	Peqlab E.Z.N.A. miniprep kit	37
2.3.1.4.	Plasmid DNA maxiprep by CsCl gradient ultracentrifugation	37
2.3.1.5.	Restriction endonuclease digestion of DNA	38
2.3.1.6.	Preparation of DNase free RNase	38
2.3.1.7.	Phenol-chloroform purification of DNA samples.....	38
2.3.1.8.	Polymerase chain reaction	39
2.3.1.9.	Agarose electrophoresis of DNA	39
2.3.1.10.	Preparation of dialysis tube.....	40
2.3.1.11.	Recovery of DNA fragments from agarose gel	40
2.3.1.12.	Measurement of nucleic acid concentration and purity	40
2.3.1.13.	Dephosphorylation of DNA 5' ends	40
2.3.1.14.	Creating blunt ended DNA	41
2.3.1.15.	Dialysis of DNA samples.....	41
2.3.1.16.	Ligation of DNA ends.....	41
2.3.1.17.	Preparation of electrocompetent E. coli cells.....	41
2.3.1.18.	Transformation of Escherichia coli by electroporation.....	42
2.3.1.19.	Transformation of Agrobacterium tumefaciens.....	42
2.3.1.20.	Site-directed mutagenesis	43
2.3.2.	Protein analytical techniques	44
2.3.2.1.	SDS polyacrylamide gel electrophoresis	44
2.3.2.2.	Staining SDS polyacrylamide gels with Coomassie Brilliant Blue R250 and colloidal blue stain	44
2.3.2.3.	Tris-Tricine buffered SDS-polyacrylamide electrophoresis of peptides.....	45
2.3.2.4.	Two-dimensional electrophoresis	46
2.3.2.5.	Western blot analysis of proteins.....	46
2.3.2.6.	Chemical and enzymatic manipulation of proteins.....	47
2.3.2.7.	In vitro kinase reactions	48
2.3.2.8.	Recombinant protein expression in Escherichia coli cells.....	49
2.3.2.9.	Purification of proteins	49
2.3.2.10.	Tandem affinity purification of plant proteins on NiNTA and Strep-tactin resins	52
2.3.2.11.	Mass spectrometry	57
2.3.3.	Plant techniques	57
2.3.3.1.	Crossing Arabidopsis plants	57
2.3.3.2.	Arabidopsis seed sterilization	57
2.3.3.3.	Transformation of Arabidopsis using the floral dip method [229]	57
2.3.3.4.	Selection of Arabidopsis transformants	58
2.3.3.5.	Arabidopsis genomic DNA extraction by the CTAB method [230].....	58
2.3.3.6.	Transformation and maintenance of Arabidopsis cell suspension cultures	59
3.	RESULTS	61
3.1.	T-DNA INSERTION MUTATIONS IN GENES ENCODING ARABIDOPSIS SNRK1 KINASE SUBUNITS AND UPSTREAM ACTIVATING KINASES	61
3.1.1.	Isolation of a T-DNA insertion mutation in the SNRK1 α catalytic subunit gene AKIN10 (At3g01090)	61
3.1.2.	SnRK1 β subunit alleles in public T-DNA insertion mutant collections.....	62
3.1.3.	Isolation of SnRK1 β subunit mutations in the Koncz collection.....	65
3.1.4.	Analysis of transcript level of mutated SnRK1 beta subunit genes.....	65

3.1.5.	Generation of double AKIN beta subunit mutants.....	66
3.1.6.	Isolation of homozygous T-DNA insertion mutants for two SnRK1 upstream activating kinases.....	67
3.1.7.	Phenotypic analysis of SnRK1 subunit mutants.....	68
3.2.	OVEREXPRESSION OF SNRK1 BETA SUBUNITS.....	70
3.2.1.	Construction of a CaMV35S promoter driven GFP tagging vector.....	70
3.2.2.	Overexpression of GFP-tagged SnRK1 β subunits.....	70
3.2.3.	Analysis of SnRK1 β -GFP overexpressing plants and suspension cultures.....	70
3.2.4.	Transcription regulation of AKIN β and other SnRK1 subunit genes.....	72
3.3.	DEVELOPMENT OF A BIOCHEMICAL APPROACH FOR ISOLATION OF SNRK1 COMPLEXES FROM ARABIDOPSIS.....	74
3.3.1.	Construction of an expression vector for tandem His-Strep tag affinity purification of plant proteins.....	75
3.3.2.	Cloning of SnRK1 subunits into the p3xtag tandem affinity tagging vector.....	77
3.3.3.	Immunoblot analysis of the overexpressed PIP-L-tagged SnRK1 subunits.....	77
3.3.4.	Purification of PIP-L tagged SnRK1 beta subunits from Arabidopsis cell suspension culture.....	78
3.4.	IN VITRO PHOSPHORYLATION OF CANDIDATE PROTEASOMAL SUBSTRATES.....	80
3.4.1.	Generation of Arabidopsis SnRK1 α bacterial expression constructs.....	80
3.4.2.	Preparation of point mutant SnRK1 α kinase variants.....	81
3.4.3.	Candidate SnRK1-proteasome substrates.....	83
3.4.4.	Cloning bacterial expression and purification of the selected proteasomal substrates.....	84
3.4.5.	In vitro kinase reactions with radioactive γ 32P-ATP.....	84
3.4.6.	Two-dimensional gel electrophoresis of phosphorylated SnRK1 substrates.....	89
3.4.7.	Constitutively active kinase variants.....	90
3.4.8.	Inactive kinase variants.....	91
3.4.9.	Testing the effect of SnRK1 upstream activating kinases on AKIN10 activity.....	91
3.4.10.	Testing the activity of truncated kinase forms.....	92
3.4.11.	Partial reconstruction of the SnRK1 kinase complex.....	94
3.5.	IDENTIFICATION OF PHOSPHORYLATION SITES IN SNRK1 KINASE SUBSTRATES.....	94
3.5.1.	Mass spectrometric analysis of phosphorylated substrates.....	94
3.5.2.	Phosphopeptide mapping of IAA6.....	95
3.5.3.	Site-directed mutagenesis of the IAA6 S39E residue in bacterial expression clones.....	97
3.5.4.	Preparation of IAA6 plant overexpression constructs.....	98
3.5.5.	Analysis of phenotypes conferred by overexpression of IAA6 phosphorylation site variants and immunoblot analysis of modified IAA6 in transgenic plants.....	98
3.6.	ANALYSIS OF THE EFFECT OF SNRK1 KINASES ON SUBSTRATE STABILITY IN VIVO.....	100
3.6.1.	Preparation of DNA constructs for <i>in vivo</i> test of stability of candidate AKIN10 substrates.....	101
3.6.2.	<i>In vivo</i> stability test of candidate substrate proteins in combination with AKIN10 overexpression.....	102
4.	DISCUSSION.....	105
4.1.	IDENTIFICATION OF INSERTION MUTATIONS IN SNRK1 SUBUNIT GENES.....	105
4.2.	FUNCTIONAL ANALYSIS OF SNRK1 SUBUNITS.....	106
4.3.	SEARCHING FOR CANDIDATE SNRK1 SUBSTRATES.....	107
4.4.	AN ASSAY SYSTEM FOR ANALYSIS OF STABILITY OF CANDIDATE SNRK1 SUBSTRATES IN VIVO.....	111
4.5.	IMPROVED TECHNOLOGY FOR AFFINITY PURIFICATION OF SNRK1 KINASES.....	112
4.6.	SNRK1-ACTIVATING KINASES.....	113
4.7.	OUTLOOK.....	113
5.	APPENDIX.....	115
5.1.	GERMINATION DATA OF T-DNA INSERTION MUTANTS IN SNRK1 SUBUNIT AND SNAK KINASE GENES.....	115
5.2.	MAP OF PPILY VECTOR.....	118
5.3.	MASS SPECTROMETRIC IDENTIFICATION OF PHOSPHORYLATION SITES IN ABI5, DPBF4 AND IAA6 PROTEINS.....	119
6.	REFERENCES.....	125
7.	ACKNOWLEDGEMENTS.....	137

I FIGURES

Figure 1.	Location of the T-DNA inserts in the GABI_579E09 mutant AKIN10 allele.	61
Figure 2.	Identification of a homozygous AKIN10 GABI_579E09 T2 insertion mutant lines by PCR-analysis.	62
Figure 3.	Details of SnRK1 β subunit mutations	63
Figure 4.	Isolation of homozygous <i>akinβ2</i> mutants	64
Figure 5.	Identification of homozygous mutant lines for the AKIN β 1 and AKIN β 2 KONCZ alleles	66
Figure 6.	RT-PCR analysis of the SnRK1 beta subunit mutants	67
Figure 7.	T-DNA insertion mutations in genes of SnRK1 upstream kinases SnAK1 and SnAK2	68
Figure 8.	Isolation of homozygous SnAK mutants	69
Figure 9.	Expression of GFP-tagged SnRK1 beta subunits	71
Figure 10.	Developmental regulation of transcription of <i>SnRK1</i> subunit genes	73
Figure 11.	AKIN β 1-GFP (A) and AKIN β 2-GFP (B) proteins are stable and accumulate in vascular tissues of overexpressing plants	73
Figure 12.	Imidazole gradient elution of TRX-AKIN11-PIP-L	76
Figure 13.	Physical map and sequence of the coding region of PIP-L-Strep-HA tag of p3xtag tandem affinity tagging vector	77
Figure 14.	Proteasomal degradation of the SnRK1 α and β subunits	78
Figure 15.	Tandem affinity purification of AKIN β 2-PIP-L-Strep-HA protein from Arabidopsis cell suspension culture	79
Figure 16.	Purification of recombinant SnRK1 α catalytic subunits AKIN10 and AKIN11	82
Figure 17.	Bacterial expression and purification of the hypothetical substrates	86
Figure 18.	<i>In vitro</i> kinase assays of candidate proteasomal substrates with AKIN10 using radioactive γ 32P-ATP	87
Figure 19.	Kinase reactions of candidate proteasomal substrates with AKIN10 using radioactive γ 32P-ATP	88
Figure 20.	Purification of recombinant PRL1 protein and testing its SnRK1 inhibitor activity	89
Figure 21.	Two-dimensional electrophoresis of phosphorylated IAA6 and DPBF4	90
Figure 22.	Dominantly active SnRK1 α kinase variants	90
Figure 23.	AKIN10 and AKIN11 do not activate each other <i>in vitro</i>	91
Figure 24.	TLK upstream kinases phosphorylate AKIN10 but do not significantly increase its activity <i>in vitro</i>	92
Figure 25.	Activity of the truncated AKIN10 variants	93
Figure 26.	Partial reconstruction of the AKIN10 SnRK1 kinase complex with AKIN β 3	93
Figure 27.	Conserved phosphorylation sites were identified in ABI5 and DPBF4 by mass spectrometric analysis	95
Figure 28.	The phosphorylation site revealed in IAA6 is conserved in many members of the Aux/IAA protein family of auxin signalling repressors	95
Figure 29.	Proteolytic map of IAA6 and the molecular mass of resulting peptides	96
Figure 30.	Phosphopeptide mapping of IAA6 with Arg-C enzyme and CNBr	97
Figure 31.	Bacterial expression and kinase assay of the IAA6 S39A and IAA6 S39E mutants	97
Figure 32.	Overexpression of IAA6 S39E mutant protein strongly reduces plant development	99
Figure 33.	Flowers and siliques of IAA6 overexpressor plants	100
Figure 34.	Schematic presentation of the pUBRX protein stability testing vector	101
Figure 35.	Results of <i>in vivo</i> substrate stability tests	103

II ABBREVIATIONS AND SYMBOLES

A	adenine
ABA	abscisic acid
ADP	adenosine 5'-diphosphate
AMP	adenosine 5'-monophosphate
Amp	ampicillin
<i>A. thaliana</i>	<i>Arabidopsis thaliana</i>
ATP	adenosine 5'-triphosphate
bp	base pair
βME	2-mercapto ethanol
BSA	bovine serum albumin
C	cytosine
CaMV	Cauliflower Mosaic Virus
cDNA	complementary DNA
C-terminal	carboxyterminal
C-terminus	carboxyl terminus
CTAB	cetyl trimethylammonium bromide
2,4-D	2,4-Dichlorophenoxy acetic acid
DMSO	dimethyl sulfoxide
DNA	Deoxyribonucleic acid
dNTP	deoxyribonucleotide triphosphate
DTT	dithiotreitol
<i>E. coli</i>	<i>Escherichia coli</i>
EDTA	ethylenediaminetetraacetic acid
EtBr	ethidium bromide
G	guanine
Gm	gentamycin
GST	glutathione-S-transferase
Hyg	hygromycin B
IAA	indole-3-acetic acid
IPTG	isopropyl-β-thiogalactoside
kb	kilobase
kDa	kilo Dalton (1,000 Da)
Km	kanamycin
<i>lacZ</i>	<i>E. coli</i> β-galactosidase gene
MBP	maltose binding protein
μg	microgram
μl	microliter
μM	micromolar
mg	milligram
min.	minute
ml	milliliter
mM	millimolar
mRNA	messenger RNA
Ni	nickel

NiNTA		nickel-nitrilotriacetic acid matrix
N-terminal		amino terminal
N-terminus		amino terminus
OD		optical density
P		phosphor
PAGE		polyacrylamide gel electrophoresis
PCR		polymerase chain reaction
pH		negative logarithm of the proton concentration
PMSF		phenylmethylsulfonyl fluoride
PVDF		polyvinylidene difluoride
RNA		ribonucleic acid
RNase		ribonuclease
Rif		rifampicin
rpm		revolution per minute
RT-PCR		reverse transcription PCR
<i>S. cerevisiae</i>		<i>Saccharomyces cerevisiae</i>
SDS		sodium dodecylsulfate
sec.		second
SSC		standard saline citrate
T		thymine
TAE		Tris-acetate (40 mM); EDTA (1mM)
Tc		tetracyclin
TCA		trichloroacetic acid
TE		Tris.HCl (10mM); EDTA (1mM)
TEMED		N,N,N',N' tetramethylethylenediamine
Tris		Tris(hydroxymethyl) aminomethane
TRX		thioredoxin
U		unit
UTR		untranslated region
UV		ultraviolet light
V		Volt
wt		wild type
Aminoacids		
A	Ala	Alanine
C	Cys	Cysteine
D	Asp	Aspartic acid
E	Glu	Glutamic acid
F	Phe	Phenylalanine
G	Gly	Glycine
H	His	Histidine
I	Ile	Isoleucine
K	Lys	Lysine
L	Leu	Leucine
M	Met	Methionine
N	Asn	Asparagine
P	Pro	Proline
Q	Gln	Glutamine
R	Arg	Arginine
S	Ser	Serine

T	Thr	Threonine
V	Val	Valine
W	Trp	Trptophan
Y	Tyr	Tyrosine
X		any aminoacid

III SUMMARY - ZUSAMMENFASSUNG

Summary

AMP-activated protein kinases (AMPK) are structurally and functionally highly conserved in all eukaryotes. The most profoundly studied yeast AMPK ortholog, Snf1, plays a role in the sensing and response to low energy and nutrient levels. There is much less information available about the function of plant Snf1 orthologs, termed Snf1-related protein kinases (SnRKs) and their regulatory roles in plant specific nutrient regulated mechanism, such as photosynthesis, plant hormone signaling and metabolism.

Genetic studies of plant SnRK1 kinases are impeded by the lack of T-DNA insertion mutants in the SnRK1 catalytic subunits and the lack of male transmission of mutations affecting the SnRK γ subunit. The present work describes the isolation of T-DNA insertion mutations in SnRK1 β subunit genes and characterization of these mutants. Single and double mutant plants did not show any observable developmental or sugar signaling phenotype. Triple SnRK1 β mutant could not be generated because no mutant allele is available for the third beta subunit. In our experiments overexpression of GFP-tagged SnRK1 beta subunits did not show subcellular relocalization in response to nutritional stress, a mechanism which was described in yeast. Instead, rapid proteasomal degradation of *Arabidopsis* SnRK1 subunits was observed in response to sugars and light. Proteasomal degradation of SnRK1 subunits prevented their efficient overexpression for biochemical studies. Former *in vitro* and *in vivo* studies found SnRK1 kinases in proteasomal complexes in *Arabidopsis*. This observation correlates with the fact that numerous nutrient status regulated metabolic enzymes are proteasomal substrates in *Arabidopsis* as in yeast and their degradation is controlled by phosphorylation and sugar availability. In order to identify SnRK1 interacting partners *in vivo*, it was attempted to isolate protein complexes from *Arabidopsis* through tagged SnRK1 subunits. In contrast to a former and mostly unsuccessful immunoaffinity purification approach, this work applies a rapid tandem affinity chromatography-based protein purification method. In addition to developing a biochemical approach for identification of SnRK1 interacting partners, we further explored the proteasomal connection of SnRK1 kinases and searched for their potential substrates using *in vitro* phosphorylation studies. Several sugar-regulated proteasomal substrates and F-box proteins were overexpressed in *E. coli* and purified to near homogeneity along with similar purification of SnRK1 kinase catalytic subunits. The purified proteins were subjected to *in vitro* kinase reactions using radioactive $\gamma^{32}\text{P}$ -ATP and phosphorylation was detected in more cases. Some of the phosphorylation sites were successfully identified by mass spectrometric analysis. Site-directed mutagenesis of the phosphorylation site on IAA6 and overexpression of the mutant construct indicates the importance of phosphorylation site *in vivo*. In order to provide further evidence for interaction of SnRK1 kinases with their substrates *in vivo*, an assay system for testing the stability of kinase substrates was developed.

Zusammenfassung

AMP-aktivierte Proteinkinasen (AMPK) sind in allen Eukaryoten strukturell und funktionell in hohem Maße konserviert. Am besten ist die Hefe Protein Kinase Snf1 erforscht. Sie spielt eine große Rolle beim Erkennen und Reagieren auf niedriges Energieangebot und Nährstoffmangel. Es gibt weit weniger Information über die Funktionen der Snf1-Orthologe in Pflanzen. So sind zum Beispiel deren regulatorische Rolle in pflanzenspezifischen, ernährungsabhängig regulierten Mechanismen wie Photosynthese und Pflanzenhormon-Signal Transduktion unbekannt.

Genetische Studien an Pflanzen-SnRK1 Kinasen werden durch den Mangel an T-DNA Insertionsmutanten in katalytische Untereinheiten der SNRK1 und durch Mutationen in der SnRK γ -Untereinheit, die männliche Sterilität verursacht, erschwert. Die vorliegende Arbeit beschreibt die Isolation von T-DNA Insertions-Mutanten in SnRK1- β -Untereinheiten und deren Charakterisierung. Einfach und zweifach mutierte Pflanzen zeigten keine sichtbaren Entwicklungs- oder Zucker anzeigenden Phänotypen. Dreifach mutierte Pflanzen konnten nicht aufgezogen werden, da für die dritte Beta –Untereinheit kein Mutantenallel erhältlich ist. Überexpression der GFP-markierten SnRK1 Beta-Untereinheiten zeigte keine subzelluläre Relokalisation als Antwort auf ernährungsbedingten Stress, ein Mechanismus, der in Hefe beschrieben wurde. Stattdessen wurde als Antwort auf Zucker und Licht ein rascher proteosomaler Abbau der Arabidopsis SnRK1 Untereinheiten beobachtet. Der proteosomale Abbau von SnRK1-Untereinheiten verhinderte ihre effiziente Überexpression für biochemische Studien. Frühere *in vivo* und *in vitro* Studien entdeckten Arabidopsis SNRK1 Kinasen in proteosomalen Komplexen. Diese Beobachtung wird dadurch unterstützt, dass zahlreiche durch die Ernährung regulierte metabolische Enzyme in Arabidopsis wie auch in Hefe proteosomale Substrate sind, und ihr Abbau durch Phosphorylierung und die Verfügbarkeit von Zucker kontrolliert wird. Um SnRK1 interagierende Partner *in vivo* zu identifizieren, wurde versucht, Proteinkomplexe aus Arabidopsis durch markierte SnRK1-Untereinheiten zu isolieren. Im Gegensatz zu früheren, meist erfolglosen Versuchen durch Immunoaffinitätsreinigung, verwendet diese Arbeit eine rasche auf Tandem-Affinitäts-Chromatographie basierende Proteinreinigungsmethode. Außer der Entwicklung eines biochemischen Versuchs zur Identifizierung SnRK1 interagierenden Partner, erforschten wir auch die proteosomale Verbindung der SnRK1 Kinasen und suchten durch die Anwendung von *in vitro* Phosphorylierungsexperimenten nach deren potentiellen Substraten. Einige Zucker-regulierte proteosomale Substrate, F-box - Proteine und auch SnRK1-Kinase Untereinheiten wurden in *E.coli* überexprimiert und mittels einer chromatographische Reinigung nahezu homogen gereinigt. Die gereinigten Proteine wurden durch Einsatz von radioaktivem γ 32-ATP in *in vitro* Kinase-Reaktionen unterworfen, wobei mehrere Phosphorylierungen detektiert wurden. Einige der Phosphorylierungsstellen wurden durch Massenspektrometrie erfolgreich identifiziert. Zielgerichtete Mutagenesis der IAA6 Phosphorylierungsstelle und Überexpression des Mutantenkonstruktes bestätigte die Bedeutung dieser Phosphorylierungsstelle *in vivo*. Um weitere Belege für die Interaktion

der SnRK1 Kinasen und ihre Substrate *in vivo* zu liefern, wurde ein Versuchs-System zum Test der Stabilität der Kinase-Substrate entwickelt.

1. INTRODUCTION

1.1. NUTRIENT AVAILABILITY AND PLANT GROWTH CONTROL

Nutrient availability is an environmental and physiological factor that controls growth and development. Growth retardation is the most general consequence of nutrient limitation. The growth limiting effect of nutrient shortage was first recognized in agricultural science and formulated in the principle of “Liebig’s law of the minimum”, which states that plant growth is limited by the lowest amount of an essential nutrient (Carl Sprengel 1828 [1]). A more precise examination of this phenomenon was carried out on isolated plant meristematic cells in the 1960s. When pea root tips were cultured in a medium depleted for sucrose or treated with uncouplers of oxidative phosphorylation the roots stopped growing and the cells became arrested in either G1 or G2 phase of the cell cycle [2,3]. Regulation of cell cycle by nutrient starvation implies the existence of nutrient status sensing and signal transduction mechanisms.

Nutrients and their shortage are not mere metabolic growth signals but are able to evoke specific physiological and developmental responses similarly to hormones. In response to carbon and energy source depletion budding yeast (*Saccharomyces cerevisiae*) turns into an enduring form, in which metabolic activity decreases to a minimal level, growth and cell cycle stops, reserve nutrients are accumulated, and a high degree of stress tolerance develops against multiple physical and chemical environmental impacts [4]. A distinct developmental program is triggered by nitrogen source depletion that evokes drastic morphological changes: the generally unicellular yeast cells switch to multicellular pseudohyphal development that provides a higher penetrating ability and enables yeast to actively search for nitrogen.

In multicellular organisms nutrients are generally stored in differentiated storage organs, from which they are released and reallocated to other tissues of the body. Coordinated release and uptake of nutrients requires sophisticated regulatory mechanisms. Failures in this process cause life-threatening diseases, like diabetes, in mammals. Plants as photoautotroph organisms are able to produce the carbohydrates they require and have developed mechanisms to coordinate carbohydrate production with its metabolism. Carbohydrate-derived signals control photosynthesis itself through negative feedback regulation [5-8]. In addition, sucrose and glucose influence a wide range of developmental processes including seed germination, seedling development, root and leaf differentiation, floral transition, fruit ripening, embryogenesis and senescence, as well as responses to light, stress and pathogens.

Sugar signaling mechanisms are partly integrated with other nutrient and hormonal signaling cascades to form a complex signaling network [7]. For instance, carbon and nitrogen assimilation is strictly coordinated in plants at the enzymatic level [9]. Phosphate and nitrate availability controls starch accumulation [10-11] and sugar and nitrogen content regulate sulphate assimilation [12-13]. In spite of high level of integration in the nutrient signal transduction, certain nutrient species can evoke

specific responses. In order to identify components of the nutrient sensing and signaling network, genetic screens were carried out in yeast and *E.coli*, and also in *Arabidopsis*.

1.2. GLUCOSE REGULATED MECHANISMS IN YEAST

Glucose-dependent regulatory mechanisms are very common in fungi including the genetic model organism budding yeast [4,14]. Although yeast is capable of aerobic respiration, in the presence of high levels of glucose it prefers anaerobic fermentation. Alcoholic fermentation does not yield as many ATP molecules per moles of sugar as oxidative phosphorylation but it can proceed at much higher rate and the produced ethanol helps to compete with less ethanol tolerant organisms. High concentration of glucose induces its exclusive and optimal use in yeast, whereas the utilization of other fermentable and non-fermentable carbon sources are inhibited by glucose through a specific regulatory mechanism called *glucose* or *catabolite repression*. Approximately one sixth of genes in the *Saccharomyces cerevisiae* genome is controlled by glucose repression [14]. The metabolic changes caused by glucose repression are well represented by the distinct sets of genes, which are active during the presence or absence of glucose. For instance, glucose induces its uptake and metabolic processing by stimulating the expression of hexose transporters (HXT) and glycolytic enzymes. In the presence of glucose, the growth rate dramatically increases, which is accompanied by intensive protein synthesis and characteristic upshift in ribosomal RNA and protein expression. Conversely, the expression of genes required for transport of sugars other than glucose is inhibited similarly to the expression of enzymes involved in respiration (Krebs cycle). A large group of genes whose promoters contain the yeast stress responsive element (STRE) and are involved in the yeast's response to various stresses are also repressed by glucose.

Depletion of glucose induces gluconeogenesis from other fermentable sugars, which requires the reactivation, so-called derepression, of glucose repressed genes. After glucose depletion, first other fermentable sugars, such as sucrose, are utilized, which is followed by the catabolism of non-fermentable sugars that require the reactivation of complete respiratory system. Sucrose is a disaccharide (α -D-glucose + β -D-fructose) and its metabolic processing requires the expression of only few additional genes encoding e.g., sucrose transporters and invertase, which are subjected to glucose repression. Invertase catalyzes the first step in the breakdown of sucrose to hexose monosaccharides. In case of glucose depletion the abundant presence of sucrose still maintains high growth rate, whereas yeast growing on non-fermentable carbon sources grows slowly and shows similarity to the enduring form accumulating reserve nutrients.

Dominant mutations in the glucose repression pathway or failures in the derepression process during low glucose concentrations result in growth defect in sucrose medium. This easily recognizable growth phenotype on sucrose medium helped to identify several "sucrose non-fermenting" (*snf*) yeast mutants defective in central regulators of the catabolite repression pathway.

1.2.1. Snf1 (Sucrose non-fermenting 1)

The yeast *snf1* mutant is unable to grow on any other carbon source than glucose [15]. The Snf1 gene encodes a serine/threonine protein kinase [16, 17], which is highly conserved in all eukaryotes. In the sugar signaling pathways of yeast, Snf1 plays a role in the derepression of glucose repressed genes under glucose starvation, as Snf1 is activated by low glucose concentration. Besides its role in the response to glucose limitation, Snf1 has been implicated in several other processes including aging, thermotolerance, peroxisome biogenesis, invasive growth, biofilm formation, meiosis and sporulation [14]. Comparison of Snf1 to its relatives in other organisms resulted in the recognition that Snf1 is not merely a sugar signaling component but a general sensor and regulator of cellular energy level.

Mammalian Snf1 orthologs, the AMP-activated protein kinases (AMPK), are activated in response to AMP (i.e. high AMP/ATP ratio) [18]. AMP is produced in the adenylate kinase reaction ($2\text{ADP} \leftrightarrow \text{ATP} + \text{AMP}$), which restores residual energy of ADP into the more accessible form of ATP on the price of generating AMP. High AMP/ATP ratio refers to conditions of general cellular energy depletion and thereby AMPKs are able to sense the cellular energy level. AMPKs play a role in the maintenance of energy balance by phosphorylating metabolic enzymes, such as acetyl-CoA carboxylase [19,20] and 3-hydroxy-3-methylglutaryl-CoA reductase (HMGR) [21] representing rate limiting enzymes of energy demanding fatty acid and cholesterol biosynthesis pathways, respectively. AMPKs also respond to stimuli that do not cause detectable change in the AMP/ATP ratio, for instance to hyperosmotic stress [22] and the application of anti-diabetic agent metformin in mammals [23].

Plant Snf1 and AMPK orthologs phosphorylate and inactivate the sucrose phosphate synthase (SPS) and nitrate reductase (NR) enzymes [24]. NR catalyzes the first step in the energy consuming process of nitrate assimilation. Posttranslational control of NR is very important in the coordination of carbon- and nitrogen assimilation intensity [25]. NR produces nitrite (NO_2^-), a toxic intermediate of nitrate assimilation, which is immediately processed further, finally to ammonia, with the reducing power provided by photosynthesis (carbon assimilation and water lysis). When carbon assimilation is not intensive enough (e.g., during night) and reducing hydrogen is not abundantly available, NR activity must be stopped to prevent toxic nitrite accumulation. Nitrite is not only a harmful oxidative molecule, but might also induce apoptosis through reactive oxygen species signaling.

There are further evidences that link Snf1-related kinases to nutrient metabolism. The TOR kinase, a known regulator of nitrogen responses has been revealed to control Snf1 activity [26]. Light and glucose has been also shown to regulate sulphate assimilation [13, 27], which is also in connection with nitrate processing [12]. Therefore, Snf1 and its orthologs are considered as general metabolic regulators with important roles in stress signaling. Exposure of yeast cells to sodium ion stress, alkaline pH, or oxidative stress causes an increase in Snf1 kinase activity, whereas heat shock or osmotic shock (sorbitol treatment) not [28]. Snf1 is also involved in genotoxic stress adaptation in response to hydroxyurea and oxidative stress [29]. In natural growth conditions, yeast generally does

not live at so high sugar concentrations like in laboratory mediums or in the fermenting grape juice during wine production. Yeast cells cultured in nutrient-limiting conditions exhibit a robustly periodic metabolic cycle. Over a cycle of 4-5 hours yeast cells rhythmically alternate between glycolysis and respiration and the DNA replication takes place only during the fermentative phase that might shield DNA from oxidative damage [30].

1.2.2. Nomenclature of the Snf1-related protein kinases

The family of Snf1 orthologs is classified under the designation 5'-AMP-activated protein kinases (AMPKs) that belong to the superfamily of CDPK/SnRK protein kinases [31]. In plants, members of the AMPK family are named class 1 SNF1-related protein kinases (SnRK1). In different plant species there are specific names for SnRK1s, such as AKIN in *Arabidopsis*, RKIN in rice, NPK5 in tobacco, BKIN in barley, PKIN in potato etc. [32].

1.2.3. Structure of the AMP-activated protein kinases

The AMP-activated kinases form heterotrimeric complexes that consist of one catalytic α subunit, one β [33] and one γ non-catalytic subunits [34]. Alternative AMPK subunit isoforms exist that constitute multiple trimeric complexes due to combinatoric assembly [35] (Table 1).

	<i>Saccharomyces cerevisiae</i>	<i>Homo sapiens</i>	<i>Arabidopsis thaliana</i>
α subunit	Snf1	AMPK α 1, α 2	AKIN10,11,12
β subunit	Gal83, Sip1,Sip2	AMPK β 1, β 2	AKIN β 1, β 2, β 3
γ subunit	Snf4	AMPK γ 1, γ 2, γ 3	(AKIN γ), AKIN $\beta\gamma$

Table 1. Alternative subunit isoforms of AMP-activated protein kinase orthologs

Budding yeast contains one catalytic α subunits (Snf1), three alternative beta subunits (Gal83, Sip1 and Sip2) and one gamma subunit (Snf4). The individual loss of function mutations of beta subunits show little or no phenotypes, whereas the triple mutant displays *snf1*- phenotype, similarly to the *snf4* mutant (albeit it is less pronounced at lower growth temperatures) [34]. This indicates that the trimeric composition is obligatory for the kinase activity *in vivo* in yeast. The same can be observed in mammals, where co-expression of all three subunit types increases the kinase activity 50-110 fold with the formation of a heterotrimeric complex, whereas the catalytic subunit expressed alone or together with one other subunit shows hardly detectable activity [36].

In *Arabidopsis* there are three alternative SnRK1 α subunits (AKIN10, 11 and 12), three SnRK β subunits (AKIN β 1, AKIN β 2 and AKIN β 3) and one true SnRK γ subunit (AKIN $\beta\gamma$) [35]. A formerly reported AKIN γ is shown in parenthesis because it interacts with other *Arabidopsis* α and β subunits in the yeast two hybrid system and contains conserved domains, which are generally present in AMPK γ subunits, but it is unable to complement the yeast *snf4* mutation, unlike AKIN $\beta\gamma$ [149,150]. Some of the plant SnRK1 subunits are atypical (see below).

1.2.4. Relatives of AMPKs

The catalytic α subunit is comprised of an N-terminal kinase domain and a C-terminal regulatory domain. The kinase domain of AMPK α subunits is highly conserved and shows significant similarity to other kinases, whereas the sequence of the α regulatory domain is specific to the AMPK family. Based on sequence similarity of the kinase domain, a broader AMPK-related kinase family is defined. In yeast 5 relatives of Snf1 are found in the CaMK group of protein kinases but they don't substitute for Snf1 [31,37,38]. In mammals, in addition to the two genuine orthologs, AMPK1 and 2 which can complement the yeast *snf1* mutation, there are 13 other members of the family [39, 40]. In *Arabidopsis* the AMPK-related kinases can be further classified into SnRK1 class which contains three true Snf1 orthologs, AKIN10, 11 and 12, and the likewise stress-related SnRK2 and SnRK3 classes, which are plant specific and fail to complement the yeast *snf1* mutation. The 10 SnRK2 kinases of *Arabidopsis* are monomers and involved in ABA and osmotic stress responses, whereas the SnRK3 family counts 25 members [31]. The SnRK3 kinases, which are also termed the SOS2 (salt overly sensitive 2)-like protein kinases (PKS), differentially interact with the SOS3 family of Ca²⁺ sensors (CBLs, calcineurin-B-like) and show trimeric structure [41]. Also, the yeast Snf1 family member Hsl1 interacts with a yeast Ca²⁺-sensor Cnb1 [42], suggesting further stress-related functional similarities among members of the complete interspecific superfamily.

1.3. REGULATION OF AMPKS

The kinase domain of AMPK alpha subunits contains a conserved activation loop threonine (also named T-loop threonine, position T175 in AKIN10), which is phosphorylated during activation. Site-directed mutagenesis of the T-loop threonine to alanine completely abolishes the kinase activity [43-46]. In its unphosphorylated state the T-loop sterically occupies the catalytic center. Phosphorylation of the activation-loop threonine causes an outward rotation of the activation loop, thus making the catalytic cleft accessible to substrates and aligning the active site residues for catalysis [47-48]. Upstream activating kinases have been identified in yeast (Pak1 recently renamed as Sak1, Elm1 and Tos3 encoded by paralogous genes) [49-52], in mammals (LKB1, CaMKK α and β , TAK1 MAPKKK) [53-57] and recently in *Arabidopsis* (Tos3-like kinase 1 and 2 or alternatively SnAK1, SnAK2) [38, 58]. In yeast, upstream activation is essential for the kinase function, because the *elm1pak1tos3* triple mutant shows *snf1* phenotype [49]. Similarly, bacterially expressed and reconstructed mammalian heterotrimeric AMPK is not active *in vitro*, but can be activated by upstream kinase treatment [59]. In contrast, the *Arabidopsis* SnRK1 catalytic subunits AKIN10 and AKIN11 show basic activity due to autophosphorylation and phosphorylate SPS-KD (sucrose phosphate synthase catalytic domain peptide) as artificial substrate *in vitro* [60]. The different upstream kinases represent distinct signaling pathways [61]. Other phosphorylation sites were identified on purified AMPKs by mass spectrometric analysis (T258 and S485 in AMPK α 1) but their mutations don't affect the kinase activity [62].

Specific phosphatase activity removes T-loop phosphorylation during inactivation. In yeast Reg1, one of the targeting subunits of the essential PP1 phosphatase Glc7, directly interacts with and

negatively regulates the Snf1 kinase [63,64]. Reg1 is phosphorylated by Snf1 upon glucose limitation but dephosphorylated by Glc7 in the presence of glucose [65]. Other poorly investigated components, such as Sip5, might play a role in the kinase regulation. Sip5, binds to both Reg1/Glc7 and Snf1 kinase complex, and may stabilize their interaction thereby facilitating glucose repression [66]. Decrease of Glc7 phosphatase activity in the *reg1* mutant and in the absence of glycolytic enzyme and metabolic glucose sensor hexokinase2 (*hvk2*) also contribute to Snf1 activation [64-65,67]. Hvk2 is part of a nuclear glucose repressor complex [68-69], constitutively interacts with Snf1 under both low and high glucose concentration [70] and inhibits Snf1 activity at high glucose concentrations [71]. Assumingly, the glucose-binding of Hvk2 plays a role in the inactivation process. Hvk2 also interacts with the Glc7 phosphatase complex [72].

The other major mechanism that activates AMPKs is mediated by the γ subunit. Yeast two hybrid experiments indicate that the kinase domain (KD) and C-terminal regulatory domain directly interact with each other within the catalytic subunit. This conformation represses the kinase activity and depends on high glucose concentration in yeast. The C-terminal autoinhibitory domain (AID) alternatively interacts with the γ subunit [73]. Upon glucose removal the AID is released by the kinase domain and at the same time bound by the γ subunit leading to an intramolecular rearrangement and relief of kinase activity.

Mammalian and plant AMPKs can be activated by AMP *in vitro* [18,74] that is mediated by the γ subunit. Despite high level of conservation between yeast Snf4 and other AMPK γ subunits, purified and active Snf1 could not be further activated by AMP *in vitro* [75]. However, dephosphorylated and thereby inactivated trimeric Snf1 can be reactivated by mammalian AMPK upstream kinase and this process is facilitated by the presence of 100 μ M AMP. So, although not evident, it seems that AMP might directly activate also the yeast Snf1 complex. Snf1 activity correlates with changes in the AMP/ATP ratio also *in vivo*. AMP-activation of Snf1 is further supported by the fact that Snf4 binds AMP and ATP *in vitro*. Trimeric Snf1 complex from *Saccharomyces pombe* could be crystallized in association with AMP and ATP and the partial three-dimensional structure of the complex was resolved recently by X-ray crystallography, shedding light on the mechanism of AMP/ATP-regulation [76]. It is the conserved cystathione-beta-synthase-repeat based nucleotide-binding pocket of γ subunits that binds AMP or alternatively ATP [77]. The binding imposes different electrical charge distribution on the molecular surface, controlling the interactions within the kinase complex. AMP-binding activates whereas ATP binding inhibits the AMPK kinase. The binding depends on the AMP/ATP concentration ratio, but AMP has higher affinity.

High glucose concentration inhibits the interaction of Snf1 with Snf4 in the yeast two hybrid assay [75, 78]. In contrast to the KD-AID interaction, the binding of isolated AID to γ subunit is not dependent on glucose in the yeast two hybrid assay [73]. Moreover, in experiments with the full length α subunit the T-loop phosphorylation is a prerequisite of the γ subunit – AID binding, because site-directed mutagenesis of the T-loop threonine to alanine prevents it. Conversely, the inhibition by glucose depends on PP1 phosphatase activity [79], and Reg1 overexpression interferes with the AID-

Snf4 interaction at low glucose levels [65]. Therefore, it is likely that the glucose inhibition is transmitted by T-loop dephosphorylation by Glc7, and conversely T-loop phosphorylation by an upstream kinase leads to the release of AID, which is taken over by the AMP-bound γ subunit resulting in Snf1 activation. Importantly, the T-loop phosphorylation itself is not sufficient for activation because the yeast *snf4 Δ* mutant shows a *snf1*- phenotype [34].

1.3.1. Domain structure of the catalytic subunit

The sequence motifs involved in autoinhibition of Snf1 were precisely mapped in yeast. Deletion analysis located the AID to amino acid position 392-518 in Snf1, which is nearly identical to the γ -binding sequence (392-495) [73]. In mammals, the role of a short motif immediately downstream of the kinase domain was revealed in rat AMPK (315-392) as autoinhibitory sequence [80]. This motif was verified and also structurally analyzed in human AMPK (313-335) [81]. At the same steric and sequence position a UBA1 domain is present in plant AMPK orthologs and in many of human AMPK-related family members. The UBA1 domain is approximately 45 amino acids long and folds into a bundle of three tightly packed helices, exposing a hydrophobic patch that generally interacts with monoubiquitin or polyubiquitin chains [82-83]. In the yeast Snf1 kinase, the sequence of AID locates to the area of a UBA2 domain (309-482). Notwithstanding their low sequence homology, both UBA1 and UBA2 domains are generally able to bind ubiquitin.

Ubiquitin has various functions in the cell. Monoubiquitin acts as a sorting signal throughout the endocytotic pathway. Polyubiquitin chains, which are linked through Lys48 are signals for proteasomal degradation, whereas Lys63-linked chains are implicated in DNA damage repair, signal transduction and endocytosis [84]. One major role of UBA1 domain is to inhibit ubiquitin chain elongation and thereby prevent the degradation of proteasomal substrates [85-86]. In mammals, protein kinases containing UBA domain can only be found in the AMPK-related kinase family [87]. The presence of UBA domain in many AMPKs supports the observation that *Arabidopsis* SnRK1 kinases were found in association with the 26S proteasome and SCF type E3 ubiquitin ligases [88], and thereby could be regulatory components of the proteasomal degradation machinery. However, a recent publication showed that surprisingly none of the isolated UBA domains found in AMPK-related kinases can interact with any form of ubiquitin or ubiquitin-like molecules (SUMO1, SUMO2, SUMO3, NEDD8) *in vitro* [87] and this observation is also supported by crystallographic data. Compared to published structures of mono- and polyubiquitin docked onto UBA domains of other proteins there would be a steric clash between the ubiquitin and the N-terminal lobe of the kinase domain, indicating that binding of the two would be mutually exclusive. Also the conformation of the UBA domain is abnormal in AMPK-related protein kinases [89]. However, it is still possible that the UBA domain might bind ubiquitin in the active state of the kinase, which is accompanied by major structural changes and might shift also the UBA domain structure into its regular conformation.

Recently, it has been proposed that instead of binding ubiquitin the UBA domain of the AMPK-related kinases might be involved in regulating the kinase activity. Still it is not clear how,

because the results are inconsistent. Jaleel et al (2006) [87] reported that the UBA domain is necessary for efficient T-loop phosphorylation of the MARK2 AMPK-related kinase by an upstream kinase *in vitro*. Deletion of the UBA domain leads to complete loss of activity of this kinase. In case of the autophosphorylating and thereby self-activating MELK, a mammalian AMPK-related kinase, the UBA domain is also essential for the kinase activity *in vitro* [90]. In contrast, Marx et al (2007) [91] could not verify the activating role of UBA domain. Instead, they found it modestly inhibitory in MARK2, suggesting that the UBA domain probably enforces an inactive open conformation of the catalytic domain. This is also supported by the fact that the autoinhibitory α helix identified in the human AMPK1 (residues 313-335) overlaps with the position of UBA domain in AMPK enzymes. Based on the structural information of multiple AMPK-related kinases (MARK1, MARK2 and MARK3) the binding ability of the UBA domain to the N-terminal kinase lobe has probably evolved on the expense of loosing ubiquitin-binding ability [92].

The extreme C-terminus of the α subunit (515-633) of Snf1 is responsible for β subunit binding, which is also indispensable for the activity [93]. In the *Arabidopsis* AKINs and some related kinases the extreme C-terminus forms a distinct KA1 domain (kinase associated) that has been implicated in autoinhibition [81].

1.4. THE ROLE OF BETA SUBUNITS IN REGULATION

The beta subunits serve as scaffold for the trimeric kinase complex, having distinct interaction domains on their conserved C-termini for both the catalytic (KIS domain, kinase interaction sequence) and activator subunits (ASC domain, association with the Snf1 complex) [33, 93-94]. In addition to their structural roles, the beta subunits determine the subcellular localization of trimeric kinase complexes, and play important roles in selective substrate recognition. The beta subunits are essential for the kinase function because deletion of genes encoding all beta isoforms inactivates the Snf1 kinase in yeast and leads to *snf1*- phenotype.

1.4.1. Subcellular localization

In response to nutritional stress the localization patterns of beta subunits change in yeast [95]. When the cells are grown on glucose, each beta subunit is predominantly cytoplasmic but upon shift to non-fermentable carbon source Gal83 is imported into the nucleus, Sip1 moves into the vacuolar membrane, whereas Sip2 seems to remain cytosolic. Yeast Sip2 is implicated in the control of aging in response to metabolic stress [96]. In this process a plasma membrane bound form of Sip2 tethers Snf1 and Snf4 to the cell membrane, and thereby prevents their nuclear import, and assumingly negatively regulates nuclear Snf1 activity [97]. Location of the Snf1 kinase complex at the nuclear periphery was observed recently, and the nuclear membrane-associated form of Snf1 might play role in the release of glucose repression [98].

Post-translational modifications of the beta subunits also affect the Snf1 kinase activity and its cellular localization [99-100]. The variable β N-terminal sequence is necessary and sufficient factor

for the correct localization [101]. The membrane binding ability of some beta subunits is provided by N-terminal myristoylation, a secondary modification which targets proteins to membranes. Sip1 and Sip2 of yeast are optionally myristoylated on their Gly2 residue [97, 102-104] and the same potential myristoylation site is present in the *Arabidopsis* SnRK1 beta subunits AKIN β 1 and AKIN β 2. Mutation of the critical glycine to alanine in the myristoylation site prevents relocalization of Sip1 in yeast [103]. Very recently the myristoylation site mutations were studied also in the *Arabidopsis* AKIN β 1 and AKIN β 2 proteins [104]. Wild type AKIN β 1 and AKIN β 2 were mostly associated with the plasma membrane. When myristoylation is inhibited by a Gly₂Ala substitution, AKIN β 1 is relocalized into the nucleus, whereas AKIN β 2 moves to the cytosol. In another approach, bimolecular fluorescent complementation (BiFC) was used to explore the localization and interactions of *Arabidopsis* SnRK1 kinase subunit isoforms in a highly artificial system, using overexpressed kinase subunits in *N. benthamiana* leaf epidermis [105]. This resulted in the detection of all three beta subunits incorporated into trimeric kinase complexes in the cell membrane, cytoplasm and nucleus.

The beta subunits are also phosphorylated at multiple sites *in vivo* and *in vitro* in yeast [105-107] and mammals [100]. In case of AMPK β 1, the phosphorylation sites were identified by mass spectrometry [62, 99]. Site-directed mutagenesis of serine 108 to alanine resulted in loss of AMPK kinase activity, whereas the SS 24, 25 AA double mutation and S182A mutation resulted in nuclear redistribution of the β subunit [107].

Using trimeric Snf1 complex purified from yeast cells, Snf1 itself was found to be implicated in phosphorylation of its beta subunits *in vitro* [107]. However, the possibility couldn't be excluded that the phosphate incorporation is mediated by a different kinase copurified in minor amounts with Snf1. Bacterially expressed and reconstituted trimeric AMPK complex is entirely inactive but can be activated by externally added upstream kinase [59]. However, so far such kinase sample has not been assayed for beta subunit phosphorylation. Other protein kinases acting in the sugar signaling pathways have been implicated in the regulation of subcellular AMPK movements, including the upstream Snf1-activating kinase Pak1 [109] and the cyclic-AMP dependent protein kinase PKA [110]. Nevertheless, subcellular movements of beta subunits are clearly independent of Snf1 and Reg1 because they are normally localized in a *snf1 Δ* strain [95].

1.4.2. Substrate definition

Genetic and biochemical observations indicate that in yeast only the nuclear Gal83 beta subunit containing Snf1 kinase complex phosphorylates the transcriptional activator Sip4 protein [111,112]. Subcellular localization probably plays a major role in the selectivity of various Snf1 complexes by allowing access to sequestered substrates. Interestingly, the conserved Snf4-binding ASC domain, and not the variable N-terminus, of Gal83 was shown to be necessary and sufficient for Sip4 interaction [111].

The β subunits contain a functional glycogen-binding domain (GBD) positioned N-terminally of KIS and ASC domains, which certainly plays a role in the substrate definition. The GBD (residues

68-163 in AMPK β 1) is most closely related to iso-amylase domains found in glycogen and starch branching enzymes [113-115]. The GBD of beta-subunit is able to bind glycogen *in vitro* in a saturating manner. Moreover, overexpressed AMPK β 1 co-localizes with glycogen-bound phosphatase (glycogen phosphorylase) *in vivo*. Mutations in AMPK γ subunits cause glycogen storage disease in humans [116] and glycogen synthase is an identified AMPK substrate [117]. Phosphorylation site mutation S108A of AMPK β partially inhibits glycogen binding. There might be additional sequences in the holoenzyme involved in glycogen association because binding affinity of the trimeric kinase to glycogen is about 10-fold higher than the GBD alone. AMPK activity is not inhibited by glycogen.

1.5. GLUCOSE SIGNALING IN YEAST

For more exact illustration of the role of Snf1 in cell signaling, the following section provides a short overview of key components of yeast glucose signal transduction machinery [4,14,118].

Extracellular glucose is sensed by plasma-membrane integrated receptors. Such intramembrane glucose receptor is Gpr1 that belongs to the G-protein coupled receptor family. Upon external glucose binding, Gpr1 releases its trimeric G protein α -subunit partner (Gpa2) that activates the cyclic-AMP producing enzyme adenylate cyclase (Cyr1). An alternative way for adenylate cyclase activation is through small G-proteins Ras1 and Ras2, but less is known about this part of the cascade. They might be activated by intracellular glucose signal that finally leads to cAMP production through Cyr1. In yeast, cAMP enhances proliferation and down-regulates stress resistance. Cyclic-AMP allosterically activates the cAMP-dependent protein kinase A (PKA), which directly phosphorylates and regulates metabolic enzymes and transcription factors. For instance, PKA phosphorylates and inactivates the Msn2 and Msn4 transcriptional activators of stress-induced genes that carry the stress responsive element (STRE) in their promoter. Transcription factor Rap1, another direct PKA substrate, regulates the expression of ribosomal proteins and thereby is an indicator of general intensity of protein synthesis. An important link between nutrient limitation and cell cycle control is established through translational regulation of yeast cyclin 3 by PKA. PKA integrates multiple nutrient responses including glucose, sulphate, phosphate and nitrogen sources. The convergence is in part due to antagonistic interaction with the TOR kinase pathway, another major nutrient signaling cascade mostly described in nitrogen responses. Interestingly, glucose availability correlates with PKA activity but not with high cAMP levels, because cAMP is present only during the transition from repressed state to derepressed state.

Other glucose receptors, evolved from glucose transporters and enzymes of glucose metabolism, have intrinsic ability to bind glucose. Such glucose transporter-derived intra-membrane receptors are Rgt2 and Snf3 that lost their transporting activities. In response to extracellular glucose they interact with casein kinase1 (Yck1), which in turn phosphorylates the cytoplasmic form of Mth1 and Std1 transcriptional repressor proteins marking them for proteasomal degradation through the SCF^{GRR1}-E3 ubiquitin ligase. When localized in the nucleus, Mth1 and Std1 participate in the

repression of hexose transporter gene expression (Hxt family) through interaction with the Rgt1 transcriptional repressor.

The main glucose repression pathway requires the intracellular presence of glucose. Once glucose is imported to the cytoplasm it becomes phosphorylated, which has multiple purposes. The addition of a phosphate group to the sugar acts to trap it in the cell, since the negatively charged phosphate cannot easily traverse the plasma membrane. From metabolic aspect, phosphorylation of glucose is the entry step into glycolysis. Glucose phosphorylation is also implicated in the activation of glucose repression pathway. Glucose phosphorylation is catalyzed by hexokinase1, hexokinase2 and glucokinase (Hxk1, Hxk2 and Glk1) in yeast. Mostly Hxk2, but to less extent also Hxk1, is able to mediate glucose repression, whereas glucokinase not. Hxk1 and Hxk2 are therefore not only metabolic enzymes but also glucose sensors. Long-term glucose repression specifically requires Hxk2, which is the most active glucose-phosphorylating enzyme and exists as phosphorylated monomer and unphosphorylated active dimer. Overexpression of Glk1 does not restore glucose repression in *hxk* mutants indicating that not phosphorylated glucose but instead the active forms of hexokinases play important roles in glucose signal transduction. Mannoheptulose, a specific inhibitor of hexokinases, blocks the glucose repression pathway. Interestingly, mutant alleles of Hxk2 have been identified in which catalytic activity and signal transducing abilities are uncoupled. Hxk2 is present also in the nucleus and its nuclear localization is dependent on glucose [119].

An additional pathway with emerging importance is linked to trehalose metabolism. Trehalose is a disaccharide comprised of two glucose subunits linked in α,α -1,1 configuration. Being a non-reducing sugar, trehalose is chemically more inert than glucose whose aldehyde and ketone groups react with lysine or arginine residues of proteins. Trehalose is involved in desiccation tolerance and known as a general stress protectant and storage carbohydrate in microorganisms, accumulated mainly during starvation conditions. Similarly to glucose-6-phosphate, trehalose-6-phosphate (T6P) is not only a metabolic intermediate but a regulator of enzyme activity. In yeast T6P inhibits Hxk2 and thereby controls the flux of sugars into glycolysis. Mutant alleles of trehalose-6-phosphate synthase (Tps1) confer general glucose-sensing defect.

There is a prevalent crosstalk between the glucose signaling cascades represented by the above mentioned receptors. Therefore, this pathway is considered as a complex signaling web, which is also interconnected with other nutrient and hormone signal transduction cascades. For example, cAMP synthesis through Ras2 requires glucose phosphorylation by the hexokinases or glucokinase [120]. On the other hand, full glucose response (glucose induction and also repression) can be triggered by expressing either activated Ras2 or Gpa2. Therefore, Hxk2 must generate the glucose repression signal through G-proteins [121]. The transcriptional response of Snf3/Rgt2 target genes (e.g. Hxt1-4) can also be generated in the absence of glucose by the expression of hyperactive Ras or Gpa2. Snf3 and Rgt2 appear either to act upstream of Ras/cAMP/PKA or to play an ancillary, redundant role in the initial detection of glucose. PKA, activated by cAMP, is involved in glucose-induced removal of Rgt1

repressor, and thereby activates the expression of Hxk2, hexose transporters (Hxt) and Snf3 receptor genes.

1.5.1. Snf1 is a central regulator in yeast glucose signaling

The canonical Snf1 function is the release of glucose repressed gene expression. Glucose repression is transmitted by the Hxk2 pathway, which indeed shows interactions with Snf1 and with its negative regulator, the Glc7 PP1 phosphatase. However, Snf1 and Glc7 interact with several other elements of glucose signaling network and therefore they cannot be obviously assigned to any of the signaling cascades represented by the above described receptors. It is also unknown, which signals activate and which signaling cascades integrate the Snf1-activating upstream kinases. Moreover, AMPKs are directly activated by AMP, which is a metabolic signal, so they can be interpreted as a sensor or receptor component of a distinct signaling pathway.

Both Snf1 and the Reg1-targeted Glc7 PP1 phosphatase directly interact with Hxk2 [70,72]. This is a substrate level interaction at least in case of Glc7, which directly dephosphorylates and thereby activates Hxk2. Since Snf1 and Glc7 are direct interacting partners and functional antagonists, Snf1 might phosphorylate and inactivate Hxk2. In support of this hypothesis, increasing extracellular glucose concentration and hyperactivation of PKA (that are both opposing the conditions when Snf1 is active) result in reduced Hxk2 phosphorylation, whereas attenuation of PKA activity increases ³²P labeling of HXK2 [122]. Snf1 also prevents Hxk2 gene expression through multisite phosphorylation and activation of Rgt1 transcriptional repressor. Snf1 phosphorylates Mig1 (the binding partner of Hxk2) on at least four sites [70]. Phosphorylation of serine 311 causes nuclear export of Mig1 and thereby prevents Hxk2 to access to its promoter targets by heterodimerization with Mig1. In yeast cells grown in glucose medium, Mig1 is nuclear whereas in cells grown in ethanol medium it is cytoplasmic. However, in *hxx2* mutant cells Mig1 has always cytoplasmic localization even in cells grown on glucose, which is due to its Snf1-mediated phosphorylation because in *hxx2snf1* double mutant Mig1 is constitutively nuclear. Furthermore, Hxk2 appears to regulate Snf1 activity, perhaps through Glc7. In the Snf3-Rgt2 glucose induction pathway Snf1 phosphorylates Mth1 and Std1, thereby preventing their proteasomal degradation targeted by Grr1. In the PKA signaling route Snf1 phosphorylates Msn2 and thereby probably regulates its nucleo-cytoplasmic distribution. Snf1 also interacts with the Nrg1 and Nrg2 transcriptional repressors of stress responsive genes involved in the transcriptional control of about 150 genes, including a set of genes regulating haploid invasive growth.

1.5.2. Snf1 and controlled protein degradation

Protein products of many genes whose expression is regulated by glucose are also controlled post-translationally by glucose signaling. These control mechanisms include conformational changes, subcellular redistribution (e.g., Rgt1, Mig1, *etc.*) and proteolytic degradation by the 26S proteasome. Many of these events are mediated by phosphorylation. Grr1 (glucose repression resistant 1), the F-box protein substrate recognition subunit of an SCF type E3 ubiquitin ligase, was identified in genetic

screens as component of glucose signal transduction but it is also involved in nitrogen response and cell cycle regulation [123]. SCF^{Grr1} recognizes phosphorylated substrates via the cationic surface of its leucine-rich repeat (LRR) protein interaction motif [124] but phosphorylation of substrates on other residues can prevent their degradation. In case of Mth1 and Std1, it is casein kinase (Yck1) which facilitates their degradation, whereas phosphorylation by Snf1 stabilizes them. Other proteasomal substrates, such as Gis4, are also known to be ubiquitylated by SCF^{Grr1} and to interact with Snf1 [125]. Gis4 has been implicated in glucose responses [126] and is also a regulator of ion homeostasis in yeast [127]. SCF^{Grr1} mediates the degradation of several other glucose regulated proteins, for instance, Gal2 [128] and Mks1 [129]. One major means of cell cycle regulation by nutrient availability is represented by proteasomal degradation of G1 cyclins Cln1 and Cln2 targeted by Grr1.

Reg1, the targeting subunit of Glc7 phosphatase also interacts with Grr1 in a complex with 14-3-3 proteins [130]. Snf1 does not bind to Grr1 directly but it also co-purifies with the 14-3-3 proteins Bmh1 and Bmh2 of yeast [52] as well as the γ subunit Snf4 [131]. Members of the 14-3-3 protein family are binding partners of phosphoproteins [132]. It has been shown in some cases that the phosphorylated 14-3-3 binding partners are also substrates for the Glc7 phosphatase [133]. Through interaction with numerous binding partners, the 14-3-3 proteins play important roles in the regulation of diverse cellular processes including transcription, signaling, cell cycle control and metabolic regulation [134]. Moreover, it is established that the 14-3-3 proteins Bmh1 and Bmh2, together with Reg1, actively participate in glucose-induced degradation of maltose permease [135]. The involvement of 14-3-3 proteins in the control of proteasomal degradation explains their interaction with Grr1. Genetic evidence indicates that the yeast 14-3-3 proteins Bmh1 and Bmh2 are involved in the regulation of glucose repression. Deletion of *Reg1* and both *Bmh* genes causes a synergistic relief of glucose repressed gene expression [136]. Supporting this, among 14-3-3 interacting partners there are several proteins involved in gluconeogenesis [137]. In addition, 14-3-3 proteins also respond to the Ras/PKA pathway [138]. 14-3-3 proteins are also involved in glucose signaling related mechanisms, including the control of DNA damage [139] and replication checkpoints in yeast [140].

Phosphoprotein binding ability of 14-3-3 proteins can stabilize active or inactive conformation of enzymes, it can stimulate protein-protein interactions and anchor proteins to cellular compartments through which 14-3-3s regulate nucleo-cytoplasmic distribution of proteins [141]. Since active Snf1 is predominantly located in the nucleus, whereas fluorescently tagged Reg1 appears to be exclusively cytoplasmic, it was proposed that upon glucose-related signals Snf1 would rapidly shuttle between the nuclear and cytoplasmic compartments allowing inactivation by Glc7/Reg1 in the cytoplasm [142]. Based on this assumption, Snf1 might be exported from the nucleus still in an active form and 14-3-3 proteins might serve as mediators of Glc7/Reg1 function. In the mammal QSK and SIK kinases, which are members of the AMPK-related protein kinase family, it is the phosphorylated T-loop which has been shown to confer binding to a 14-3-3 protein that controls their activity and localization [143]. Phosphorylated form of another mammalian AMPK-related kinase MARK3 also interacts with 14-3-3 proteins. Wild type MARK3 is present in both cytoplasm and plasmamembrane, whereas mutation of

the T-loop phosphorylation sites to alanine results in a loss of 14-3-3 binding ability and exclusive plasmamembrane localization of MARK3. Nevertheless, 14-3-3-binding of MARK3 does not affect its activity [144]. 14-3-3 proteins themselves are also regulated by phosphorylation which further complicates the understanding of their regulatory interactions with kinases. The above listed examples assume a complex regulatory mechanism in which AMPK kinases in cooperation with 14-3-3 proteins control proteasomal degradation of enzymes and components of various signaling pathways.

1.6. SNF1-RELATED KINASES IN PLANTS AND THEIR ATYPICAL SUBUNITS

Snf1-related kinase subunits were identified in plants based on sequence homology to yeast Snf1 and its related subunits [145]. In *Arabidopsis* three SnRK1 α subunits (AKIN10, AKIN11 and AKIN12), three SnRK1 β subunits (AKIN β 1, AKIN β 2 and AKIN β 3) and at least one true SnRK1 γ (AKIN β γ) subunit were identified [35]. Based on data available in the *Genevestigator* microarray database AKIN10 and AKIN11 represent the variants expressed in most tissues, whereas AKIN12 expression is restricted to siliques and its expression level is very low.

In contrast to the two typical β subunits in *Arabidopsis* (AKIN β 1 and AKIN β 2), AKIN β 3 is a shorter variant and does not carry N-terminal GBD. Nonetheless, it still contains the KIS and ASC domains. Therefore, AKIN β 3 is still able to mediate interactions within the trimeric SnRK1 complex *in vitro* and *in vivo* [146]. Although atypical, AKIN β 3 can complement the yeast mutations *sip1 Δ sip2 Δ gal83 Δ* . Such short β subunit variant exists also in other plant species. The GBD-containing N-terminal sequence, which is missing from the short beta subunits, appears on the N terminus of the plant specific γ subunit as a result of natural domain swap [147], therefore the *Arabidopsis* SNF4/ γ subunit is named AKIN β γ . This longer γ subunit version also complements the yeast *snf4* mutation. A putative distant ortholog of SnRK1 γ subunit was found in *Arabidopsis* (At3g48530) that contains CBS repeats, but its overall homology to other γ subunit orthologs is very low [148]. Although it interacts with other *Arabidopsis* SnRK1 subunits in the yeast two-hybrid system, it is unable to complement the yeast *snf4* mutation. Therefore, this protein might not be a true γ subunit but rather another CBS-repeat protein with different function. Interestingly in maize (*Zea mays*) two *ZmAKIN β γ* sequences were found [147].

An atypical functional feature of plant SnRK1 kinases is, at least in tobacco and *Arabidopsis*, that the catalytic subunits AKIN10 and AKIN11 can autophosphorylate and show a moderate substrate phosphorylating activity *in vitro*, unlike yeast Snf1 and mammal AMPK orthologs [60]. Nevertheless, recently upstream activating kinases had been identified also in *Arabidopsis* [38,58].

1.6.1. Physiological roles of SnRK1 kinases in plants

Reverse genetic approach of functional dissection of *Arabidopsis* SnRK1 subunit genes is limited because no T-DNA insertion mutations are available for *AKIN11*, and only one T-DNA tag is found in the 3'-region of *AKIN10* gene (not studied yet in detail). For *AKIN12* more T-DNA insertion mutant lines exist.

Two SnRK1-encoding genes, PpSnf1a and PpSnf1b, have been cloned from the moss *Physcomitrella patens* and shown to functionally replace Snf1 in yeast [149]. In *Physcomitrella*, gene function can be studied by homologous recombination based mutagenesis method (gene targeting), which is applied in the haploid gametophyte. The *snf1asnf1b* double mutant of *Physcomitrella* is viable but requires continuous light for survival and deficient in starch accumulation. This phenotype correlates with properties of the yeast *snf1* mutant, which is able to grow only on glucose medium and unable to accumulate reserve nutrients. (However, the analogy between plant SnRK1 and yeast Snf1 function is not obvious because yeast accumulates reserve nutrients when glucose is depleted, whereas plants accumulate mesophyll starch when performing photosynthesis and producing sugars in the light). The *snf1asnf1b* double knockout grown on continuous light shows developmental abnormalities, premature senescence and altered sensitivity to plant hormones (hypersensitivity to auxin and reduced sensitive to cytokinin). The increased senescence phenotype is similar to enhanced aging phenotype of the yeast *sip2Δ* mutant [97,98] and AMPK-related aging phenotype of human fibroblasts [150]. In potato, antisense expression of Snf1-related protein kinase sequence results in decreased expression of sucrose synthase in tubers and loss of sucrose-inducibility of sucrose synthase transcripts in leaves [151], whereas SnRK1 overexpression leads to increased starch accumulation and low glucose concentration in tubers [152]. In barley, the absence of SnRK1 expression causes abnormal pollen development and lack of starch accumulation in pollen and thereby results in male sterility [153]. In cultured wheat embryos, embryo specific expression of an antisense SnRK1 variant represses transient expression of α -amylase promoter thereby inhibits starch breakdown [154]. (The result is the latter quite artificial experiment is opposite to those mentioned before, indicating that there are still questions in the role of SnRK1 kinases in starch metabolism.)

Reserve nutrient reallocation occurs also in other cases during development, in which SnRK1 kinases play a role. For instance, herbivore attack during early phases of development increases root reserves, which in turn delays senescence and prolongs flowering. In *Nicotiana attenuata*, reallocation of reserve carbon to root in response to herbivore attack is mediated by the downregulation of a SnRK1 β -subunit *NaGal83* in the leaves [155].

In pea (*Pisum sativum*), antisense expression of SnRK1 causes defects in seed maturation, reduced conversion of sucrose into storage products, lower globulin content, frequently altered cotyledon surface, shape and symmetry, as well as occasional precocious germination. Gene expression analysis of pea embryos using macroarrays of 5548 seed specific genes revealed 183 differentially expressed genes in two clusters, either delayed down-regulated or delayed up-regulated during the phase transition from intensive cell division to maturation [156]. The delayed down-regulated genes are related to mitotic activity, gibberellin and brassinosteroid synthesis, stress response and Ca^{2+} -signal transduction. The delayed up-regulated genes are mainly related to storage protein synthesis and stress tolerance. Most of the phenotypes exhibited by antisense SnRK1 expressing plants resemble abscisic acid (ABA) insensitivity. The close connection between SnRK1 and hormone signaling, especially with ABA responses, was also studied in tomato seeds where ABA

and gibberellin were shown to differentially regulate SnRK1 expression [157]. The role of γ subunit was studied in *Medicago truncatula* seeds [158]. *MtSnf4b* accumulated during seed filling whereas it disappeared during water uptake by mature seeds. However, desiccation stress lead to reactivation of the Snf1 complex in seedlings. Silencing of *MtSnf4b* using an RNA interference (RNAi) approach resulted in the accumulation of 60% more sucrose in the seeds and caused reduced seed germination.

In *Arabidopsis* no mutant phenotype of any SnRK1 subunit has been published so far. Very recently, phenotypes of AKIN overexpressor transgenic *Arabidopsis* plants were published as well as knock-down lines using virus-induced gene silencing (VIGS) [159]. AKIN10 overexpression showed some advantage in seedling primary root growth and development under low light with limited energy supply, whereas exogenous glucose application resulted in reduced root and shoot growth. In contrast, AKIN10 silenced lines were able to use exogenously supplied sucrose and glucose and exhibited enhanced shoot and root growth. Whereas wild type plants undergo rapid senescence in response to nutrient deprivation, AKIN overexpressing lines display delayed flowering and delayed onset of senescence. In contrast, the AKIN10 and 11 double knock-down plants exhibit so rapid aging that in the most severe cases senescence occurs before flowering. Unlike in *Physcomitrella*, the growth phenotypes could not be rescued by exposure to continuous light. RNA-silencing of AKINs also causes defects in starch metabolism. In the double knock-down lines leaf starch content remained high at the end of the night suggesting a failure of carbon transport from source leaves to the roots during the dark period. However, this result is opposite to the majority of former observations in different plant species engineered for overexpressing or silencing SnRK1 kinases. Most of the former results suggest that SnRK1 kinases enhance the accumulation of starch whereas this recent observation suggests that SnRK1 kinases intensify starch breakdown.

Global transcript analysis of AKIN overexpression in an artificial protoplast system identified 1021 putative AKIN target genes belonging to various catabolic pathways including cell wall, starch, sucrose, amino acid, lipid and protein degradation that provide alternative sources of energy and metabolites [159]. Similarly to the glucose repression mechanism of yeast, also in *Arabidopsis* a large set of genes were repressed, which are involved in the ribosome biogenesis. Importantly, the results also revealed an extended role of SnRK1 in signal transduction, since mRNA levels of a large number of transcription factors, chromatin remodeling factors and signal transduction components changed in response to AKIN expression. These microarray data suggested that AKIN function should be repressed by sugar abundance. This is again opposite to the prevailing view, which supposes that SnRK1 kinases enhance starch accumulation that can only be supported with sugars abundantly available [60, 151, 160].

Data from *Physcomitrella* indicate that the day/night changes play a critical role in the control of SnRK1 kinases. In *Arabidopsis* light regulation of the transcript levels of AKIN β 1, β 2 and AKIN γ subunits was proposed. AKIN β 1 and AKIN γ transcripts reversibly accumulate in the darkness whereas AKIN β 2 expression seems to be repressed in the dark [148]. In addition, public transcriptome database survey revealed that dark-induced genes are activated under various stress conditions and repressed

not only by light but also by sugars, obviating the connection between sugar-, light- and stress responses [159].

Several SnRK1 kinase substrates have been identified in plants. Most of them are enzymes related to metabolism, although an important role of SnRK1 kinases is expected in signal transduction as well. For example, SnRK1 kinases phosphorylate and inactivate nitrate reductase (NR), sucrose phosphate synthase and 3-hydroxy-3-methylglutaryl-coenzyme A reductase in spinach [161]. A genetic example for the involvement of SnRK1 kinases in signal transduction was published recently: coexpression of AKIN10 with the G-box binding basic leucine-zipper transcription factor GBF5/bZip2 resulted in a strong synergistic effect on the activation of the dark and stress induced DIN6, a candidate target gene for the GBF5 bZIP transcription factor [159].

1.6.2. Involvement of SnRK1 kinases in plant sugar signaling

Our knowledge about the roles of plant SnRK1 kinases in cell signaling at the molecular level is very limited. Neither the recently identified upstream SnRK1-activating kinases are characterized yet, nor their orthologs in yeast. On the other hand, SnRK1 kinases are in close connection with nutrient-, especially sugar signal transduction pathways. Therefore, it is reasonable to study SnRK1 kinases in the context of sugar signaling and its cross-talk with stress-, light- and hormone signaling.

In multicellular organisms sugars are produced or taken up and temporarily stored in specialized organs from where they are reallocated to every tissues of the body. The necessity for long-distance sugar transport, tissue specific and cell autonomous sugar signaling mechanisms, and coordination with complex hormonal networks makes sugar signaling far more complicated in multicellular organisms than in single cell organisms. In plants, depending on the net flux of sugar, net sugar exporting (source) and sugar importing (sink) tissues can be distinguished. Leaf mesophyll cells are considered as source tissue whereas the non-photosynthetic root contains sink tissues, similarly to developing embryos and other rapidly developing organs, such as ripening fruits and meristematic regions. Diurnal changes in sugar allocation are well known in plants. Accumulated excess carbohydrates are transported from the leaves to the roots during the night. Sugar fluxes also dramatically change through development and in response to biotic and abiotic stresses [5].

The major form of transported sugars in plants is sucrose. Sucrose can be imported to sink tissues through plasmodesmata or by apoplastic transport through the cell wall and sucrose transporters. In sink tissues sucrose is cleaved by cytoplasmic, vacuolar and cell wall invertases generating glucose and fructose. The convertibility of sucrose to glucose gives a possible explanation why most sucrose-induced responses can also be triggered by glucose. In case of sugar repression of photosynthesis genes, hexoses are effective at lower concentration than sucrose indicating that sucrose is perhaps not the primary signaling molecule. However, in a few known cases sucrose and glucose exhibit distinct signaling functions. An important example is that the presence of glucose induces intensive cell division during early embryo development, whereas embryonic cell expansion in the following developmental phase is triggered in response to sucrose signal [6].

In plants sucrose and glucose influence a wide range of developmental processes including seed germination, seedling development, root and leaf differentiation, floral transition, fruit ripening, embryogenesis and senescence, as well as responses to light, stress and pathogens. The sugar induced phenotypes used in genetic screens reflect the effects of high concentrations of externally applied sugars (e.g. 6% glucose) that repress photosynthesis, cause stunted growth and inhibit lateral root formation and true leaf development. (The germination arrest on high-sugar media occurs only in a sensitive period during the initial stages of seedling development.) Similarly to yeast, trehalose and some enzymes of its metabolism are sugar-signaling components of emerging importance [162, 163].

1.6.3. Conserved and divergent elements in yeast and *Arabidopsis* glucose signal perception

Although there is a candidate G-protein coupled glucose receptor in *Arabidopsis*, intriguingly no obvious ortholog of PKA has been identified [38]. Therefore, it is not clear how these receptors contribute to glucose signal transduction in plants. *Arabidopsis* apparently contains only one G-protein α -subunit, GPA1, which is implicated in various developmental, light, hormone, phospholipid and stress responses. GPA1 interacts with two putative G-protein coupled receptors GCR1 and RGS1. Loss of RGS1 increases GPA1 activity, which results in increased hypocotyl elongation in the darkness and increased cell production in roots grown in the light. RGS1 overexpressors are hypersensitive to glucose, whereas the *rgs1* mutant is insensitive to glucose inhibition of germination [6].

Other potential cell surface located glucose receptors are found also in plants, but our knowledge about them is limited. The SUT2 sucrose transporter homolog in *Arabidopsis* and tomato is reminiscent to Snf3 and Rgt2 of yeast showing no transporter activity but possessing a long cytoplasmic loop not present in active transporters [6].

Hexokinases are the most ancient and evolutionarily conserved sugar sensors in *E.coli*, yeast, mammals and plants, but there are differences between the orthologs. In *Arabidopsis* two hexokinases AtHXK1 and AtHXK2 and four additional hexokinase-like (AtHKL) genes exist, from which AtHKL1 has detectable kinase activity and therefore is also named AtHXK3. Null mutation of AtHXK1 leads to glucose insensitivity, which cannot be compensated by overexpression of HXK2. AtHXK1 overexpression confers glucose hypersensitivity. *Arabidopsis hxx1* mutants still have about 50% of the wild type glucose kinase activity provided by AtHXK2 and HXLs, and accumulate sugar phosphates to normal levels. These data indicate that as in yeast, the product glucose-6-phosphate itself does not play a role in HXK1-dependent glucose signaling in *Arabidopsis*. However, the glucose analogues 6-deoxyglucose and 3-O-methylglucose, which are transported to the cytoplasm but not phosphorylated, do not trigger sugar responses, unlike 2-deoxyglucose which can undergo phosphorylation. Similarly to Hxk2 of yeast, mutants of *Arabidopsis* AtHXK1 were also generated with impaired kinase activity, which still show normal glucose signal transducing ability. These mutants are deficient in ATP-binding and phosphoryl transfer and not in glucose binding.

Interestingly, yeast Hxk2 and *Arabidopsis* HXK1 are only interchangeable with respect to glucose kinase activity, but they fail to replace each other in their glucose signaling function [6].

Similarly to yeast, AtHXK1 can also translocate to the nucleus where it was reported to participate in a DNA-binding signaling complex together with RPT5B proteasomal 19S cap subunit and VHA-B1 vacuolar H⁺-ATP-ase [164]. Plant hexokinases also associate with membranes of subcellular compartments [165], for instance mitochondria, where they participate in the control of programmed cell death in response to oxidative stress [166].

1.6.4. Sugar response mutants and developmental impact of sugar signaling

Further components of plant sugar signal transduction pathways were identified in several genetic screens based on either enhanced or reduced sugar responses [8]. The screening strategies followed changes either in transcriptional activity of sugar responsive promoter elements in mutants or alterations in the sugar-induced germination arrest phenotype. The mutants were screened on various sugar concentrations using different types of sugars. (The osmotic effects of sugar treatments were excluded by comparison with plants treated with non-metabolizable sugars.) For instance, *glucose insensitive* (*gin*) mutants are able to establish seedling growth on 330mM externally applied glucose (6%), which induces developmental arrest and bleaching in wild type seedlings. By contrast, in *glucose overly sensitive* (*glo*) mutants developmental arrest occurs already at 220mM glucose concentration (4%). These mutant screens identified AtHXK1 as *gin2* and unravelled many formerly annotated hormone signal transduction components showing sugar response phenotypes. In addition to being glucose insensitive, the *gin2* mutant is also hypersensitive to cytokinin and insensitive to auxin, exhibits delayed leaf senescence and retarded growth under high light irradiance [167]. These observations also underscore a close connection between sugar, hormone and light signal transduction cascades.

The interaction of sugar responses with abscisic acid and ethylene signal transduction is especially close. The mutations identified in the sugar-related screens include both hormone biosynthesis genes and downstream hormone signaling elements indicating a broad interaction interface between sugar and hormone signaling cascades. ABA2, a sort chain dehydrogenase/reductase enzyme involved in ABA biosynthesis, was defined by the *gin1* [168], *sis4* (sucrose insensitive4) [169] and *isi4* (impaired sucrose induction4) mutations [170], whereas *aba3* proved to be allelic with *gin5* [171]. Genetic analysis of the *gin2* mutant indicated that AtHXK1 acts upstream of *aba2* in the glucose signaling pathway [168]. *Abscisic acid insensitive 4* was originally isolated because of its ability to germinate on ABA containing media normally inhibitory for germination of wild type *Arabidopsis* seeds [172]. The encoded gene was identified to code for an AP2-domain transcription factor [173], and has been since found in a large number of sugar response screens (*sun6* [174], *sis5* [169], *gin6* [171], *isi3* [170]) and also in salt tolerance screens [175]. ABI4 regulates lipid mobilization in the embryo and is also involved in the repression of seed germination [176]. Although ABI4 is mostly expressed in developing seeds, it is able to repress the expression of plastocyanin, a

nuclear encoded photosynthetic gene. Moreover, ABI4 mediates the effects of exogenous trehalose on *Arabidopsis* growth and starch breakdown [177]. Another ABA-signaling transcription factor identified in sugar response screens is ABI5 [172], which contains a basic leucine zipper DNA binding domain [178]. Expression studies suggest that ABI5 is present during a short post-germination developmental window that correlates with the sugar sensitive period [179]. ABI5 is posttranslationally modified by phosphorylation on multiple residues, which is essential for its activity [179,180]. ABI5 is not only a sugar signaling factor but, in contrast to ABI4, it plays a role in the sugar-mediated regulation of senescence [181], which is an important link also towards SnRK1 kinases. (ABA promotes senescence but it is not required for the sugar-dependent induction of leaf senescence.) Not all ABA signal transduction components play a role in sugar response. For instance, the *abi1* and *abi2* mutations affecting two closely related PP2C type phosphatases and *abi3* do not cause alteration in germination-related sugar responses [182].

ABA and sugar signal transduction is so closely related that the existence of mutants specific only to sugar signaling is an important question. Some mutants with *gin* or *sis* (sugar insensitive) phenotypes (e.g. *sis3* [9]) seem to be unrelated to plant hormone responses. High concentrations (100µM and higher) of externally applied ABA evokes the same developmental arrest phenotype in seedlings as sugars do. Considering also the sugar response phenotypes of mutants in ABA biosynthesis and signaling, it is likely that sugars exhibit many of their developmental effects through components of ABA signal transduction. However, all this applies only to high concentrations of these agents accordingly to their application in genetic screens. Low concentrations of sugars (15 to 90 mM glucose, fructose and sucrose but not sorbitol or mannitol) strongly repress the inhibition of seed germination by exogenous ABA [183]. Low concentration effects of sugars and ABA are not completely revealed yet. ABA has long been considered as a stress hormone and growth inhibitor but relatively recent data indicate that low concentration of ABA is essential for normal shoot and root development [183-185].

The antagonism between abscisic acid and ethylene signaling pathways is a well known phenomenon: generally the positively acting elements of ethylene signal transduction down-regulate ABA signaling and *vice versa*, except of some cases when ethylene and ABA act synergistically for instance in root, where ABA promotes growth at low concentrations [186-187]. The opposite effect of ethylene and ABA reflects also in their interaction with sugar responses: sugar acts synergistically with ABA, but in antagonism with ethylene [188]. This finding is also supported by the fact that ethylene promotes hypocotyl elongation in the light (which inhibits it) even in the presence of high sugar levels, but inhibits the same process in the dark [189]. Furthermore, *gin1/aba2* and *gin2/hxk1* mutations down-regulate a branch of ethylene signaling pathways that stimulates germination, and cotyledon and leaf development [188]. Mutations affecting the negatively acting factors in ethylene responses were identified also as glucose insensitive mutants (e.g., *eto1*, ethylene biosynthesis mutant [188], and *ctr1*, which is allelic to *gin4* [183], and *sis1* [190]), whereas mutations of positive regulatory elements in ethylene signaling confer glucose overly sensitive phenotype (*etr1*, *ein2*, *ein3*,

ein6 [7]). However, analysis of the double mutants *gin1 etr1* and *gin1 ein2*, that display the glucose insensitive phenotype of the *gin1/aba2*, indicate that ethylene probably affects glucose signaling through ABA [8].

HXK1 (*GIN2*) plays an important role also in growth promotion because under high light irradiance *gin2* plants remain small with reduced cell expansion whereas wild type plants benefit from the increased energy supply and their growth is accelerated [167]. Analysis of the effects of proliferation promoting plant hormones on *gin2* revealed that *gin2* is relatively insensitive to auxin-induction of cell proliferation and root formation, but hypersensitive to shoot induction by cytokinin. Consistent with this observation, seedling development of the auxin resistant *axr1*, *axr2* (IAA7), and *tir1* (transport inhibitor response) mutants, as well as that of plants that display constitutive cytokinin response (or are supplemented with exogenous cytokinin), are insensitive to high glucose levels and also relatively insensitive to ABA and ethylene suggesting a possible convergence point between the three signaling pathways [191]. Mutation in *AXR2/IAA7* and other Aux/IAA family members, such as *AXR3/IAA17* and *SHY2/IAA3*, also result in constitutive photomorphogenesis in the dark including true leaf development and greening [192].

Metabolizable sugars alter the responsiveness of plants to light, which has been described for the PhyA-specific far-red light signaling pathway. Sugars can inhibit the far-red light-induced block of greening that is caused by the PhyA-specific repression of protochlorophyllide oxidoreductase [193]. In the *sun6/abi4* (sucrose uncoupled 6) mutant PhyA signaling is no longer inhibited by sugars [194]. Intriguingly, the vegetative developmental mechanisms controlled by PhyA and B are repressed by ethylene [195] that, at least in the above mentioned aspects, acts antagonistically to sugars.

In most cases the effects of sugars on complex developmental events are only described at the phenotypic level but are not completely understood molecularly. Sugars regulate the timing of many developmental phase-changes, such as the progression from juvenile to adult phases, floral transition, senescence and phases of embryo development. Expression of antisense RUBISCO small subunit transcript in tobacco resulted in decreased leaf source strength with concomitant extension of early phase of shoot development [196]. In *Arabidopsis*, a species that flowers earlier under long-day conditions, a correlation was found between greater export of carbohydrates from the leaves and enhanced induction of flowering [197]. Application of exogenous sucrose to the aerial part of plant has also been observed to induce flowering in *Arabidopsis* even in complete darkness [198]. In accordance, trehalose-6-phosphate synthase (*AtTPS1*), a regulator of glucose, ABA and stress responses is an essential factor for flowering in *Arabidopsis* [199]. However, growth on high and low concentration of sucrose (5%, 150mM, 30mM) has been shown to significantly delay flowering [200]. From another view, instead of sugars rather the C:N ratio might be important to regulate the timing of flowering transition [201] and other developmental processes, such as lateral root formation [202], which is a potential interference point with SnRK1 signaling. A major determinant of flowering transition is the day length, which is perceived in plants by comparing diurnal light changes and outputs of the circadian clock. In addition to the characterized close interaction between sugar

signaling and diurnal expression changes, whose regulation involves SnRK1 kinases [159], global transcriptome analysis revealed that sugars also modify the gene expression of about 50% of known clock regulated genes [203].

1.7. SUGAR SIGNALING AND PROTEIN DEGRADATION

Arabidopsis SnRK1 kinases have been found to interact with components of the 20S proteasomal central cylinder ($\alpha 7$ proteasomal subunit) and the common SKP1 subunit of SCF type E3 ubiquitin ligases in yeast two hybrid screen and *in vivo* [89]. Recent bioinformatics analyses suggest that over 5% of the *Arabidopsis* proteome may be involved in ubiquitin- and 26S proteasome-dependent protein degradation [6]. In the most prevalent type of SCF type E3 ubiquitin ligases that contain CULLIN1 subunit, the estimated number of alternative substrate recognition F-box protein subunits is 694 in plants [204]. F-box proteins themselves have also been shown to become ubiquitylated and degraded in a proteasome-dependent mechanism [205]. There are identified ubiquitin ligase components and proteasomally degraded elements in hormone response (AIP2, ABI5 family, EBF1, EBF2, EIN3 EILs, DELLA proteins, TIR1 family, AUX/IAA family, COI1, SLY1 etc.), light signaling (HY5, COP1), flowering (FKF1, CDF1, CO, ZTL), circadian clock (ZTL, TOC1, LKP2), leaf senescence (ORE9) and many other pathways. Sugar signal transduction pathways also utilize controlled protein degradation in their regulation. Solely based on sequence similarity, there are no obvious *Arabidopsis* orthologs of yeast F-box protein GRR1, which was assigned to glucose signal transduction [123]. However, there are several potential functional orthologs, which show considerable similarity to GRR1, including the F-box proteins EBF1 and EBF2 assigned to ethylene signaling and the nuclear auxin receptor F-box protein TIR1 (and its three other family members, the AFB proteins) [206], which function as auxin hormone receptors. EBF1- and EBF2-dependent proteasomal degradation of EIN3 transcription factor in ethylene signaling is enhanced by glucose but inhibited by ethylene [207]. In addition, the TIR1 family member AFB1/AtGRH1 (GRR1 homolog 1) can restore glucose repression activity in the *grr1* mutant yeast, in a way still dependent on the Mig1 repressor [208].

Integration of metabolic signals with cell division has been proposed to be controlled at the level of CyclinD proteins. Cyclins are essential cofactors of cyclin-dependent kinases that are main regulators of the cell cycle. Whereas wild type *Physcomitrella patens* exhibits a prolonged juvenile phase when grown in the presence of glucose, the CyclinD knockout is insensitive to this glucose-mediated developmental delay [209]. In *Arabidopsis*, cyclinD3;1 is transcriptionally upregulated by sugars and cytokinins to enable G1/S transition [210] and appears to be a highly unstable protein which is degraded in a 26S proteasome-dependent fashion upon sucrose depletion [211]. Moreover, cyclinD3;1 is phosphorylated in response to sugar starvation, and the hyperphosphorylated form accumulates in response to proteasome inhibitor treatment [211]. Cyclin D1 is also proteasomally degraded and its stability is controlled by phosphorylation [212].

1.7.1. Conserved mechanisms suggest involvement of SnRK1 kinases in sugar dependent proteolysis

14-3-3 proteins participate in sugar signal transduction also in plants. In cultured sugar-fed *Arabidopsis* cells many proteins are phosphorylated and bound to 14-3-3 proteins, whereas in response to sugar starvation the 14-3-3 binding partners are subjected to selective proteolytic degradation [213]. The identity of protease involved is still a question, but it can be inhibited by MG132, a cysteine protease inhibitor of 26S proteasome, and cannot be inhibited by PMSF, a serine protease inhibitor. Importantly, the corresponding protease can only cleave target proteins *in vitro* when they are free of 14-3-3 proteins. Phosphorylation and 14-3-3-binding completely protect the proteolytic substrates from degradation [214]. Another potential connection with SnRK1 kinases is the involvement of 14-3-3 proteins in the regulation of senescence. 14-3-3 protein overexpressing potato displays prolonged stay-green phenotype with delayed leaf senescence, whereas antisense 14-3-3 plants show early senescence [214]. Additionally, in a screen searching for *Arabidopsis* suppressors of yeast *grr1* mutation, the 14-3-3 protein AtGF14 was identified [208].

Many 14-3-3 binding partners are enzymes of carbon and nitrogen metabolism, for instance nitrate reductase (NR) [215], glutamine synthetase [216], sucrose phosphate synthase (SPS) [217], trehalose-6-phosphate synthase 1 (TPS1) [218] and 6-phosphofructo-2-kinase/fructose-2,6-bisphosphatase [219]. Phosphorylation of NR, SPS and HMGR by SnRK1 inhibits their activity in spinach and 14-3-3-binding of NR in response to darkness is also inhibitory [24]. In contrast, an *Arabidopsis* protein kinase, PKS5, inactivates a plasmamembrane H⁺-ATP-ase by preventing its interaction with a 14-3-3 protein [220]. Leaf NR is rapidly inhibited by phosphorylation and 14-3-3 binding in response to darkness. In addition, after a prolonged dark period NR is degraded. These results led to the assumption that 14-3-3-binding is a prerequisite for degradation. Furthermore, immunodepletion of 14-3-3 proteins from leaf extracts prevented NR degradation. Therefore, 14-3-3 proteins might play a role in targeting NR for proteolysis in the dark. However, other experiments provide evidence for the contrary mechanism, in which 14-3-3 binding would prevent the degradation of proteolytic substrates. Consistent with the latter scenario, the relative abundance of 14-3-3 proteins has been reported to decline gradually during prolonged darkness [214]. In conclusion, the function of 14-3-3 proteins is not completely understood, but their conserved roles in the control proteasomal degradation and their connection to SnRK1 kinases supports the model that SnRK1 kinases are components of the sugar-dependent proteasomal degradation machinery.

1.8. AIMS OF THE PRESENT WORK

The yeast AMPK kinase, Snf1, plays a widely conserved role in cell signaling. Plant orthologs of yeast Snf1 represented by the class I SnRK1 kinases have been so far characterized concerning their roles in the regulation of activity and stability of key metabolic enzymes. Therefore, major aim of the present work was to obtain information about the roles of SnRK1 kinases in cell signaling.

The project was based on former yeast two-hybrid and *in vivo* studies of interactions of *Arabidopsis* SnRK1 kinases with the proteasome and the conserved common ASK1/SKP1 component of SCF-type E3 ubiquitin ligase complexes. These results provided the first data about the presence of SnRK1 kinases in proteasomal complexes. However, the number of proteasome containing complexes is very high because of the associated variable ubiquitin ligases are represented by 694 different substrate receptor F-box proteins in *Arabidopsis*. Therefore, one aim of the project was to determine, whether the presence of SnRK1 kinases in proteasomal-SCF complexes is general or restricted to some specific complexes. This part of the work was supported by a grant of the German National Science Foundation (DFG Ko1438/3-3) for two years. The project employed epitope-tagging and subsequent immunoaffinity chromatography of proteasomal substrates and F-box proteins but failed to produce sufficient resolution of SnRK1-SCF-proteasome complexes by mass spectrometry. In contrast to yeast and mammal cells, intensive proteolytic degradation in plant tissues and low level production of affinity tagged proteins proved to be serious technical obstacles.

In parallel with the biochemical approach, genetic analysis of T-DNA insertion mutations in genes encoding SnRK1 kinase subunits was performed to obtain information on possible regulatory roles of SnRK1 kinases in the plant signaling web. This approach is described in the present thesis. Other approaches, such as transcript profiling of SnRK1 α overexpressing plants and characterization of *Arabidopsis* SnRK1 $\beta\gamma$ subunit involved other members of our laboratory. To identify and characterize candidate SnRK1 substrate, this work was largely devoted to study the phosphorylation of transcription factors and other proteins by the purified SnRK1 kinase AKIN10. Major aims of the PhD thesis work were

- Isolation and characterization of SnRK1 α and SnRK1 β subunit T-DNA insertion mutants in *Arabidopsis*, in order to gain information about the role of SnRK1 kinases in cell signaling
- Improvement of protein purification strategy to increase protein complex stability and yield
- Study of subcellular localization of individual SnRK1 β subunits, in order to identify nuclear components of SnRK1 kinases
- Identification of candidate SnRK1 substrates
- Localization and mutagenesis of phosphorylation sites in SnRK1 substrates
- Verification of *in vitro* SnRK1-substrate interactions *in vivo*
- Characterization of upstream SnRK1-activating kinases in order to get information about the signals that activate SnRK1 kinases.

2. MATERIALS AND METHODS

2.1. MATERIALS

2.1.1. Chemicals and laboratory supplies

2.1.1.1. *General chemicals*

Beckman Instruments Inc., Palo Alto, USA	Centrifuge tubes
Biomol GmbH, Hamburg, Germany	MG132
BIO-RAD, München, Germany	Bradford Reagent
	Precision Plus, pre-stained molecular weight standard for protein electrophoresis
	Polypeptide SDS-PAGE Molecular Weight Standard
	Cat. No. 161-0326
Calbiochem Corp., Darmstadt, Germany	Miraclloth
Cambrex Bio Science Inc., Rockland, USA	Seakem LE Agarose
Corning Inc., Corning, USA	Costar, Disposable Serological Pipettes
Eppendorf AG, Hamburg, Germany	Safe-lock microcentrifuge tubes (0.5, 1.5 and 2.0 ml)
Invitrogen GmbH, Karlsruhe, Germany	1kb molecular mass marker for agarose electrophoresis
	Tris-HCl, ultrapure
Grenier bio-one GmbH Kermsmünster, Austria	Petri dishes
	Falcon tubes (15 and 50ml)
Heirler Cenovis GmbH, Radolfzell, Germany	milk powder
Lehle Seeds, Round Rock, TX, USA	Vac-in-stuff, Silwet L-77
Merck, Darmstadt, Germany	General chemicals:
	ethanol, methanol, 2-propanol, acetone, chloroform, glycine, N,N dimethylformamide, acetic acid, Na-acetate, NaCl, NaOH, MgCl ₂ , NaH ₂ PO ₄ , Na ₂ HPO ₄ , NaF, TCA, Isoamyl alcohol, EDTA (TitriplexIII),
Metabion International AG, Martinsried, Germany	oligonucleotides
Millipore, Badford, USA	Nitrocellulose filter VSWP 0.025µm
	Sterivex filter units
	Immobilon-P (PVDF membrane for immunoblot)
	Glass vacuum filter set
Peqlab Biotechnologie GmbH, Erlangen, Germany	E.Z.N.A. plasmid miniprep kit I.
Riedel da Haen, Seelze, Germany	Ca-hypochlorite
Roche Diagnostics GmbH, Mannheim, Germany	anti HA antibody
	anti c-Myc antibody
Carl Roth GmbH, Karlsruhe, Germany	dNTP solutions
	preequilibrated phenol (Rotiphenol)
	Acrylamide mix, Rotiphorese 40, 29:1
	Alufoil, 30µm thick

	IPTG
Sartorius AG, Göttingen, Germany	Minisart, 0.22µm and 0.45µm filter units
Serva Electrophoresis GmbH, Heidelberg, Germany	Bromophenol Blue – Na Salt Visking® dialysis tubes, 6mm diameter Dodecyl sulphate, Na-salt (SDS) Ponceau S solution
Whatman, Maidstone, USA	3MM paper
Sigma-Aldrich	General chemicals: abscisic acid, D-glucose, TEMED, EtBr, Sucrose, APS, CNBr, 2-estradiol, 2-mercaptoethanol, DTT, ATP, PMSF, tricine, Na ₃ VO ₄ , CTAB, Triton X-100, Tween-20 Protease inhibitor cocktail for plant cells (Cat.No.P9599)
Fluka Biochemika	TFA
GE Healthcare	ECL Detection Reagent, chemiluminescence kit disposable chromatographic columns (PD-10 column)
Starlab GmbH, Ahrensburg, Germany	disposable pipette tips, TipOne
Thermo, Electron Corporation, Milford, MA, USA	electroporation cuvette, 2mm diameter

2.1.1.2. *Enzymes*

Boehringer Mannheim, Germany	RNaseA Calf Intestinal Phosphatase
New England Biolabs, Frankfurt am Main, Germany	Restriction endonucleases T4 DNA ligase T4 DNA polymerase Antarctic Phosphatase
Takara Bio Inc., Otsu, Shiga, Japan	TaKaRa LA Taq DNA polymerase
Invitrogen GmbH, Karlsruhe, Germany	Taq DNA polymerase, recombinant
Roche Diagnostics GmbH, Mannheim, Germany	Endoproteinase Arg-C Sequencing Grade
Worthington	DNase

2.1.1.3. *Culture media and hormones*

Duchefa, Haarlem, the Netherlands	Phytoagar
BD Biosciences, Franklin lakes, NJ, USA	Bacto® Yeast Extract (Ref. No. 212750) BBL™ Beef Extract (Ref. No. 212303) Bacto® Peptone (Ref. No. 211677) BD Difco Beef extract
Carl Roth GmbH, Karlsruhe, Germany	Trypton / peptone (from casein pancreatically digested)
Invitrogen GmbH, Karlsruhe, Germany	Select Agar
Sigma-Aldrich	Murashige & Skoog Medium basal salt mixture (MS) Murashige & Skoog Medium basal salt with minimal

	organics (MSMO) (Plant cell culture tested) (M6899)
	2,4 dichlorophenoxy acetic acid
	α Naphtaleneacetic Acid
	Nicotinic acid
	Pyridoxin HCl
	Thiamine HCl
	Myo-inositol

2.1.1.4. *Antibiotics*

Sigma-Aldrich	Ampicillin
	Carbenicillin
	Kanamycin
	Tetracyclin
	Spectinomycin
	Chloramphenicol
	Streptomycin
	Sulphadiazine
	Rifampicin
	Gentamycin
Roche Diagnostics GmbH, Mannheim, Germany	Hygromycin B
Duchefa Biochemie, Haarlem, the Netherlands	Cefotaxime sodium (Claforan)
	Ticarcillin disodium mixture 15:1 & Potassium Clavulanate

2.1.1.5. *Chromatography resins*

Glutathion Sepharose 4B (GE Healthcare)
 Ni-NTA resin (Qiagen)
 Amylose resin (New England Biolabs)
 StrepII-tactin sepharose (IBA)
 Sephadex G-25, G-50 (GE Healthcare)
 HiTrapDEAE FF 1ml IEX column (GE Healthcare)
 Talon resin (Clontech)

2.1.1.6. *Antibodies*

2.1.1.6.1. Primary antibodies

Anti-HA Rat monoclonal antibody (clone 3F10) against a peptide derived from influenza haemagglutinin peptide (Roche). Dilution 1:1000
 Anti-c-Myc Mouse monoclonal antibody raised against a peptide from human c-Myc protein (Roche). Dilution 1:1000

2.1.1.6.2. Secondary antibodies

Goat anti-rat heavy plus light chains, horseradish peroxidase conjugate, dilution 1:5000 (Sigma, A9037)
 Goat anti mouse heavy plus light chains, horseradish peroxidase conjugate, dilution 1:10000 (Pierce 31430)

2.1.1.7. *Radiochemicals*

γ ³²P-ATP (GE Healthcare)

2.1.2. Bacterial strains

2.1.2.1. *E. coli* strains

DH10b (Invitrogen)

(*E. coli* F⁻ *mcrA*Δ(*mrr-hsdRMS-mcrBC*)Φ80*lacZ*ΔM15Δ*lacX74recA1endA1araD139*Δ(*ara, leu*)7697*galUgalKλrpsLnupG*)

BL21(DE3)pLysS (Novagen)

(*E. coli* B F⁻ *dcm ompT hsdS*(r_B⁻ m_B⁻)*galλ*(DE3)[pLysS Cam^r])

BMH 71-18 *mutS* (BD Biosciences)

(*E. coli thi supE* Δ(*lac-proAB*) [*mutS*::Tn10][F' *proAB, lacI^q* ZΔM15])

S17.1

(*E. coli* 294::RP4-2 (Tc::Mu) (Km::Tn7))

2.1.2.2. *Agrobacterium* strains

Agrobacterium tumefaciens GV3101 (pMP90)

C58C1, rif, pMP90 (pTiC58ΔT-DNA), Gm^r [221]

Agrobacterium tumefaciens GV3101 (pMP90RK)

C58C1, rif, pMP90RK (pTiC58ΔT-DNA), Gm^r, Km^r [221]

2.1.3. Plasmid vectors and constructs

2.1.3.1. Plasmid vectors

vector	drug resistance in bacteria	drug resistance in plants	reference
pER8 XVE	Sp50, Hyg50	Hyg15	Zuo et al, 2000 [222]
pPCV002	Amp100, (Cb100)	Km50	Koncz et al 1994 [223]
pPCV812	Amp100, (Cb100), Hyg50	Hyg15	Koncz et al 1994 [223]
pPILY	Amp100, (Cb100)	-	Ferrando et al 2000 [224]
pMENCHU	Amp100, (Cb100)	-	Ferrando et al 2000 [224]
pLOLA	Amp100, (Cb100)	-	Ferrando et al 2000 [224]
pGEM-T	Amp100, (Cb100)	-	Promega
pGEX-5X-1	Ap100, (Cb100)	-	GE Healthcare
pMAL-c	Ap100, (Cb100)	-	New England Biolabs
pET201	Ap100, (Cb100)	-	-

pET201 is an unpublished vector similar to pET32 (Novagen). It is a thioredoxin-His₆ double tagging bacterial expression vector, Amp^R, IPTG inducible, driven by T7 promoter.

2.1.3.2. Plasmid constructs

2.1.3.2.1. Formerly published constructs

PRL1-pMAL-c2 [59]

AKIN10 pGEX-5X-1 [59]

AKIN11 pGEX-5X-1 [59]

2.1.3.2.2. *Newly prepared vectors and constructs*

AKIN β 1-pGFP	GST-EBF1 in pGEX-5X-1
AKIN β 2-pGFP	TRX-EBF2-His in pET201
AKIN β 3-pGFP	GST-EBF2 in pGEX-5X-1
AKIN β 1-pPCV812	TRX-FKF1-His in pET201
AKIN β 2-pPCV812	GST-FKF1 in pGEX-5X-1
AKIN β 3-pPCV812	GST-ZTL in pGEX-5X-1
p3xtag vector	TRX-AKIN β 1-His in pET201
TRX-AKIN11-PIPL	TRX-AKIN β 2-His in pET201
AKIN10-p3xtag	TRX-AKIN β 3-His pET201
AKIN10 3x in pER8 binary vector	TRX-AKIN β γ -His in pET201
AKIN11-p3xtag	GST-AKIN β γ in pGEX-5X-1
AKIN11 3x in pER8 binary vector	TRX-TLK1-His in pET201
AKIN β 1-p3xtag	TRX-TLK2-His in pET201
AKIN β 1 3x in pPCV002 binary vector	TRX-AKIN10_280aa-His in pET201
AKIN β 2-p3xtag	TRX-AKIN10_T175D_280aa-His in pET201
AKIN β 2 3x in pPCV002 binary vector	TRX-AKIN10_340aa-His in pET201
AKIN β 3-p3xtag	TRX-AKIN10 T175D_340aa-His in pET201
AKIN β 3 3x in pPCV002 binary vector	IAA6 HA-pPILY
GST-AKIN10-His in pGEX-5X-1	IAA6 S39A HA-pPILY
GST-AKIN11-His in pGEX-5X-1	IAA6 S39E HA-pPILY
TRX-AKIN10-His in pET201	IAA6 HA-pPCV002
TRX-AKIN11-His pET201	IAA6 S39A HA-pPCV002
TRX-AKIN10 T175D -His in pET201	IAA6 S39E HA-pPCV002
TRX-AKIN11 T176D-His in pET201	pUPRX vector
TRX-AKIN10 K48R-His in pET201	IAA6-HA in pMenchu(Sall-)
TRX-AKIN11 K49R-His in pET201	IAA6-HA in pUPRX
TRX-ABI5-His in pET201	IAA6-HA UPRX in pPCV002
TRX-DPBF4-His in pET201	IAA7-HA in pMenchu(Sall-)
TRX-ABI4-His in pET201	IAA7-HA in pUPRX
TRX-EIN3-His in pET201	IAA7-HA UPRX in pPCV002
GST- EIN3 in pGEX-5X-1	ABI5-HA in pMenchu(Sall-)
MBP-EIN3-His in pMAL-c2	ABI5-HA in pUPRX
TRX-CYCD1-His in pET201	ABI5-HA UPRX in pPCV002
TRX-CYCD2-His in pET201	EIN3-HA in pMenchu(Sall-)
TRX-CYCD3;1-His in pET201	EIN3-HA in pUPRX
TRX-CYCD3;3-His in pET201	EIN3-HA UPRX in pPCV002
TRX-IAA3-His in pET201	TIR1-HA in pMenchu(Sall-)
TRX-IAA6-His in pET201	TIR1-HA in pUPRX
TRX-IAA6 S39A-His in pET201	TIR1-HA UPRX in pPCV002
TRX-IAA6 S39E-His in pET201	EBF1-HA in pMenchu(Sall-)
TRX-IAA7-His in pET201	EBF1-HA in pUPRX
TRX-CO-His in pET201	EBF1-HA UPRX in pPCV002
TRX-CDF1-His in pET201	EBF2-HA in pMenchu(Sall-)
TRX-HY5-His in pET201	EBF2-HA pUPRX
TRX-TIR1-His in pET201	EBF2-HA UPRX in pPCV002
TRX-EBF1-His in pET201	

2.1.4. Plant material

2.1.4.1. *Arabidopsis thaliana* wild type and mutant lines

wild type: Col-0 ecotype	AKIN β 1 SALK 008325	AKIN β 2 Koncz 87453
AKIN10 GABI 579E09	AKIN β 1 Koncz 66465	SnAK1 SALK 000044
AKIN β 1 SALK 235B06	AKIN β 1 Koncz 14344	SnAK1 SALK 015230
AKIN β 1 SAIL 40A07	AKIN β 2 SALK 037416	SnAK2 SALK 142938

2.1.4.2. *Arabidopsis* cell suspension cultures

All constructs were transformed into *Arabidopsis* plants, dark and green cell suspension cultures.

35S-AKIN β 1-GFP in pPCV812 (Hyg)
 35S-AKIN β 2-GFP in pPCV812 (Hyg)
 35S-AKIN β 3-GFP in pPCV812 (Hyg)
 35S-AKIN β 1-PIPL-Strep-HA in pPCV002 (Km)
 35S-AKIN β 2-PIPL-Strep-HA in pPCV002 (Km)
 35S-AKIN β 3-PIPL-Strep-HA in pPCV002 (Km)
 estradiol inducible AKIN10-PIPL-Strep-HA in pER8 (Hyg)
 estradiol inducible AKIN11-PIPL-Strep-HA in pER8 (Hyg)
 35S-IAA6wt-HA in pPCV002 (Km)
 35S-IAA6S39E-HA in pPCV002 (Km)
 IAA6-UBRX in pPCV002 (Km)
 IAA7-UBRX in pPCV002 (Km)
 TIR1-UBRX in pPCV002 (Km)
 EIN3-UBRX in pPCV002 (Km)
 EBF1-UBRX in pPCV002 (Km)
 EBF2-UBRX in pPCV002 (Km)
 ABI5-UBRX in pPCV002 (Km)

2.1.5. *Arabidopsis* cDNA libraries

To obtain cDNA clones of plant genes, I have used several *Arabidopsis* cDNA libraries prepared from different starting materials: e.g., *Arabidopsis* suspension cultures, *Arabidopsis* roots, rosette leaves and stems; seedling and flowers. These libraries were either provided by other laboratories or prepared by in our group by former lab members. One frequently used library was prepared by Klaus Salchert in 1997, where the cDNA products were cloned in fusion with the Gal4-DNA activation domain (GAD), using EcoRI (5') and XhoI (3') adaptors, in the plasmid pACT2 [225].

2.1.6. Oligonucleotides

2.1.6.1. Oligonucleotides for cloning

GFPfwd	5'-CGCCCATGGGTAAAGGAGAAGAAC-3'
GFPrev	5'-CGCGGATCCTTATTTGTATAGTTCATCCATG-3'
AKIN β 1GFPfwd	5'-CCGCCATGGGAAATGCGAACGGC-3'
AKIN β 1GFPrev	5'-GGGCCATGGGCCGTGTGAGCGGTTTGTAGAG-3'
AKIN β 2GFPfwd	5'-GGGCCATGGGTAACGTGAACGCGAGAG-3'
AKIN β 2GFPrev	5'-GGCCATGGTCCTCTGCAGGGATTTGTAGAG-3'
AKIN β 3GFPfwd	5'-GCGCCATGGCGATGAACAGTCAAAATCCTGATG-3'
AKIN β 3GFPrev	5'-CGCCCATGGGAACATTGGCGCTCCCTCTTC-3'
Piplfwd	5'-CCCGAATTCGGTCATGATGATCATCACC-3'
Piplrev	5'-GGCGAATTCTCAGTCATGGGTGTGATCATGAG-3'
3xtagfwd	5'-CGAAGCTTATGGTCGACAGATCTAGAGGTCATGATGATCATCACCATG-3'
3xtagrev	5'-GCGGATCCTTTTTCGAACTGCGGGTGGCTCCAGTCATGGGTGTGATCA TGAGAATG-3'
A10_3xfwd	5'-GGGGTCGACATGGATGGATCAGGCACAGGC-3'
A10_3xrev	5'-CCTCTAGAGAGGACTCGGAGCTGAGCAAG-3'
A11_3xfwd	5'-GGGGTCGACATGGATCATTTCATCAAATAGATTTG-3'
A11_3xrev	5'-GGAGATCTGATCACACGAAGCTCTGTAAG-3'
AKIN β 1_3xtag_fwd	5'-GGGGTCGACATGGGAAATGCGAACGGCAAAGAC-3'
AKIN β 1_3xtag_rev	5'-GGGTCTAGACCGTGTGAGCGGTTTGTAGAGGAC-3'
AKIN β 2_3xtag_fwd	5'-GGGGTCGACATGGGTAACGTGAACGCGAGAG-3'

IAA6_fwd_Pily	5'-GCGGGCCATGGCAAAGGAAGGTCTAG-3'
IAA6_rev_Pily	5'-GCGCGAGATCTATCTTGCTGGAGACCAAAAC-3'
IAA6_UBR_fwd	5'-GCGCGCCATGGGTCGACCTTACATCTTGTCTTAAGACTTAGAGGTGGTATG- GCAAAGGAAGGTCTAG-3'
IAA6_UBR_rev	5'-GCGCGAGATCTATCTTGCTGGAGACCAAAACC-3'
IAA7_UBR_fwd	5'-GCGCGAAGCTTGTGCGACCTTACATCTTGTCTTAAGACTTAGAGGTGGTATG- ATCGGCCAACTTATGAAC-3'
IAA7_UBR_rev	5'-GCGCGAGATCTGTTCTTGCAGTACTTC-3'
ABI5_UBR_fwd	5'-GGCCGGGATCCGTCGACCTTACATCTTGTCTTAAGACTTAGAGGTGGTATG- GTAAGTAGAGAAACGAAGTTG-3'
ABI5_UBR_rev	5'-GCGCGGATCCGAGTGGACAACCTCGGGTTCCTC-3'
EIN3_UBR_fwd	5'-GCGCGCCCATGGGTCGACCTTACATCTTGTCTTAAGACTTAGAGGTGGTATG- ATGTTTAATGAGATGGGAATG--3'
EIN3_UBR_rev	5'-GGCGGGGATCCGAACCATATGGATACATCTTG-3'
TIR1_UBR_fwd	5'-GCGCGAGATCTGTCGACCTTACATCTTGTCTTAAGACTTAGAGGTGGTATG- CAGAAGCGAATAGCCTTG--3'
TIR1_UBR_rev	5'-GCGCGAGATCTTAATCCGTTAGTAGTAATGATTTGC-3'
EBF1_UBR_fwd	5'-GGCCGCCATGGGTCGACCTTACATCTTGTCTTAAGACTTAGAGGTGGTATG- TCTATCTTTAGTTTTG-3'
EBF1_UBR_rev	5'-GGCGGGGATCCGGAGAGGATGTCACATTTG-3'
EBF2_UBR_fwd	5'-GGCCGCCATGGGTCGACCTTACATCTTGTCTTAAGACTTAGAGGTGGTATG- TCTGGAATCTTCCAGATTTAG-3'
EBF2_UBR_rev	5'-GGCGGGGATCCGTAGAGTATATCGCACCTC-3'

2.1.6.2. *Oligonucleotides for sequencing*

pETF	5'-TAATACGACTCACTATAGG-3'
pETR	5'-CTAGTTATTGCTCAGCGG-3'
35S promoter primer	5'-TCCTTCGCAAGACCCTTCTCTAT-3'
nosT(R)	5'-GCAAGACCGCAACAGGATT-3'
GEX5	5'-GGGCTGGCAAGCCACGTTTGGTG-3'
GEX3	5'-CCGGGAGCTGCATGTGTACAGAGG-3'
AKIN10midrev (559-539bp in AKIN10)	5'-CTGGAGCGGCATAATTTGGAC-3'
AKIN10midfwd (409-429bp in AKIN10)	5'-AACATGGTGTTCACAGAGAC-3'
AKIN10endfwd (1078-1102bp in AKIN10)	5'-GAAAGCGTTGCTTCACCTGTTAGC-3'
AKIN11midrev (559-539bp in AKIN11)	5'-CGGGAGCAGCGTAGTTGGGGC-3'
AKIN11midfwd (417-437bp in AKIN11)	5'-TGTCCATAGAGACCTGAAGCC-3'
AKIN11endfwd (951-974bp in AKIN11)	5'-CAACAGAACACAAAACGATGCTAC-3'

2.1.6.3. *Oligonucleotides for site-directed mutagenesis*

AKIN10 T175D	Pho5'---GATGGTCATTTTTGAAG GAC AGTTGTGGAAGTCCAAATT---3'
AKIN10 K48R	Pho5'---GGACATAAGGTTGCTATC CGG ATCCTCAATCGTCGCAAAATC ---3'
AKIN11 T176D	Pho5'---GATGGTCATTTCTAAAG GAC AGTTGTGGAAGCCCCAAC---3'
AKIN11 K49R	Pho5'---GGCATAAGGTTGCTATC CGA ATCCTTAATCGTCGTAAG ---3'
IAA6 S39A	Pho5'---AAGAAGAAGAGGGTGCTC GCT GATATGATGACCTCATCAG---3'
IAA6 S39E	Pho5'---AAGAAGAAGAGGGTGCTC GAG GATATGATGACCTCATCA---3'
pET201 AfeI-	Pho5'---CTCAGGTCAATGCCA GAG CTTCGTTAATACAGATG---3'

2.1.6.4. *Oligonucleotides for T-DNA insertion mutant screens and RT-PCR*

2.1.6.4.1. *screening primers*

AKIN10 5'	5'-TCATTTCTGAATCGGGTACGAGAGAT-3'
AKIN10 3'	5'-CAGGCGACGACACGAAGCGAGTTT-3'
AKINbeta1 5'	5'-GACCATCTCTATTCTAACCCACC-3'
AKINbeta1 3'	5'-GGTTACCGTGTGAGCGGTTTGTAG-3'

AKINbeta2 5'	5'-GAAGCTTCAGATCACGACTTGTTC-3'
AKINbeta2 3'	5'-ATCACGGGCTCAGCAGGTTGGTTCAG-3'
AKINbeta3 5'	5'-AGTCTGAGAAGCATAGACAAGGAGTGAAG-3'
AKINbeta3 3'	5'-TACAAACAAACAATGCCACGTCTATCAGC-3'
SnAK1 5'	5'-TTGAAGCCCTCGAAACCCCTTTTATC-3'
SnAK1 3'	5'-AGCTATGGTCTCCTGGACGCACACAA-3'
SnAK2 5'	5'-CATTTCTTCTCATGTGCCATGGATATTG-3'
SnAK2 3'	5'-TTGGAGTTGATTTTGGCCGTTTTACCC-3'
SALK LB	5'-TTTGGGTGATGGTTCACGTAGTGGG-3'
FISH1	5'-CTGGGAATGGCGAAATCAAGGCATC-3'
FISH2	5'-CAGTCATAGCCGAATAGCCTCTCCA-3'
GABI RB	5'-TTCCATTGCCAGCTATCTGTAC-3'

2.1.6.4.2. RT-PCR primers

AKINβ1 5' RTPCR:	5'-GGTAGCGGTGGTGCAGATGTTACCTC-3'
AKINβ1 3' RTPCR:	5'-GTGGCACTGAATTTTAGGGTTACCGTGT-3'
AKINβ2 5' RTPCR:	5'-GCTGAGATTTGTTCTCCTCGTGAAGCTATGT-3'
AKINβ2 3' RTPCR:	5'-GAATTGCATCATCTTCACTCACCTCTGC-3'
FISH1 (LB)	5'-CTGGGAATGGCGAAATCAAGGCATC-3'
FISH2 (RB)	5'-CAGTCATAGCCGAATAGCCTCTCCA-3'
tubulin fwd (At5g62690)	5'-AGGAACTGGATCTGGTATGGGAACAT-3'
tubulin rev	5'-GTCACACCAGACATAGTAGCAGAAATCAAG-3'

2.2. GROWTH MEDIA AND STOCK SOLUTIONS

2.2.1. Stock solutions

2.2.1.1. Antibiotics

Antibiotics	Stock solution mg/ml	Working concentration µg/ml
Ampicillin	50 in water	100
Carbenicillin	50 in water	100
Kanamycin	100 in water	25 (for <i>Arabidopsis</i> 50-100)
Tetracyclin	15 in 50% ethanol, light sensitive	25-50
Spectinomycin	50 in water	50 (in <i>Agrobacterium</i> 100)
Chloramphenicol	25 in ethanol	25
Streptomycin	50 in water	50
Hygromycin B	15 in water	15 (for <i>E.coli</i> 50)
Sulphadiazine	7,5 in water	15
Cefotaxime sodium (Claforan)	200 in water	200
Ticarcillin disodium mixture 15:1 & Potassium Clavulanate	150 in water	150
Rifampicin	25 in methanol	100 <i>Agrobacterium</i>
Gentamycin	25 in water	25 <i>Agrobacterium</i>

Antibiotics stock solutions were sterilized by filtration through Millipore filters of 22µm pore size.

2.2.1.2. Plant hormones

All hormone solutions were filter sterilized and stored at -20°C.

Hormone	Solvent	Stock
abscisic acid (ABA)		1mg/ml in methanol
1-naphtyl-acetic acid (NAA)	1N KOH	1mg/ml in water
2,4 dichlorophenoxy acetic acid (2,4D)		2mg/ml in ethanol
kinetin	1N NaOH	1mg/ml in water

2.2.1.3. *Protease inhibitors*

Material	Stock	Working concentration
PMSF	200mM in ethanol	1mM (half life time in water is approximately 30 min)
leupeptin	1mg/ml in water	5 μ g/ μ l
aprotinin	1mg/ml in water	1 μ g/ μ l
benzamidine hydrochloride	50mM in water	1mM
pepstatin	1mg/ml in water	1 μ g/ μ l

2.2.1.4. *Other stock solutions*

Material	Stock	Working concentration
β -estradiol	10mM in DMSO	5-20 μ M
MG-132	50mM in DMSO	20-50 μ M
IPTG	1M in water	1mM
NaF phosphatase inhibitor	2M	50 mM
Na ₃ VO ₄ phosphatase inhibitor	200mM	0,2 mM
EtBr	10mg/ml in water	250 μ g/l

2.2.2. Culture media

2.2.2.1. *LB medium*

(Luria-Bertani medium)

Bacto-tryptone	10g
Bacto-yeast extract	5g
NaCl	10g
	1 liter

The components are dissolved by stirring and the pH is adjusted to 7.2 with 5N NaOH (approx. 0.2 ml). Upon adjusting the volume to 1 liter with distilled water, the medium is autoclaved for 20 minutes. If desired, solidified medium is prepared by adding 6.4g of agar powder before autoclaving. Antibiotics are added after sterilization, when the temperature of the medium decreases to approximately 50°C.

2.2.2.2. *YEB medium*

Beef extract	5g
Yeast extract	1g
Peptone	5g
Sucrose	5g

1 liter

The pH is adjusted to 7.2, and add 18 g bacto-agar is added optionally for solidified medium. The medium is autoclaved for 20 minutes. After autoclaving the YEB medium is supplemented with filter-sterilized $MgCl_2$ to a final concentration of 1.4 mM. (Stock solution of $MgCl_2$ is 2M.)

2.2.2.3. *Culture medium for root-derived dark grown Arabidopsis cell suspension culture*

- 4.3g/l MS basal salt mixture
- 30g/l sucrose (87 mM final concentration, isotonic to 90mM sorbitol (18g/l). If desired isotonic low sugar medium is prepared with 5g sucrose (14.5mM) plus 14.5g sorbitol (72.5mM) for 1l medium
- 4 ml/l 100x stock B5 vitamin (filter-sterilize and store at 4°C):
 - Nicotinic acid 1mg/ml
 - Pyridoxin HCl 1mg/ml
 - Thiamine HCl 10mg/ml
 - Myo-inositol 100mg/ml

After adjusting the pH to 5.8 with 0.5M KOH the medium is sterilized by autoclaving for 20 min. Sterile stock solution of 2,4D is added to final concentration of 1mg/l. (Stock 2mg/ml dissolved in 0.5M KOH and adjusted to pH 6-7 with HCl, filter sterilized and stored at 4°C.)

2.2.2.4. *Culture medium for leaf-derived light-grown green (photosynthetic) Arabidopsis cell suspension culture*

- 4.4g/l MSMO (Sigma M6899)
- 30g/l sucrose

The pH is adjusted to 5.7 with 0.5M KOH. The medium is sterilized by autoclaving for 20 min and after cooling it down to room temperature supplemented with hormones: α Naphthaleneacetic acid to 0.5mg/l and kinetin 0.1mg/l final concentrations.

2.2.2.5. *Culture medium for Arabidopsis seedlings*

<u>MSAR medium</u> [223]:	Macroelements 25.0 ml/l
	Microelements 1.0 ml/l
	Fe-EDTA 5.0 ml/l
	$CaCl_2 \cdot 2H_2O$ 5.8 ml/l
	KI 2.2 ml/l
	B5 vitamin 2.0 ml/l
	sucrose 5g/l

pH is adjusted to 5.8 with 1M KOH and 0.6 g/l phytoagar is added

Macroelements: 20g/l NH_4NO_3 , 40 g/l KNO_3 , 7.4 g/l $MgSO_4 \cdot 7H_2O$, 3.4 g/l KH_2PO_4 ,
2 g/l $Ca(H_2PO_4)_2 \cdot H_2O$

Microelements: 6.2g/l H_3BO_4 , 16.9 g/l $MnSO_4 \cdot 4H_2O$, 8.6 g/l $ZnSO_4 \cdot 7H_2O$,
0.25 g/l $Na_2MoO_4 \cdot 2H_2O$, 0.025 mg/l $CuSO_4 \cdot 5H_2O$,

0.025 mg/l $\text{CoCl}_2 \cdot 6\text{H}_2\text{O}$

Fe- Na_2 -EDTA: 5.56 g/l $\text{FeSO}_4 \cdot 7\text{H}_2\text{O}$, 7.46 g/l Na_2 -EDTA $\cdot 2\text{H}_2\text{O}$

KI: 375 g/l KI

CaCl_2 : 75 g/l $\text{CaCl}_2 \cdot 2\text{H}_2\text{O}$

2.3. METHODS

2.3.1. DNA methods

2.3.1.1. *Precipitation of DNA with ethanol or isopropanol*

DNA is precipitated in the presence of 0.3M final concentration of sodium acetate (pH 6.0) with either 1 volume isopropanol for 30 min at room temperature or on ice, or with 2 volume ethanol for at least 20 minutes at -20°C and then collected by centrifugation at 14000rpm in a benchtop centrifuge. The DNA pellet is washed two times with 400 μl 70% ethanol and finally with 200 μl absolute ethanol. The pellet is dried in vacuum desiccator and dissolved in sterile distilled water.

2.3.1.2. *Plasmid DNA miniprep (Alkaline lysis method)*

(Sambrook et al 1989 [226], modified):

- Harvest 1.5ml of overnight grown bacterial culture by centrifugation at 8000rpm in a tabletop centrifuge.
- Resuspend the bacterial pellet in 200 μl **Solution I**
- Add 200 μl **Solution II**. Mix the contents gently by inverting the tube many times.
- Add 200 μl **Solution III**. Mix the contents gently, precipitation of protein occurs.
- Centrifuge at 13000 rpm for 10 minutes in a tabletop centrifuge at room temperature
- Decant the supernatant into a new tube.
- Add 1 vol isopropanol or 1ml ethanol and mix gently. (Optional: for a compact pellet place the tube for 20 minutes to -20°C , otherwise the precipitate might spread on the inner wall of the microcentrifuge tube.)
- Centrifuge at 13000 rpm for 10 minutes preferentially at 4°C .
- Wash the pellet two times with 400 μl 70% ethanol and finally with 200 μl absolute ethanol.
- Dry the pellet at 37°C .
- Dissolve the pellet in 50 μl redistilled water

Solution I: 50mM glucose, 25 mM Tris-HCl (pH 8.0), 10mM EDTA

Solution II: 0.2N NaOH (freshly diluted from a 10N stock), 1% SDS

Solution III: 3M sodium acetate pH 4.8 (Adjust pH with glacial acetic acid. The resulting solution will be 3M with respect to sodium and 5M with respect to acetate.).

2.3.1.3. *Peqlab E.Z.N.A. miniprep kit*

This kit was used only to extract plasmid DNA for sequencing, where higher quality is advisable. From 5ml well grown bacterial suspension, if eluted in 50µl water, 100µg/µl plasmid concentration is attainable.

2.3.1.4. *Plasmid DNA maxiprep by CsCl gradient ultracentrifugation*

(based on Sambrook et al, 1989 [226])

- Inoculate 1l or more LB medium with an overnight culture of E. coli containing the required plasmid DNA
- Incubate it in a shaker at 37°C for 16 hrs (reaching stationary phase of growth)
- Centrifuge bacteria in a Beckman centrifuge at 6000g for 6 min (250ml tubes)
- Suspend the pellet 30ml solution I (50mM glucose, 25mM Tris-Cl pH 8.0, 10mM EDTA pH 8.0)
- Add 60ml of freshly prepared solution II (0.2N NaOH, 1% SDS). Mix well but gently till full lysis of bacteria (5-10 min)
- Add 45ml of solution III (3M NaOAc pH 4.8) and incubate the solution for 30 min on ice. Invert the tube many times gently while precipitate forms
- Centrifuge in GSA rotor at 12000 rpm at 4°C for 20 min
- Filter the supernatant through Miracloth into a new Beckman tube
- Add 100ml of 2-propanol and mix gently. Keep the tubes on ice for 30min.
- Centrifuge at 12000 rpm in a GSA rotor for 20 min. The pellet contains the plasmid DNA
- Pour off the supernatant and wash the pellet with 70% ethanol then with abs. ethanol, and dry the pellet in vacuum (not completely because then it takes longer to dissolve it)
- Dissolve the pellet in 23.3ml THE buffer (50mM Tris.HCl, 20mM EDTA pH 8.0) and after it has dissolved add 24.00g CsCl
- Fill the DNA solution into a Quick-seal ultracentrifuge tube and add 600µl 10mg/ml EtBr solution, the fill up the tube with 1.00g/ml CsCl solution (approx. 8,5ml). Balance the tubes with accuracy
- Centrifuge at 45000rpm in a VTi55 rotor at 20°C for 14-16 hrs in a Beckman ultracentrifuge
- Take the DNA band in 5ml (visualised with 365nm UV light)
- Fill it in 5ml Quick-seal tube, balance the tubes and seal them, and then run at 55000rpm in a VTi65 rotor at 20°C for 4-6 hrs
- Collect the DNA band and transfer it to eppendorf tubes
- Remove EtBr by adding 300µl of isoamyl alcohol saturated with 20xSSC (do this step in the chemical hood), shake it and centrifuge in a tabletop centrifuge at 8000rpm for 1min. EtBr passes to the organic phase (upper layer). Repeat the extraction 4-5 times while the DNA solution becomes colorless
- Split the DNA solution into 300µl aliquots in eppendorf tubes and add to each 300µl sterile distilled water, 60µl 3M NaOAc pH 6.0, and 420µl (0.7volume) 2-propanol. Mix gently by inverting the tubes and precipitate the DNA for 1h at room temperature.
- Collect the DNA by centrifugation for 15min at 13000rpm in a benchtop centrifuge

- Wash the pellet with 70% ethanol then with abs. ethanol and dry
- Dissolve the DNA in 100-200µl sterile distilled water and measure OD at 260nm. (1 Abs equals to 50µg/ml DNA concentration)

2.3.1.5. *Restriction endonuclease digestion of DNA*

Generally, restriction endonucleases from the New England Biolabs company were used in combination with appropriate buffer sets. In a plasmid analysis reaction, the following components were used:

- 4µl plasmid DNA (as written above)
- 2µl buffer
- 2µl RNase
- 2µl BSA (if the enzyme requires for stability in solution)
- 10µl redistilled water
- 0.2µl restriction endonuclease

The reactions were incubated for 2 hours at 37°C, unless the enzyme required other special condition.

2.3.1.6. *Preparation of DNase free RNase*

Pancreatic RNase (RNase A) was dissolved at a concentration of 10mg/ml in 0.01M sodium acetate (pH 5.2) and heat treated at 100°C for 15 minutes. After cooling the solution slowly to room temperature the pH was adjusted by adding 0.1 volumes of 1M Tris-HCl (pH 7.4) and the RNase stock was dispense into aliquots and stored at -20°C.

2.3.1.7. *Phenol-chloroform purification of DNA samples*

The standard way to remove protein contaminations from nucleic acid samples is protein extraction with a mixture of phenol and chloroform, then in a second step with chloroform alone. The method takes advantage of the fact, that deproteinization is more efficient in the presence of two organic solvents instead of one alone. Although phenol denatures proteins very effectively, it does not completely inhibit RNase activity and is a solvent for RNA molecules that contain long poly(A) tracts. Both problems can be prevented by adding isoamyl-alcohol in a 25:24:1 ratio (phenol:chloroform:isoamyl-alcohol). Pure phenol is crystalline, which can dissolve about 8% water. Phenol is pre-equilibrated to pH 8.0 prior to use which prevents DNA losses (DNA tends to participate to the phenolic phase when using acidic phenol) and saturates phenol with water. Optionally 0.1% hydroxyquinoline can be added, which indicates oxidation by changing its color from yellow to reddish. Oxidation, which might lead to DNA damage, can be prevented by keeping phenol under a layer of 2mM β-mercapto-ethanol in Tris-HCl pH 8.5. During phenol extraction an equal volume of phenol:chloroform mixture is added to the sample and mixed thoroughly until an emulsion is formed. The sample is centrifuged in a tabletop microcentrifuge at 13000 rpm for 10 min. Normally the aqueous phase forms the upper layer, which is carefully removed by a micropipette, not disturbing the

potentially cloudy interphase, which might contain precipitated proteins. Discard the organic phase and the interphase. Repeat this extraction until no protein precipitate is visible in the interphase. After extraction is complete, the lingering amount of phenol is removed by extracting the sample with an equal amount of chloroform. Finally DNA is collected by alcohol precipitation.

2.3.1.8. *Polymerase chain reaction*

For amplification of DNA fragments recombinant Taq polymerase was used from Invitrogen.

Generally 32 PCR cycles were performed. The T_m value of oligonucleotide primers was calculated by the manufacturer, but normally the following rough calculation was used: $T_m = 4x(G+C)+2x(A+T)$.

Ingredients of the PCR reaction mixture for 100 μ l:

- 3 μ l 50mM MgCl
- 2 μ l 10mM (each) dNTP mixture
- 1 μ l template DNA
- 10 μ l buffer
- 5 μ l primer mix, 10 μ M each
- 1 μ l Taq polymerase
- 78 μ l distilled water

The reactions were carried out in 10-20 μ l for analysis and in 100 μ l for cloning a PCR fragment. The following program scheme was followed:

32x	[1. initial denaturation	95°C	5 min
		2. denaturation	95°C	30 sec
		3. primer annealing	T_m	30 sec
		4. chain extension	72°C	1min/kb DNA fragment length
		5. final extension	72°C	10min
		(6. storage	4-15°C)	

2.3.1.9. *Agarose electrophoresis of DNA*

The concentration of agarose gel varies depending on the size of DNA fragments, which should be separated. 1g/100ml agarose concentration was used for most fragments up to 5kb, whereas above 5kb 0.8g/100ml gel was poured. The measured amount of agarose powder was filled up with the necessary volume of 1xTAE buffer supplemented with 250 μ g/l ethidium bromide, and dissolved by warming in a microwave oven for a few minutes. The solution was allowed to cool down to approximately 50°C then poured into a tray formerly sealed by both ends by scotch tape and equipped by electrophoresis combs. The solidified gel was immersed into 1xTAE buffer in a gel tank (Horizon 11-14 GibcoBRL). The DNA samples were supplemented with 6x loading dye and pipetted into the gel wells. As a molecular size marker generally the 1kb DNA ladder from Invitrogen was used. For separation of DNA fragments 80V voltage was applied. DNA bands were visualized using a UV light transilluminator (TFX35M Gibco BRL) at 254nm except for the recovery of DNA bands for cloning

when the less destructive 365nm wavelength was used. Gel images were captured by an imaging system consisting of a Kodak DC-120 zoom digital camera and the Kodak Digital Science 1D V 3.0.2. software.

1xTAE buffer	50X stock solution
40mM Tris-acetate (pH 8.0)	242g Tris base
1mM EDTA	57.1 ml glacial acetic acid
	100ml of 0.5M EDTA
	Do not adjust pH

6x loading dye: 50% glycerol, 10mM Tris.HCl (pH 8.0), 1mM EDTA, 0,25% bromophenol blue

2.3.1.10. *Preparation of dialysis tube*

Unrolled dialysis tube was boiled in large volume of 1mM EDTA (pH 8.0) and 2% (w/v) sodium bicarbonate buffer for 10 minutes using a ballast (Erlenmeyer flask with water) to keep the tubes immersed. The liquid may become yellowish. Rinse the tubing thoroughly in distilled water and boil the tubes again for 10 minutes in 1mM EDTA. Allow the tubing to cool and then store it at 4°C. From this point onward handle the tubing with gloves. Before use wash it inside and out with distilled water.

2.3.1.11. *Recovery of DNA fragments from agarose gel*

Separate sufficient amount of DNA fragments on agarose gel (generally few micrograms). It is useful to bind more wells with scotch tape to create a large well, in which the DNA runs more dispersed what prevents trailing and overlapping. Visualize by ethidium bromide staining and exposure to 365nm UV light, which does minimal damage on DNA (in contrast to 254nm). Cut out the required DNA bands with a scalpel using minimum of gel size. Put the gel slice into a suitable sized dialysis tube with forceps, fill it sterile TAE buffer leaving no bubbles, close the ends with medical clips and place it to the agarose electrophoresis running chamber. Run until the band leaves the gel completely and reverse the current for 15 sec to release the DNA from the wall of dialysis tubing. (It can be checked with 365nm UV light without opening the tube.) The DNA solution is removed with a pipette and subjected to phenol-chloroform extraction and i-propanol or ethanol precipitation.

2.3.1.12. *Measurement of nucleic acid concentration ad purity*

DNA concentration is measured photometrically at OD₂₆₀ (1 unit equals to 50µg/ml double stranded DNA concentration or 40µg/ml RNA concentration). The OD₂₆₀/OD₂₈₀ ratio should be approximately 1.8 in pure nucleic acid samples.

2.3.1.13. *Dephosphorylation of DNA 5' ends*

Dephosphorylation prevents self-ligation of linear plasmid DNA vectors. The dephosphorylation is carried out using Antarctic Phosphatase from NEB following the manufacturer's instructions. I used 1µl of enzyme in 20µl reaction volume for 1h duration. The enzyme can be heat inactivated in contrast

to calf intestinal phosphatase, whose activity can be safely removed only by an additional phenol-chloroform purification step. After dephosphorylation, the DNA was concentrated by ethanol precipitation.

2.3.1.14. *Creating blunt ended DNA*

For creating blunt ended DNA fragments by 3' overhang removal or 3' recessed end filling I used T4 DNA polymerase (NEB) according to the protocol given in the manufacturer's catalog.

Reaction conditions:

1x NEBuffer 2

Supplemented with 100 μ M dNTPs

1 unit of T4 DNA polymerase per μ g DNA

1xBSA (provided by NEB)

Incubate at 12°C for 15 minutes

Stop reaction by adding EDTA to a final concentration of 10mM

Heat inactivation of enzyme by incubating at 75°C for 20 minutes

In addition to heat inactivation, I usually further purified the DNA fragment by phenol-chloroform extraction.

2.3.1.15. *Dialysis of DNA samples*

Dialysis of DNA may be necessary before electroporation of ligated DNA to eliminate salts. It is a good alternative of alcohol precipitation when a buffer exchange is needed (e.g. two subsequent restriction endonuclease digests). A Millipore nitrocellulose filter disk (type VSWP, pore size 0,025 μ m diameter 25mm) is placed on the surface of deionized water so that one side remain dry. The dialyzing DNA solution is pipetted on the upper face of the disk. The dialysis is complete in one hour then the solution can be removed with a pipette. In case the dialysis follows digestion with an endonuclease which cannot be inactivated by heat, the dialysis can be carried out at 4°C.

2.3.1.16. *Ligation of DNA ends*

For ligation NEB T4 DNA ligase was used with the supplied buffer. The buffer contains ATP, which is essential cofactor of T4 DNA ligase. The reaction was usually carried out in 10 μ l final volume using 1 μ l of T4 DNA ligase, and an approximate vector to insert concentration ratio of 1:3 that was determined from band intensity by agarose gel electrophoresis. Generally the reaction was incubated at 14°C overnight, or for blunt end ligation for 2h at room temperature and then overnight at 12°C.

2.3.1.17. *Preparation of electrocompetent E. coli cells*

Streak out the selected *E. coli* strain onto an LB agar plate containing the corresponding antibiotics, if the strain has any antibiotics resistance. Grow it for 12 hours at 37°C. With a sterile toothpick,

inoculate a single bacterial colony in 5ml liquid LB medium, including the antibiotics, in a test tube. Grow it overnight at 37°C in a shaker with 160rpm or in a rotator. Inoculate with the overnight culture 500ml LB medium without antibiotics in a sterile 2 l Erlenmeyer flask and grow at 37°C at 160rpm shaking until the optical density at 600 nm reaches 0.4-0.5. Harvest the cells in sterile 200ml Beckman centrifuge tubes (cap and tube wrapped in alufoil and autoclave separately) in a Sorvall centrifuge in a GSA rotor or compatible at 6000rpm (approx. 6000g) at 4°C for 6 minutes. Gently resuspend the bacterial pellet in ice cold, sterile deionized water, and centrifuge again with the same parameters. Repeat the washing step twice more then resuspend the pellet in 1-2ml ice-cold 10% glycerol or 10% DMSO in sterile deionized water, and aliquot in eppendorf tubes in 50-80µl quantities. Snap freeze the aliquots in liquid nitrogen and store at -80°C.

2.3.1.18. ***Transformation of Escherichia coli by electroporation***

After thawing a frozen aliquot of *E. coli* electrocompetent cell on ice, the dialyzed DNA solution is added to the bacteria and mixed gently with a pipette. The mixture is transferred into a sterile transformation cuvette (Peqlab, 2mm) pre-chilled on ice. An electric pulse is applied (in BioRad Gene Pulser electroporator) with the following settings: voltage = 2.5kV, capacitance = 25µF, resistance = 200Ω. After the pulse 600µl LB medium is added and the bacterial suspension is transferred into a glass test tube and shaken in a thermostat at 37°C for 30 minutes. When the incubation period is over, different aliquots are streaked out on LB plates containing the proper antibiotics. If a ligation mixture is transformed, usually 50µl is streaked out, in case of plasmid DNA 5µl or less.

2.3.1.19. ***Transformation of Agrobacterium tumefaciens***

Transformation of *Agrobacterium* cells is performed by electroporation for which the protocol is basically the same as for *E.coli*. The main differences are that *Agrobacterium* cells are grown on 28°C in YEB medium. It takes approximately 3 days while *Agrobacterium* cell grow out on a plate. Plasmid preparation from *Agrobacterium* is not convenient because of low yield. The analysis of agrobacterial plasmid content can be facilitated by heating the miniprep solution in the lysis phase to 55°C for a few minutes. The extracted plasmid DNA is analyzed by the polymerase chain reaction or transformed into *E.coli* for further analysis after a plasmid extraction. An alternative *Agrobacterium* transformation method is conjugation with *E.coli* cells, which works in both directions. In the conjugation donor S17-1 (Sm^R) *E.coli* strain is used with GV3101(pMP90RK) *Agrobacterium* host cells. Both cell types are grown to mid-log phase, then centrifuged and resuspended in 0.5 ml antibiotics free medium then mixed with each other. Always that medium is used which is required for the recipient bacterium, during the transfer of plasmid DNA from *E.coli* into *Agrobacterium* the medium is YEB. 50µl amounts from the bacterium mixture are pipetted on the surface of a plate with the corresponding medium and let evaporated by leaving the plate open in a sterile hood for approximately 15 minutes. The plates are incubated for one day at the growth temperature required for the recipient bacteria. Then all the bacteria are collected from the plate in 0.5-1 ml liquid medium and streaked onto a

selection plate, which contains antibiotics for the recipient bacterial strain and the transferred plasmid. The grown up *Agrobacterium* colonies are analyzed by back conjugation to *E.coli* cells and a subsequent plasmid DNA extraction and restriction analysis.

2.3.1.20. *Site-directed mutagenesis*

Site directed mutagenesis was carried out according to the unique site elimination method of Deng and Nickoloff [228]. The protocol was based on the Transformer™ Site-Directed Mutagenesis Kit (Clontech), with modifications. The mutagenesis occurs on plasmid DNA. Two oligonucleotide primers are required, both of them are phosphorylated at their 5'-ends to facilitate ligation. One of them introduces a mutation in the target gene (which can be nucleotide exchange, small deletion or insertion, as well). The other, selection primer mutates a unique restriction endonuclease cleavage site by which it destroys the site in the resulting plasmid. In addition to the mutagenic central part, the oligos must contain 15-20 base pairs flanking regions at both ends, complementary to the plasmid DNA. The primers are extended by T4 DNA polymerase and the ends are joined by T4 DNA ligase. The parental plasmids are eliminated by selective restriction endonuclease digest aided by the mutation introduced by the selection primer. The hybrid plasmids are transformed into mismatch repair deficient *E. coli* (BMH 71-18 *mutS*, *tet*^R), and the bacteria are pooled and grown in liquid culture for 12-16 hours under antibiotics selection. A second round of plasmid extraction, restriction endonuclease cleavage and transformation provides high frequency of homogenous mutant plasmids in the resulting single colonies. The mutagenesis is carried out using the following steps:

1. Denaturation of double-stranded plasmid DNA by boiling for 15 minutes and then cooled down slowly to room temperature. The primers are included in the mixture, so during the cooling step primer annealing occurs.

Plasmid DNA 50ng/μl final cc.
 Mutagenic primer 1μl 100pmol/μl
 Selection primer 1μl 100pmol/μl
 10x Annealing Buffer 2μl
 DW to a total volume of 20μl

10X Annealing Buffer
 200mM Tris-HCl pH 7.5
 100mM MgCl₂
 500mM NaCl

2. Add dNTP mixture to 100μM final cc.
 ATP to 1mM final cc.
 BSA 50 μg/ml
 1μl T4 polymerase (3U)
 1μl T4 ligase (400U)
 DW to 30 μl end volume

Incubate for 30-60 min at room temperature

3. Inactivation of T4 polymerase by adding 10mM EDTA and heating to 75°C for 10 minutes
4. Dialysis of DNA (as written above)

5. Restriction endonuclease digestion for 2 hours with the nuclease according to the selection primer
6. Dialysis of DNA
7. Transformation by electroporation into BMH 71-18 *mutS E. coli* strain (tet^R). All the transformant bacteria are pooled and grown in 5ml liquid LB medium, supplemented with corresponding antibiotics, for 12-16 hours at 37°C in a test tube in a rotator.
8. Plasmid DNA miniprep is prepared. Digested again with the selective restriction endonuclease to eliminate parental plasmids, then the DNA is dialyzed, and transformed into any basic *E coli* strain suitable for cloning. The bacteria are plated and grown for 12 hours.
9. A single colony is inoculated into 2ml LB medium, plasmid DNA is extracted and the mutation is confirmed by sequencing.

2.3.2. Protein analytical techniques

2.3.2.1. SDS polyacrylamide gel electrophoresis

SDS polyacrylamide gel electrophoresis was carried out as described in the laboratory manual Molecular Cloning (Sambrook J., Fritsch E.F. and Maniatis, T.). Here only the buffer and gel compositions are listed. The gel component values are accommodated to 40% acrylamide stock solution (29:1 acrylamide : metylene-bis acrylamide) instead of using 30%.

5x Tris-glycine electrophoresis buffer:

15.1g	Tris base
94g	glycine
50ml	10% SDS
filled up to 1000ml with deionized water	

5x SDS gel loading buffer:

250mM	Tris-HCl pH 6.8
0.5M	DTT (measured from powder)
10%	SDS (measured from powder)
50%	glycerol

Components for 10ml gel volume (values in ml)	8%	10%	12%	15%	stacking gel 2ml (5%)
H ₂ O	5,275	4,825	4,3	3,55	1,48
40% acrylamide mix (29:1)	2,025	2,475	3,0	3,75	0,25
1,5M Tris (pH8,8)	2,5	2,5	2,5	2,5	0,25
10% SDS	0,1	0,1	0,1	0,1	0,02
10% ammonium persulfate	0,1	0,1	0,1	0,1	0,02
TEMED	0,006	0,004	0,004	0,004	0,002

2.3.2.2. Staining SDS polyacrylamide gels with Coomassie Brilliant Blue R250 and colloidal blue stain

Staining solution for CBB-R250:

0.25g	Coomassie Brilliant Blue R250
45ml	H ₂ O
45ml	methanol
10ml	glacial acetic acid

The polyacrylamide gel is immersed into at least 5 volumes of staining solution and placed on a slowly rotating platform for minimum 4 hours at room temperature. The gel is destained in the same solution without the dye generally for 4-8 hours, changing the destaining solution three times. For

colloidal Coomassie staining Novex Colloidal Blue Staining kit was used from Invitrogen, and the staining was carried out following the manufacturer's instructions.

2.3.2.3. *Tris-Tricine buffered SDS-polyacrylamide electrophoresis of peptides*

Peptide electrophoresis uses a tricine-based buffer system, which in contrast to glycine-based buffers allows the separation in the low molecular weight range. We used a three layer gel system that consists of a stacking gel, a spacing gel layer and a separating gel.

Special reagents:

1. Separating/spacer gel acrylamide: 48g acrylamide, 1,5g N,N'-methylene-bis-acrylamide. Bring to 100ml and filter through paper to remove cloudiness.
2. Alternative: separating/spacer gel (2x crosslinked): 48g acrylamide, 3g N,N'-methylene-bis-acrylamide.
3. Stacking gel acrylamide: 30g acrylamide, 0.8g N,N'-methylene-bis-acrylamide. Bring to 100ml and filter through paper to remove cloudiness.
4. Separating/spacer gel buffer: 3M Tris base (ultra pure), 0.3% SDS. Bring to pH 8.9 with HCl.
5. Stacking gel buffer: 1M Tris-HCl, pH 6.8
6. Cathode (top) running buffer (10x stock): 1M Tris base, 1M tricine, 1% SDS. Dilute 1:10 immediately before use. Do not adjust pH, it will be about 8.25
7. Anode (bottom) running buffer (10x stock): 2M Tris base. Bring to pH 8.9 with HCl. Dilute 1:10 immediately before use

2.3.2.3.1. Gel recipes:

<u>Separating gel:</u>	6.7ml	deionized water
	10ml	separating/spacer gel buffer
	10ml	separatin/spacer gel acrylamide (1x or 2x crosslinked)
	3.2 ml	glycerol
	10µl	TEMED
	100µl	10% ammonium persulphate
<u>Spacer gel:</u>	6.9ml	deionized water
	5.0ml	separating/spacer gel buffer
	3.0ml	separating/spacer gel acrylamide (1x crosslinked only)
	5µl	TEMED
	50µl	10% ammonium persulphate
<u>Stacking gel:</u>	10.3ml	deionized water
	1.9ml	stacking gel buffer
	2.5ml	stacking gel acrylamide
	150µl	EDTA
	7.5µl	TEMED
	150µl	10% ammonium persulphate
<u>Tris-tricine sample buffer</u>	4.0 ml	deionized water
	2.0 ml	0.5M Tris-HCl pH 6.8
	2.4 ml	glycerol
	1.0 ml	10% SDS
	0.2 ml	β-mercapto-ethanol
	0.4 ml	0.5% Coomassie G-250

Insufficient amount of β-mercapto-ethanol may result in doublets or diffuse bands.

Fixation	50%	methanol
	10%	glacial acetic acid
		in water

Place the gel into this polypeptide fixative solution for 30 min

<u>Staining, destaining</u>	25%	isopropanol
	7%	glacial acetic acid
	68%	deionized water
	(0.25 g/l	coomassie brillant blue in the staining solution)

Stain the prefixed gel for 1 hour. Destaining: 3x15 minutes or until the desired destaining has reached.

Molecular weight standard: Polypeptide SDS-PAGE Molecular Weight Standard (Bio-Rad)

2.3.2.4. *Two-dimensional electrophoresis*

Two-dimensional gel electrophoresis was carried out by the proteomics service group of our institute. Reference: J Walker: The Protein Protocols Handbook [228].

2.3.2.5. *Western blot analysis of proteins*

For blotting proteins generally Immobilon-P PVDF membrane was used in a Bio-RAD mini cell or house-made wet blotting system. The Immobilon-P membrane was first wetted with pure methanol for a few seconds before using it in a water-based buffer. The gel and membrane is straddled by three layers of Whatman paper on both sides and this “sandwich” is covered by a pair of a sponge sheet. The transfer is performed in transfer buffer at 25V for 2 hours or alternatively 10V for overnight blotting.

1x transfer buffer (stock is 5x concentrated):

50mM boric acid
50mM Tris base
Do not adjust pH

When the transfer is complete, the chamber is disassembled and the membrane is gently shaken in blocking solution for two hours.

Blocking solution

5% milk powder
0.05% Tween 20
in 1x TBS buffer

10x TBS, (1litre)

80g NaCl
2g KCl
30g Tris base
Adjust pH to 8.0 with HCl

The primary antibody was applied in 10ml blocking buffer for 2 hours with respect to the characteristic dilution ratio of specific antibodies. Before applying the secondary antibody the membrane was washed three times in wash buffer (1xTBS + 01% Tween 20). The secondary antibodies were also applied for 2 hours in blocking solution in their required concentrations. After the

incubation period, the blot was washed 3 times with wash buffer and detected by ECL reagent (equal mixture of two components, approximately 200 μ l each for a 6 x 9cm minigel blot) and hypersensitive X-ray film for different exposition times.

2.3.2.6. *Chemical and enzymatic manipulation of proteins*

2.3.2.6.1. *Trichloro-acetic acid (TCA) precipitation of proteins*

TCA precipitation of proteins was performed using the following protocol: Add 2 volumes of 10% TCA in acetone to 1 volume of protein solution in an eppendorf tube. Allow the mixture to stand for at least 2 hours at -20°C. Improved recovery can be achieved by allowing the mixture to stand at -20°C overnight. Centrifuge the sample at 14.000 rpm in a tabletop centrifuge for at least 10 minutes at 4°C. Immediately and carefully decant the supernatant and remove the residual liquid with a pipette. Wash the pellet with pure acetone. Dry the pellet under vacuum (10-15 min). Dissolve the precipitated protein by vortexing in a minimal volume (50 μ l) of either neutral or alkaline buffer.

2.3.2.6.2. *Selective chemical cleavage of proteins at methionyl groups by CNBr*

Cyan bromide cleavage of proteins was carried out using the following working steps:

1. Dry down the sample under vacuum. Heating is necessary to remove bicarbonate completely if that was used as a buffer component. Solubilize the sample in 70% aqueous TFA or 70% formic acid to protein concentration of 1-5mg/ml.
2. Add CNBr to the sample in 10 x molar excess to the methionyl groups. In practice, this means equal amount of CNBr to protein pellet. (Other protocols apply 3 x more CNBr or even more). For very small amounts of samples add one crystal of CNBr. Alternatively 5M CNBr in acetonitrile solution can be used.
3. Let the reaction proceed for 24 hours at room temperature with gentle stirring. Cover the reaction vessel with alufoil.
4. Dry the sample in vacuum centrifuge. If the sample was solubilized in formic acid, dissolve it in water and dry again, which should get rid of the residual formic acid.
5. Dissolve the sample in 20-40 μ l of tricine-SDS-PAGE sample buffer. If it turns yellow, residual acids are present and the sample will run badly. Tris buffer can be added to raise pH.
6. To deactivate CNBr in a solution not exceeding 60g CNBr/liter the recommended method is to add 1M NaOH and NaOCl in volumes of ratio 1:1:2 (CNBr solution : NaOH : NaOCl). With low concentration of CNBr simply hypochlorite solution can be used. Wait until effervescence stops.

2.3.2.6.3. *Enzymatic cleavage of proteins*

In this work we used only Arg-C protease, which cleaves at arginine residues at position P1. Sequencing grade Arg-C protease was applied from Roche, which product contains the necessary buffer and activation solution.

2.3.2.6.4. *In-gel digestion of proteins*

(Reference: Shevchenko, A., Wilm, M., Vorm, O and Mann M. (1996) Mass spectrometric sequencing of proteins from silver stained polyacrylamide gels. *Anal Chem.* 68, 850-858)

Excision of protein bands from polyacrylamide gels: Wash the gel with water (2 changes, 10 minutes each). Excise the spots or bands of interest from the gel. Cut the excised piece into 1mm³ cubes and transfer them to a 0.5 µl microfuge tube.

Washing of gel pieces: Wash the gel particles with water and 50mM NH₄HCO₃/ acetonitrile 1:1 (v/v) for 15 min. Remove all remaining liquid and add enough acetonitrile to cover the gel particles. The gel shrinks and sticks together. Remove acetonitrile and rehydrate the gel pieces in 50mM NH₄HCO₃. After 5 min, add an equal volume of acetonitrile and then remove all liquid after 15 min of incubation. Add enough acetonitrile to cover the gel particles. After the gel pieces have shrunk, remove acetonitrile. Dry down the gel particles in a vacuum centrifuge.

Reduction and alkylation: Swell the gel particles in 10mM dithiothreitol/25mM NH₄HCO₃ (freshly prepared) and incubate them for 45 min at 56°C. Chill tubes to room temperature, remove excess liquid and replace it quickly by roughly the same volume as above of freshly prepared 55mM iodoacetamide (light sensitive) in 25mM NH₄HCO₃. Incubate for 30 min at room temperature in the dark and then remove iodoacetamide solution and wash the gel particles with 50mM NH₄HCO₃ and acetonitrile (1:1 v/v), one or two changes each, 15 min per change. Add enough acetonitrile to cover the gel particles. After the gel pieces have shrunk remove the acetonitrile and dry down the gel particles in a vacuum centrifuge.

In-gel digestion: Add just enough freshly prepared enzyme solution (25mM NH₄HCO₃ with for instance 5ng/µl trypsin solution, sequencing grade) to cover the gel. Incubate at 37°C for 30 minutes. Add enough 25mM NH₄HCO₃ to keep the gel wet overnight, but avoid excess liquid and incubate at 37°C overnight.

Extraction of peptides: Make sure that about 3µl of liquid is in the tube (it might be necessary to add some water) and sonify for 10 min. Recover the supernatant and add 3µl of 50% acetonitrile with 1% trifluoro-acetic acid or formic acid. Sonify for 10 min and recover the supernatant. Repeat the acetonitrile/acid step and pool the supernatants.

Peptide analysis: If purification is necessary, perform microcolumn purification

2.3.2.7. *In vitro kinase reactions*

In general, 1µg of purified recombinant protein kinase and 1µg substrate was mixed with 1µl of fresh radioactive $\gamma^{32}\text{P}$ ATP in a reaction buffer containing 100mM Tris-HCl (pH 8.0), 5mM MgCl₂, and 50mM NaCl. High buffering capacity is needed to balance the effect of the acidic ATP. Mg²⁺ is an essential cofactor needed for ATP activation. The reaction runs for at least 1 hour at room temperature.

The reagents are separated by SDS-PAGE so, that the front line, which contains most of the unincorporated radioactive ATP should not leave the gel. (The bottom of the gel can be cut and discarded, which reduces contamination of the equipment.) In order to remove background activity of the unincorporated ATP molecules, the gel slab is immersed into 10% acetic acid solution for one hour. Subsequently the gel is placed between a Whatman paper and a layer of cellophane and dried in a heated vacuum-assisted gel dryer machine. The dried gel is placed into a photo cassette and subjected to autoradiography with an X-ray film. With high activity, 5-10 minutes of exposition should be sufficient whereas in case of weaker activity the exposition can be extended to hours or even days. The signal is fading very slowly, because the half-life time of the ^{32}P isotope is approximately 2 weeks. To exploit the intensifier layer found inside many photo cassettes, the cassette is placed into a -70°C deep freezer. After the assay, all the equipment is decontaminated by wiping or immersing into deconex solution.

2.3.2.8. *Recombinant protein expression in Escherichia coli cells*

For expression of recombinant proteins *E. coli* strain BL21DE3pLysS was used as host in most experiments. This strain is deficient in the lon intracellular protease and ompT extracellular protease therefore facilitates the purification of intact proteins. In addition, the strain carries the gene of T7 RNA polymerase under the control of *lacUV5* promoter and therefore is compatible with IPTG inducible expression. The pLysS vector plasmid carries the gene of T7 lysozyme, a natural inhibitor of T7 RNA polymerase, which provides a more strict regulation of transgene expression.

After electroporation of the recombinant plasmid into BL21DE3pLysS *E. coli* and selection of transformants, a starter culture for protein expression was inoculated in 5ml LB with a sterile toothpick and grown overnight at 37°C in the presence of the bacterial strain specific (Cm) and plasmid specific (Amp) antibiotics. The grown-up starter culture was inoculated into larger amount of LB medium (0.5-2.0l, depending on the abundance and solubility of the recombinant protein) and grown until it reached $\text{OD}_{600}=0.6$, when 1mM IPTG was added to induce protein expression. Proteins were expressed for different time intervals ranging from 3 hours to 10 hours. The protein expression was generally carried out at 37°C , although in some cases lower temperature was tried, which increases recombinant protein solubility inside the bacterial cells and reduces losses by inclusion body formation. After the expression period, the bacteria were pelleted in a Sorvall RC5B centrifuge in 250ml Beckman centrifuge tubes at $6000\times g$ for 6min at 4°C . The bacterial pellet was frozen in order to facilitate the lysis of bacteria or for storage at -80°C .

2.3.2.9. *Purification of proteins*

2.3.2.9.1. *Affinity purification of His-tagged recombinant proteins on Ni-NTA resin*

cDNA clones for expression of 6xHis tagged proteins were generally cloned in the non-commercial pET201 vector (very similar to pET32 from Novagen), which provides an N terminal thioredoxin tag to increase solubility of recombinant proteins in *E. coli* and a 6xHis tag in C-terminal position.

(Reference: The QIAexpressionist™. A handbook for high-level expression and purification of 6xHis-tagged proteins, QIAGEN).

The bacterial pellet was taken up in prechilled lysis buffer (2ml/g bacterial pellet, but not less than 20ml):

Lysis/binding buffer: 1xPBS pH=8.0 (phosphate buffered saline: 40mM phosphate buffer, 300mM NaCl)
 10% glycerol
 1% Triton X-100
 40mM imidazole
 5mM 2-mercapto ethanol
 protease inhibitors (PMSF, leupeptin, pepstatin, aprotinin, but no EDTA)

The bacteria were lysed by sonication on ice. The cell debris was pelleted in a benchtop centrifuge at 14000rpm at 4°C for 10-20min. All subsequent steps were carried out in a cold room at 4°C.

- The supernatant was applied on 1ml (bed volume) pre-equilibrated Ni-NTA matrix filled in a disposable chromatographic column (QIAGEN) and was let flow through by gravitation. (The binding capacity of Ni-NTA is in the range of 5-10mg His-tagged protein /ml matrix, therefore this was the amount generally used.) The flow-through fraction was frozen for further analysis. The column was washed with 50-100 ml pre-chilled wash buffer by gravity flow (identical to lysis buffer).
- The His-tagged proteins were eluted from the column in elution buffer containing increasing imidazole concentration gradient ranging from 40-250mM in 500 µl fractions or by constant 300mM imidazole in elution buffer in 6x500µl fractions.

Elution buffer: 1xPBS (pH 7.0, 40mM Na_x(PO₄)_x, 300mM NaCl)
 5mM 2-mercapto ethanol
 different imidazole concentrations (elution starts at 100mM)
 protease inhibitors

- The fractions were assayed on SDS-PAGE, stained with coomassie brilliant blue R250. The protein containing fractions were dialyzed against 1l dialysis buffer with one buffer change or size exclusion chromatography was used to change the buffer.

Dialysis buffer: 20mM TRIS-HCl (pH 7.5)
 50mM NaCl
 5mM 2-mercapto ethanol
 0.2mM PMSF
 10% glycerol (not applied for gel filtration)

- After buffer exchange, the protein concentration was measured by Bradford assay (Bio-RAD). Protein solutions were further purified or aliquoted and frozen in liquid nitrogen, stored at -80°C. When buffer exchange was done by gel filtration, 10% glycerol was added before freezing.

2.3.2.9.2. Affinity purification of GST-tagged recombinant proteins on glutathion-Sepharose 4B

(Reference: GST gene fusion system, Handbook, GE Healthcare)

GST-tagged recombinant proteins were purified using the following protocol:

1 The bacterial pellet was taken up in prechilled lysis/binding buffer (2ml/g bacterial pellet, but not less than 20ml).

Lysis/binding buffer: 1× PBS (ice-cold) (140 mM NaCl, 2.7 mM KCl, 10 mM Na₂HPO₄, 1.8 mM KH₂PO₄, pH 7.3)
10% glycerol
1% Triton X-100
5mM 2-mercapto ethanol
1mM EDTA
protease inhibitors (0.2mM PMSF, leupeptin, pepstatin, aprotinin, or combined protease inhibitor cocktail for bacterial extracts (Sigma))

The bacteria were lysed by sonication on ice. The cell debris was pelleted in a benchtop centrifuge at 14000rpm at 4°C for 10-20min.

2. All further steps were carried out in a cold room at 4°C. The supernatant was applied onto 1ml (bed volume) pre-equilibrated Glutathione-Sepharose 4B matrix filled in a disposable chromatographic column (GE Healthcare) and was let flow through by gravitation. (The binding capacity of Glutathione Sepharose 4B is approximately 8mg glutathione S-transferase /ml matrix). The flow-through liquid was frozen for further analysis. The column was washed with 50-100 ml pre-chilled wash buffer by gravity flow (identical to lysis buffer).

3 Elution was performed using 6x500µl elution buffer (50 mM Tris-HCl (pH 8.0) and 25 mM reduced glutathione, pH is adjusted to 8.0 after adding glutathione).

4 Analysis of purified proteins by SDS-PAGE, buffer exchange, protein concentration measurement and storage were as described in the Ni-NTA purification protocol.

2.3.2.9.3. Affinity purification of MBP-tagged recombinant proteins on MBP-Sepharose

(Reference: pMAL™ Protein Fusion and Purification System, New England Biolabs.)

The bacterial pellet was taken up in prechilled lysis/binding buffer (2ml/g bacterial pellet, but not less than 20ml).

Lysis/binding buffer: 20mM Tris-HCl (pH 7.4)
200mM NaCl
1mM EDTA
10% glycerol
5mM 2-mercapto ethanol
protease inhibitors (0.2mM PMSF, leupeptin, pepstatin, aprotinin, or combined protease inhibitor cocktail for bacterial extracts (Sigma))

All further steps were carried out in a cold room at 4°C. The supernatant was applied on 1ml (bed volume) pre-equilibrated MBP-sepharose matrix filled in a disposable chromatographic column (NEB) and was let flow through by gravitation. (The binding capacity of MBP-Sepharose is approximately 3mg MBP tagged recombinant protein /ml matrix) The flow-through liquid was frozen for further

analysis. The column was washed with 50-100ml prechilled wash buffer by gravity flow (identical to lysis buffer). Elution was performed with 6x500µl

elution buffer: 20mM Tris-HCl pH 7.4
 200mM NaCl
 5mM 2-mercapto ethanol
 10mM maltose
 0.2mM PMSF

The analysis of purified proteins by SDS-PAGE, buffer exchange, protein concentration measurement and storage were as described in the Ni-NTA purification protocol.

2.3.2.9.4. *Affinity purification of proteins on StrepII-tactin resin*

(Reference: Strep-tag[®] Purification Protocol, 2005, IBA GmbH, Germany)

For purification of Ster-tag labeled proteins, the StrepII-tactin column was pre-equilibrated with

bufferW: 100mM Tris-HCl (pH 8.0), 150 mM NaCl and 1 mM EDTA
 (protease inhibitors can be applied but use buffer without EDTA for metalloproteins)

The bacterial pellet is resuspended in ice cold bufferW, which might be supplemented with bacterial protease inhibitors (PMSF, leupeptin, pepstatin, aprotinin, benzamidin, or use combined protease inhibitor cocktail). The bacterial cells are homogenized by sonication or French-press cell. The cell debris is removed by centrifugation in a cold tabletop microcentrifuge at 14000rpm for 10-20 min. Subsequently, the cell extract is loaded onto the column (binding capacity is 50-100nmol protein/ml matrix, in the range of 1-2 mg protein). When the sample has passed, the column is washed with 5 column volume of bufferW. The wash fractions are collected for further analysis. The bound proteins are eluted with 6 times 0.5 column volume of

elution buffer: bufferW containing 2.5mM desthiobiotin

- To prevent covalently linked contaminations use 5mM β-mercapto-ethanol
- To prevent non covalently linked contaminations the following additives can be used:
 NaCl up to 1M concentration, glycerol up to 25% and mild non-ionic detergents (Triton-X 100, Tween 20, CHAPS) in 0.1% concentration.

2.3.2.10. *Tandem affinity purification of plant proteins on NiNTA and Strep-tactin resins*

2.3.2.10.1. *Simplified protocol for total cell extract*

Freeze the plant material in liquid nitrogen. Grind the frozen tissues with liquid nitrogen in a mortar with pestle to a fine powder. In case the starting material is a cell suspension culture, it is recommended to add sand during mortaring or alternatively perform the extraction with dry ice (i.e., solid CO₂). Let the nitrogen evaporate. When evaporated the color of the tissue changes from gray-white to dark green in case of leaf material. Transfer the powder to another container e.g. a beaker to

prevent freezing of the buffer in the cold mortar. Alternatively, a blender machine can be used especially with leaf material. All following steps are carried out at 4°C. Add 3ml/g tissue

Buffer A: 1xPBS pH=8.0 (phosphate buffered saline: 40mM phosphate buffer, 300mM NaCl)
5mM 2-mercapto-ethanol
10% glycerol
0.1% Triton-X 100
1mM Na₃VO₄ (activated)
1mM PMSF and 1/100 volume Protease inhibitor cocktail
for plant extracts (SIGMA P9599)
(add 2mM ATP pH7.0 if proteasomal complex is to be purified)

Filter slurry on nylon mesh, pore size 100 and 50 µm. Centrifuge in 200ml Beckman centrifuge tubes in Sorvall GSA rotor or equivalent with 12500 rpm (approx. 25000g) for 20-30 min at 4°C. Carefully decant the supernatant into a new vessel and apply it onto pre-equilibrated NiNTA column in a cold room. The volume of the NiNTA resin used should be 2ml/each 20g of fresh sample weight.

Wash the column with 50-100ml bufferA, containing 10mM imidazole, and then wash the column shortly with elution buffer to remove glycerol. Elute proteins with an increasing step gradient of imidazole concentration in

Elution buffer (bufferA without glycerol):

1xPBS (pH 8.0) (phosphate buffered saline: 40mM phosphate buffer, 300mM NaCl)
5mM 2-mercapto-ethanol
1mM Na₃VO₄ (activated)
1mM PMSF + 1/100 volume plant protease inhibitor cocktail
(add 2mM ATP pH 7.0 if proteasomal complex is to be purified)

The imidazole step gradient starts at 40 mM and increases by 20-40mM intervals. The volume of fractions should be equal to the bed size of the column. The fractions can be analyzed on SDS-PAGE and western blotting. Typically, the specifically eluted proteins can be found in the 100mM-200mM fraction range. It is advisable to proceed further immediately.

Pool the eluted fractions between 100mM and 200mM imidazole and apply it on 1-2ml Strep-tactin Sepharose column pre-equilibrated with elution buffer. (Strep tactin Sepharose is compatible with 250mM imidazole and up to 1M NaCl.). Wash the column with 50ml

Strep-washing buffer:

150mM NaCl
10mM Tris-HCl (pH 8.0)
10% glycerol
0.1% Triton-X 100
5mM β-mercapto-ethanol
0.2mM PMSF
1mM Na₃VO₄
(2mM ATP for purification of proteasome-associated proteins)

Wash the column shortly with elution buffer without desthiobiotin to remove glycerol and detergent.

Elute proteins with 6 x 0.5-1ml of

Strep-elution buffer:
 150mM NaCl
 10mM Tris-HCl (pH 8.0)
 5mM β -mercapto-ethanol
 2.5mM desthiobiotin (it dissolves in water quite slowly)
 (2mM ATP)
 1/100 volume Protease inhibitor cocktail for plant extracts (SIGMA P9599)

The fractions are analyzed on SDS-PAGE and western blotting. If abundant proteins were purified, it might be attempted to measure protein concentration by the Bradford assay (BIO-RAD). The protein containing fractions can be concentrated by vacuum centrifugation. If the sample is to be frozen, 10% glycerol is added prior snap freezing. If the sample is to be processed by mass spectrometry, do not add glycerol. Buffer exchange may be necessary to reduce salt concentration for which dialysis or gel filtration on a small volume Sephadex-G25 column are the alternatives.

2.3.2.10.2. Alternative protocol for separated handling of nuclear and cytoplasmic fractions

After tissue homogenization add 3ml/g tissue nuclear grinding buffer:

Nuclear grinding buffer (NGB):
 1M hexylene-glycol
 10mM PIPES-KOH pH 7.0
 5mM 2-mercapto-ethanol
 10mM MgCl₂
 0.2% TritonX-100
 2mM ATP (pH neutralized prior use)
 1mM Na₃VO₄ (activated)
 0.8mM PMSF (Add extra 0.4mM PMSF in every 20 min of preparation time)
 (Effective concentration 0.1-1mM, half life at pH 7.5 1 hr)
 [Alternatively 0.5mM AEBSF (4-(2-aminoethyl)-benzenesulfonyl-fluoride hydrochloride)]

Filter slurry on nylon mesh, pore size 100 and 50 μ m. Use a wide mouth funnel for filtering especially in case of large amount of starting material. It is advisable to rinse the slurry with NGB. Squeeze the filter to collect all liquid. Centrifuge in 50ml falcon tubes at 1260xg for 10 minutes at 4°C. Alternative: centrifuge in Sorvall GSA tubes with 3,000 rpm at 4°C for 15 min (approx 1400xg). Carefully decant the supernatant into new GSA tubes and spin at 12,500 rpm (25,000 g) for 30 min at 4°C and process further with this fraction as cytoplasmic fraction by binding to Ni²⁺ or Co²⁺ beads.

Extraction of nuclear proteins:

Gently resuspend the nuclear pellet in nuclear wash buffer (1ml/10g starting material, minimum 0.5ml). The nuclei are very easily damaged and lysed, therefore handle with care. Use wide-mouth pipette tips. The buffer contains 0.3% Triton X-100 for cell membrane lysis (experimentally determined concentration, specific for *Arabidopsis*, CellLytic™ PN Isolation/Extraction Kit, Sigma). In the presence of Mg²⁺ the Triton X-100 does not solubilize the DNA and may only strip away the outer of the two nuclear membranes. Optionally, view the sample under microscope to see the cells are broken but nuclei are intact.

Nuclear wash buffer (NWB):

- 0.5M hexylene-glycol
- 10mM PIPES-KOH pH 7.0
- 10mM MgCl₂
- 0.3% TritonX-100
- 5mM 2-mercapto-ethanol
- 0.8mM PMSF
- 2mM ATP
- 1mM Na₃VO₄
- 1/100 volume Protease inhibitor cocktail for plant extracts (SIGMA P9599, does not contain EDTA)

High purity preparation of nuclei:

Prepare 40% Percoll in NWB and 2.3M sucrose solution in 10mM PIPES-KOH (pH 7.0), 10mM MgCl₂. The sucrose solution is dense, may be warmed up to 50-65°C to facilitate solution of sucrose, but must be chilled to 4°C before use. Prepare nuclei isolation tube in a 50 ml falcon tube by filling 10ml sucrose solution to the bottom and carefully adding a 10ml 40% Percoll layer on the top. Two separate phases should be formed. The nuclei isolation tube can be scaled in 2ml eppendorf tubes (with 0.7ml of each layer) or in 15ml falcon tubes (3ml of each layer). Carefully apply the nuclear suspension on the top of the isolation tube. Centrifuge at 3200xg for 30 min at 4°C. Most of the nuclei are banded at the interface between the sucrose and Percoll layers. Gently collect the nuclei with a Pasteur pipet and transfer into a new 14ml tube. Wash the nuclei to remove Percoll and sucrose in 2x the nuclei band volume using NWB. Centrifuge at 3200xg for 5 minutes, decant supernatant and invert the tube to remove the hypotonic NWB buffer.

Nuclear lysis: Resuspend the nuclei pellet in 2/3 pellet volume nuclear lysis buffer.

Nuclear lysis buffer (NLS):

- 150mM KCl
- 20mM HEPES-KOH (pH 7.5)
- 10% glycerol
- 10mM MgCl₂
- 5mM 2-mercapto-ethanol
- 1/100 volume protease inhibitor cocktail (or 1/50)
- 2mM ATP
- 1mM Na₃VO₄
- (NH₄)₂SO₄ (Concentration must be experimentally determined, should be as low as possible e.g. 80mM, maximum 0.4M).

Add 5U/ml Benzoase (Novagen) or 100µg/ml DNase (Worthington, electrophoretically homogenous) and 100 µg/ml RNase (electrophoretically homogenous, Serva) and 50U/ml micrococcal nuclease (Worthington). Rock the tube for 60 min at 4°C. Check the lysis of nuclei under microscope, DNA can be stained with DAPI. Dounce homogenizer can be used to enhance shearing. Centrifuge in SS34 with 14,000 rpm (25,120g) for 30 min. Keep the pellet, in case re-extraction would be needed. If yes, sonicate the pellet in 1ml nuclear lysis buffer, centrifuge and check protein content of the supernatant by Bradford reagent and then combine with the first nuclear extract. Measure protein concentration by bicinchonic acid method (Pierce).

Proceed further with the chromatographic steps. The use of $(\text{NH}_4)_2\text{SO}_4$ is not recommended with NiNTA resin (by the manufacturer), whereas the Strep-tactin Sepharose is compatible with $(\text{NH}_4)_2\text{SO}_4$ up to 2M. (Application of ammonium-sulphate containing samples onto NiNTA resin was carried out by us, and ammonium did not reduce Ni^{2+} ions up to 400mM in the binding phase). However, plant tissues contain biotin (vitamin H), which strongly binds to the Strep-tactin Sepharose and interferes with sample binding. Therefore, in case of small sample volumes the nuclear extract can be first applied to Strep-tactin followed by NiNTa chromatography if necessary, otherwise ammonium salts must be first removed by a quick buffer exchange using gel filtration with a diluted sample. Alternatively the homogenization of the nuclei can be performed with French-pressure cell, and the ammonium free lysate can be first applied to NiNTA resin.

2.3.2.10.3. Gel filtration

Size exclusion chromatography was used for quick and efficient buffer exchange of protein solutions. Generally, 10-15 ml Sephadex G25 or G50 was used filled in disposable plastic columns (e.g. PD-10 columns, GE Healthcare). Dry Sephadex powder was pre-swollen for 3 hours in distilled water with slow shaking, autoclaved and then equilibrated with the chosen buffer. The elution volume (void volume) was measured by running Blue-Dextran 2000 on the column. Fractions were collected in 500 μ l aliquots and assayed with Bradford reagent (BIO-RAD). The eluted proteins were immediately applied to the second chromatographic column (in case of double GST-His tagging or Strep-his tandem tagging).

2.3.2.10.4. Anion exchange chromatography

The purification of AKIN10 kinase included an anion-exchange chromatography step. 1ml pre-packed HiTrap DEAE-Sepharose FF anion exchange matrix was used with Tris-HCl buffer pH 8.0. Elution was performed by increasing NaCl concentration in a step gradient using 50mM intervals. The anion exchange chromatography was otherwise carried out according to the manufacturer's instructions (GE Helathcare).

2.3.2.10.5. Activation of sodium orthovanadate (phosphatase inhibitor)

Isolation of active protein kinases requires the inhibition of protein phosphatases during the kinase purification procedure. This protocol is applied to depolymerisation of vanadate converting it into a more potent inhibitor of protein phosphatases. DTT application in the chromatography buffers should however be avoided as DTT rapidly inactivates sodium orthovanadate. 200mM stock solution of sodium orthovanadate Na_3VO_4 is adjusted to pH to 10.0 using either 1N NaOH or 1N HCl. At pH 10.0 the solution will be yellow and is boiled until it turns colorless (approximately 10 minutes) and then cooled to room temperature. The pH is readjusted to 10.0 and the boiling procedure and pH

readjustment is repeated until the solution remains colorless. The stock solution is stored in aliquots at -20°C. Applied final concentration of sodium orthovanadate is 0.2mM

2.3.2.11. *Mass spectrometry*

Mass spectrometry was carried out by the help of the MS service group of our institute. We used MALDI-TOF and ESI-Q-TOF mass spectrometers equipped with an ion-trap device.

2.3.3. Plant techniques

2.3.3.1. *Crossing Arabidopsis plants*

There are approximately 3 to 5 flower buds on each floral axis at a given day that are feasible for crossing Arabidopsis. These are the most developed flower buds, which are still closed and did not undergo self-pollination as their anthers are immature. These flower buds are emasculated with pointed forceps taking off the sepals and petals under a stereomicroscope or using a magnifying glass headset. An open mature flower is taken from the crossing partner plant and its stamens are used to fertilize the prepared carpel by touching it several times.

2.3.3.2. *Arabidopsis seed sterilization*

Instead of regular bleach, Arabidopsis seeds are sterilized with Ca-hypochlorite, which secured better viability and germination. Seeds in an eppendorf tube (not more than 200 µl) are treated with 1ml of hypochlorite solution with gentle shaking for 10 minutes (note: prolonged exposition time might reduce the seed's germination ability) and subsequently collected by centrifugation at 6000 rpm for 1 min in a tabletop centrifuge). The hypochlorite solution is removed using sterile pipette tip and the seeds are washed three times with 1ml sterile distilled water. Subsequently, the seeds are suspended in 1ml sterile water, stratified overnight at 4°C and spread on the surface of an MS agar plate. Alternatively the seeds can be dried after the final washing step leaving the open eppendorf tube for 4-5h or overnight in a sterile hood. In this case sterile toothpicks are used to loosen the cohesive seeds.

Hypochlorite solution: Dissolve 5g Ca(OCl)₂ in 100ml distilled water and then add 1ml 10% Triton X-100 and mix well the solution using a magnetic stirrer. Centrifuge the solution in a 50ml Falcon tube at minimum 2000 rpm and then decant the supernatant into a clean 50ml Falcon tubes. The solution might be stored at 4°C for 2-3 weeks.

2.3.3.3. *Transformation of Arabidopsis using the floral dip method [229]*

Agrobacterium is grown in YEB medium to OD600 1.2-1.5 in the presence of antibiotics to select for the resistance marker of binary vector. Bacteria from 500ml culture are collected by centrifugation and resuspended in 200ml IM medium (0.5 concentration of MS basal salt mixture (Sigma), 1 x B5 vitamins (Sigma), 5% sucrose, 0.05µM BAP and 0.005%(v/v) Silwet L-77 (Ambersil). Inflorescences of 3-4 week-old plants (10-15 cm high) are immersed into the bacterial suspension for 3-5 min and

then the plants are covered with plastic bags for 24h. In order to obtain more susceptible flowers per plant, the stems can be cut back once in the growth period prior to transformation when the first stems are few cm high. This results in a branching stem structure.

2.3.3.4. *Selection of Arabidopsis transformants*

Sterile *Arabidopsis* seeds are resuspended in 1ml water and pipetted on the surface of a (15cm diameter) MSAR plate, containing the corresponding antibiotics (Km100, Hyg15). Some more milliliters of sterile water is added and the seeds are equally spread by the tilting the plate. Seed density should be 5-10 seeds to cm². When the seeds are settled, the water is removed by the circumference of the plate with a pipette. When using kanamycin selection the sensitive seedlings will turn yellow soon after germination whereas the resistant seedlings remain green. Under hygromycin the selection the sensitive seedlings remain green for about 10 days, but do not develop leaves and subsequently become stunted and brown, and their root development is strongly inhibited.

2.3.3.4.1. *Seed storage*

Arabidopsis seeds are dried in a demisted chamber (silica particles absorb humidity from its air). The seeds are stored at -20°C.

2.3.3.5. *Arabidopsis genomic DNA extraction by the CTAB method [230]*

CTAB (Hexadecyl trimethyl ammonium bromide) is a cationic detergent.

Approximately 300mg *Arabidopsis* tissue (seedlings, leaves) is collected into a 1.5ml eppendorf tube and frozen in liquid nitrogen. The sample is grinded with a glass rod while it becomes unfrozen and subsequently 0.3ml of preheated CTAB 2x buffer is added. Upon mixing the extract is incubated at 65°C for at least 5 minutes with repeated shaking and then placed on ice. Following addition of 0.3 ml chloroform, the extract is mixed and centrifuged for 5 minutes at top speed in a benchtop centrifuge. 0.4ml from the upper phase of the samples is pipetted into new eppendorf tubes containing 40µl preheated CTAB 10x buffer (it is too viscous at room temperature) and 0.4ml chloroform is added. The samples are mixed and centrifuged again for 5 minutes. 0.3ml of the upper phase is pipetted into new eppendorf tube containing 0.3ml CTAB precipitation buffer, the solution is mixed and upon 5 min incubation is centrifuged for 10 minutes. After removal of the supernatant the pellet is dried briefly and then dissolved in 0.3ml high salt TE buffer. The DNA is precipitated with 0.6ml ethanol at -20°C for 30 min and collected by centrifugation for 10 min at maximum speed in a tabletop centrifuge. The pellet is washed two times with 70% ethanol, and then with absolute ethanol and dried to dissolve the DNA in 100µl distilled water. For PCR analysis 1µl DNA sample is used.

CTAB 2x buffer:

2% (w/v) CTAB
100mM Tris-HCl pH 8.0
20mM EDTA
1.4M NaCl
1% (w/v) polyvinylpyrrolidone

CTAB 10x buffer:

10% (w/v) CTAB
0.7M NaCl

CTAB precipitation buffer:

1% CTAB
50mM Tris-HCl pH 8.0
10mM EDTA pH 8.0

High salt TE buffer:

10mM Tris-HCl pH 8.0
1mM EDTA pH 8.0
1M NaCl

2.3.3.6. *Transformation and maintenance of Arabidopsis cell suspension cultures*

Cell suspension culture is a homogenous population of rapidly dividing plant cells in liquid media. It is ideal to get larger amount of plant material relatively quickly for e.g. biochemical purposes. Protein expression can be easily and relatively quickly studied in this system. Nevertheless, its disadvantage is that it has no organ and tissue structure. Basic organ modeling is possible using root derived or leaf originated culture forms or by triggering cell differentiation (e.g., embryogenesis) using various combination of plant hormones. Culture media ingredients for both types of cell cultures are described under 2.2.2.3. and 2.2.2.4.

Propagation of cell culture: To 10-15 ml one week old culture 35-40 ml fresh media is added, supplemented with the corresponding antibiotics.

2.3.3.6.1. *Cell culture transformation by Agrobacterium tumefaciens*

All the following steps are carried out in sterile conditions.

1. 20-25ml Agrobacterium (OD₆₀₀: 0.8-1.0) suspension is collected by centrifugation in a Falcon tube in a suitable centrifuge at 4000rpm for 20 min
2. The bacteria are gently resuspended in the corresponding Arabidopsis cell suspension medium and centrifuged again. (This step removes the antibiotics from the bacterial medium). The pellet should be about 100-200µl. Resuspend the bacteria in 1-2 ml Arabidopsis cell culture medium, then the bacteria are ready to use.

3. Collect Arabidopsis cells from 50ml 1-week-old cell suspension culture in a falcon centrifuge at 1000rpm for 1 min.
4. When preparing a double transformant cell suspension line, wash the starting single transformant cell suspension once with sterile cell suspension medium containing no antibiotics.
5. Resuspend 10-20 ml of Arabidopsis cell pellet in the corresponding cell culture medium to 50ml in the sterile hood. Transfer the cells into a sterile 250ml Erlenmeyer flask with a 25 ml serological pipette.
6. Add 1ml of the Agrobacterium suspension to 50ml Arabidopsis cell suspension. Close the flask with a sterile paper plug (sterilized together with the flask) and cover the plug with alufoil.
7. Incubate the cells with gentle agitation (120rpm) for 2-3 days. When using root derived culture, incubate in the dark.
8. After 3 days the cells are centrifuged in a Falcon centrifuge at 1000rpm for 1min, which separates the Arabidopsis cells from the majority of Agrobacteria. Discard the supernatant, and transfer the plant cells into a fresh flask.
9. Add cefotaxime to 200 μ g/ml and tricarcillin to 150 μ g/ml end concentration to stop bacterial growth. Add selection antibiotics in the required concentration (Km 50, Hyg 15). Incubate the culture for a few days, but check it every day. If the cell lysis is too intensive, change the medium.
10. In the first weeks subculture is performed by keeping the majority of living cells. If there are many cells, half of the culture is transferred into new medium, if there are fewer cells, the cells are sedimented by leaving the flask undisturbed for a few minutes and the supernatant is removed by a sterile pipette. Then, the cells are supplied with fresh medium (with antibiotics) and transferred into a new flask. The cultures have to be passed regularly in every 7 days.

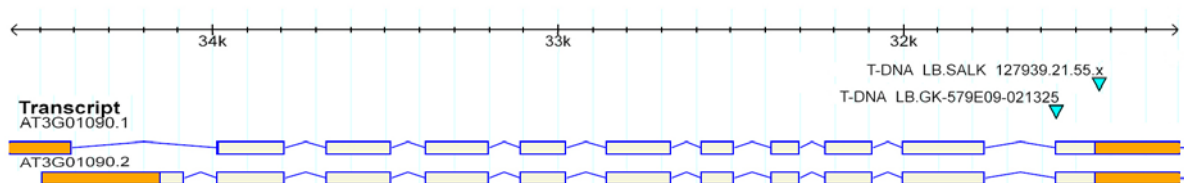
3. RESULTS

3.1. T-DNA INSERTION MUTATIONS IN GENES ENCODING ARABIDOPSIS SNRK1 KINASE SUBUNITS AND UPSTREAM ACTIVATING KINASES

3.1.1. Isolation of a T-DNA insertion mutation in the SNRK1 α catalytic subunit gene AKIN10 (At3g01090)

In our research group, Kenneth Berendzen has previously identified two insertion mutant alleles SAIL_834G03 and SALK_127939 of the *AKIN10* gene encoding a catalytic α -subunits of *Arabidopsis* SnRK1 kinases. Both of these insertions are located outside of the *AKIN10* coding region, one 603 bp upstream of the start codon and the other 4 bp downstream of the stop codon, respectively. These insertion mutants did not show any phenotypic alteration related to SnRK1 kinases. Screening of the Koncz and Wisconsin collections could not identify additional SnRK1 α mutant alleles in *AKIN10* and in its close relative *AKIN11*, but three T-DNA insertion mutants could be isolated in the *AKIN12* (At5g39440) gene that encodes a seed specific third *Arabidopsis* SnRK1 α variant (SAIL_598H08, SALK_053616 and Koncz 7986). Due to overlapping expression patterns of *AKIN11* and *AKIN12* during embryo and seed development, none of the *akin12* mutants showed alteration in seed development, and stress, sugar and hormone responses. In addition, 9 point mutations were identified by TILLING in the *AKIN* genes without yielding a reliable mutant phenotype.

Recently, we found that an additional AKIN10 mutant allele exists in the GABI-KAT collection (GABI_579E09), which is discussed here. Sequence data deposited in the Arabidopsis thaliana Integrated Database (www.atidb.org) indicated that the insertion is located in the last exon corresponding the extreme C-terminus of AKIN10 at the sequence position 1426 of AKIN10 ORF, which is 1539 bp (Figure 1). Upon selecting sulfadiazine resistant plants carrying the GABI_579E09 T-DNA insertion genomic DNA was extracted from 10 x 10 T2 lines using the CTAB method, and analyzed by polymerase chain reaction to search for homozygous mutant lines. For genotyping two gene specific oligonucleotide primers were designed to the ends of AKIN10 gene (AKIN10 5' and AKIN10 3') and two additional primers were used which were specific to the right and left border sequences of the T-DNA (GABI RB and FISH1, respectively; Figure 2).



Junction sequence: AKIN10_GABI_579E09
 TGATGGTGAAACAGTGTATAAAACTCGGGACGACAAGTATCTACTG
 LB 2593

Figure 1. Location of the T-DNA inserts in the GABI_579E09 mutant AKIN10 allele.

The downstream junction of the T-DNA insert is located in the last exon at position 1426 of At3g01090.1 coding sequence. Deletion of the original sequence due to T-DNA integration is indicated in red. (The upstream junction sequence has not been determined.) The number indicates nucleotide position in the genomic sequence related to the start codon.

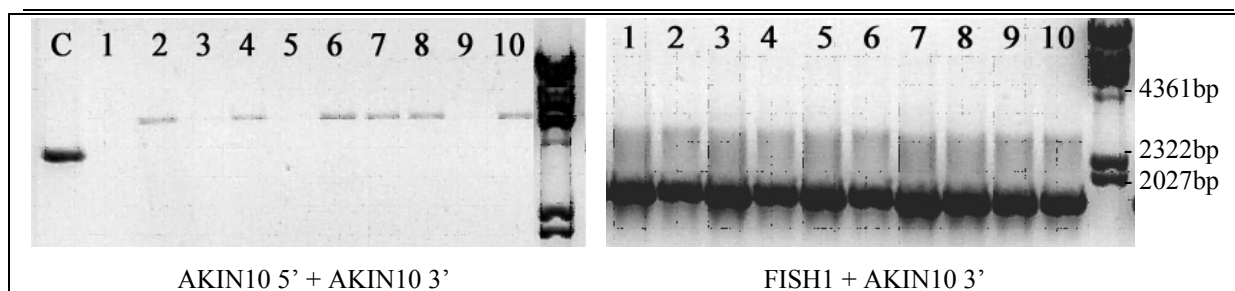


Figure 2. Identification of a homozygous AKIN10 GABI_579E09 T2 insertion mutant lines by PCR-analysis.

Ten individual T2 progeny was analyzed by PCR using combinations of AKIN10 5' (5'-TCATTTCTGAATCGGGTACGAGAGAT-3') and AKIN10 3' (5'-CAGGCGACGACACGAAGCGAGTTT-3') gene specific primers with the FISH1 (5'-CTGGGAATGGCGAAATCAAGGCATC-3') left border specific and GABI RB (5'-TTCCATTGCCAGCTATCTGTAC-3') right border specific primers. The AKIN10 5' + GABI RB and AKIN10 5' + FISH1 combinations did not yield a PCR product. Therefore, the upstream junction sequence remained unknown. The expected product size of gene specific primers is 4.3 kb (C = wild type genomic DNA template control).

3.1.2. SnRK1 β subunit alleles in public T-DNA insertion mutant collections

In *Arabidopsis* there are three SnRK1 beta subunits, AKIN β 1 (At5g21170), AKIN β 2 (At4g16360) and the atypical AKIN β 3 (At2g28060) that contains no N-terminal glycogen binding domain (Figure 3.). We have identified mutant alleles for AKIN β 1 in the GABI-KAT (GABI_235B06), Syngenta (SAIL_40_A07) and SALK (SALK_008325) collections. Characterization of these insertion mutants showed that in all three alleles the T-DNA insertions were located in the first intron. Here we present therefore only the GABI and SALK alleles. We also identified a T-DNA insertion mutation (SALK_037416) in the AKIN β 2 gene but failed to find an insertion mutation in AKIN β 3 in the publicly available collections and by screening insertion mutant lines generated in our laboratory (Figure 3.). The mutant screening approaches yielded also T-DNA insertion mutations in the 5'-UTR regions of AKIN β 2 and AKIN β 3, but these were not used because the SALK, SAIL and GABI T-DNA insertions contain a CaMV35S promoter upstream to the left border junction and thus in these lines the AKIN β 2 and AKIN β 3 genes are transcribed by the 35S promoter (i.e., leading to overexpression of corresponding transcripts).

For PCR-based genotyping gene specific oligonucleotides AKIN β 1 5', AKIN β 1 3', AKIN β 2 5', AKIN β 2 3', AKIN β 3 5' and AKIN β 3 3' were used in combinations with T-DNA border sequence specific primers [FISH1 (LB), FISH2 (RB), SALK LB, GABI RB] (Figure 4). The GABI mutants were selected on sulfadiazine but in the SALK lines silencing of the kanamycin resistance gene (NPTII) prevented the identification of transformants using antibiotics selection and therefore they were not selected prior to genotyping. We found that in both SALK and GABI lines the T-DNA insertions were frequently represented by inverted repeats formed by ligation of T-DNA right boundaries. In such arrangement, the LB left border regions are joined to plant DNA and therefore the CaMV35S and mannopine synthase 2 promoters located upstream of LB junctions transcribe in both 5' and 3' direction of truncated genes. Therefore, all screens were first performed with the LB + 3' gene specific primer combination along with gene specific primer pairs.

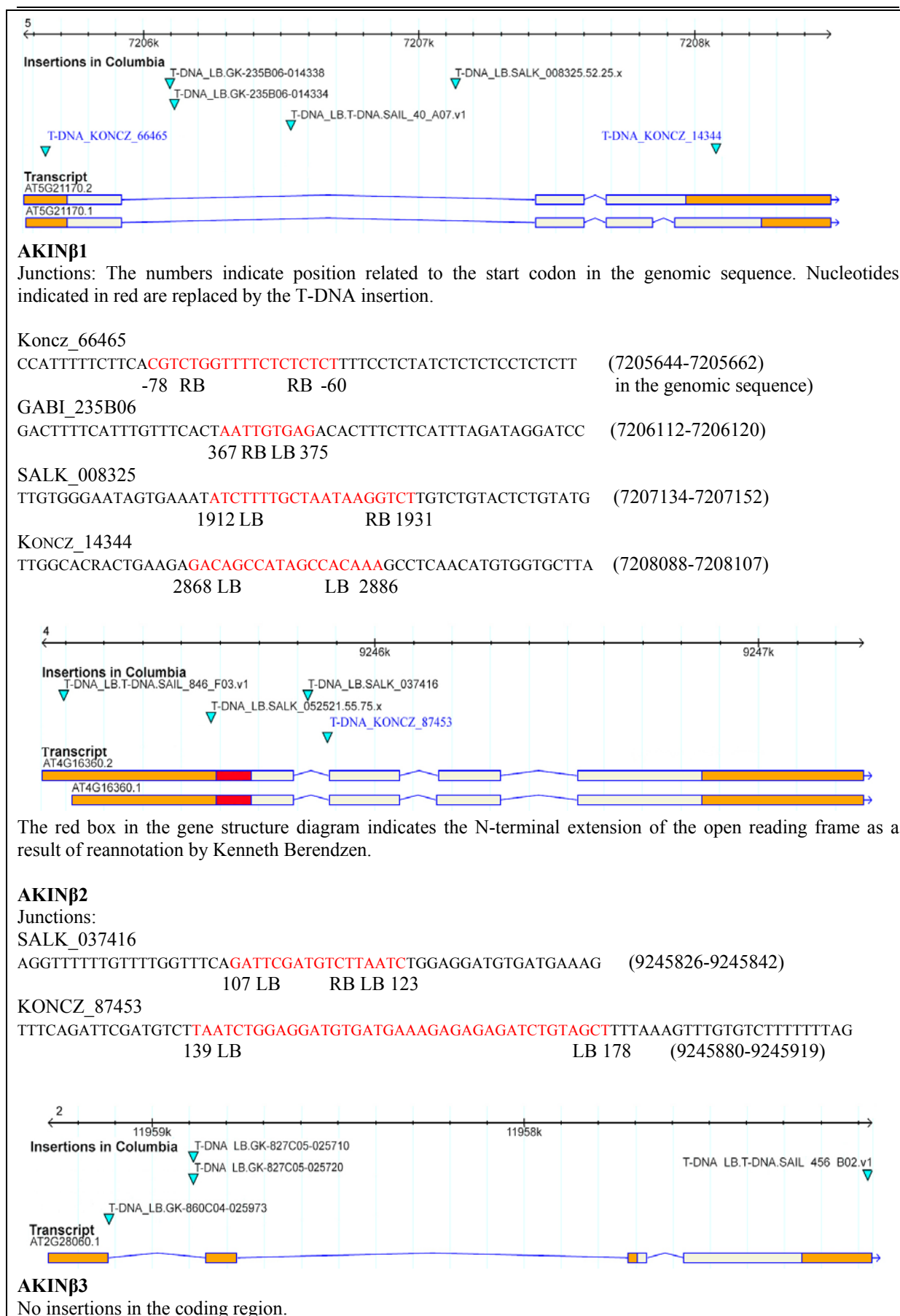
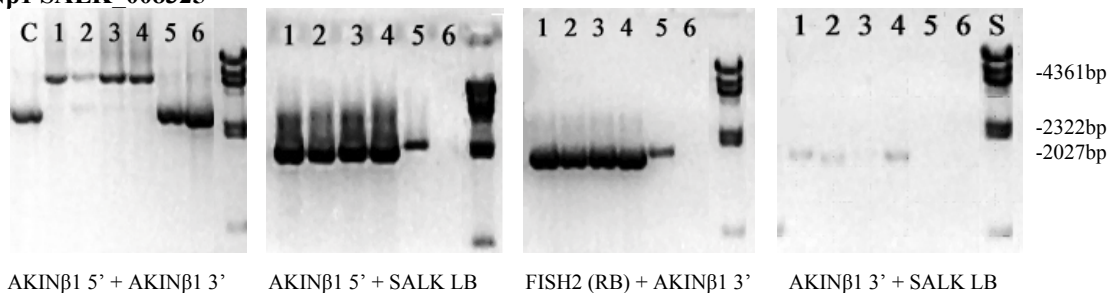


Figure 3. Details of SnRK1 β subunit mutations

AKINβ1_SALK_008325

AKINβ1 5' + AKINβ1 3' AKINβ1 5' + SALK LB FISH2 (RB) + AKINβ1 3' AKINβ1 3' + SALK LB

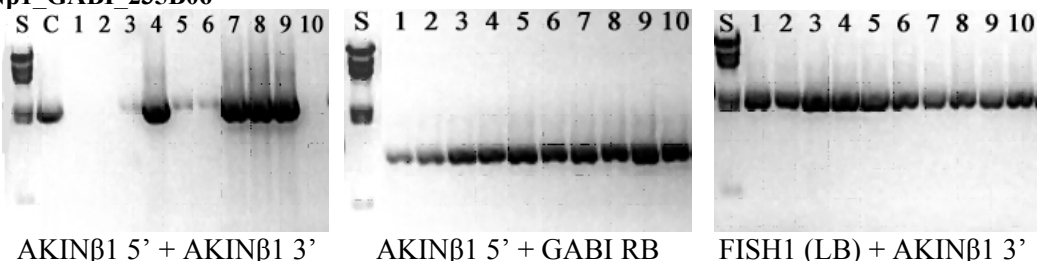
expected sizes: 3.0 kb for wt

1.9 kb

1.1 kb

-

Samples 1, 2, 3 and 4 are homozygous mutants, sample 5 is heterozygous and sample 6 is wild type
[C = genomic DNA control, S = molecular weight standard (bacteriophage λ *Hind*III digest)]

AKINβ1_GABI_235B06

AKINβ1 5' + AKINβ1 3'

AKINβ1 5' + GABI RB

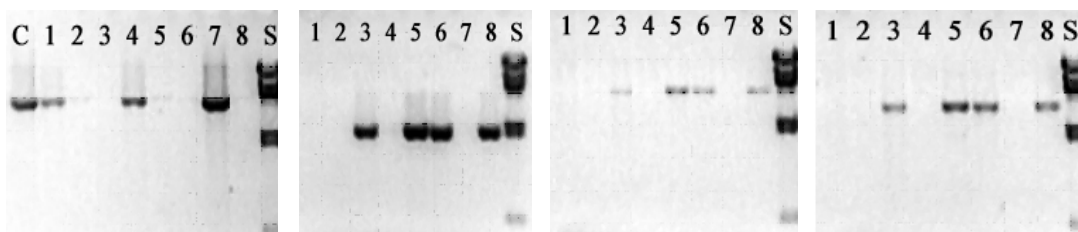
FISH1 (LB) + AKINβ1 3'

expected sizes: 3.0kb

0.8 kb

2.2 kb

Samples 1, 2, and 10 were selected as homozygous mutants (3, 5 and 6 are ambiguous)

AKINβ2_SALK_037416

AKINβ2 5' + AKINβ2 3'

AKINβ2 5' + SALK LB

AKINβ2 5' + FISH2

AKINβ2 3' + SALK LB

expected sizes: 5.24 kb

-

3.3 kb

1.9 kb

Samples 3, 5, 6 and 8 are homozygous for the AKINβ2 mutation.

primers

AKINbeta1 5' 5'-GACCATCTCTATTCTAACCCACC-3'
 AKINbeta1 3' 5'-GGTACCGTGTGAGCGGTTTGTAG-3'
 AKINbeta2 5' 5'-GAAGCTTCAGATCACGACTTGTTCC-3'
 AKINbeta2 3' 5'-ATCACGGCTCAGCAGGTTGGTTCAG-3'
 SALK LB 5'-TTTGGGTGATGGTTCACGTAGTGGG-3'
 GABI RB 5'-TTCCATTGCCAGCTATCTGTCC-3'
 FISH2 5'-CAGTCATAGCCGAATAGCCTCTCCA-3'
 FISH1 5'-CTGGGAATGGCGAAATCAAGGCATC-3'

Figure 4. Isolation of homozygous *akinβ2* mutants

3.1.3. Isolation of SnRK1 β subunit mutations in the Koncz collection

In order to isolate additional mutant alleles for the SnRK1 β subunit genes, a T-DNA insertion mutant collection (referred to as “Koncz collection”) generated by our laboratory was also screened. The Koncz collection of T-DNA-tagged *Arabidopsis thaliana* plants contains 92500 transgenic lines. Identification of individual mutations in the Koncz collection employs a PCR based screen in two rounds. The mutant population was split into pools each containing 100 different mutant lines. Genomic DNA was extracted from the pools and arranged into a two dimensional array. Aliquots of the DNA extracts located in one row or one column of the array are pooled again and serve as a template for PCR reaction, thereby reducing the total number of PCR reactions necessary for the identification of one pool. The result of this screen is a pool of 100, which is screened further with the same strategy by arranging its 100 members into a 10x10 array. Each screen requires a pair of gene specific primers designed upstream and downstream to the gene of interest and these primers are used in combination with T-DNA right and left border specific primers.

The screen resulted in the identification of a mutation in the *AKIN β 1* coding sequence (KONCZ_14344) and another tag in the 5'-UTR (KONCZ_66465), from which the one in the coding sequence was processed further. Due to alternative splicing event the KONCZ_14344 mutation is located in the open reading frame only in case of the longer splicing variant (At5g21170.1) whereas in the shorter variant the insertion is found in the 3'-UTR. One additional mutation was identified in the first intron of *AKIN β 2* (KONCZ_87453), but no mutations were found in *AKIN β 3*.

The T2 generation of mutant seeds was germinated on hygromycin and the 3:1 resistant to sensitive segregation ratio indicated that there is probably one insert in the mutant lines. Homozygous mutants were identified by PCR analysis (Figure 5). As additional test, the T3 generation progeny of identified homozygous plants was germinated on hygromycin plates and no sensitive seedlings had been found.

3.1.4. Analysis of transcript level of mutated SnRK1 beta subunit genes

In order to test whether the T-DNA insertions caused knockout mutations, RNA was extracted from the mutant plants, cDNA was prepared and the samples were analyzed by RT-PCR. Potential transcription of the target gene sequences located downstream of LB insert junctions carrying the CaMV35S promoter was also tested. Primers were designed to the 5' and 3' ends of coding sequences of each SnRK1 beta subunit genes and used in combination with right and left border specific primers (Figure 6.) In case of *AKIN β 1* SALK_008325 allele the 5'-segment of coding is transcribed from either direction. The RT-PCR reaction was carried out with 40 cycles with 60°C annealing temperature and 8 min extension time.

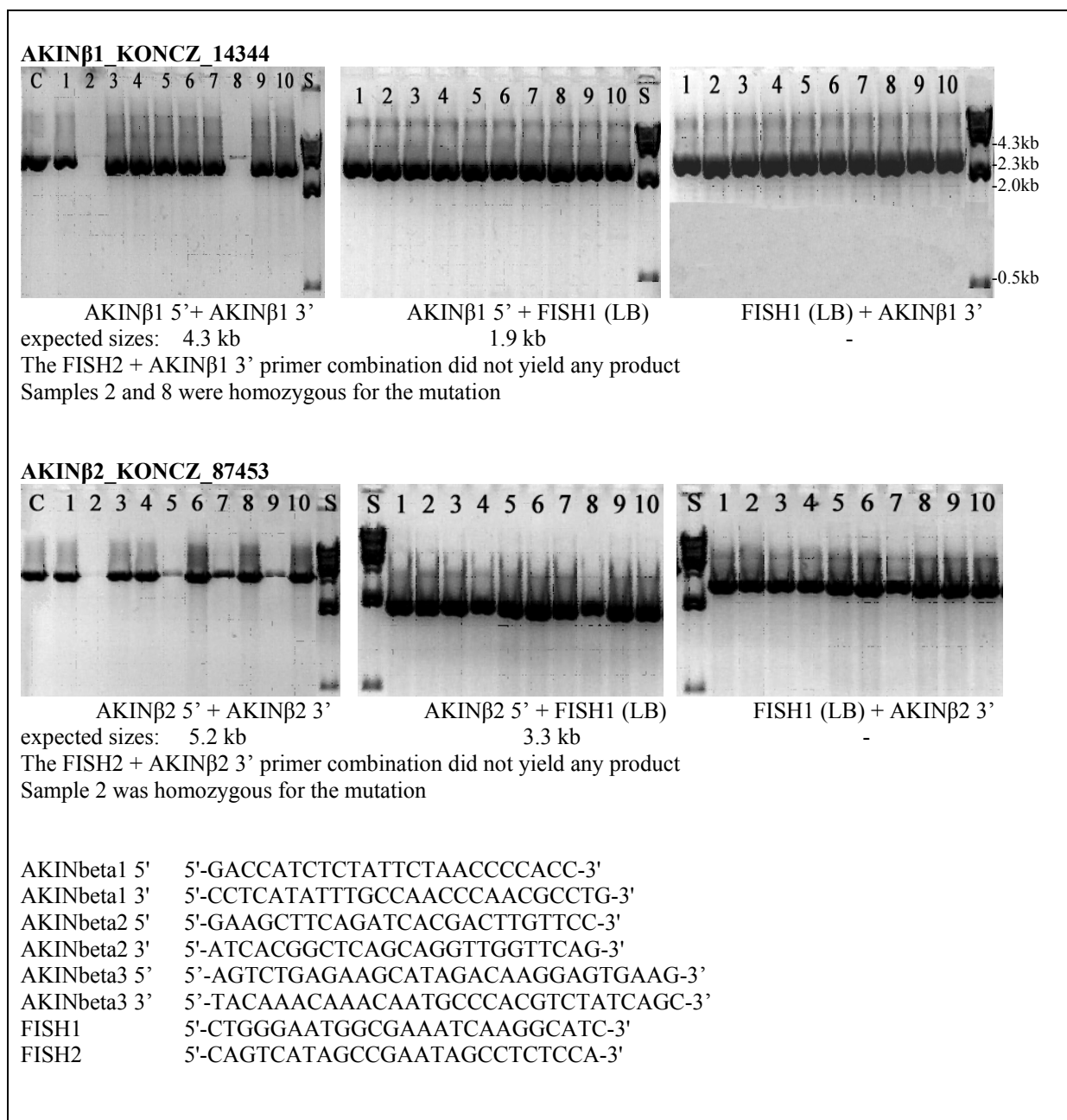


Figure 5. Identification of homozygous mutant lines for the AKINβ1 and AKINβ2 KONCZ alleles

3.1.5. Generation of double AKIN beta subunit mutants

AKINβ1 SALK 008325 x AKINβ2 KONCZ 87453 and AKINβ1 SALK 008325 x AKINβ2 SALK 037416 double mutants were generated by crossing the mutant *Arabidopsis* plants. Double homozygous plants were identified in the F2 generation using PCR screening with the same combinations of primers used for the analysis of single mutants.

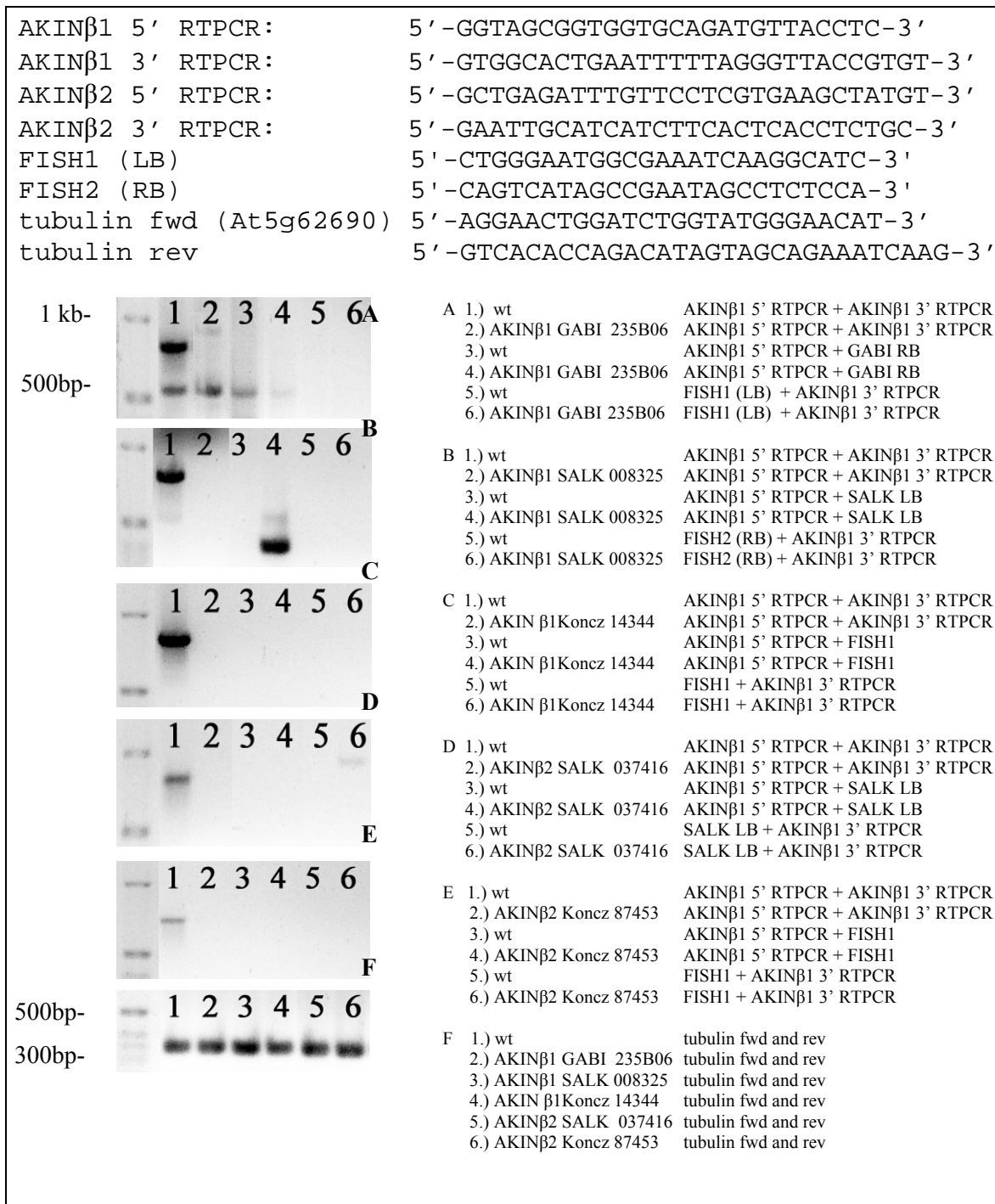


Figure 6. RT-PCR analysis of the SnRK1 beta subunit mutants

3.1.6. Isolation of homozygous T-DNA insertion mutants for two SnRK1 upstream activating kinases

Based on sequence homology to yeast Snf1 upstream activating kinases, two genes were identified recently in *Arabidopsis* as putative SnRK1 upstream kinases [37, 57], AtSnAK1 (At5g60550) and AtSnAK2 (At3g45240), which can complement the yeast *elm1sak1tos3* triple mutation. T-DNA insertion mutants are available for both genes in the public collections (Figure 7.). Here the

AtSnAK1_SALK_015230, AtSnAK1_SALK_000044 and AtSnAK2_SALK_142938 mutations are described.

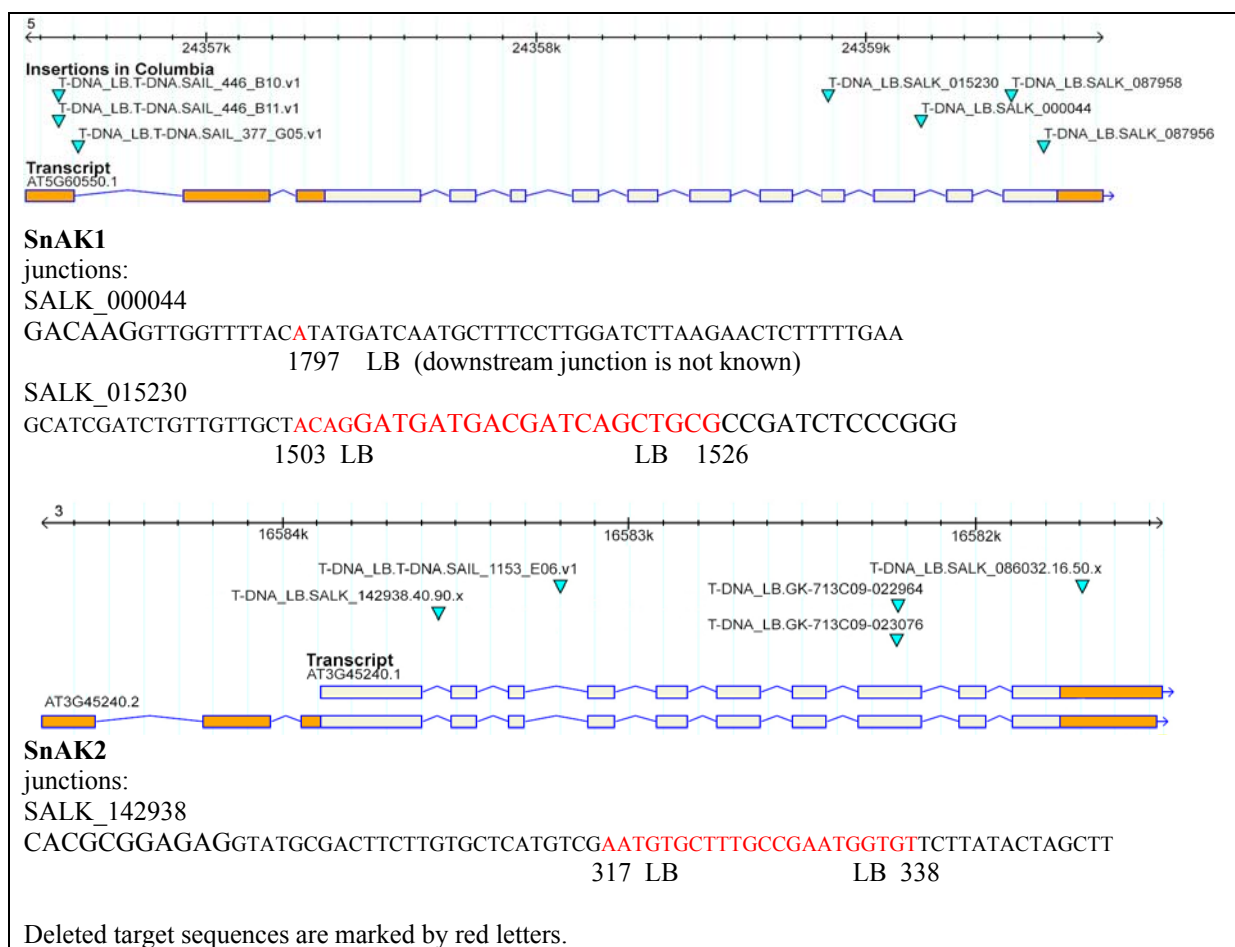


Figure 7. T-DNA insertion mutations in genes of SnRK1 upstream kinases SnAK1 and SnAK2

In order to isolate homozygous mutants, genomic DNA was extracted from 10 individual T2 lines and analyzed by PCR. A gene specific oligonucleotide pair was designed for both genes, which were used in combination with T-DNA border specific primers (FISH2, SALK LB, Figure 8.)

3.1.7. Phenotypic analysis of SnRK1 subunit mutants

During germination, seedling development and growth in soil none of the homozygous plants showed any obvious phenotypic alteration compared to wild type plants. To test for possible alteration of normal sugar and ABA responses, homozygous mutant seeds were germinated on 0.5x MS medium containing either 3% glucose, or 5% sucrose, or 1 μ M ABA or 2 μ M ABA. Germination of the mutant seeds was followed by monitoring the liberation of cotyledons from the testa. No difference could be observed between the germination speeds of the seeds. Despite 3 days of stratification treatment at 4°C, the germination speed showed relatively great differences between and within the sample populations, especially when treated with ABA. Although, the germination kinetics was different between the samples, it was not consequent between repeated experiments. (The results are

summarized in Appendix 1.) As sugar content of 0.5MS seed medium (i.e., 0.5% sucrose) could also cause some variation in the germination speed, we also tested germination characteristics of mutants on sugar free medium, as well as the development of seedlings on agar solidified distilled water plates and germination of the mutants for 10 days in the dark. These assays revealed no significant differences between the different single *akin10*, *akinβ1*, *akinβ2*, *snak1*, *snak2* and *akinβ1akinβ2* double mutants compared to wild type seedlings. The latter observation indicated that *Arabidopsis* can tolerate inactivation of two from three known putative subunits of SnRK1 kinases without showing observable alterations in sugar and ABA responses and development.

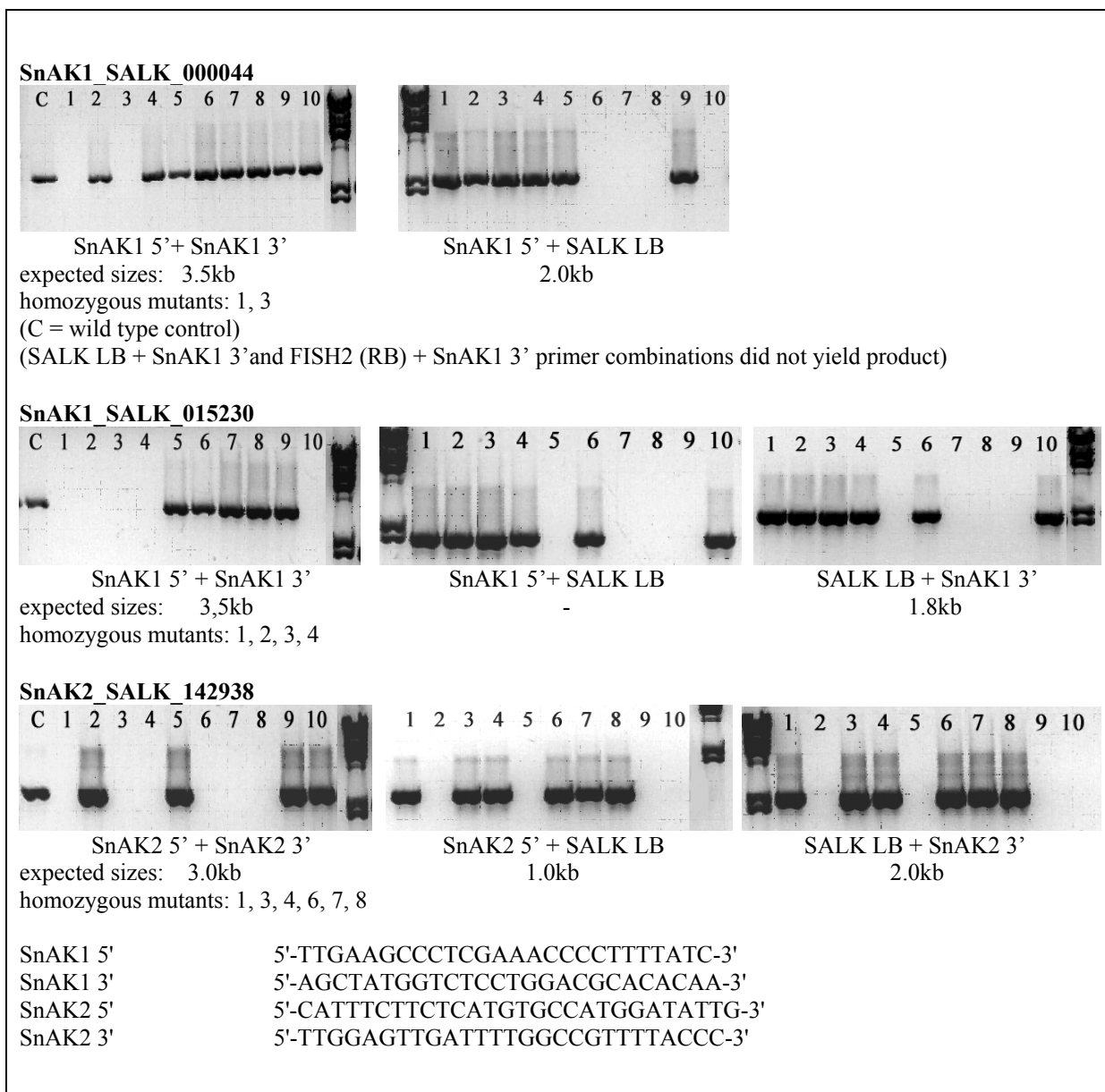


Figure 8. Isolation of homozygous SnAK mutants

3.2. OVEREXPRESSION OF SNRK1 BETA SUBUNITS

3.2.1. Construction of a CaMV35S promoter driven GFP tagging vector

In order to test, whether the *Arabidopsis* SnRK1 β subunits undergo subcellular relocalization in response to nutritional stress analogously to the yeast Snf1 β subunits, GFP-tagged SnRK1 β constructs were prepared. A CaMV35S promoter driven GFP tagging vector was created by reconstruction of the pPILY HA epitope tagging vector [224] (see Appendix 2 for the map of pPILY). The intronic HA tag was substituted with the GFP version “emerald” (the “emerald” GFP template was a courtesy of Dr Guido Jach). The GFP fragment was obtained by PCR amplification using the primers GFPfwd and GFPprev, which incorporated an *NcoI* restriction endonuclease site to the 5' end of the PCR product (including the start codon within the *NcoI* site), and a *BamHI* site downstream of the stop codon. This PCR fragment was inserted into *NcoI*-*BamHI* sites of pPILY vector. In the resulting GFP tagging vector (pGFP), the *NcoI* site provides a cloning site for creating and expression of C-terminal GFP fusion constructs. The expression cassette can easily be subcloned into the pPCV002 (Km^R) or pPCV 812(Hyg^R) binary vectors by the rare cutting *NotI* restriction endonuclease.

3.2.2. Overexpression of GFP-tagged SnRK1 β subunits

Coding sequences of all three AKIN β subunits were cloned to the *NcoI* site of pGFP vector. The AKIN β subunit cDNAs were PCR amplified from a cDNA library formerly prepared from *Arabidopsis* cell suspension culture (provided by a former colleague, Klaus Salchert). Primer pairs were designed for all three AKIN β subunits by incorporating *NcoI* sites to both ends of the PCR product (AKIN β 1GFPfwd + AKIN β 1GFPprev, AKIN β 2GFPfwd + AKIN β 2GFPprev, AKIN β 3GFPfwd + AKIN β 3GFPprev. *NcoI* does not cut in any of the AKIN β subunits.) After cloning the AKIN β cDNAs into pGFP, the orientation of inserts was determined (i.e., by *HindIII* + *BglII* for AKIN β 1, *HindIII* for AKIN β 2 and *NaeI* + *BglII* for AKIN β 3) and subsequently the correct clones were sequenced with a 35S promoter primer (AKIN β 1 is 855bp, AKIN β 2 is 870bp and AKIN β 3 is 345 bp therefore unidirectional sequencing was sufficient). The expression cassettes were excised by *NotI* and inserted into a single *NotI* site of pPCV 812-*NotI* binary vector (Hyg^R). The resulting binary vectors were transformed into the *Agrobacterium* strain GV3101 (pMP90RK) and used for transformation of *Arabidopsis* plants, as well as root- and leaf-derived cell suspension cultures. All plant materials were selected for hygromycin resistance marker of pPCV812-*NotI* T-DNA.

3.2.3. Analysis of SnRK1 β -GFP overexpressing plants and suspension cultures

GFP signal in cultured cells grown in MS medium was compared to that of cells transferred to 90mM sorbitol solution or distilled water kept in darkness for 3-4 hours. Re-localization of the AKIN β proteins could not be assessed, because no GFP signal was detectable in the samples that were cultured in MS medium with 3% sucrose regardless growing them either in the light or in darkness. In contrast, in samples incubated in sugar free medium in the dark GFP signal could be readily detected,

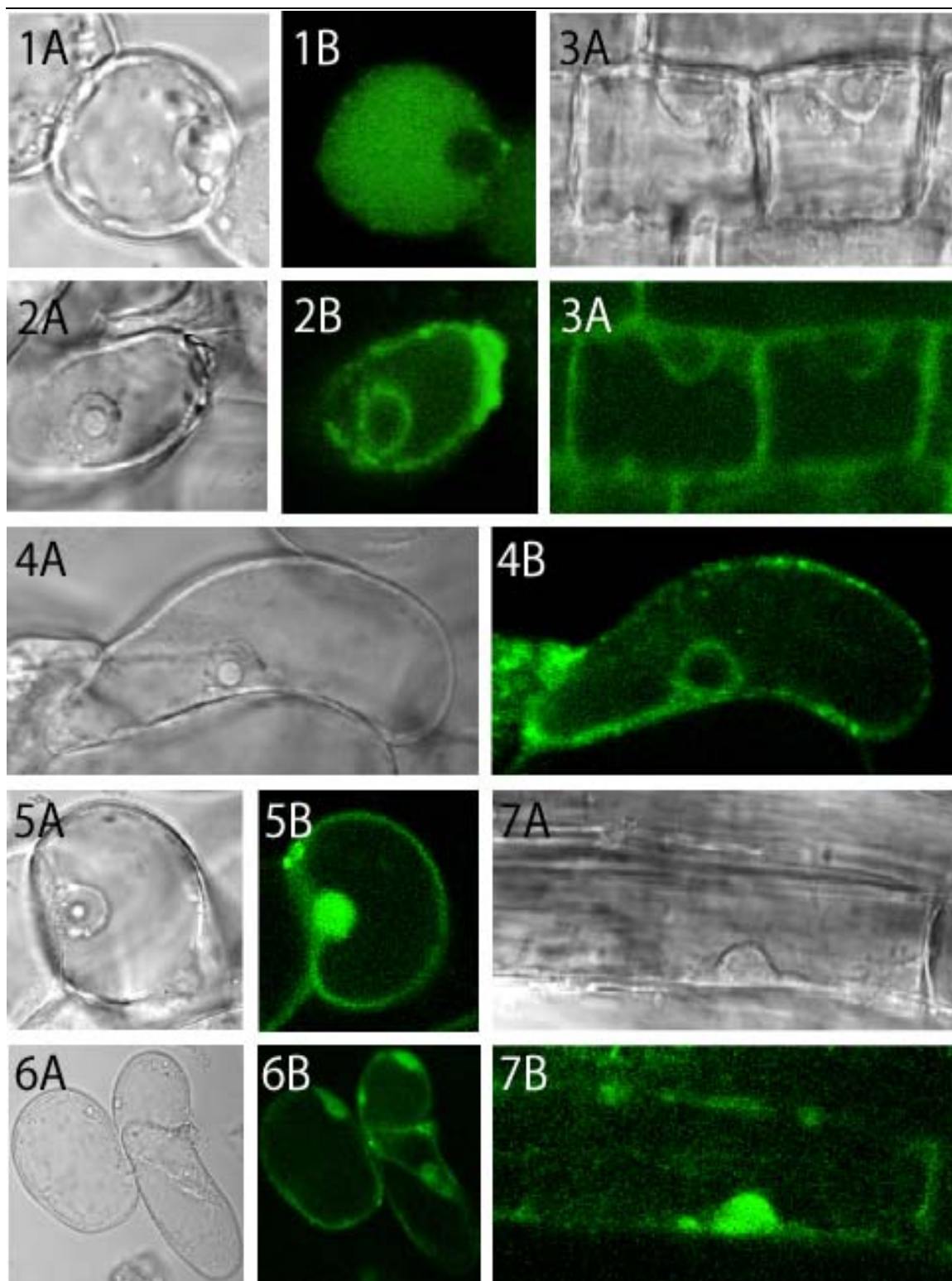
but it faded extremely quickly when exposed to strong blue light in the confocal microscope. The fading was quicker than normal photobleaching, since the initial GFP signal faded within a few seconds, causing a technical problem in capturing the images.

The GFP signal produced in AKIN β 1-GFP overexpressing suspension cultures appeared to be abnormal, since GFP was detectable throughout the cell excluding the nuclear matrix. (The image is shown only to illustrate that even in this abnormal state of the cell AKIN β 1 is excluded from the nuclear matrix.) AKIN β 1 in seedlings and AKIN β 2 in both cell suspensions and seedling material looked mostly associated to the plasma-membrane and the nuclear envelope, but were not detected in the nuclear matrix. At lower levels, AKIN β 1 and AKIN β 2 were also detected in the cytoplasm as intense fluorescent spots that may represent artificial aggregates (pers. comm. with Dr Elmon Schmelzer). By contrast, AKIN β 3 was present mostly in the nuclear matrix but at lower level was also detected in the cytoplasm (see cytoplasmic bridges in Figures 9/6B). AKIN β 3 was also found in the peripheral region of the cell. This localization probably corresponds to periplasmic cytoplasm, because AKIN β 3 does not carry a myristoylation motif, which would target it to the plasma membrane. In comparison, AKIN β 1 and AKIN β 2 could not be detected in cytoplasmic bridges. Expression of all three AKIN β proteins could be detected in both photosynthetic and root tissues of seedlings and in green and root derived cell suspension cultures depleted for sucrose. The observed rapid sugar-induced degradation of AKIN β proteins suggested the possibility of proteasomal degradation, for which evidence is given below in the biochemical chapter. The AKIN β -GFP fusion protein overexpressing heterozygous plants were grown to adult phase, but no phenotypic alteration could be observed compared to wild type *Arabidopsis* plants.

Figure 9. Expression of GFP-tagged SnRK1 beta subunits

The Figure is displayed on the next page. All photos were taken from cells and tissues exposed to sugar free medium and darkness.

1.A and 1B	AKIN β 1-GFP in root derived cell suspension culture. Aberrant cells, but no signal is detected in the nucleus.
2A and 2B	AKIN β 2-GFP in root derived cell suspension culture. GFP signal is detected in the plasmamembrane and nuclear envelope.
3A and 3B	AKIN β 1-GFP in <i>Arabidopsis</i> root cells.
4A and 4B	AKIN β 2-GFP in root derived cell suspension culture. GFP signal is detected mostly in the plasmamembrane and nuclear envelope.
5A and 5B	AKIN β 3-GFP in root derived cell suspension culture. GFP signal is detected in the nucleus and subcortical cytoplasm.
6A and 6B	AKIN β 3-GFP in root derived cell suspension culture. GFP signal is detected in the nucleus and cytoplasm. Note the signal in the cytoplasmic bridge.
7A and 7B	AKIN β 3-GFP in root epidermal cell of an <i>Arabidopsis</i> seedling.



3.2.4. Transcription regulation of AKIN β and other SnRK1 subunit genes

Data from the Genevestigator database were collected to get information about the expression profiles of SnRK1 β subunit genes in diverse *Arabidopsis* tissues and developmental stages (Figure 10.). In our experiments the most abundant accumulation of GFP-tagged SnRK1 β subunit proteins were observed in vascular tissues (Figure 11).

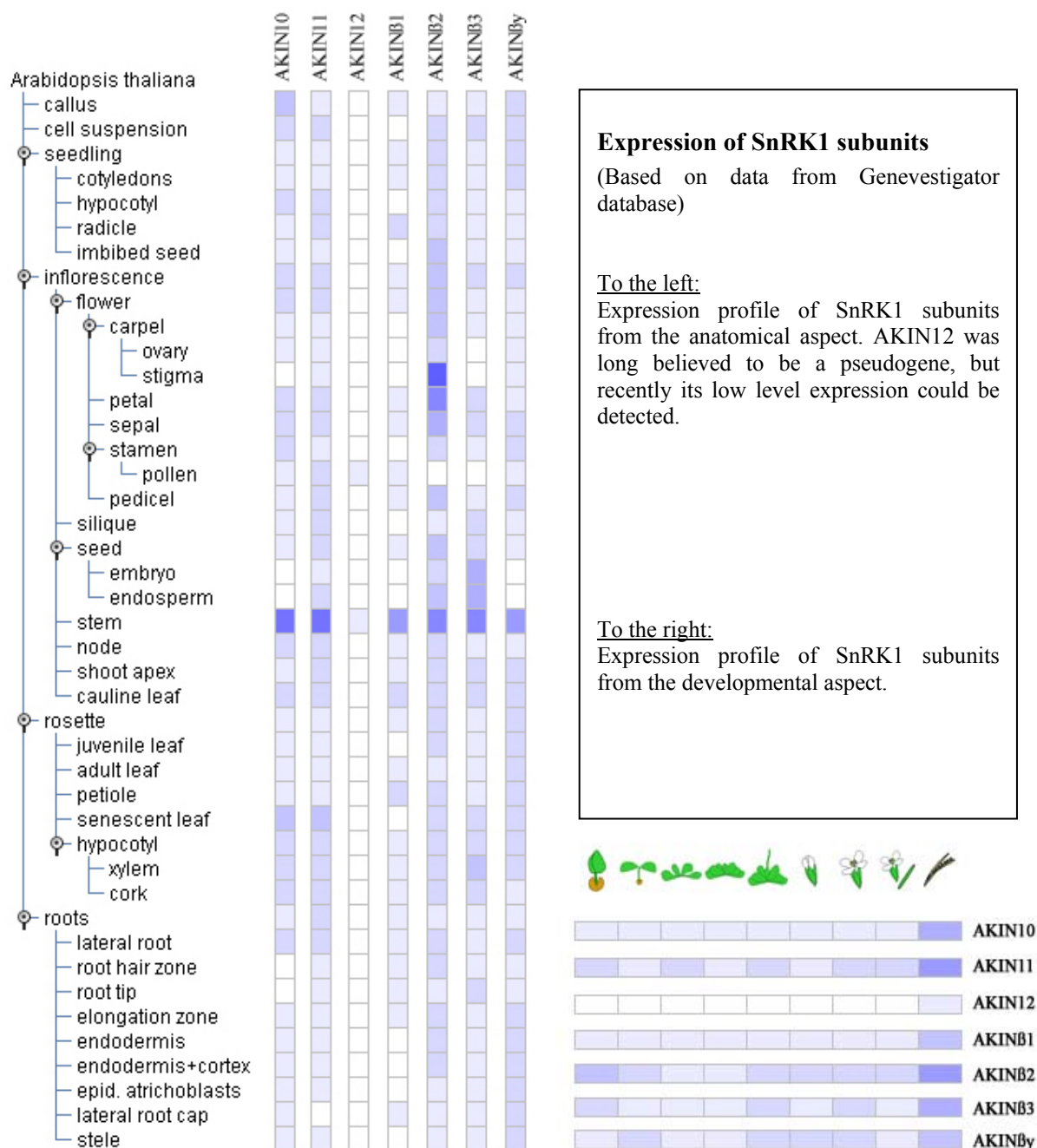


Figure 10. Developmental regulation of transcription of *SnRK1* subunit genes

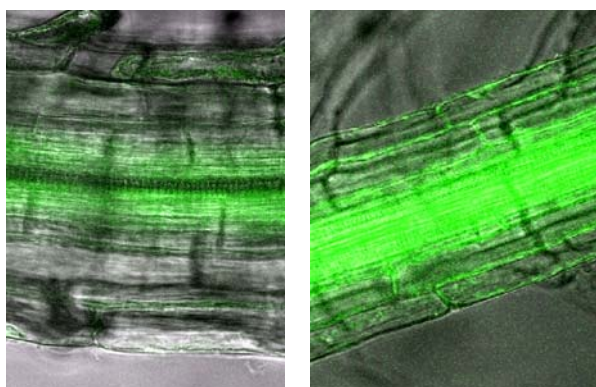


Figure 11. AKINβ1-GFP (A) and AKINβ2-GFP (B) proteins are stable and accumulate in vascular tissues of overexpressing plants

3.3. DEVELOPMENT OF A BIOCHEMICAL APPROACH FOR ISOLATION OF SNRK1 COMPLEXES FROM ARABIDOPSIS

In the past years, our laboratory invested a considerable effort into isolation of proteasome-associated SnRK1 complexes from various plant materials. This approach primarily aimed at the identification of SnRK1-interacting proteins, especially in the proteasomal context. In these trials, generally ion exchange chromatography was applied as the first step followed by gel filtration or glycerol gradient centrifugation to separate differently sized protein complexes, and finally immunoaffinity chromatography to pull-down the epitope labeled SnRK1 subunits. Generally, two candidate interacting proteins (i.e., SnRK1 subunit and its candidate interacting partner) were tagged with HA (influenza haemagglutinin) and cMyc (human cMyc peptide) epitope tags, respectively, against which monoclonal antibodies and immunoaffinity matrices were commercially available. One of the tags was used for isolation of protein complexes by immuno-affinity chromatography and the other for detection of the interacting partner. Additionally, several specific antibodies were used to detect proteasomal components in the purified complex. Final aim was the isolation of sufficient amounts of protein complexes for mass spectrometric analysis and identification of yet unknown subunits of SnRK1-proteasome complexes. However, due to high cost and high background of immunoaffinity chromatography matrices and low yield of protein complexes obtained by specific peptide elution and competition, these approaches were severely handicapped. Further potential problems were caused by the high proteolytic activity. As proteasomal inhibitors, such as MG132, are extremely expensive, their application throughout all steps in processing large sample quantities was not feasible. In addition, after ion exchange chromatography and gel filtration or glycerol gradient centrifugation immunoblot detection was necessary to identify the chromatographic fractions, which contained the protein complexes of interest. During this lengthy procedure the samples were either stored on ice (i.e., exposed to proteolytic activity), or frozen (i.e., which might lead to disintegration of high molecular mass protein complexes). These technical barriers raised a demand for a fast and robust purification method that provide high selectivity and sufficient capacity for handling large amounts of samples.

The use of histidin tag in nickel chromatography to purify proteins is a widespread technique in bacterial, yeast and human applications. However, in plants there are high levels of metal-binding proteins and therefore this method results in a high background. StrepII tag based affinity chromatography has also been used with success in plants, but only relatively small quantities of starting material can be applied to the Strep-affinity matrices because plant tissues contain biotin (vitamin H), which binds to the Strep-tactin Sepharose matrix and blocks the binding sites. (Avidin can be used to block the biotin in the sample before application to the chromatographic matrix, but it is extremely expensive and therefore not a practical solution with large sample quantities.) The combination of His and StrepII tags provides extremely high purification efficiency and widely used for isolation of proteins from yeast and mammals that are expressed by the help of commercially available vectors. However, so far no instance was reported on the use of this combination of affinity

chromatographies for successful isolation of recombinant proteins and protein complexes from plant tissues although, when using Ni-chromatography as first purification step biotin can be theoretically removed, and the subsequent Strep-purification is thus predicted to provide high purity.

3.3.1. Construction of an expression vector for tandem His-Strep tag affinity purification of plant proteins

In trials to isolate His-tagged proteins from *Arabidopsis* one contaminating protein accumulated to especially high level during nickel affinity purification (personal communication with Andreas Bachmair). This component was identified by mass spectrometric analysis and proved to be a putative cobalt-binding protein (PIP-L, PRL1 interacting partner-L, At1g15730), which carries homology to the *Pseudomonas denitrificans* CobW cobalt-binding protein. Certainly, the cobalt-binding properties are responsible for the high affinity to the Ni-matrix. We identified a histidine-rich low complexity sequence region carrying the putative cobalt-ion-binding domain. This histidine-rich region also contains several negatively charged residues (D, E), residues with non binding electron pair (N, S, T) and a cysteine, which might also play a role in metal-ion binding. The putative metal-binding sequence (highlighted in red bold) was exploited as natural histidine tag and it is referred to as PIP-L-tag.

PIP-L amino acid sequence:

MATLLKLDIATTFILAFIVPRANTSLNHRFASARLSTATVSLRTRKSSSFYSAALYSDSRRRRFHSAVASDSSL
AVVDDDEDIFDVASEILPDNRIPATIIITGFLGSGKTLLNHILTGDHGKRIAVIENEFGEVDIDGSLVAAQTA
GAEDIMMLNNGCLCCTVRGDLVRMISEMVQTKKGRFDHIVIETTGLANPAPIIQTFYAEDEIFNDVKLD
GVVTLVDAKHARLHLDEVKPEGYVNEAVEQIAYADRIIVNKTDLVGEPELASVMQRIKTINSMAHMKR
TKYGKVDLDYVLGIGGFDLERIESSVNEEEKEDRE**GHDDHHHGHDCDHHEHEHEHEHEHHSH**
DHTHDPGVGSVSIVCEGLDLEKANMWLGALLYQRSEDIYRMKGILSVQDMDERFVFQGVHEIFEGSP
DRLWRKDETRTNKIVFIGKNLNREELEMGFRACLI.

First, the Ni-binding capability and efficiency of the selected peptide sequence was tested using a bacterially overexpressed TRX-AKIN11-PIP-L protein. The clone was prepared by incorporating the PIP-L sequence into the AKIN11pET201 construct (see 3.4.1.). The PIP-L sequence was obtained by PCR amplification from an *Arabidopsis* cDNA library using the primers pip1fwd and pip1rev which both incorporated an EcoRI site. The PCR product was inserted to the EcoRI site at the downstream junction of the AKIN11pET201 construct. Pip1rev contained a stop codon, therefore the His tag in the original vector is not translated. The Ni-binding properties of PIP-L tag were practically identical to that of the conventional His₆-tag (Figure 12). The TRX-AKIN11-PIP-L protein also showed specific binding to a Co²⁺-containing resin (TALONTM BD Biosciences) and the purification factor achieved with Ni and Co²⁺ matrices was comparable (data not shown), although the patterns of contaminating proteins differed.

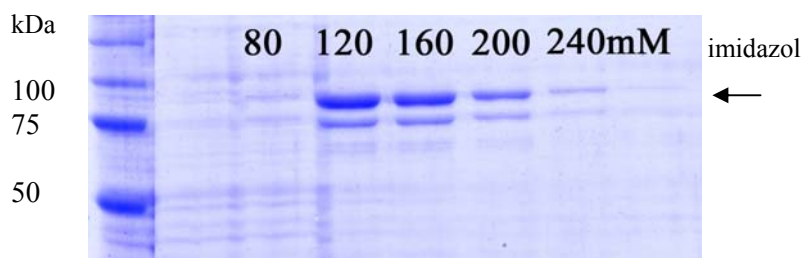
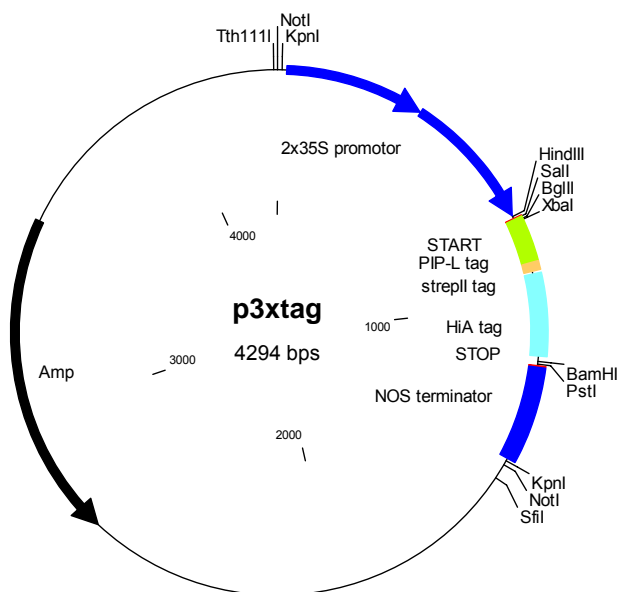


Figure 12. Imidazole gradient elution of TRX-AKIN11-PIP-L

An arrow shows the position of TRX-AKIN11-PIP-L protein. His₆-tagged proteins generally start to elute at 100 mM imidazole.

A vector for tandem affinity tag labeling (p3xtag) was designed to fuse genomic and cDNA sequences with coding sequences of PIP-L, StrepII and intronic HA tags to express C-terminally labeled proteins in plants (Figure 13.). In this combination, the HA tag was designed for control immunodetection, but in principle it can also be used as a third, immunoaffinity tag. The vector was created by modification of pMenchu (Sall-) HA-tagging vector. The 105 bp long PIP-L fragment was obtained by PCR-amplification from a cDNA library using 3xtagfwd and 3xtagrev oligonucleotide primers. 3xtagfwd incorporated *Hind*III-ATG-*Sal*I-*Bgl*II-*Xba*I sites upstream of the PIP-L coding region, whereas 3xtagrev contained a StrepII-tag (the bacterial version of Strep-tag was modified for optimal *Arabidopsis* codon usage) and a *Bam*HI site. The PCR-product was inserted into pMenchu (Sall-) vector as *Hind*III-*Bam*HI fragment into the *Hind*III-*Bgl*II sites. In this way, the vector carried a destroyed *Bgl*II site along with a formerly removed *Sal*I site located downstream of the cloning site. Therefore, the introduced *Sal*I, *Bgl*II and *Xba*I sites are unique sites, comprising the multicloning polylinker of the new vector. This pMenchu vector cassette can be transferred to the pPCV binary vectors as *Not*I fragment.



```

      HinDIII      Sall      BglIII  XbaI      PIP-L tag
AAGCTTATG GTC GAC AGA TCT AGA GGT CAT GAT GAT CAT CAC CAT GGT CAT GAC TGC
CAT GAT CAC CAC AAT GAG CAT GAG CAT GAG CAT GAA CAC GAG CAT CAC CAT TCT

                                StrepII tag (A.t. codon usage)      BamHI/BglII
CAT GAT CAC ACC CAT GAC AAG TGG TCT CAT CCT CAA TTC GAA AAA GGA TCT TAT CCA

      HA tag      intron
TAC GAT gtaagttctgcttctacctttgatatatataataaattatcattaattagtagtaataataatattttaaatatttttcaaaaataaaagaa

                                intron
tgtagtatatagcaattgcttttctgtagttataagtgtgtatattcaattataacttttctaatatatgaccaaaaattgtgtatgtgcag GTT CCA

      HA tag  filled Sall from pMenchu  BamHI  PstI  STOP
GAT TAT GCT ggt ega tcg acG GAT CCa CTG CAG TGA att c

```

Figure 13. Physical map and sequence of the coding region of PIP-L-Strep-HA tag of p3xtag tandem affinity tagging vector

3.3.2. Cloning of SnRK1 subunits into the p3xtag tandem affinity tagging vector

cDNAs encoding AKIN10 and AKIN11 were cloned into the p3xtag vector as *SalI-BglIII* and *SalI-XbaI* fragments respectively, after amplification with A10_3x fwd, A10_3x rev, A11_3x fwd and A11_3x rev oligonucleotide primers. Since constitutive overexpression of AKINs was predicted to be problematic based on former experiments, the tagged open reading frames were subcloned into the estradiol-inducible 35S promoter driven expression cassette of pER8 (Hyg^R) vector. To achieve this, the complete tagged reading frames of *AKIN10* and *AKIN11* were excised as *SalI-EcoRI* fragments from p3xtag thereby losing the 2x35S promoter. (Since an extra start codon was integrated into the construct with the primers, losing the vector's start codon by the *SalI* digest did not cause a problem.) The pER8 binary vector contains only unique *SpeI* and *XhoI* cloning sites. Therefore, the cloning was managed through an intermediary vector, into which the tagged reading frame was inserted as *SalI-EcoRI* fragment and then subcloned into pER8 by *SpeI-XhoI* using the flanking cleavage sites in the intermediary vector. In addition, all three AKIN β subunits were cloned into the p3xtag vector as *SalI-XbaI* fragments and transferred into pPCV002 (Km^R) as *NotI* fragments.

3.3.3. Immunoblot analysis of the overexpressed PIP-L-tagged SnRK1 subunits

All five AKIN subunit constructs were transformed into root-derived cell suspension cultures through *Agrobacterium*-mediated transformation using *Agrobacterium* GV3101 (pMP90RK) as host for the pPCV002 constructs and GV3101 (pMP90) for the pER8 constructs. The expressed proteins were detected by western blot analysis using α -HA antibody. All five SnRK1 subunits were expressed at a low level in the cultures maintained with 3% sucrose confirming that the stability of these proteins is regulated by the levels of sucrose as seen in chapter 3.2.3.

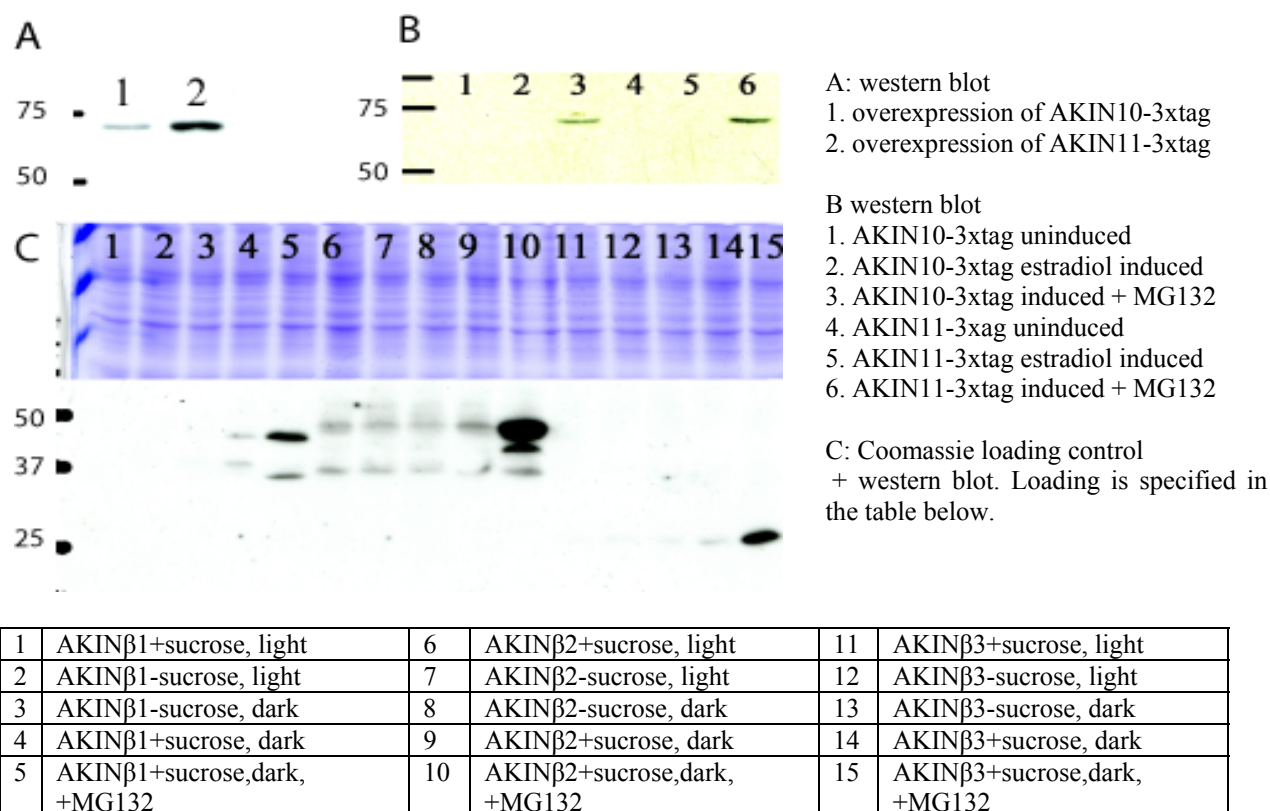


Figure 14. Proteasomal degradation of the SnRK1 α and β subunits

The expression level of the SnRK1 β subunits could not be significantly increased by changing light conditions or sugar availability in the medium.

The role of light and the presence or absence of sucrose in the medium was tested in case of β subunits, but in the root-derived cell suspension culture these conditions did not significantly alter the protein stability. Application of the proteasome inhibitor MG132 greatly increased protein amount of all the tested α and β subunits indicating proteasomal degradation of all five subunits.

3.3.4. Purification of PIP-L tagged SnRK1 beta subunits from Arabidopsis cell suspension culture

It was attempted to purify heterotrimeric SnRK1 kinase complex and identify its associated protein components from plants using the PIP-L-StrepII tagged constructs (detailed protocol is given in the materials and methods chapter). In the first step, total protein extract was purified on NiNTA resin through the PIP-L tag, and imidazole gradient elution was applied (Figure 15.). The fractions were analyzed by Coomassie-staining and immunoblotting with α -HA antibody. The positive fractions were pooled and applied onto Strep-tactin resin, washed, and eluted with 2.5mM desthiobiotin. The samples were analyzed by western blotting and concentrated by vacuum centrifugation or TCA-aceton precipitation. Purification of AKIN β 2 yielded the best result from the SnRK1 subunits, but the extracted protein amount was still not sufficient for subsequent mass spectrometric analysis. The extracted AKIN β 2 appeared as a double band indicating secondary modification *in vivo*.

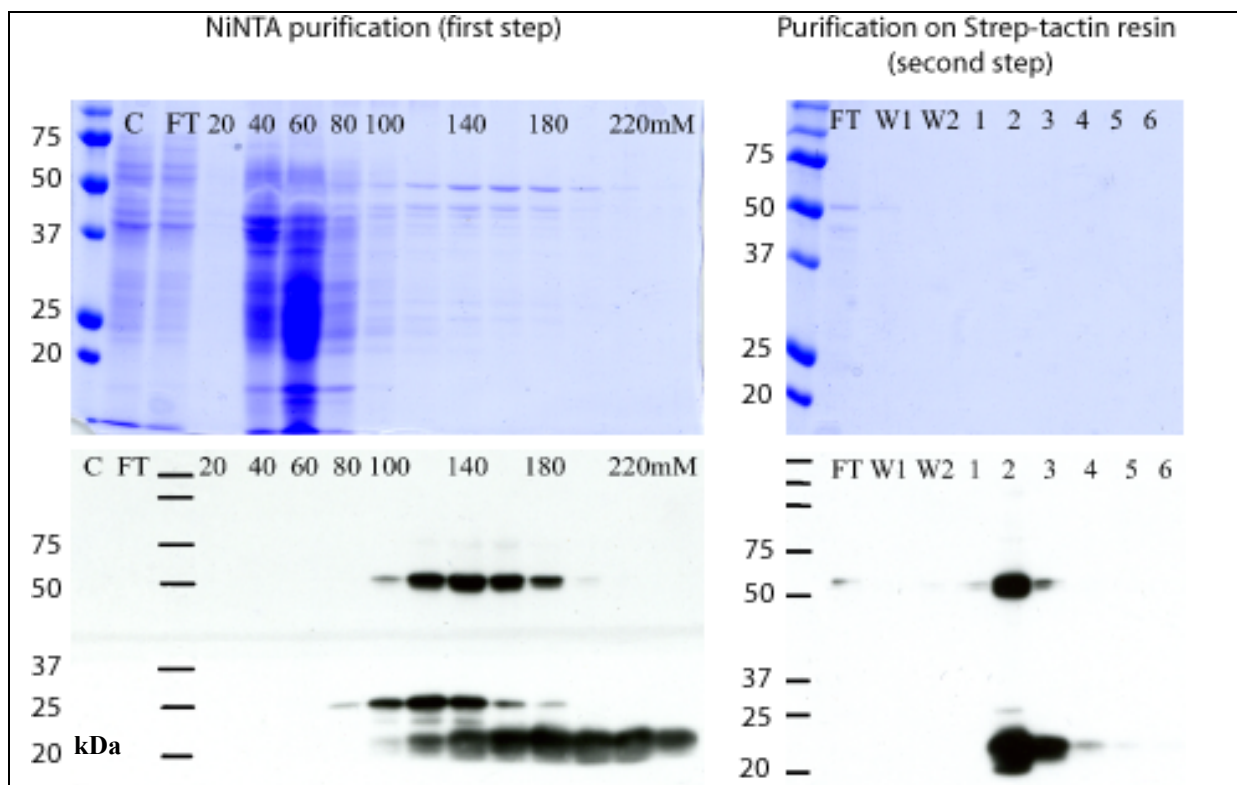


Figure 15. Tandem affinity purification of AKIN β 2-PIP-L-Strep-HA protein from Arabidopsis cell suspension culture

Elution from the NiNTA matrix was performed with imidazole gradient ranging from 20mM to 250mM using 20mM steps with 500 μ l fraction volumes. Elution from Strep-tactin matrix was done with 2.5mM desthiobiotin with 500 μ l fractions. C: crude extract, FT: flowthrough, W: wash.

It was noteworthy that in the crude extract the immunoblot analysis did not detect HA signal, which implies that the AKIN β 2-PIP-L-StrepII-HA protein concentration was under the detection level. However, the method was capable to enrich the PIP-L-Strep-tagged protein. The protein concentration was 1.350 mg/ml in the crude extract and 0.148mg/ml in the 140mM imidazole fraction of NiNTA column (measured by Bradford assay). Therefore, the calculated purification was extremely high, 9122-fold in the first step. After the second chromatography the protein concentration was too low to be measured by Bradford assay, therefore the purification rate could not be determined.

Although the protein amount can be significantly increased by the use of MG132 proteasome inhibitor, this is not the method of choice with large amounts of samples because of the very high price of this chemical. In addition, accumulation of one member of a protein complex does not help to identify other members, since their amount may not increase simultaneously. The above described purification method could also be useful to identify phosphorylation sites on monomer proteins. When working with plant protein samples, two relatively successful protein monomer isolation techniques are used: phenol extraction and TCA-aceton precipitation followed by 2D gel analysis and mass spectrometry of the redissolved proteins. These approaches prevent protein degradation due to denaturation and also preserve secondary modifications, but the proteins are precipitated and need to be dissolved. Proteins can be dissolved efficiently in chaotropic agents (8M urea or 6M guanidinium hydrochloride) which are compatible with Ni-chromatography. Chaotropic agents can be washed out

during the NiNTA purification, and afterwards the sample can be applied to the Strep matrix. Therefore, the method described here could add a highly selective purification step to these protein extraction methods.

3.4. IN VITRO PHOSPHORYLATION OF CANDIDATE PROTEASOMAL SUBSTRATES

SnRK1 kinases have been already investigated from many aspects with limited success. Reverse genetic approach and overexpression analyses were performed with nearly all subunits (PhD theses Kenneth Berendzen and Vijaya Shukla, and this work). A microarray experiment based on 2 pairs of chips was recently published by Jen Sheen and a similar pilot experiment was also carried out in our lab (PhD thesis of K.B.). Isolation of protein complexes including SnRK1 subunits was also attempted, as well as phosphorylation site determination on the SnRK1 β subunits, but finally ended with no success of MALDI analyses. Moreover, GFP localization and AKIN promoter-GUS fusion analysis have been also completed except using GFP labeling of full-length genomic constructs (PhD thesis K.B.).

Yeast two-hybrid screens with AKIN10 and AKIN11 identified the $\alpha 7$ proteasomal subunit and SKP1, a component of SCF type E3 ubiquitin ligase complexes, as SnRK1 α -interacting partners. These interactions were verified also *in vivo*. The presence of a UBA domain in SnRK1 kinases further supports their proteasomal interaction since polyubiquitin chain formation on proteins is the signal for their proteasomal degradation. Since the proteasomal $\alpha 7$ subunit and SKP1 were proved to be no substrates for SnRK1 kinases *in vitro*, we searched SnRK1 kinase substrates amongst several known and candidate proteasomal substrates. Phosphorylation of proteasomal substrates often precedes their proteasomal degradation. In yeast, Snf1 has been shown to control proteasomal degradation of multiple components of sugar signalling and metabolic pathways. The mechanism might be conserved because sugar-controlled degradation of sugar-related enzymes was also demonstrated in *Arabidopsis* at the physiologic level. Participation of 14-3-3 proteins in the process both in yeast and *Arabidopsis* further supports the existence of a conserved mechanism. Therefore, proteasomal substrates and also F-box proteins, substrate recognition subunits of SCF-type E3 ubiquitin ligase complexes, were expressed in and purified from *E. coli* and subjected to *in vitro* kinase reactions with recombinant AKIN10 and AKIN11. These assays were possible because in contrast to yeast and mammal AMPKs *Arabidopsis* SnRK1 α catalytic subunits show autophosphorylation and some degree of substrate phosphorylation activity *in vitro*.

3.4.1. Generation of *Arabidopsis* SnRK1 α bacterial expression constructs

N-terminally GST-tagged AKIN10 and AKIN11 constructs were prepared by Bhalerao et al (1999) [60] by cloning *EcoRI-SalI* cDNA inserts in the pGEX-5X-1 vector (GE Healthcare, Ref number 27-4584-01). These clones were used for large-scale protein purification starting from 2l of *E. coli*

suspension, and the protein extracts were purified on Glutathion-Sepharose 4B columns. In our hand, most of the recombinant proteins precipitated in inclusion bodies in the bacteria and the minor soluble fraction was heavily degraded. Therefore, an additional histidin-tag was introduced to the C-termini of these constructs to allow double affinity purification and selection for intact full-length recombinant proteins. The C-terminal 3'-segments of *AKIN10* and *AKIN11* cDNAs were PCR amplified using MISI2 and MISI4 forward oligonucleotide primers designed to the intrinsic *Bgl*III and *Xba*I sites located at 1144 and 1026bp positions of *AKIN10* and *AKIN11* cDNAs, respectively. These primers were used in combination with reverse oligos incorporating the coding sequence of the His-tag upstream and a *Sal*I site downstream to the stop codon (MISI1 and MISI3 primers for *AKIN10* and *AKIN11*, respectively). The PCR amplified fragments were cloned into the original pGEX-5X-1 constructs replacing the C-terminal coding sequences. Recombinant proteins were prepared from these construct and purified on Ni-NTA agarose and subsequently on Glutathion-Sepharose 4B matrix. Although high purity was achieved, the protein amount was very low and not sufficient for regular routine assays. Therefore, another bacterial tag, a thioredoxin-tag was tried in order to increase bacterial solubility of AKIN10 and AKIN11. The clones were prepared by subcloning the original GST-AKIN fragments into pET201 double-tagging vector, which contains coding sequences for an N-terminal thioredoxin and a C-terminal His tag. The open reading frames of AKINs were excised as *Sal*I and blunted *Eco*RI fragment and ligated into *Sal*I and filled-in *Bam*HI sites of pET201. As expected, the solubility of AKIN kinase proteins was greatly increased. Phenylarsine-agarose for the purification through thioredoxin tag is not available any more unfortunately. Therefore, other ways had to be found to achieve maximal purity. Imidazole gradient elution from NiNTA column and subsequent ion exchange chromatography was used to attain high purity recombinant proteins. The GST-His-tagged variants were kept for certain kinase assays where a higher sized AKIN kinase was necessary, because the GST tagged forms are approximately 10 kDa larger than the TRX-tagged versions due to differences in tag size (Figure 16.).

3.4.2. Preparation of point mutant SnRK1 α kinase variants

To generate constitutively activated AKIN kinase versions, the activation-loop threonine residue was exchanged to asparagine (T175D in AKIN10 and T176D in AKIN11) by site-directed mutagenesis in order to mimick phosphorylated state of the T-loop. Inactive kinase variants were also created by site-specific mutagenesis of the ATP-binding site (K48R in AKIN10 and K49R in AKIN11). The inactive variants are still phosphorylable on their T-loop threonine by upstream activating kinases. All mutant clones were generated using pET201 bacterial expression clones and recombinant proteins were prepared with the same protein purification strategy as described above. The site-directed mutagenesis was carried out by the unique site elimination method [227]. One primer was designed to the *Afe*I site of the pET201 vector backbone (pET201AfeI-) and used with combination with one of the mutagenic primer specific for each construct (primers AKIN10T175D, AKIN10K48R, AKIN11T176D and AKIN11 K49R). (See 2.1.6.3. in the Materials and Methods chapter).

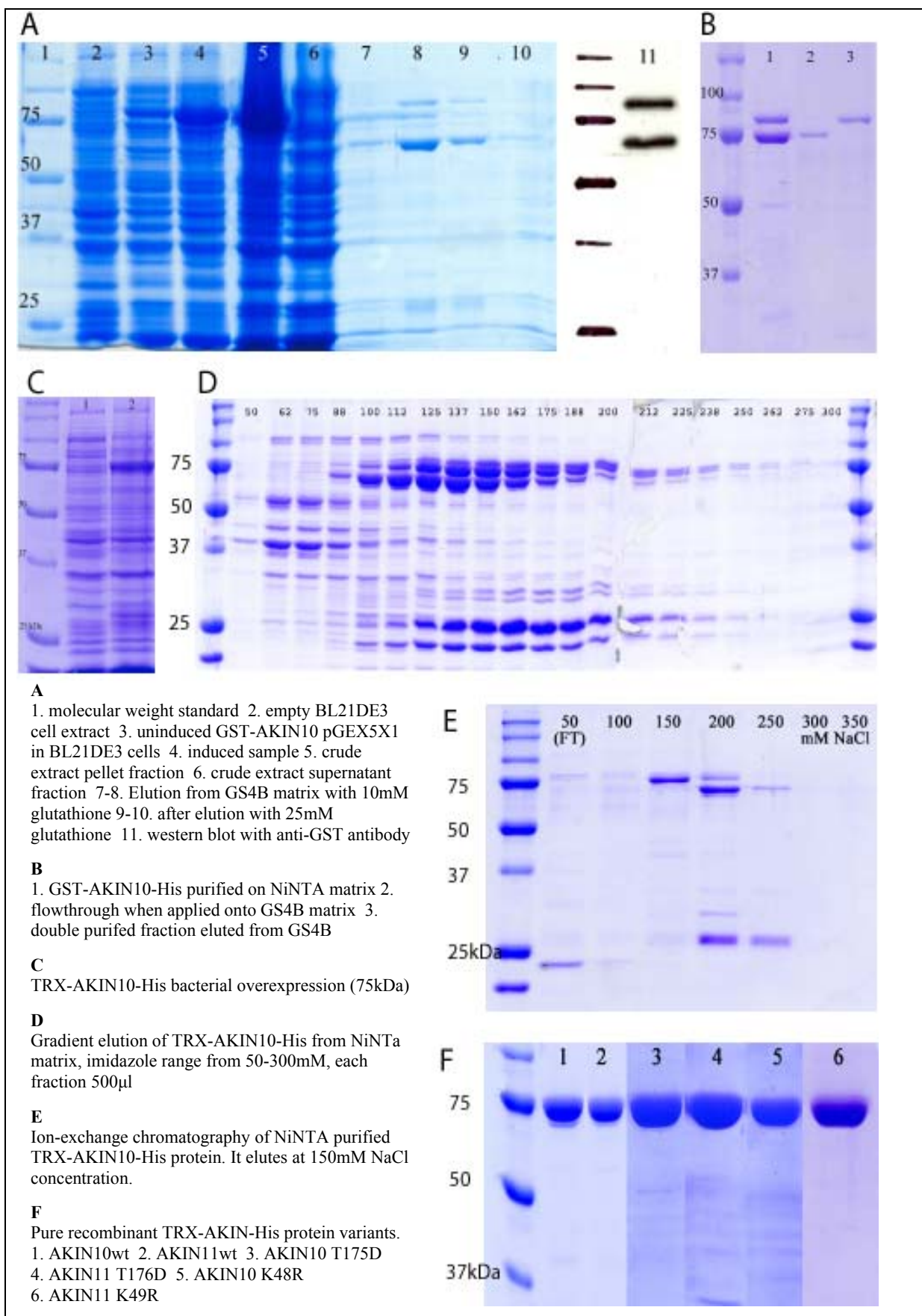


Figure 16. Purification of recombinant SnRK1 α catalytic subunits AKIN10 and AKIN11.

3.4.3. Candidate SnRK1-proteasome substrates

To search for candidate SnRK1 substrates, we choose proteasomal substrates which have been reported to either undergo sugar- or light-dependent degradation or affected by mutations causing sugar related phenotypes. ABI5 (At2g36270) is a proteasomal substrate and its mutation causes insensitivity to sugar-induced germination arrest. ABI5 is phosphorylated by SnRK2 kinases, and phosphorylation is necessary for its biological activity. Three phosphorylation sites were already determined on ABI5 based on *in vitro* kinase reactions. We hypothesized that ABI5 might be a key factor in sugar-induced developmental arrest, and sugar signal could be transmitted by SnRK1 kinases. DPBF4 (At2g41070) is another member in the ABI5 family of bZIP transcription factors and contains the conserved phosphorylation sites determined previously in ABI5.

EIN3 (At3g20770) is a transcriptional activator in the ethylene signal transduction pathway, and it is a proteasomal substrate. Glucose enhances EIN3 degradation. D-type cyclins are implicated in the sugar control of cell cycle. Proteolytic degradation of cyclinD3;1 (At4g34160) is inhibited by sugars, unlike that of CycD2 (At2g22490), but it is regulated by sugars at the level of transcription similarly to CycD3. Just like CycD3;1, CycD1 (At1g70210) is also a phosphoprotein, and phosphorylation enhances its proteasomal degradation. As control, CycD3;3 was also used as substrate in the assays.

The stability of CO protein (CONSTANS, At5g15840), a key regulator of flowering transition, is controlled by day-length and CO is degraded in the dark, where SnRK1 kinases are supposed to be active. The CDF1 (At5g23040) transcription factor, a repressor of CO expression and proteasomal substrate was also tested in our *in vitro* kinase assays.

shy2, a mutant form of Aux/IAA3 (At1g04240) transcriptional repressor in the auxin signaling pathway also shows sugar-related phenotypes similarly to *axr2* (dominant mutation of IAA7, At3g23050). Another member of the Aux/IAA family, IAA6 (At1g52830) was also tested to determine whether potential phosphorylation sites are found in the conserved domains of this protein family. Some F-box proteins were also selected for investigation. They are the substrate recognition subunits of SCF type E3 ubiquitin ligase complexes, but generally are also proteasomal substrates and their stability is oppositely regulated compared to their targets. TIR1 (At3g62980) and the EBFs (EBF1, At2g25490 and EBF2, At5g25350) are amongst the closest plant relatives of yeast GRR1 and involved in the degradation of IAA proteins and EIN3, respectively. The F-box protein FKF1 (At1g68050) is responsible for degradation of CDF1, and thereby involved in the control of CO level and flowering transition. The F-box *Zeitlupe* (ZTL, At5g57360) is a component of the circadian clock system and its function is thus connected to CO regulation.

To reconstruct trimeric SnRK1 kinases *in vitro*, the purification of non-catalytic SnRK1 kinase subunits was also attempted. Beta subunits are known phosphoproteins, but their kinase partner has not yet been identified. Since the gamma subunit is an important regulator of the kinase activity, its purification was critical for *in vitro* reconstruction of trimeric kinases to increase their activities.

3.4.4. Cloning bacterial expression and purification of the selected proteasomal substrates

Cloning strategies used for generation of individual constructs are summarized in Table 2. (Corresponding primers are listed under 2.1.6.1. in the Materials and methods chapter). Photos of Coomassie-stained SDS-PAGE gels documenting the purity of obtained recombinant proteins are depicted in Figure 17. GST, MBP and TRX tags were used as control proteins. Some of the listed proteins could not be purified under natural conditions, like the AKIN β subunit, ABI4 and CyclinD3. In these cases, only the overexpression is illustrated. The EIN3 protein could not even be overexpressed in *E.coli*, although thioredoxin-, GST- and MBP tagged constructs were all tested.

The identity of the recombinant substrate proteins was verified by mass spectrometric analysis. Therefore, western blot analysis was not performed in the majority of cases. Protein samples purified on NiNTA resin frequently contained a major bacterial contamination band at 74kDa, which was analyzed by mass spectrometry. This contamination corresponds to a bifunctional polymyxin resistance *arnA* protein (Swissprot database accession P77398). The reason for co-purification is that it contains vicinal histidine residues, which behave as a quasi His-tag. In some cases, like in the TRX-EBF1-His purification experiment, this contaminating protein gives approximately 95% of the total protein in the sample. (The purified recombinant proteins can be distinguished by comparing with the overexpression band in the crude extract gel lane.)

3.4.5. In vitro kinase reactions with radioactive $\gamma^{32}\text{P}$ -ATP

In the kinase reactions generally 1 μg kinase and 1 μg substrate protein were used in 20 μl reaction volume. The reaction was carried out at room temperature in a buffer containing 5mM MgCl_2 , 50mM NaCl, 20mM Tris-HCl (pH 7.5), 5mM β -mercapto-ethanol and 1 μl $\gamma^{32}\text{P}$ -ATP (5000 $\mu\text{Ci/mol}$). In some cases, the recombinant substrate protein could be purified only in a very low quantity. In these cases generally 0.2 μg substrate was used instead of 1 μg (TIR1, EBF1, FKF1 and CycD1). Exposition times were ranging from 20 min to 1 day. Long exposition times were necessary due to the relatively low activity of recombinant AKIN10. For comparison, the monomeric SnRK2.6/OST1 kinase was also tested as control kinase in parallel reactions (not shown) on ABI5 and DPBF4 and its activity was found one or two magnitude higher compared to AKIN10. (A potential reason for lower AKIN10 activity was the lack of the γ activator subunit, but its effect could not be tested since the γ subunit could not be purified from bacteria). Autophosphorylation intensity of AKIN10 served always as good internal control for comparison of phosphate incorporation intensities of various substrates.

Although AKIN11 could be also purified using the thioredoxin-His tag combination, neither substrate phosphorylating activity nor autophosphorylation of AKIN11 could be observed (Figure 18E). This result is in contrast to formerly published data using GST-AKIN11, and therefore it might be due to a technical problem. Therefore, only results with AKIN10 are shown here.

Construct	Vector	Cloning strategy	Protein size and comments
TRX-ABI5-His	pET201	PCR product cut by XhoI inserted to Sall site	63 kDa
TRX-DPBF4-His	pET201	PCR product to NheI +Sall	44 kDa
TRX-ABI4-His	pET201	PCR product on genomic DNA template was inserted to Sall (no intron in ABI4)	purification is not possible, 50 kDa
TRX-EIN3-His	pET201	PCR product, filled BamHI to filled NheI + filled NotI	overexpression is not possible, 86kDa
GST-EIN3-His	pGEX-5X-1	PCR product of EIN3_pGEXfwd + EIN3rev was inserted to BamHI + Sall	overexpression is not possible, 99kDa
MBP-EIN3-His	pMAL-c2	PCR product of EIN3:pMAL_fwd + EIN3rev was inserted to BamHI + Sall	overexpression is not possible, 114kDa
TRX-CyclinD1-His	pET201	PCR product was cut by XhoI and inserted to Sall site	low amount 54 kDa
TRX-CyclinD2-His	pET201	PCR product, filled BamHI + filled BglII was inserted to filled NotI	56 kDa
TRX-CyclinD3-His	pET201	PCR product, filled Sall + filled BamHI was inserted to filled NotI site	58 kDa
TRX-CyclinD3b-His	pET201	PCR product cut by XhoI and inserted to Sall site in vector	57 kDa
TRX-IAA3-His	pET201	PCR product was cut by Sall + XhoI and inserted to Sall site	35 kDa
TRX-IAA6-His	pET201	PCR product was inserted to filled NheI + filled NotI	35 kDa
TRX-IAA7-His	pET201	PCR product inserted as HindIII+XhoI	42 kDa
TRX-CO-His	pET201	PCR product inserted as BamHI+HinDIII	57 kDa
TRX-CDF1-His	pET201	PCR product was inserted to Sall site	42 kDa
TRX-HY5-His	pET201	PCR product cut by XhoI inserted to Sall site	32 kDa
TRX-TIR1-His	pET201	cut out from pMenchuSall clone, filled BglII to filled NotI	low amount, 84kDa
GST-EBF1	pGEX-5X-1	PCR, EBF1pGEX + EBF1UBR_rev, BamHI	low amount, 94kDa
TRX-EBF1-His	pET201	filled BamHI to filled NheI + filled NotI	low amount, 81kDa
GST-EBF2	pGEX-5X-1	PCR, EBF2pGEX + EBF2UBR_rev, BamHI	low amount, 94kDa
TRX-EBF2-His	pET201	filled BamHI to filled NheI + filled NotI	low amount, 81kDa
GST-FKF1	pGEX-5X-1	PCR product, Sall to XhoI	low amount, 97kDa
TRX-FKF1-His	pET201	PCR product to Sall site	low amount, 85kDa
GST-ZTL	pGEX-5X-1	It was subcloned as BamHI + XhoI	low amount, 93kDa
Kinase subunits			
TRX-AKIN β 1-His	pET201	PCRproduct, NcoI blunt + BamHI blunt to Sall blunt + NotI blunt	46 kDa
TRX-AKIN β 2-His	pET201	PCR product to Sall site	47 kDa
TRX-AKIN β 3-His	pET201	PCR product blunted, inserted to filled NotI	29 kDa
TRX-AKIN β γ -His	pET201	PCR product to <i>NheI</i> + <i>HindIII</i>	purification is not possible, 68kDa
GST-AKIN β γ	pGEX-5X-1	PCR product, BamHI+Sall to BamHI+XhoI	purification is not possible, 81kDa
Controls			
TRX tag (+His)	pET201	empty vector	14 kDa
GST tag	pGEX-5X-1	empty vector	27 kDa
MBP tag	pMAL-c2	empty vector	42 kDa

Table 1. Cloning details of of constructs used for expression of candidate kinase substrates and SnRK1 kinase subunits.

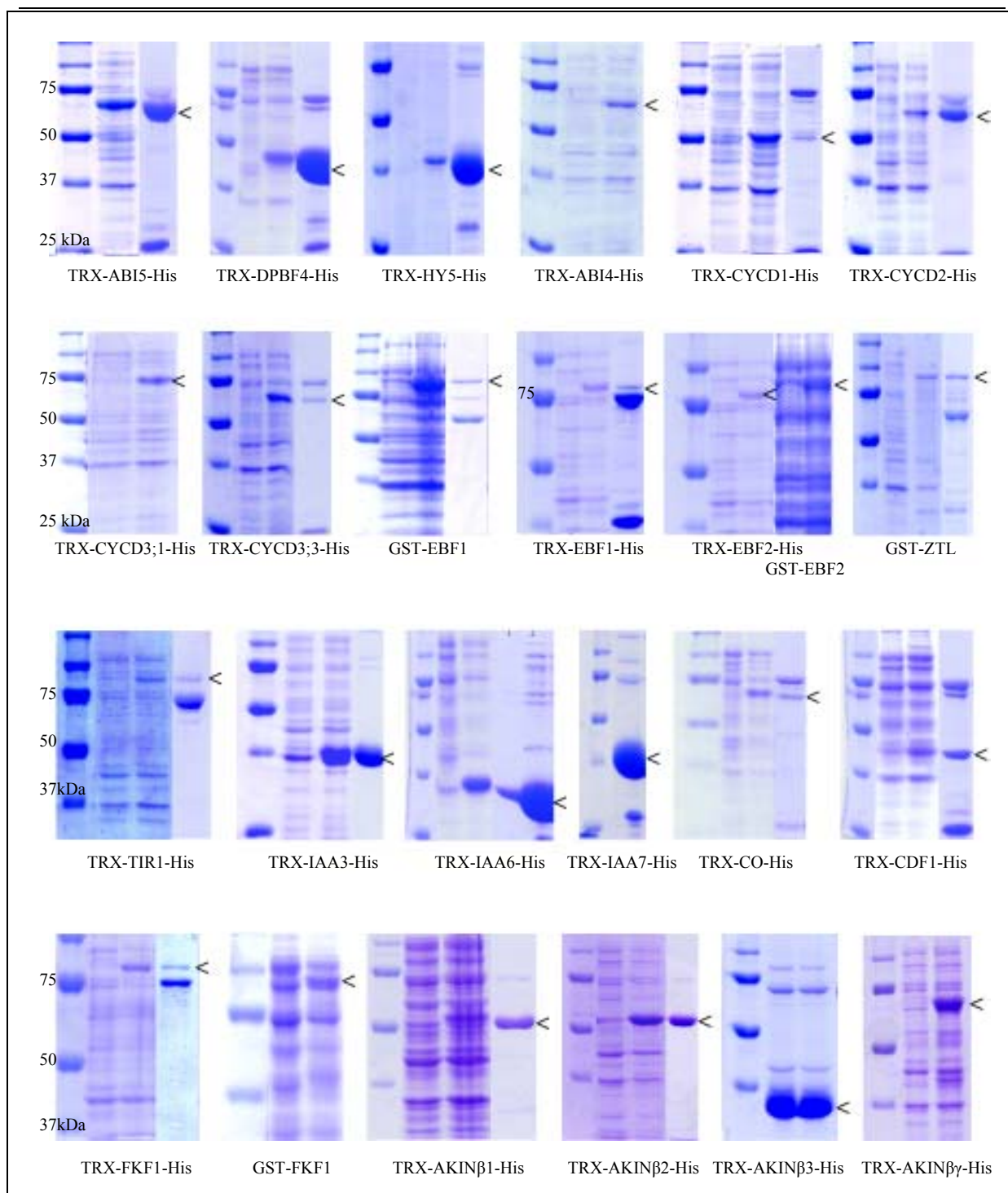


Figure 17. Bacterial expression and purification of the hypothetical substrates

cDNA sequences of selected substrates were cloned into IPTG-inducible vectors that were transformed into the *E. coli* strain BL21DE3pLysS for protein expression. First lane: non-induced bacteria, crude extract (control). Second lane: IPTG induced expression, crude extract. (Note the overexpression of protein of interest). Third lane: Purified protein. (The protein of interest is indicated with a “<” mark, and it is not always identical to the most intensive protein band. The size of protein of interest equals to the overexpression band in the second lane.) A frequent contamination was the bifunctional polymyxin resistance *arnA* protein (Swissprot database accession P77398), which contains two vicinal histidines; therefore under less stringent washing conditions co-purifies with His6-tagged proteins. Less stringent wash conditions were necessary when the molecular mass of protein of interest was high (80-100kDa) or when its soluble fraction was limiting.

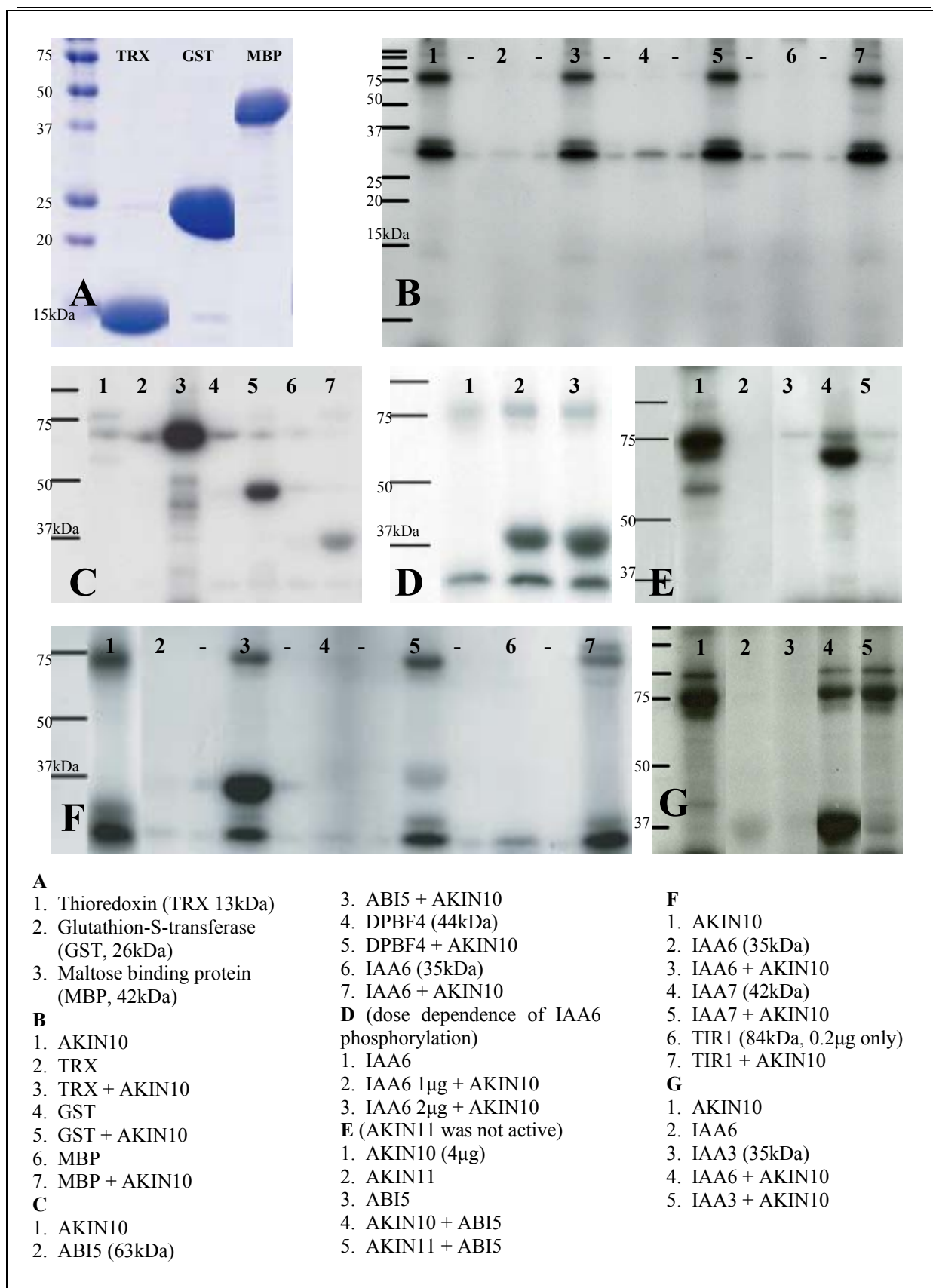


Figure 18. *In vitro* kinase assays of candidate proteasomal substrates with AKIN10 using radioactive $\gamma^{32}\text{P}$ -ATP.

The reactions generally contained 1 μ g kinase and 1 μ g substrate. In few cases very low amount of substrate protein could be purified that limited the amount used in the kinase assay to less than 1 μ g.

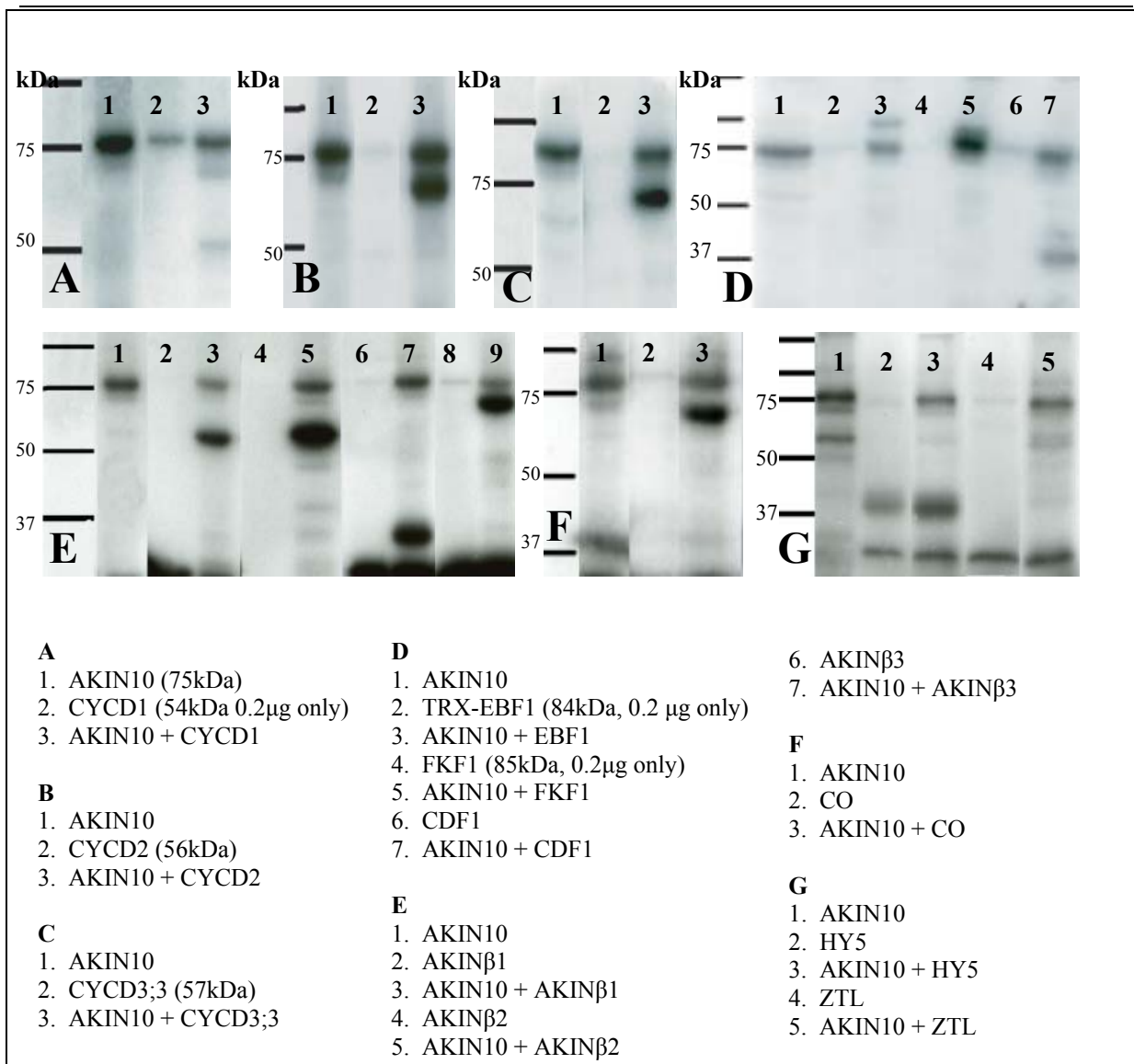


Figure 19. Kinase reactions of candidate proteasomal substrates with AKIN10 using radioactive γ 32P-ATP.

The reactions generally contained 1µg kinase and 1µg substrate (for detailed information about the reaction conditions see the text). In few cases very low amount of substrate protein could be purified, that limited the amount used in the kinase assay to less than 1µg.

Among all substrates tested, ABI5 and DPBF4 showed the most intensive phosphorylation. Relatively intensive phosphate incorporation could be detected with all three AKIN β subunits. IAA6, CycD2, CycD3;3 and CO gave also well detectable signals, although one magnitude lower than ABI5 and DPBF4. The rest of proteins showed very low intensity of phosphorylation, questioning the specificity of kinase reactions. Control samples without kinase did not show phosphate incorporation into the substrate proteins. Specificity of the kinase reactions was further tested by dose dependence of IAA6 substrate phosphorylation (Figure 18D): double amount of substrate has proportionally increased phosphate incorporation. In another approach, the specificity of kinase reactions was tested by the application of a formerly published specific SnRK1 inhibitor, the PRL1 WD40 repeat protein [60]. Recombinant PRL1 protein could be purified by the help of MBP-PRL1-His construct, which was prepared formerly by Bhalerao et al. Purification of recombinant PRL1 was carried out on NiNTA

matrix followed by application to maltose resin (Figure 20.). Inhibition was tested in a radioactive kinase reaction with one of the best substrates tested, DPBF4. In the reaction 1 μ g amount of each proteins were used. In this experiment PRL1, did not inhibit SnRK1 activity on DPBF4, at least at the concentration applied, but instead some radioactive phosphate incorporation was detected in PRL1. Phosphorylation of PRL1 is supported by an unpublished observation of Dóra Szakonyi showing that PRL1 appears as a double band in immunoblot analysis that indicates secondary modification.

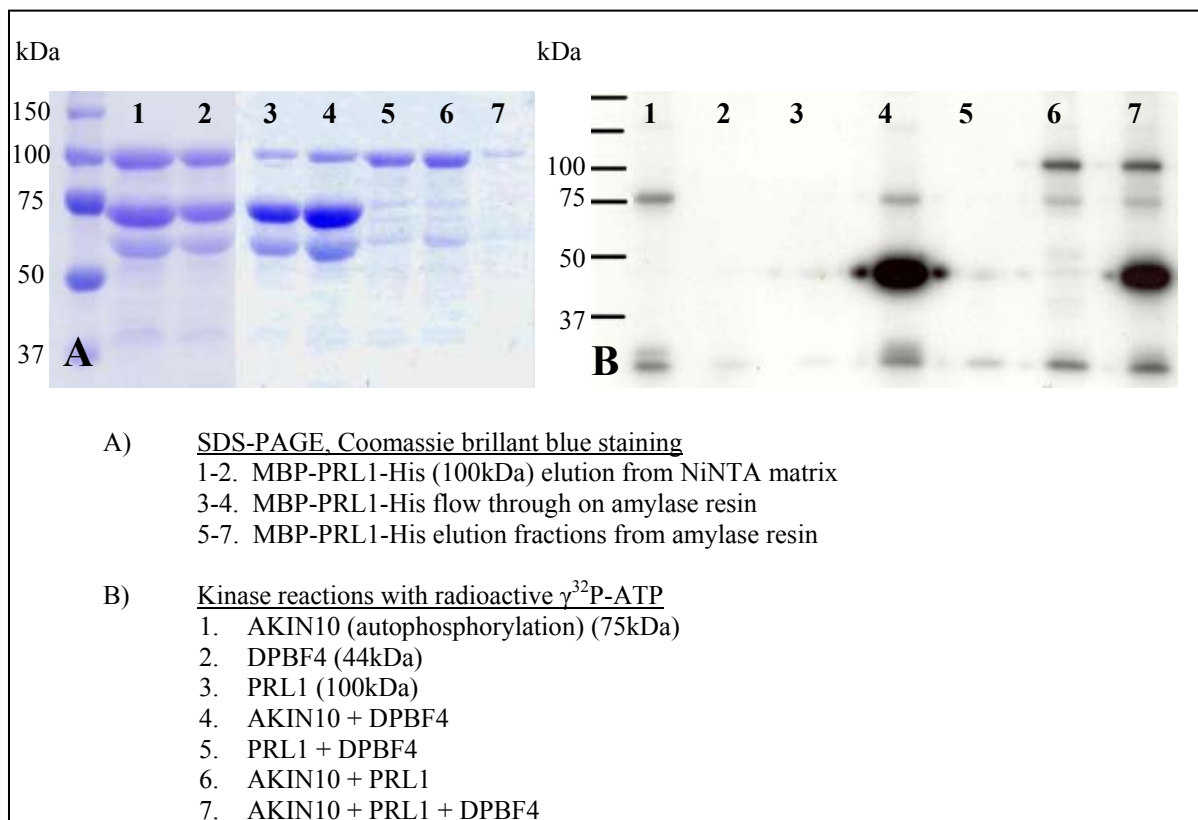


Figure 20. Purification of recombinant PRL1 protein and testing its SnRK1 inhibitor activity

3.4.6. Two-dimensional gel electrophoresis of phosphorylated SnRK1 substrates

To prepare samples for mass spectrometry study of substrate phosphorylation sites, *in vitro* kinase reactions were carried out using non-radioactive ATP. The phosphorylated proteins were concentrated by TCA-acetone precipitation. Proteins with different phosphorylation states were separated by two-dimensional gel electrophoresis and stained by Sypro-Ruby fluorescent stain. The analysis revealed multisite phosphorylation in ABI5 and DPBF4 (5-6 peaks could be distinguished that equals to 4-5 phosphorylation sites), whereas IAA6 showed only two separated spots upon separation in the second dimension (Figure 21).

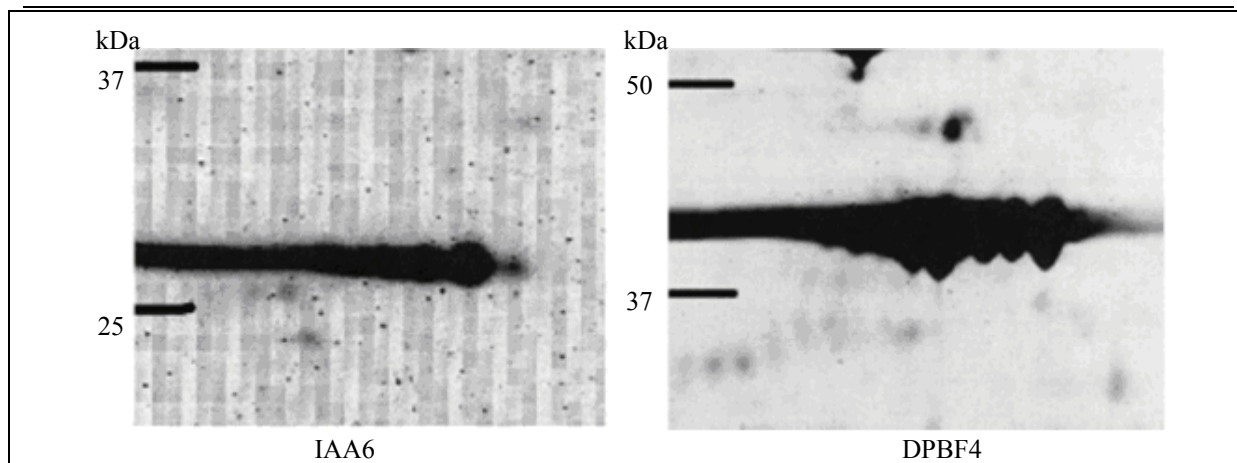


Figure 21. Two-dimensional electrophoresis of phosphorylated IAA6 and DPBF4

3.4.7. Constitutively active kinase variants

Relatively low *in vitro* activity of AKIN10 made it difficult to evaluate the radioactive phosphorylation data. ABI5 and DPBF4 were strongly phosphorylated and were clearly substrates for AKIN10. In case of IAA6, CyclinD2, CyclinD3;3 and CO, the levels of phosphate incorporation were substantially lower. The reason for the different levels of phosphorylation intensity may be that ABI5 and DPBF4 are phosphorylated at multiple sites, whereas the other substrates may contain single phosphorylation sites, which would cause nearly a magnitude weaker signal. To improve these results, it was attempted to generate more active kinase forms. Dominantly active T-loop mutant variants were prepared by the site-directed mutagenesis of the T-loop threonine to aspartate (T175D in AKIN10, T176D in AKIN11). The aspartate residue mimicks the phosphorylated T-loop threonine but the activation mutant kinase cannot be inactivated by phosphatases. Therefore, they could be useful also for *in vivo* studies of kinase functions. Mutant constructs of AKIN10 and AKIN11 were prepared and recombinant proteins purified as described above (Chapter 3.4.2. Figure 16F). As expected, the major autophosphorylation site is at the T-loop threonine and autophosphorylation disappears in the T-loop mutant AKIN10 (Figure 22.). The activity of AKIN10 T175D variant was approximately 3-5 times higher compared to the wild type AKIN10 (the activity increase is not pronounced in Figure 22 but see also Figure 25.). As with the thioredoxin-His-tagged AKIN11, no activity could be detected with AKIN11 T176D.

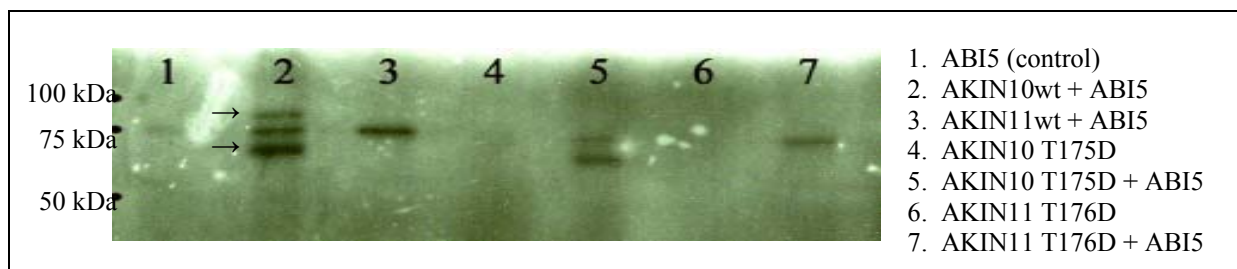


Figure 22. Dominantly active SnRK1 α kinase variants

The upper band corresponds to autophosphorylation AKIN10. The lower arrow indicates the position of ABI5. The third band in sample 2 is a background activity, which is also present in the ABI5 control sample. The autophosphorylation band of AKIN10 disappeared in the T175D mutant, but ABI5 phosphorylation activity was retained. This indicated that the autophosphorylation site is at the T-loop. AKIN11 and its “dominantly active” variant T176D did not show any activity in these experiments. The T175D mutation caused 3-5 times increase in AKIN10 activity (on this image it is not visible but see also Figure 25.)

3.4.8. Inactive kinase variants

Inactive SnRK1 α kinase variants were generated by site-directed mutagenesis of a lysine residue to arginine at the ATP-binding site (K48R in AKIN10, K49R in AKIN11). These variants lack autophosphorylation activity, but their intact T-loop threonine can still be phosphorylated by an upstream activating kinase. It was tested by using these inactive variants whether AKIN10 can activate AKIN11 and *vice versa* by being potential substrates for each other. In order to be able to distinguish the size of the two kinases, the active kinase variants were purified as GST-tagged versions, which have approximately 10kDa higher molecular mass than the thioredoxin tagged inactive variants. GST-AKIN11 was not active, and AKIN10 did not phosphorylate itself or AKIN11 in an intermolecular reaction (Figure 23.).

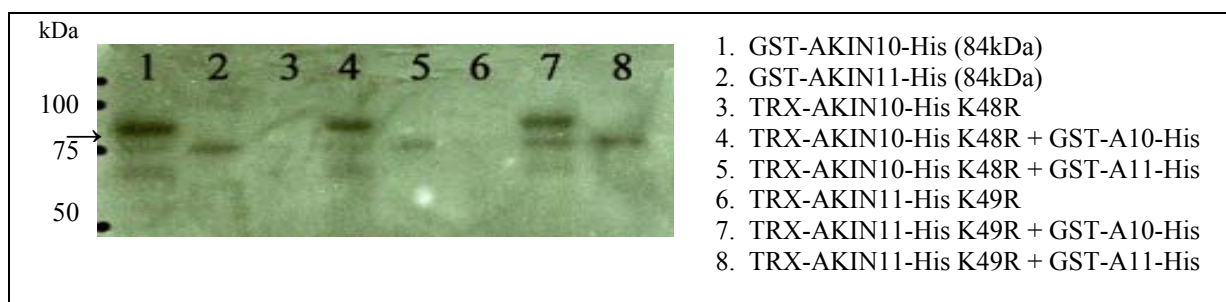


Figure 23. AKIN10 and AKIN11 do not activate each other *in vitro*

The arrow indicates a 84kDa molecular weight band that corresponds to the GST-tagged AKIN10 autophosphorylation. Similarly to TRX-AKIN11, GST-AKIN11 was also not active *in vitro*. AKIN10 did not activate AKIN11 or itself by intermolecular phosphorylation.

3.4.9. Testing the effect of SnRK1 upstream activating kinases on AKIN10 activity

An *in silico* systematic trans-genomic comparison of all yeast and *Arabidopsis* kinases in 2003 revealed that the *Arabidopsis* genome contains two protein kinases, the sequences of which are closely related to the yeast Snf1 upstream activating kinases Elm1, Sak1 and Tos3. As the *Arabidopsis* kinase sequences are most similar to Tos3, they were named by our laboratory Tos3-like kinases, TLK1 (At5g60550) and TLK2 (At3g45240). Parallely to our work, another group recently published that these kinases can restore Snf1 activity in yeast, which has lost all three of its Snf1 upstream activating kinases. We obtained the open reading frames of TLK1 and TLK2 by PCR amplification from an *Arabidopsis* cDNA library using gene specific oligonucleotide primers (TLK1fwd, TLK1rev, TLK2fwd and TLK2rev). The two open reading frames were cloned into the *SalI* site of pET201 vector to generate thioredoxin-His double tagged bacterial expression constructs. Recombinant proteins were expressed in *E. coli* cells, purified on NiNTA matrix and subjected to *in vitro* kinase reactions to test whether TLKs can increase AKIN10 activity *in vitro* or not (Figure 24). TLK1 could indeed phosphorylate AKIN10 *in vitro*, but surprisingly it did not lead to increased AKIN10 kinase activity on substrates, such as DPBF4 and IAA6, *in vitro*. In comparison to AKIN10, much higher autophosphorylation activity was observed by TLK1, whereas TLK2 was completely inactive.

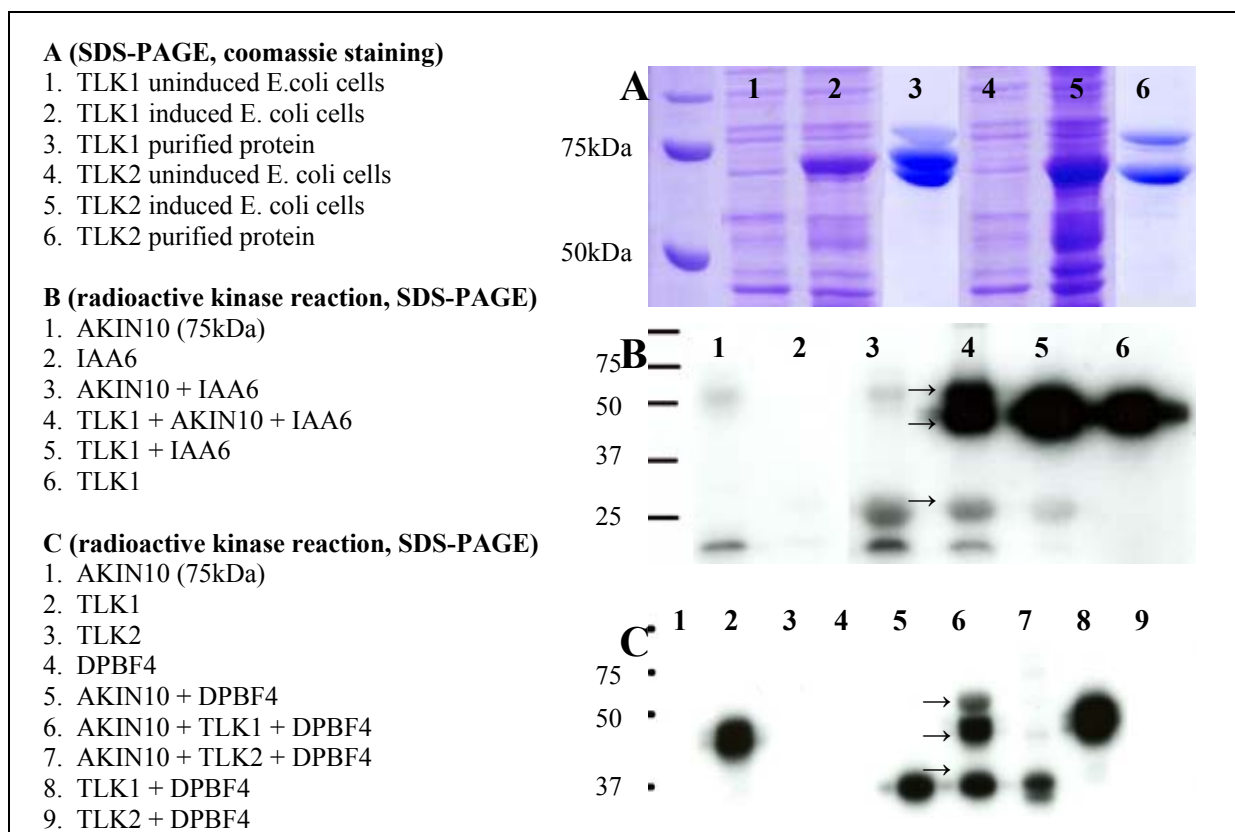


Figure 24. TLK upstream kinases phosphorylate AKIN10 but do not significantly increase its activity *in vitro*.

In B) the middle arrow indicates TLK1 autophosphorylation, whereas the upper arrow shows increased phosphate incorporation into AKIN10 compared to its autophosphorylation activity. The lower arrow shows the substrates, IAA6 in picture B, and DPBF4 in picture C.

3.4.10. Testing the activity of truncated kinase forms

In addition to the autoinhibitory domain, also the UBA domain of AMPKs and AMPK-related kinases appears to play a role in the kinase activation. However, it is still not clear whether the UBA domain plays a negative or positive regulatory role, because it was reported as both activator and inhibitor in the literature in different AMPK-related kinases. In order to generate a more active kinase form, two truncated AKIN10 variants were prepared with C-terminal deletions. The first construct lacked only the autoinhibitory domain, whereas in the second a larger deletion removed also the UBA domain. The location of the UBA domain was determined by *in silico* domain analysis (using the SMART homepage: smart.uni-heidelberg.de) and by alignment to other UBA domain containing AMPK-related kinases. The length of the UBA domain-containing variant was 340 amino acids, whereas the UBA domain deleted version was 280 amino acids long. Both clones were prepared by amplifying the corresponding AKIN10 cDNA sequences with the polymerase chain reaction using specific primers. The primer AKIN10fwd incorporated a *SalI* restriction endonuclease recognition site and was used in combination with AKIN10_280_rev and AKIN10_340_rev, incorporating *SalI* and *XhoI* sites, respectively. The DNA fragments were ligated to the *SalI* site of pET201 vector to generate TRX-His double-tagged constructs. Similarly, the T175D T-loop mutant, dominantly active truncated kinase variants were also prepared. Recombinant proteins were purified from all constructs and subjected to

in vitro kinase reactions (Figure 25). The T175D dominantly active variants were approximately five times more active *in vitro* than wild type AKIN10. Deletion of the autoinhibitory domain had only a minor effect on AKIN10 activity but when the UBA domain was additionally deleted, the kinase activity was greatly reduced. Therefore, the UBA domain seems be crucially important for the activity of AKIN10.

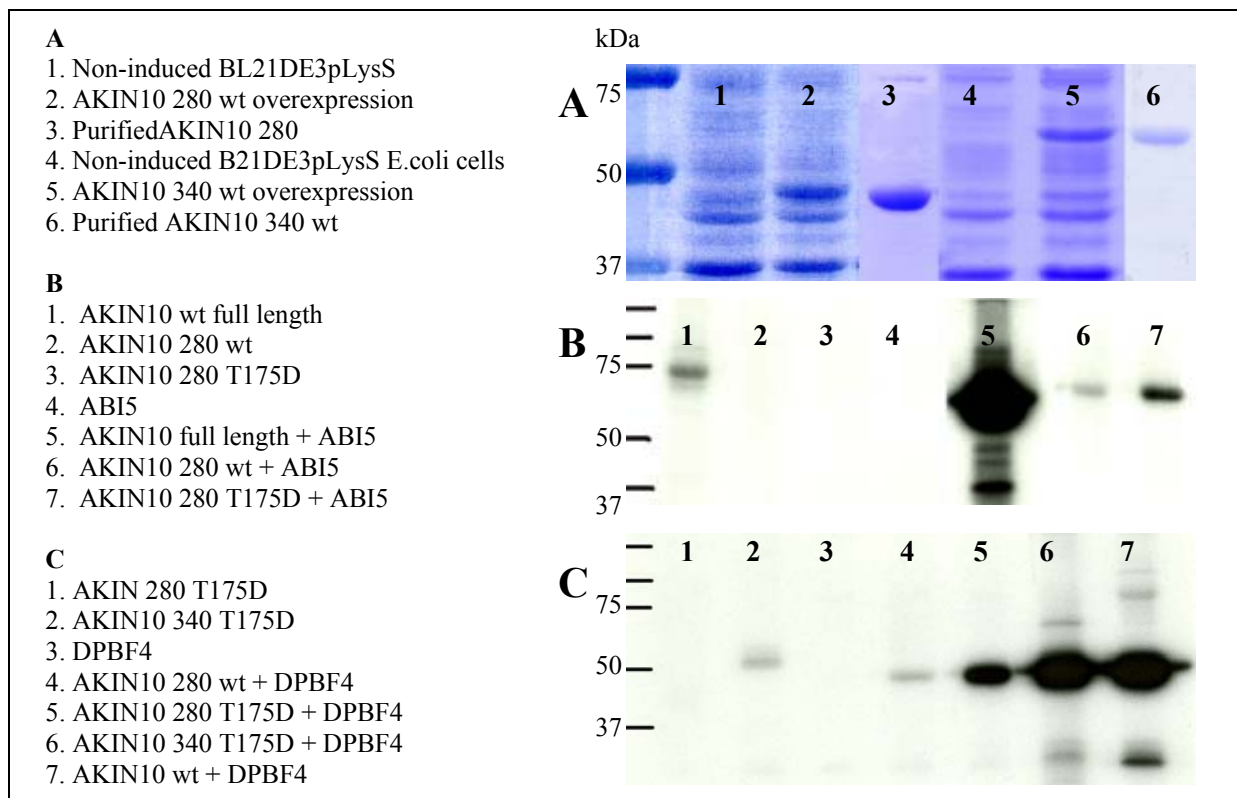


Figure 25. Activity of the truncated AKIN10 variants.

A: Bacterial expression and purification of truncated AKIN10 variants. B: Radioactive kinase reaction using the truncated AKIN10 variants. C: Radioactive kinase reaction using the truncated AKIN10 kinase variants.

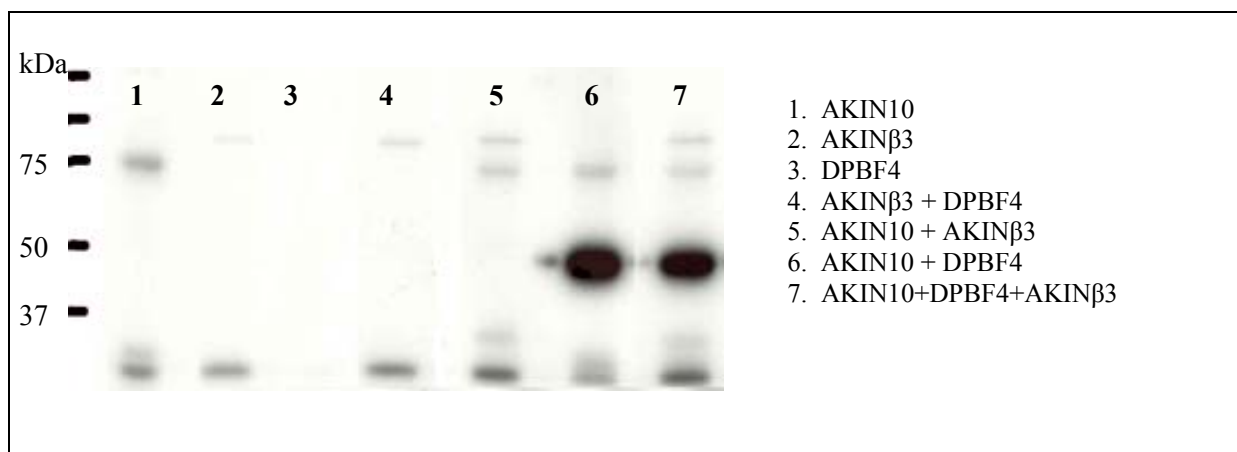


Figure 26. Partial reconstruction of the AKIN10 SnRK1 kinase complex with AKIN β 3

The addition of AKIN β 3 did not change the phosphorylation intensity of DPBF4 by AKIN10. Intriguingly, in this experiment AKIN β 3 itself was phosphorylated at a very low level (in contrast to earlier assays). (TRX-AKIN10-His = 75kDa, TRX-DPBF4-His = 44kDa, TRX-AKIN β 3-His = 29kDa)

3.4.11. Partial reconstruction of the SnRK1 kinase complex

The activator AKIN $\beta\gamma$ subunit could not be purified from bacteria under native conditions, and therefore reconstruction of trimeric SnRK1 kinase was not possible. However, the potential role of beta subunits was assayed. One of the best substrates in the *in vitro* kinase assays was the DPBF4 transcription factor, which is a nuclear protein. AMPK beta subunits might play a role in the substrate recognition and binding therefore the effect of presence of a beta subunit in the kinase reaction was tested. Based on subcellular localization of GFP-tagged beta subunits, the β_3 subunit was the most obviously nuclear. Therefore, this combination was used in the kinase assay. The addition of AKIN β_3 to the reaction mixture did not alter the intensity of DPBF4 phosphorylation (Figure 26.).

3.5. IDENTIFICATION OF PHOSPHORYLATION SITES IN SNRK1 KINASE SUBSTRATES

3.5.1. Mass spectrometric analysis of phosphorylated substrates

To determine the positions of AKIN10 phosphorylation sites, the substrate proteins were phosphorylated with non-radioactive ATP and subsequently digested either with trypsin (EC 3.4.21.) or alternatively glutamyl-endopeptidase (on other names Glu-C or V8, EC 3.4.21.19.). The resulting samples were enriched for phosphoproteins using Calbiochem ProteoExtract Phosphopeptide Capture Kit. The phosphorylated peptide fragments were identified by MALDI-TOF mass spectrometer. The identified phosphopeptides were further analyzed by tandem mass spectrometry using ESI-Q-TOF configuration equipped with an ion-trap device to precisely locate the phosphorylation sites. (The charts of the analysis are shown in Appendix 3.)

Five conserved phosphorylation sites were identified in ABI5 and DPBF4 (S42, S64, S145, T201 and S439 in ABI5 and S21, S43, S66, T104 and S259 in DPBF4) (Figure 27.). One of the sites was formerly identified in *in vitro* experiments by [232] and could not be verified in DPBF4 (S74), and shown that this site is not conserved in ABI5 (there is no phosphorylatable residue at the corresponding location). However, a new atypical site was found in both substrates (ABI5 S64, DPBF4 S43). In the new site, a positively charged amino acid residue was found in to position -4 relative to the phosphorylated serine, instead of position -3 expected according to the hypothesized kinase recognition motif. The new site is conserved in the ABI5 homologs from other organisms (rice, barley, wheat), whereas the formerly described site, which was not identified by us, is neither conserved in these proteins. A single phosphorylation site was detected in IAA6 at the amino acid position Ser39, which is conserved in many other members of the Aux/IAA protein family. No other phosphorylation sites could be detected in any other substrates examined.

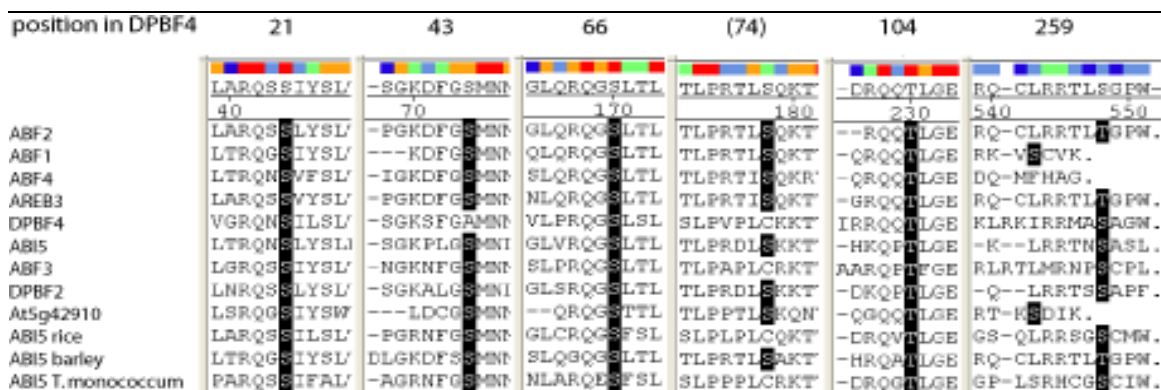


Figure 27. Conserved phosphorylation sites were identified in ABI5 and DPBF4 by mass spectrometric analysis

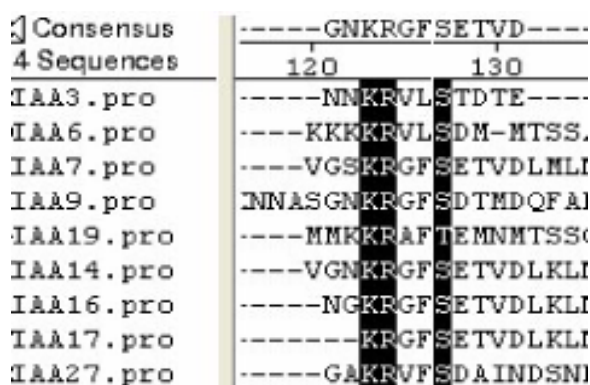
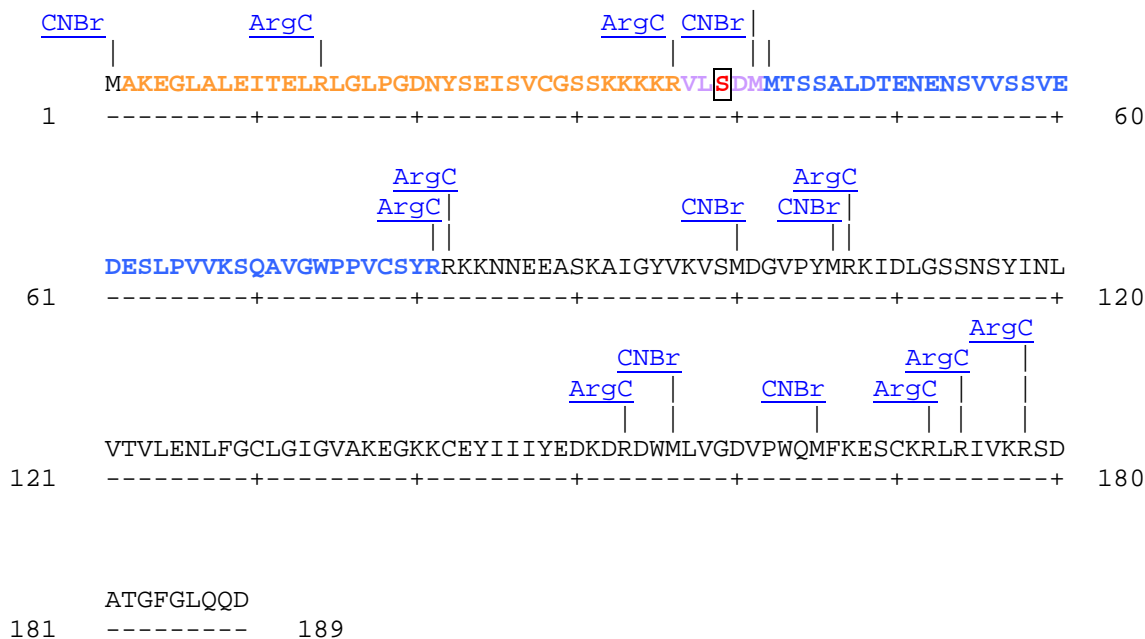


Figure 28. The phosphorylation site revealed in IAA6 is conserved in many members of the Aux/IAA protein family of auxin signalling repressors.

3.5.2. Phosphopeptide mapping of IAA6

Although the exact position of a phosphorylation site in IAA6 could be determined by tandem MS analysis, the site did not match as well the predicted consensus as the phosphorylation sites mapped in ABI5 and DPBF4. The identified IAA6 tryptic peptide contained a dehydroxy serine at position S39 after collision-induced decay (CID), which indicated the loss of phosphate group from an originally phosphorylated serine (the phosphate is generally lost during CID fragmentation mode). However, the peptide was not enriched during the phosphopeptide enrichment procedure, and the corresponding peptide could not be found in the V8 enzyme digested sample. Therefore, additional methods were applied to assure the existence of this phosphorylation site. Phosphopeptide mapping was carried out by enzymatic fragmentation of radioactively phosphorylated IAA6 protein. Unincorporated $\gamma^{32}\text{P}$ -ATP was removed by TCA-acteton precipitation of the peptides followed by washing the pellet in pure acetone. The peptides were solubilized in Tris-tricine SDS gel loading buffer and the peptide fragments were separated on Tris-tricine buffered SDS-PAGE gel system, which can resolve peptides as small as 1kDa. The radioactive peptide fragments were visualized by X-ray film exposition. The cutting agents were selected based on computer analysis of IAA6 amino acid sequence. The predicted phosphorylation motif of calcium/calmodulin dependent protein kinase superfamily, to which also SnRK1 kinases belong to, is K/R-X-X-S/T. The amino acid sequence of IAA6 contains only one such site, corresponding exactly to the site which had been identified by the MS analysis. We chose such

enzymes and chemicals, which cleave in close proximity of the predicted site resulting in peptide fragments overlapping only at the predicted position. Thus, we selected Arg-C protease (E.C. 3.4.21.35) that cuts at arginine residues at P1 position, and cyanogen bromide, which chemically cleaves proteins at methionine groups at P1 position. The selected agents cut upstream and downstream to the predicted kinase motif, respectively, resulting in not too small peptide fragments (Figure 29.). Indeed, CNBr fragmentation of IAA6 identified the expected fragment as phosphopeptide (Figure 30.).



Position of cleavage site	Name of cleaving enzyme(s)	Resulting peptide sequence	Peptide length [aa]	Peptide mass [Da]
14	Arg-C proteinase	MAKEGLALEITELR	14	1573.868
36	Arg-C proteinase	LGLPGDNYSEISVCGSSKKKKR	22	2366.718
81	Arg-C proteinase	VLSDMMTSSALDTENENSVVSSVEDESLPVVKSQAVGWPPVCSYR	45	4844.369
82	Arg-C proteinase	R	1	174.203
107	Arg-C proteinase	KKNNEEASKAIGYVKVSM DGV P YMR	25	2815.255
153	Arg-C proteinase	KIDLGSSNSYINL VTVLENLFGCLGIGVAKEGKKCEYII IYEDKDR	46	5122.924
172	Arg-C proteinase	DWMLVGDVPWQMFKESCKR	19	2355.773
174	Arg-C proteinase	LR	2	287.362
178	Arg-C proteinase	IVKR	4	514.669
189	end of sequence	SDATGFGLQQD	11	1138.156

Position of cleavage site	Name of cleaving enzyme(s)	Resulting peptide sequence	Peptide length [aa]	Peptide mass [Da]
1	CNBr	M	1	149.208
41	CNBr	AKEGLALEITELRLGLPGDNYSEISVCGSSKKKKRVLSDM	40	4337.030
42	CNBr	M	1	149.208
100	CNBr	TSSALDTENENSVVSSVEDESLPVVKSQAVGWPPVCSYRRKKNNEEASKAIGYVKVSM	58	6302.006
106	CNBr	DGV P YMR	6	680.774
156	CNBr	RKIDLGSSNSYINL VTVLENLFGCLGIGVAKEGKKCEYII IYEDKDRDWM	50	5711.606
165	CNBr	LVGDVPWQM	9	1044.234
189	end of sequence	FKESCKRLRIVKRS DATGFGLQQD	24	2783.201

Figure 29. Proteolytic map of IAA6 and the molecular mass of resulting peptides

Orange color indicates CNBr fragment, whereas the Arg-C peptide containing the putative phosphorylation site is marked in blue. Violet color shows the overlapping part of the two fragments. Red color marks the phosphorylated serine residue. The table shows the molecular mass values of peptide fragments.

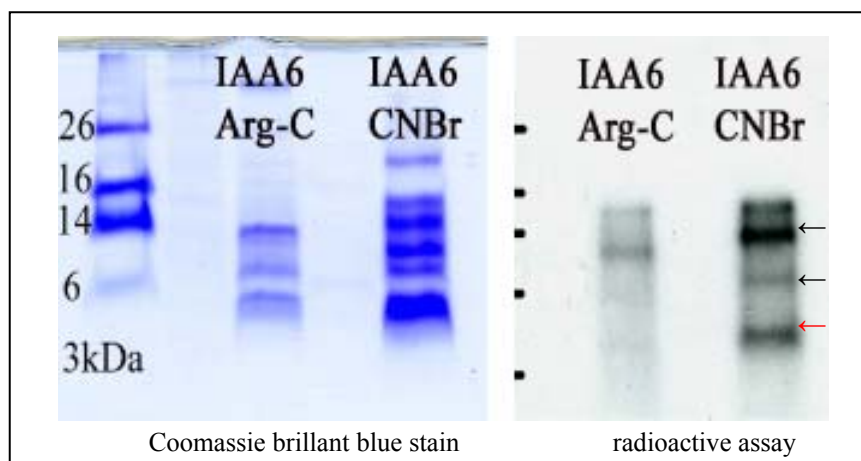


Figure 30. Phosphopeptide mapping of IAA6 with Arg-C enzyme and CNBr

Black arrow indicates partially cleaved peptides, which are larger than the size of the largest fully cut peptide fragment, 6.3kDa (see Figure 29. for peptide sizes). Red arrow indicates a peptide with a size of about 4 kDa which identifies the predicted phosphopeptide fragment.

3.5.3. Site-directed mutagenesis of the IAA6 S39E residue in bacterial expression clones

Site-directed mutagenesis was carried out on IAA6 to generate S39A non-phosphorylatable variant and S39E, in which the glutamine residue mimicks phosphoserine. The constructs were prepared in the pET201 bacterial expression vector to generate thioredoxin-IAA6-His fusion proteins, using IAA6_S39A, IAA6_S39E and pET201AfeI- oligonucleotides for the mutagenesis. In order to verify the phosphorylation sites, recombinant proteins were purified from the mutant constructs and were subjected to *in vitro* kinase assays (Figure 31.). Phosphate incorporation into the mutant proteins versions was greatly reduced compared to the wild type protein. Interestingly the solubility of IAA6 S39E construct in bacteria was also greatly reduced, but not that of IAA6 S39A. Residual phosphorylation of mutant proteins nonetheless suggested that potentially a second AKIN10 phosphorylation site is present in IAA6.

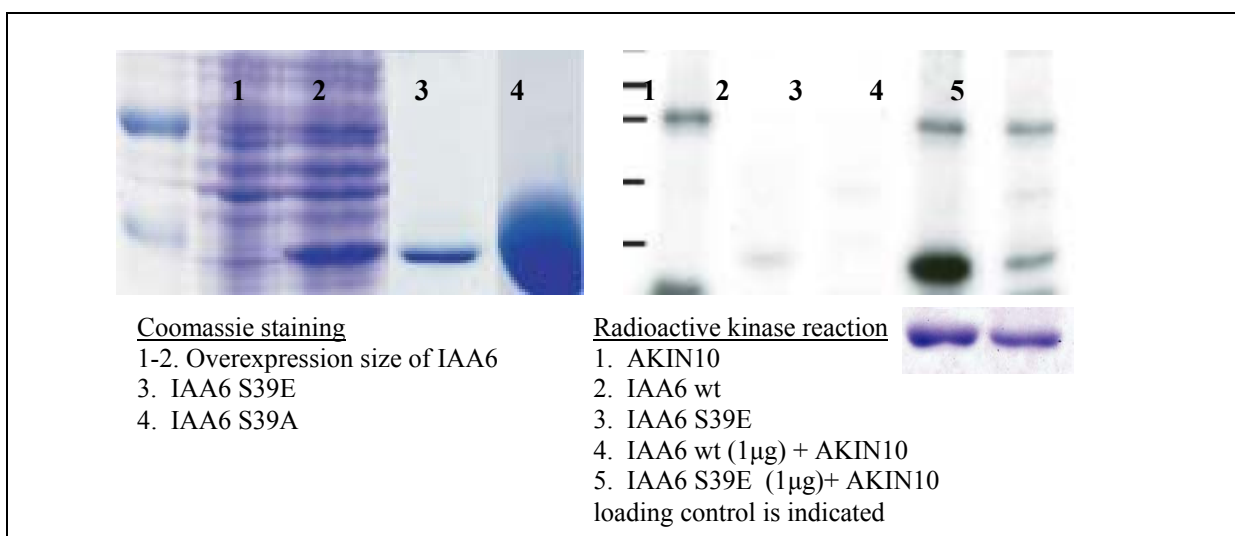


Figure 31. Bacterial expression and kinase assay of the IAA6 S39A and IAA6 S39E mutants

3.5.4. Preparation of IAA6 plant overexpression constructs

CaMV35S promoter driven overexpressor constructs of IAA6 cDNA were prepared in combination with an intron tagged C-terminal HA-tag (influenza haemagglutinin) coding sequence including all three IAA6 variants (i.e., wild type, S39A and S39E mutants). Mutant IAA6 cDNAs encoding the S39A and S39E variants were PCR amplified from the pET201 bacterial expression vector using IAA6_fwd and IAA6_rev oligonucleotide primers containing extra *NcoI* and *BglII* sites, respectively. The product was inserted into the intermediate vector pPILY [224], verified by DNA sequencing and subcloned as *NotI* fragment into pPCV002 binary vector, which carries a kanamycin resistance plant selectable marker gene. The constructs were transformed into S17.1 *E. coli* strain and conjugated into the GV3101 (pMP90RK) *Agrobacterium* host and subsequently transformed into *Arabidopsis thaliana* (Col-0) plants. Transformants were selected on kanamycin. (IAA6 S39A mutant seeds were not available by the date of submission.)

3.5.5. Analysis of phenotypes conferred by overexpression of IAA6 phosphorylation site variants and immunoblot analysis of modified IAA6 in transgenic plants

IAA6 is a proteasomal substrate, and based on data from the literature, its overexpression does not result in increased IAA6 protein concentration *in vivo*, nor does it produce phenotypic alteration. However, a point mutation in its degradation domain (amino acid residues 70-81) responsible for its interaction with the TIR1 F-box leads to increased IAA6 protein level and to slightly shorter hypocotyl phenotype during germination.

In our experiments, IAA6 overexpressor plants reached normal height, rosette size and silique length but petal development was reduced (Figure 32. and 33.). Petals and sepals also fell off earlier from the plants. The effect of overexpression of IAA6 S39E mutant for was much more pronounced. The plants were severely stunted with a maximum height of fully developed plants of approximately 10cm. In addition, silique length was reduced to approximately half size in the IAA6 S39E overexpressor plants, whereas it was wild type length in IAA6 overexpressors. The Aux/IAA proteins function as repressors in the auxin signal transduction and, based on the observed phenotype, mimicking phosphorylation of IAA6 appeared to increase the repressor activity of IAA6. One potential scenario is that phosphorylation of IAA6 would prevent its proteasomal degradation and thereby reduce the turnover speed of the protein. In order to examine the effect of Ser39 phosphorylation on the stability of IAA6 protein, western blot analysis of proteins extracted from IAA6 S39E and wild type IAA6 overexpressing lines was performed. For the immunoblot analysis one complete IAA6 S39E overexpressor plant and same weight of tissues from an IAA6wt overexpressor plant were frozen in liquid nitrogen and mortared to fine powder with a pestle. 500µl buffer ice cold buffer was added to the sample with composition of 50mM Tris-HCl (pH 7.0), 0.5%SDS, 5mM βME, 50mM NaCl, protease inhibitor cocktail (Sigma) to 5x final concentration and proteasome inhibitor (50µM MG132). No IAA6 protein could be detected in any of the samples indicating that IAA6 protein turnover is so

quick that overexpression could not increase the protein concentration to detection level. Although the IAA6 S39E mutation increases the biological activity of the protein, the mutation does not seem to affect the concentration (and likely stability) of IAA6, which in the absence of auxin treatment is under the detection limit.

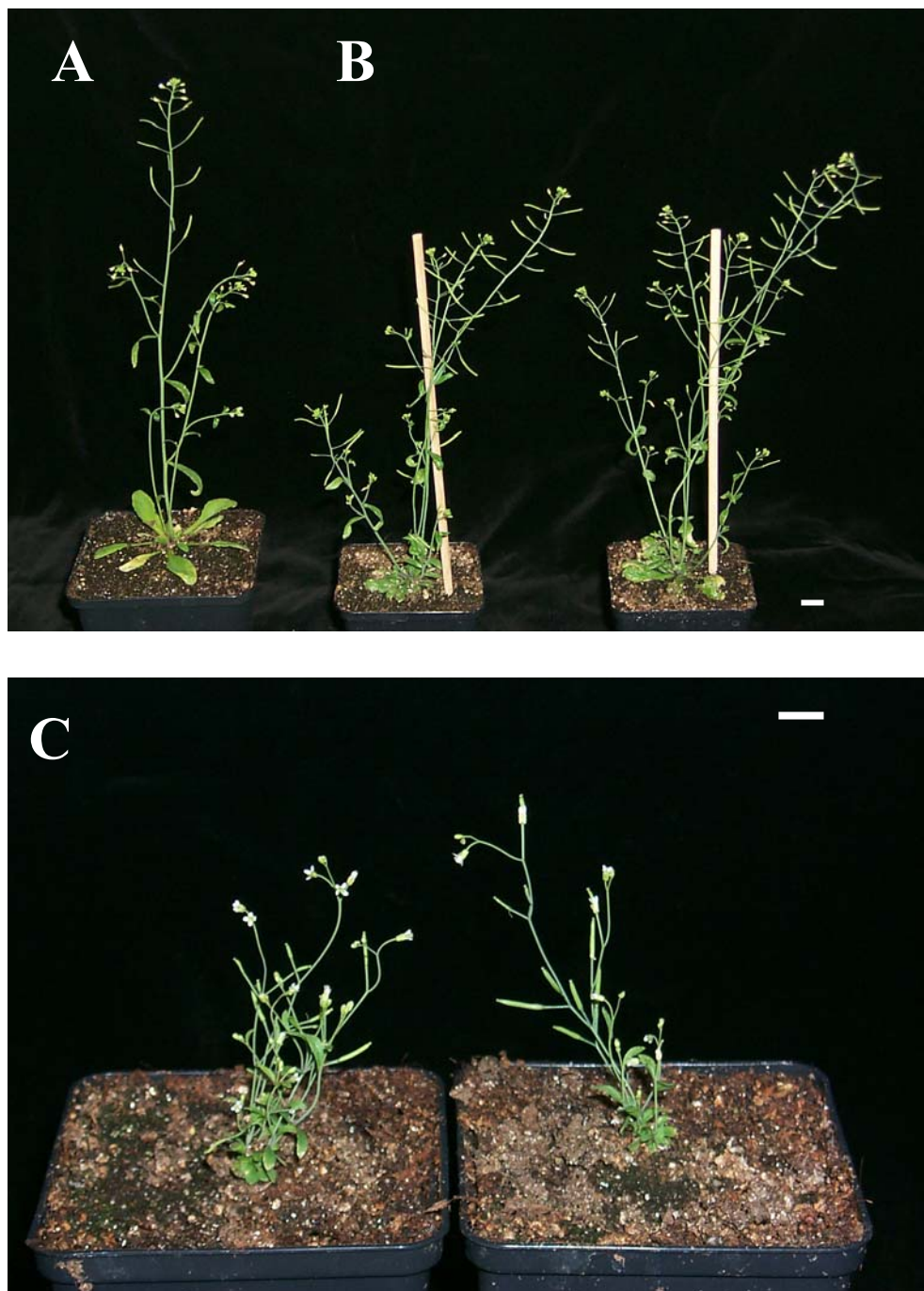


Figure 32. Overexpression of IAA6 S39E mutant protein strongly reduces plant development

The photos show 4 weeksold soil grown T1 plants. A: wild type control; B: wild type IAA6 overexpressing plants. The plants reach normal height and rosette size but petal development is reduced (see also Figure 33). C: IAA6 S39E overexpression results in severely stunted plants. Rosette diameter is approximately 1-1.5cm. Petal development and silique size is reduced. Bars are 1 cm.

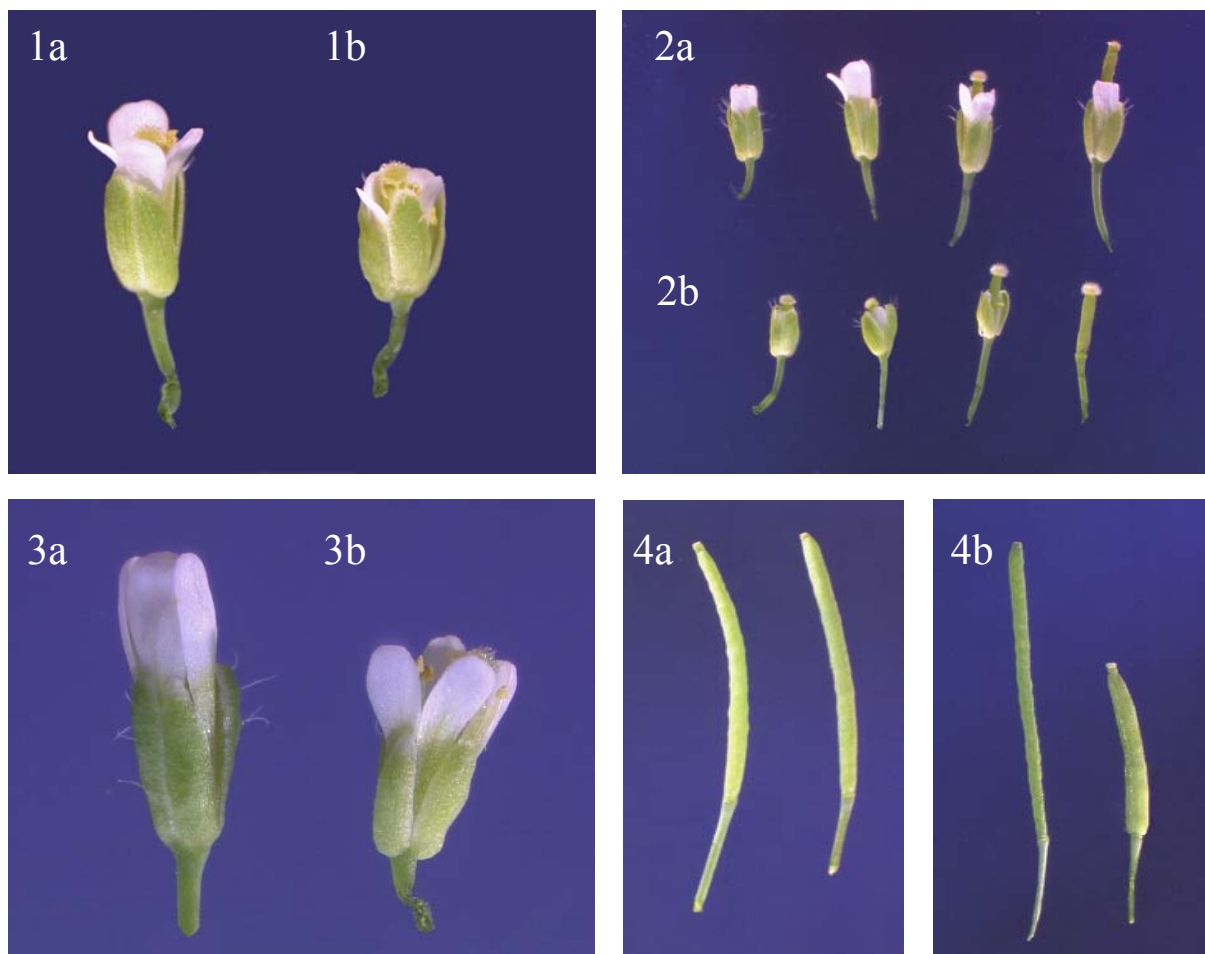


Figure 33. Flowers and siliques of IAA6 overexpressor plants

1a : Wild type flower, 1b: Flower of a wild type IAA6 overexpressing plant. Petals are underdeveloped and fall off early. 2a: Wild type flowers in different developmental stages. 2b: Flowers of IAA6wt overexpressor plants in different developmental stages. 3a: Wild type flower, 3b: Flower of an IAA6 S39E overexpressor plant. Petal development is reduced. 4a: Siliques of wt and IAA6 overexpressor plants (no difference). 4b: Siliques of IAA6 S39E overexpressor plants are shortened to approximately half length compared to those of wild type

3.6. ANALYSIS OF THE EFFECT OF SNRK1 KINASES ON SUBSTRATE STABILITY *IN VIVO*

A special protein stability testing vector was employed to study the effect of SnRK1 kinases on substrate stability *in vivo* (Figure 34.). This vector was developed by A. Bachmair [232]. The system uses a C-terminal fusion of dihydrofolate reductase (DHFR) to a defective ubiquitin as proteolysis reference protein, which is quite stable *in vivo*. DHFR-UBI is expressed in equal molar quantity with the test protein of interest in form of a translational fusion. The fusion protein construct is cleaved to DHFR-HA-UBI and target protein-HA units by ubiquitin specific proteases *in vivo*. As both DHFR-UBI and the target protein are labelled with the same C-terminal haemagglutinin (HA) tag, their amount can be precisely quantified by immunoblot detection with fluorescently labeled secondary antibodies and a laser scanning device (Odyssey). Although the protein stability testing vector was

originally designed to generate only one cleavage site downstream to C-terminal double glycine motif of DHFR ubiquitin tag, in practice the cleavage occurs both upstream and downstream to the ubiquitin tag. The ubiquitin tag carries a K48R mutation, which prevents ubiquitin chain formation on it, which would artificially target the system's components to proteasomal degradation. The reference protein serves as an internal standard to which parallel samples can be normalized and also indicates the general expression level of the fusion protein.

cDNAs of candidate SnRK1 kinase substrates were cloned into the stability testing vector and tested in combination with estradiol-inducible AKIN10 kinase in order to study the effect of AKIN10 overexpression on the stability of substrates.

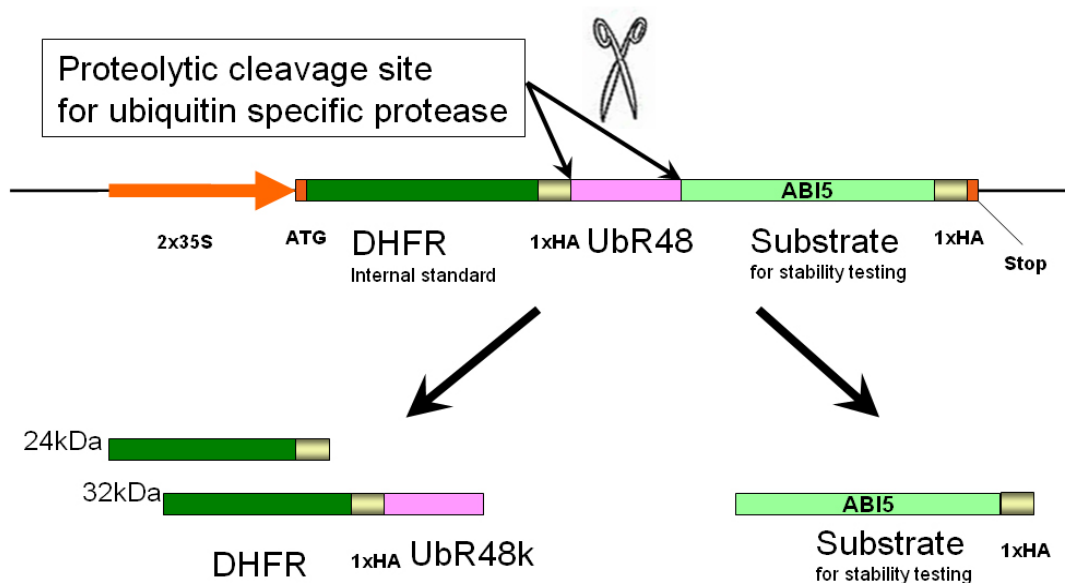


Figure 34. Schematic presentation of the pUBRX protein stability testing vector

3.6.1. Preparation of DNA constructs for *in vivo* test of stability of candidate AKIN10 substrates

First, the original stability testing vector was modified to make it compatible with the pPCV binary vector family, whose members carry a *NotI* cloning site. The DHFR-HA-UBI stability testing cassette was isolated as *HindIII* fragment and upon filling-in the ends with T4 DNA polymerase inserted into the pPCV compatible pPILY vector, from which the CaMV35S expression cassette was previously removed by *KpnI* followed by T4 polymerase treatment. Two *NotI* sites flanking the DHFR-HA-UBI stability testing cassette in the resulting vector allowed its transfer into the binary vectors pPCV002 (Km^R) and pPCV812 (Hyg^R). We named the resulting vector pUBRX similarly to its predecessor.

When cloning into this vector, it should be considered that the C-terminus of ubiquitin R48K should be fused in frame with the native N-terminal methionine of protein of interest. Any artificial amino acid introduced to the N-terminus might change the degradation speed of the protein of interest due to the N-end rule degradation pathway (referring to different degradation intensity of a

proteasomal substrate depending on the quality of its N-terminal amino acid). Thus, although there is a convenient *Bgl*II site directly downstream of the ubiquitin specific cleavage motif (Gly-Gly), it is not suitable for cloning because the sequence of all test proteins would start then with Arg corresponding to the AGA triplet in the *Bgl*II site. Instead, long primers were designed with a tail including the upstream region from the double glycine motif reaching to the nearby *Sal*I site (about 50 nucleotides upstream) and containing a complementary region to the substrate cDNA inserted directly downstream to the the position of double glycine (GGTGGT) codons.

In the construction of stability testing plasmids, the first step was tagging the PCR amplified cDNA of interest with coding sequences of the HA epitope. (We used intron-containing HA-tags, therefore the otherwise short tags become too long to incorporate them into a single primer and a second cloning step was necessary for tagging.) The forward PCR primers contained an extra *Nco*I site (IAA6, EIN3, EBF1, EBF2,) or a *Hind*III (IAA7) or a *Bgl*II (TIR1, ABI5) site upstream of the *Sal*I site and the reverse PCR primers carried a *Bgl*II site in order to insert the PCR product first in an HA-tagging vector (pMenchu *Sal*I-; i.e., to generate C-terminal HA-tagged constructs). The pMenchu *Sal*I-vector contained a destroyed *Sal*I site downstream of the HA tag sequence. Since a stop codon is positioned downstream of this *Sal*I site, it was necessary to eliminate it using an *Eco*RI site located downstream to the stop codon. So, the PCR product was inserted into pMenchu *Sal*I- as *Nco*I-*Bgl*II fragment than the cDNA fused to the intron-containing HA-tag sequence and a stop codon was transferred into *Sal*I and blunted *Xba*I sites of stability testing vector as *Sal*I and blunted *Eco*RI fragment. Finally, the complete stability testing cassette was subcloned into pPCV002 binary vector as a *Not*I fragment. (EBF1 was transferred into the stability testing vector in two pieces, because it contained an internal *Sal*I site.)

3.6.2. *In vivo* stability test of candidate substrate proteins in combination with AKIN10 overexpression

The effect of potential AKIN10 phosphorylation on substrate stability was studied *in vivo* in an inducible AKIN10 overexpressor background. As inducible AKIN10 kinase, the formerly prepared PIP-L tagged construct was used, which contained a C-terminal HA-tag for the simultaneous detection of kinase expression. The constructs were transformed into plants and root-derived dark-grown cell suspension cultures as well. Former trials of AKIN10 overexpression in green cell cultures failed, which is in accordance with recently published transcript profiling data showing antagonism between light and sugar signaling and AKIN kinase activity.

In the experiments 1-week-old stabilized double-transformant cell suspension cultures were pelleted at 200g for 1 min, resuspended in fresh medium and split into two samples. In the first sample, the kinase expression was induced with 10 μ M 2-estradiol, whereas the second sample was used as uninduced control. The samples were incubated in darkness for 4 hours, then collected and frozen in liquid nitrogen. Proteins were extracted from the samples by grinding the cells with sand in a mortar chilled with liquid nitrogen and taken up in 1ml ice cold buffer composed of 20mM Tris-HCl

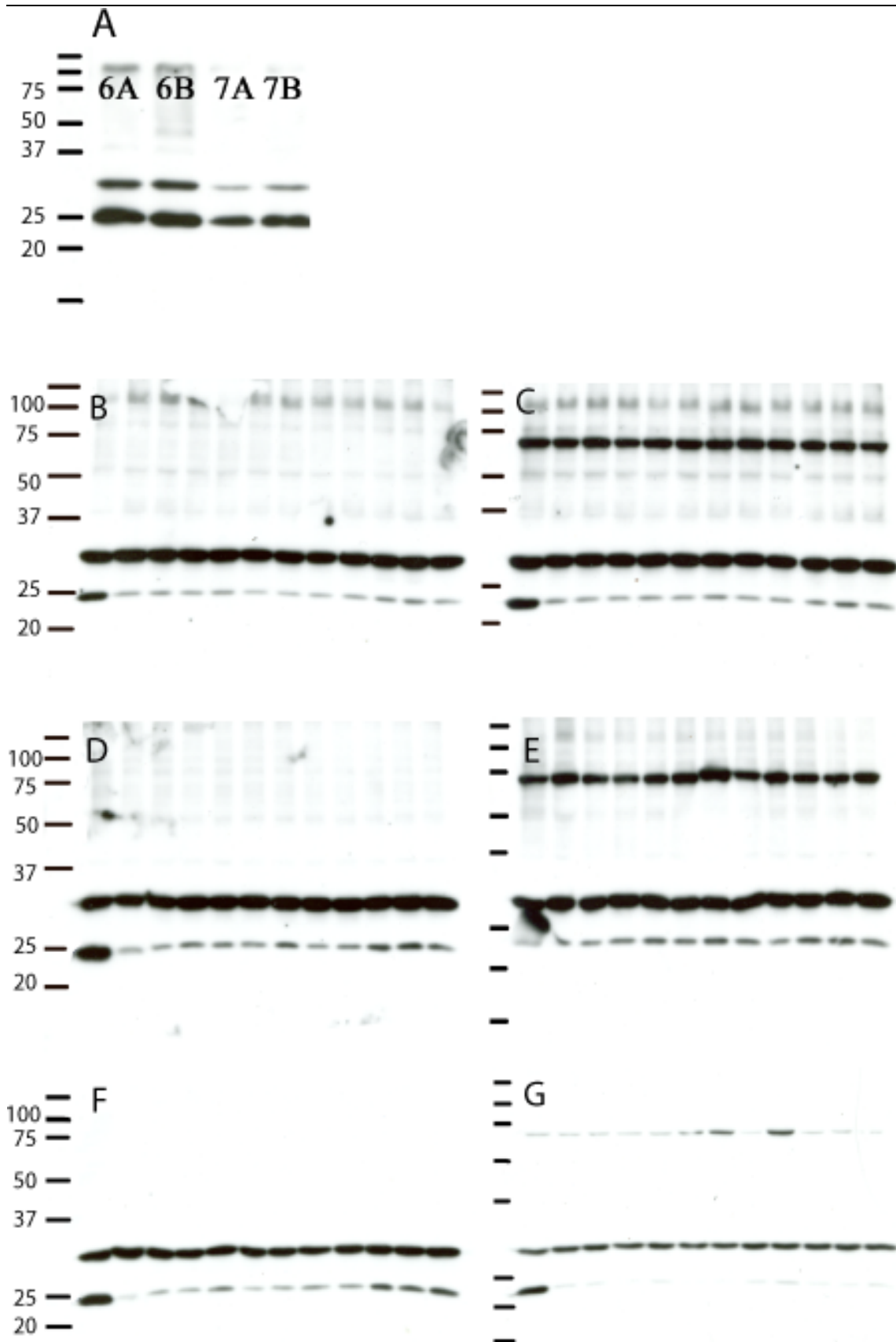


Figure 35. Results of in vivo substrate stability tests

A: stability testing of substrates in dark-grown Arabidopsis cell suspension. 6A: IAA6; 6B: IAA6 + AKIN10 induced (not detectable); 7A: IAA7; 7B: IAA7 + AKIN10 induced (not detectable). B-G: all MG132 treated samples collected in 10 min. intervals after MG132 removal. Western blot with α HA antibody. B: IAA6 (not detectable, it would be 20kDa); C: IAA6 + AKIN11 (~70kDa); D: IAA7 (not detectable, it would be 26kDa); E: IAA7 + AKIN11; F: IAA6 (not detectable); G: IAA6 + AKIN10

(pH 7.0), 10% glycerol, 5mM 2-mercapto-ethanol, 50mM NaCl and protease inhibitor cocktail in 1/100 dilution (Sigma 9939) and 25 μ M MG132. Cell debris was removed by pelleting at 20000xg in a cold tabletop centrifuge. The protein concentration of the supernatant was measured by Bradford assay (BIO-RAD) and equal amounts of 30 μ g protein samples were separated by SDS-PAGE. The result of immunoblot analysis of IAA6 and IAA7 (control) with α -HA antibody is shown in Figure 35. Unfortunately, in these experiments the formerly obtained very weak kinase expression signal could not be reproduced, nor the substrate proteins could be detected. The characteristic reference protein derived two bands could be observed in each samples, indicating expression and processing of the fusion protein. (According to personal communication of A. Bachmair, a characteristic double protein band appears as signal derived from the DHFR-HA-UBI part of the construct. The bands are approximately 34 and 24kDa, with 8kDa difference, which corresponds to the size of DHFR with and without ubiquitin.)

Since AKIN10 is degraded in a proteasome dependent way, in a second approach the cells were treated with specific proteasome inhibitor MG132 for 3 hours and then transferred into MG132-free medium to test the degradation of substrate proteins IAA6 and IAA7 by taking samples in 5-10 minute intervals. (There is data available in the literature for the half lives of a few IAA proteins, which ranges on an average between 5 to 10 minutes.) In the MG132-treated cells estradiol-induced expression of AKIN10 and AKIN11 kinases could be readily detected. Nonetheless, expression of IAA substrates was not detectable, although the characteristic bands for the proteolytically cleaved DHFR-HA-UBI reference protein were well visible. From the two expected cleavage products of DHFR-HA-UBI, the amount of lower band substantially decreased during the first 10 minutes, indicating a weakening effect of removed inhibitor proteasome inhibitor MG132.

4. DISCUSSION

The structurally and functionally conserved AMP-activated protein kinases are present in all eukaryotes. Plant and mammal AMPK orthologs can functionally replace their yeast ortholog, Snf1, *in vivo* [74, 78, 104]. Despite high level of conservation, AMPK orthologs show functional differences, indicating that their functions in single and multicellular eukaryotic organisms are considerably different. For instance, Snf1 is activated by the depletion of fermentable sugars, and its activation leads to reserve nutrient accumulation in yeast, whereas plant SnRK1 kinases also play a role in starch accumulation, but it occurs during the light period, when carbohydrates and energy are available due to photosynthetic activity. The physiological context is also different between species. For example, high concentration of external sugars causes rapid proliferation of yeast cells, whereas it inhibits early development of *Arabidopsis* seedlings. Another puzzling example is that despite high level of structural conservation of AMP/ATP binding γ subunits that confer AMP-dependent activation for mammalian AMPKs *in vitro*, AMP does not activate the trimeric yeast Snf1 complex *in vitro* [75]. These examples indicate that information gained about one ortholog might provide guidelines to studying another one, but it does not apply directly.

Snf1 controls the activity of metabolic enzymes in yeast and, importantly, it plays a wide role in nutrient signal transduction. Similarly, several metabolic enzymes were identified also in plants as targets of SnRK1 kinases. Nonetheless, our knowledge about the role of SnRK1 kinases in plant signal transduction is rather poor, although efforts have been taken to elucidate it.

4.1. IDENTIFICATION OF INSERTION MUTATIONS IN SNRK1 SUBUNIT GENES

Reverse genetic approach applied to functional dissection of *Arabidopsis* SnRK1 subunits is almost completed by now. Previously, the SNF4/AKIN $\beta\gamma$ mutations were characterized and revealed that they prevent male transmission (PhD thesis of Vijaya Shukla). Therefore, no homozygous mutant plants can be generated and the somatic phenotype of *snf4/akin $\beta\gamma$* can not be yet studied. In present work, one *akin10* insertion mutation was characterized, in which the T-DNA insertion is located in sequences encoding C-terminal regulatory sequences of the kinase. In addition, several mutant alleles of *AKIN β 1* and *AKIN β 2* subunit genes were identified, which conferred no phenotypic alterations in response to glucose and sucrose treatments during germination and seedling development. So far, no mutations are available for *AKIN11* and *AKIN β 3*. By contrast, several *akin12* knockouts are available, but the functional analysis of seed-specific AKIN12 kinase is hampered by the fact that *AKIN12* and *AKIN11* show co-expression during embryogenesis and seed development. Former experiments with *AKIN* promoter-GUS fusion constructs (PhD thesis, Kenneth Berendzen), as well as compilation of microarray data available in the *Genevestigator* database indicate that AKIN10 and AKIN11 are the

most widely expressed SnRK1 variants, probably being responsible for the majority of SnRK1 functions in *Arabidopsis*.

4.2. FUNCTIONAL ANALYSIS OF SNRK1 SUBUNITS

Transgenic RNA interference silencing of SnRK1 α subunits was carried out in several plant species, recently also in *Arabidopsis*, but the results are controversial. More recent and profound studies propose that SnRK1 kinases might play a role in starch mobilization (rice, *Arabidopsis*) and sugars inhibit SnRK1 kinase activity [233, 159], whereas former data indicate that SnRK1 is necessary for starch accumulation and sugar might induce SnRK1. SnRK1 α overexpression lead to starch accumulation in potato [152], whereas RNA interference mediated silencing resulted in reduced starch content [151]. Furthermore, SnRK1 kinase inhibition is necessary for the herbivore attack mediated carbohydrate transport from the aerial part to the root, which also indicates that SnRK1 kinase would promote starch accumulation [155]. Although several articles indicate the implication of SnRK1 kinases in starch and sugar metabolism, the exact mechanism is still not clear, after mutant analysis, overexpression and RNA interference studies. So far, very limited information could be obtained about the signalling events upstream and downstream to SnRK1 kinases at the molecular level.

The present work documents that SnRK1 kinase subunits can be expressed by 35S promoter only at a very minimal level in *Arabidopsis* because their stability of SnRK1 kinase subunits is strictly regulated by proteasomal degradation. Recently, a transcript profiling experiment was carried out in *Arabidopsis* protoplast system using transient overexpression [159]. The results suggest that SnRK1 kinase activity should be inhibited by sugars and activated by darkness and metabolic stress. One of the genes whose transcription was upregulated by AKINs is DIN6 (dark induced) and its promoter analysis revealed that a G-box element is responsible for the expression changes. Co-expression of AKINs with several G-box binding bZIP transcription factors revealed that bZIP TFs may be frequent substrates of AKINs [159].

In yeast, the Snf1 beta subunits are responsible for targeting the trimeric Snf1 kinase to different subcellular compartments and substrates. In order to reveal whether a mechanism would exist in *Arabidopsis* by which SnRK β subunit confers nuclear localization to the holoenzyme complex, GFP-tagged AKIN β subunits were overexpressed in *Arabidopsis* cell suspension culture and plants. In accordance with N-myristoylation of AKIN β 1 and AKIN β 2 [104], they were found mostly attached to membranes (plasma membrane and nuclear membrane), but AKIN β 1 and AKIN β 2 were also detected in the cytoplasm. By contrast, AKIN β 3, which carries no myristoylation site, was not associated to the membranes but found exclusively in the nucleus. Localization of AKIN β 1 and AKIN β 2 appears to be similar. This is the first instance when these proteins were found in the nuclear membrane. This finding may support the reverse recruitment model, which states that many genes – such as glucose repressed genes in yeast - are transcribed in distinct ultrastructural nuclear bodies and surfaces, such as the internal surface of nuclear envelope. Therefore, potentially all three *Arabidopsis* SnRK1 β subunits could participate in nuclear events of signal transduction. For the analysis of

potential relocation under nutritional stress conditions, AKIN β expressing suspension cells and seedlings were transferred into distilled water and kept in the dark. Instead of relocation, these experiments revealed light and sugar dependent degradation of the SnRK1 beta subunits (proteasomal degradation of β subunits was also shown in a biochemical assay). This observation supports that SnRK1 kinases are likely active in the dark and thus could indeed play a role in starch mobilization.

Previously, a key observation revealed a mechanism by which AMPK kinases participate in signal transduction. Yeast two-hybrid screen identified SKP1 (SCF-type E3 ubiquitin ligase subunit) and the proteasomal $\alpha 7$ subunit as *Arabidopsis* SnRK1 α interacting partners [88]. In support of this result, in *Arabidopsis* both trimeric SnRK1 kinases and their catalytic α -subunits alone have been detected in purified proteasomal complexes *in vivo*. Also in the better studied yeast system many instances have been found that Snf1 participates in the control of degradation of proteasomal substrates. Potential role of AMPKs in proteasomal control also appears to be underscored by the fact that most AMPK and AMPK-related kinases contain a ubiquitin-associated (UBA) domain. However, ubiquitin binding capability of UBA-domains has recently been questioned and it is now believed to UBA-domains play a structural role in AMPK regulation.

4.3. SEARCHING FOR CANDIDATE SNRK1 SUBSTRATES

As continuation of initial promising experiments, our laboratory invested a considerable effort into purification of proteasomal SnRK1 complexes from *Arabidopsis*. Epitope-tagged ubiquitin ligase subunits (SKP, Cullin, F-box proteins), proteasomal substrates and SnRK1 kinase subunits were overexpressed in *Arabidopsis*, subjected to multistep purification by conventional chromatography and immuno-affinity pull-down techniques. The isolated complexes were analyzed by immunoblot analysis and mass spectrometry. However, due to intrinsic instability of most mentioned SnRK1 and SCF components, this approach remained largely unsuccessful, despite considerable time and resources invested.

The present work describes an improved biochemical approach for purification of SnRK1 complexes. It was already tested that SKP1 and the proteasomal $\alpha 7$ subunit are not substrates for SnRK1 kinase *in vitro*. Therefore, we searched for candidate SnRK1 substrates, including known proteasomal substrates and F-box proteins (which are generally also substrates for proteasomal degradation). The number of F-box proteins and proteasome substrates is very high (in *Arabidopsis* there are 694 F-box proteins). Those proteins were selected as potential SnRK1 substrates, which are in connection with sugar signal transduction (i.e. their mutations confers sugar hypo- or hypersensitivity), and whose stability has been shown to be regulated by glucose. The candidates SnRK1 substrate proteins were overexpressed in and purified from bacteria, and subjected to *in vitro* kinase reactions using highly purified recombinant SnRK1 kinase AKIN10 and radioactive ^{32}P - γ ATP. These assays were facilitated by the unique property of plant SnRK1 catalytic subunits that allows their autophosphorylation and auto-activation, which provides moderate kinase activity *in vitro*.

ABI5 is a basic leucine zipper transcription factor that plays a key role in sugar induced post-germination developmental arrest. As mentioned above, few proteins from the bZIP family had been already suggested to function as possible SnRK substrates [159]. The cellular level and activity of ABI5 is regulated by phosphorylation and proteasome mediated degradation. Members of the ABI5 family, such as AREB1, are phosphorylated by SnRK2 kinases, which contain very similar conserved kinase domain as SnRK1 kinases. Our results indicated that AKIN10 phosphorylates ABI5 whereas no activity could be detected with AKIN11 *in vitro* (neither substrate phosphorylation nor autophosphorylation), although its activity was reported formerly.

The *Arabidopsis* ABI5 protein family contains 13 members, from which 9 show especially high homology and conservation of formerly identified AREB1 phosphorylation sites [231]. Such a closer relative is DPBF4/EEL1, which similarly to ABI5 is specifically expressed during embryo and seed development, and phosphorylated by members of the SnRK2 kinase family *in vitro* (unpublished data). We found that recombinant DPBF4 is also phosphorylated by AKIN10. *In vitro* phosphorylated ABI5 and DPBF4 proteins were analyzed by 2D-gel electrophoresis and mass spectrometry, which lead to the identification of 5 conserved SnRK1 phosphorylation sites in both proteins. In earlier studies [234], three phosphorylation sites were identified in immunoprecipitated ABI5 and additional sites were found in its somatically expressed relative, AREB1, by *in vitro* phosphorylation of its synthetic peptide fragments by SnRK2 kinases [231]. These formerly determined phosphorylation sites follow the general recognition motif of CDPK superfamily kinases (K/R-X-X-S/T), which include all SnRKs, whereas one of the newly identified site is atypical and contains a positively charged amino acid residue (K/R) in position -4 (i.e., relative to the phosphorylated S residue). This novel phosphorylation site is present in both ABI5 and DPBF4. By contrast, one less conserved site, which was reported earlier for AREB1 [231], could not be confirmed in our experiments. Site-directed mutagenesis of 5 phosphorylation sites of ABI5 to either alanine or aspartate residues is in progress in order to generate non-phosphorylatable and dominantly active ABI5 versions, respectively.

Based on these experiments, ABI5 and DPBF4 provide the first examples for that SnRK1 and SnRK2 kinases can have common substrates. Although these data derived from *in vitro* phosphorylation experiments, one may speculate that ABI5-mediated post-germination developmental arrest could be activated in response to different signals, which are transduced by different kinases through phosphorylation of ABI5 and other members of the ABI5 family. Five of the ten SnRK2 kinases are activated in response to ABA and 9 in response to hyperosmotic stress. On the other hand, our data indicate that SnRK1 kinases probably act in regulation of sugar-dependent germination arrest. SnRK1-mediated phosphorylation of ABI5 suggests that, at least in germinating seedlings, SnRK1 kinases may be activated by high sugar concentration, which is opposite to the result derived from a recent microarray experiment [159].

The recognition motives and substrate sets of SnRK1 and SnRK2 kinases are probably not identical, although overlapping. Our collaborators from the group of Jeff Leung (CNRS, Gif sur Yvette, France) experimentally determined the sequence of an optimal peptide substrate motif for both

SnRK1 and SnRK2 kinases. Synthetic peptide substrates with combinatoric amino acid sequences were phosphorylated with the distinct SnRK kinases, including our purified AKIN10, *in vitro* using $\gamma^{32}\text{P}$ -ATP. The identified motives are substantially different, although a positively charged amino acid residue in position -3 relative to the phosphorylated serine enhances the phosphorylation most. However, in nitrate reductase, a known substrate of SnRK1 kinases, the amino acid sequence around phosphorylate Ser 521 residue, which is responsible for the activity of NR, does not contain positively charged residues at positions -3 or -4 indicating considerable plasticity of the kinase motif.

ABI5 and DPBF4 also play a role in reserve accumulation phase during embryo development, when sugars are provided by the mother plant and absorbed by the embryo. In this process, the embryo develops high desiccation tolerance and its growth stops similarly to the post germination developmental arrest. Therefore, SnRK1 kinases are probably involved in the determination of source-sink relations of different tissues that provides an explanation for the starch accumulation defect observed in seeds of SnRK1 kinase knock-down plants. AKIN12 is the third SnRK1 α variant in *Arabidopsis*, which is expressed only in siliques (Genevestigator data and PhD thesis of Kenneth Berendzen). Therefore, it is possible that *in vivo* AKIN12 is responsible for ABI5 and DPBF4 phosphorylation.

Compared to ABI5 and DPBF4, many other candidate SnRK1 substrates showed weaker phosphate incorporation in the *in vitro* kinase assays. Interestingly, HY5, another bZIP transcription factor, a positive regulator of nitrate reductase whose stability is regulated by light and phosphorylation, was not phosphorylated by AKIN10 *in vitro*. A few interesting candidate substrates, such as EIN3 (whose degradation is enhanced by glucose and ABI4, a key transcriptional factor in sugar and ABA signaling) could not be purified unfortunately from bacteria. Nonetheless, we observed that several cyclins showed weak SnRK1-mediated phosphorylation, but their phosphorylation sites could not be determined by mass spectrometry. These included cyclinD3;1, which is also a proteasomal substrate, and involved in the regulation of G1/S transition of cell cycle. Abundance of cyclinD3;1 was reported to fall rapidly in response to sucrose starvation. Its degradation is probably promoted by phosphorylation similarly to CyclinD1. However, CyclinD2 seems to be a more stable protein.

IAA7, transcriptional repressor in the auxin signaling pathway, represents a well-known proteasomal substrate. We have analysed potential SnRK1-mediated phosphorylation of IAA7, because its gain of function mutation (*axr2*) confers insensitivity for externally applied glucose. Other members of the Aux/IAA protein family were also tested because of their partial sequence conservation. Similarly to IAA7, IAA3 also shows constitutive photomorphogenesis phenotype, whereas IAA6 does not. In contrast to the anticipated results, significant phosphate incorporation could be detected using IAA6 as SnRK1 substrate, whereas SnRK1 did not show significant phosphorylation activity with IAA7 and IAA3. In IAA6, a single phosphorylation site (Ser39) was successfully identified by mass spectrometric analysis. Two-dimensional gel electrophoresis analysis of *in vitro* phosphorylated IAA6 also predicted no more than one potential phosphorylation site.

Moreover, the identified phosphorylation site contains the only serine residue in the IAA6 sequence, which is flanked by a positively charged residue at position -4. Phosphopeptide mapping of radioactively phosphorylated IAA6 also supported phosphorylation of the same position. Intriguingly, a serine residue with a positively charged amino acid at this position is found in several Aux/IAA proteins, including IAA7 and IAA3, although we failed to observe *in vitro* phosphorylation of these proteins. Overexpression of S39E mutant IAA6 in *Arabidopsis* plants caused severely stunted phenotype. In comparison, overexpression of wild type IAA6 showed only petal developmental defect. IAA6 is a proteasome substrate and its degradation requires a conserved degron (domain II), which is the binding site for members of the TIR1 F-box protein family. *shy1* is a gain of function mutation in the conserved degron sequence (domain II) of IAA6. *shy1* shows only minor phenotypic changes, such as slightly reduced hypocotyl length and upcurled leaves. Clearly, the phenotype of IAA6 S39E overexpressing plants differs from the *shy1* mutant phenotype and reflect more severe disturbance of proper auxin signaling leading to drastic reduction of elongation growth and fertility.

Although our results do not probe that AKIN10 is implicated in phosphorylation of IAA6 also *in vivo*, the observed drastical developmental effect of IAA6 S39E overexpression suggests that the site is of functional importance *in vivo*. This result is in contrast to the prevailing view, which suggests that the IAA proteins are no phosphoproteins. In parallel to our data, oat PhyA was found to phosphorylate some IAA proteins *in vitro* (IAA1, IAA3, IAA9 and IAA17). The site was mapped to a fragment between domain I and domain II, which includes the position that was identified in the present work. However, these data are quite artificial, because PhyA itself does not contain a kinase domain, but only a kinase-related domain [235]. Potential regulatory role of S39 residue is indicated by the fact that at position -4 relative to the phosphorylated serine there is an invariant lysine residue, which was identified as potential ubiquitylation site [236]. This lysine residue seems to be necessary for basal degradation rate of the short-lived AUX/IAA proteins, but is dispensable for their rapid auxin-mediated degradation. Nonetheless, our preliminary results using western blot analysis of wild type and S39E mutant IAA proteins show that the S39E mutation of IAA6 does not lead to extreme stabilization of the protein. As IAA6 levels are rather low in the absence of auxin induction, further experiments are needed to determine whether the S39E mutation affects the stability of IAA6 or enhanced its activity, potentially by promoting better binding to ARFs (auxin response factors). Stabilization of IAA7 in the *axr2* gain of function mutant shows insensitivity to sugars that means under high sugar concentration the level of IAA7 should be lower. Therefore, in theory low sugar conditions should stabilize IAA7. Considering the structural similarity between yeast and plant AMPKs together with recent SnRK1 microarray data, SnRK1 should be generally activated by low sugar conditions. Therefore, in principle, phosphorylation is expected to stabilize IAA proteins, but this remains to be proven by further experiments.

4.4. AN ASSAY SYSTEM FOR ANALYSIS OF STABILITY OF CANDIDATE SNRK1 SUBSTRATES IN VIVO

In order to study the effect of SnRK1 kinases on the stability of candidate substrates *in vivo*, a special stability testing vector system was developed based on previous work of Andreas Bachmair in our department. The system takes advantage of a reference protein, which is expressed in a translational fusion with the protein of interest. The two proteins expressed in a translational fusion are separated from each other *in vivo* by ubiquitin specific proteases. The reference protein DHFR-HA-UBI is stabilized by a mutation that prevents ubiquitin chain formation and its subsequent proteasomal degradation. In fact, degradation of the reference protein occurs but it still can serve as a gel loading control for the comparison of parallel samples. The comparison is carried out in the same immunoblot experiment, because both the DHFR-HA-UBI reference protein and the protein of interest carry C-terminal HA epitope-tags for detection. cDNAs of selected test proteins (IAA6, IAA7, TIR1, EIN3, EBF1, EBF2 and ABI5) were cloned into this vector system and the stability of candidate SnRK1 substrates was tested in response to estradiol-induced SnRK1 kinase AKIN10 expression in *Arabidopsis* cell suspension cultures. (*Arabidopsis* plants transformed with these constructs were not ready by the date of submission.) The SnRK1 kinase also contains a C-terminal HA epitope tag, therefore its expression level can be monitored simultaneously with the two other proteins. The experiments showed that *in vivo* separation of the fusion DHFR-HA and test proteins occurred, because the characteristic bands of DHFR-HA-UBI and DHFR-HA internal standards could be detected. However, none of the substrate proteins could not be detected under these conditions suggesting that they are extremely unstable in the cell suspension system, which is maintained in the presence of 3% sucrose and auxin.

Another possibility and a potential trivial reason is that the tested candidate proteins are not *in vivo* substrates for the SnRK1 kinases. However, it is more likely that degradation of the tested IAA proteins, as well as that of EIN3 and others, are extremely fast and can only be monitored using chase experiments in combination with proteasome inhibitor treatments. A possible improvement may be the application of multiple tandem epitope tags (for instance 16x HA was applied in Pascal Genschik's laboratory in order to detect EBF1). However, in each case it is a question whether phosphorylation stabilizes or destabilizes the substrates and this should be experimentally answered. Another problem of the experimental set up is the very low level of SnRK1 kinase expression. To circumvent this problem, the samples were initially treated with proteasome inhibitor (MG132) to enhance SnRK1 expression. Later, the MG132 was removed and samples were collected in short time intervals, and analyzed by immunoblotting. In this way, SnRK1 expression could be readily detected. However, the IAA substrate proteins still could not be visualized, not even in the MG132-treated samples. So, it remains to be seen whether in young seedlings, where auxin induction and subsequent degradation of IAA was successfully established, an effect of SnRK1 overexpression or S39E mutation can be observed at the levels of regulation of stability of IAA6.

Another question is whether the overexpression of single SnRK1 catalytic α -subunits can effectively increase the kinase activity *in vivo*. Specific physiological conditions may be required to activate the overexpressed α -subunit involving T-loop phosphorylation and γ -subunit related activation. The overexpressed kinase may only be partially assembled into trimeric complexes because the other subunits are not present in stoichiometric amounts (or not at all) in the transformed cells. In order to enhance the effectiveness of *in vivo* experiments, we tried to increase the activity of SnRK1 catalytic subunits by mutations. The autophosphorylation site at the T-loop threonine was mutated to aspartate residue, which mimicks its phosphorylated state and prevents the inactivation of SnRK1 by specific protein phosphatases *in vivo*. The activating T-loop mutation increased the activity of SnRK1 kinase AKIN10 about 3 times *in vitro*. Furthermore, we found that the UBA domain of AKIN10 is also necessary for the kinase activation. The fact that deletion of UBA domain did not result in elevated kinase activity indicated on the other hand that the UBA domain is not part of the autoinhibitory kinase domain. Deletion of the proposed C-terminal autoinhibitory domain from the SnRK1 catalytic subunit AKIN10 did not increase the SnRK1 α activity either.

4.5. IMPROVED TECHNOLOGY FOR AFFINITY PURIFICATION OF SNRK1 KINASES

We have attempted to isolate SnRK1 kinase complexes from various plant materials, but the SnRK1 subunits proved to be very unstable proteins *in vivo*, and this caused a considerable obstacle. Immunoblot analysis could detect SnRK1 subunits in the chromatographic fractions but their quantity was not sufficient for mass spectrometric analysis of the complex components and their phosphorylation patterns. Therefore, we developed a novel tandem affinity chromatography method combining the application of His, Strep and HA affinity tags. In plant tissues, protein concentrations are generally lower than in animal cells, and after tissue homogenization the sample is exposed to a high proteolytic activity of the vacuolar contents, which in practice cannot be fully inhibited by the use of externally added protease inhibitors. Therefore, the most successfully applied protein extraction strategies from plant material involve immediate precipitation after sample homogenization and a short filtration. These approaches destroy complex protein structures, and therefore are not suitable for isolation of larger protein complexes without the application of chemical cross-linking. Conventional chromatographic approaches capture the protein of interest by ion-exchange chromatography, which does not provide high selectivity (i.e., max. purification rate is between 20 to 50-fold). Therefore, the ion-exchange chromatography fractions often are contaminated with considerably high protease activities and their subsequent processing e.g., through size fractionation by gel filtration may also result in a dilution of protein of interest below the detection threshold. Furthermore, in order to identify chromatographic fractions containing the protein of interest, immunoblot analysis has to be carried out, which takes many hours during which the proteolytic activity may destroy the samples. Alternatively, the sample can be frozen, but this is accompanied by protein precipitation, especially if more freeze-thaw cycles are needed because of multiple purification steps. Therefore, rapid and highly

selective purification is necessary to minimize protein degradation when purifying native proteins. To achieve these goals, we established tandem affinity purification using Ni-chromatography and subsequent strep-tactin chromatography. Both steps are highly selective and the elution happens in one step, and therefore immunoblot analysis between the steps is not necessary. We have demonstrated that this technology is applicable to purification of AKIN β 2 subunit and showed that already the first step Ni-affinity chromatography yields about 10,000-fold enrichment. Thus, scaling up this approach with using effective means for stabilization of SnRK1 subunits (e.g., low sucrose, darkness, proteasome inhibitors etc.) is expected to improve the efficiency of subunit analysis of SnRK1-proteasome complexes in the future.

4.6. SNRK1-ACTIVATING KINASES

To study the roles of putative SnRK1-activating kinases first genetically and later biochemically, we have identified two putative *Arabidopsis* SnRK1 activating kinases (SnAK1/TLK1 and SnAK2/TLK2) based on sequence similarity to yeast Snf1 upstream activating kinases [38]. In order to gain information about the SnRK1-activating physiological conditions, homozygous T-DNA insertional mutations were identified in both *SnAK* genes. The individual *snak* mutants do not show any phenotypic alteration compared to wild type plants, neither when treated with sugars or ABA. Therefore, we initiated the construction of double *snak* mutant lines. In addition, we have demonstrated that recombinant SnAK1 is an active enzyme, which shows intensive autophosphorylation, but nevertheless only weakly phosphorylates AKIN10 *in vitro*. In our experiments, recombinant SnAK2 was not active suggesting that potentially other proteins (i.e., SnAK subunits) may be required for proper activity of these kinases. Intriguingly, SnAKs were found by others to be able to functionally replace their yeast orthologs, which implies a considerable conservation of SnAKs and their putative regulatory partners in yeast and plants.

4.7. OUTLOOK

After four years of efforts invested into the development of genetic and biochemical tools for functional analysis of plant SnRK1 kinases, the studies have now arrived to a stage when most genetic tools are available along with improved biochemical technologies. Several observations made in this work indicate that functional analysis of plant SnRK1 kinases can be expected to reveal surprising unique regulatory functions of AMP-activated kinases in plants. Our data showing that the *akin β 1akin β 2* double knockout lines display no stress, sugar, hormone and developmental alterations contradict a recently published highlight suggesting that N-terminal myristoylation of these subunits would be required for meristem differentiation and leaf development [104]. Rather these data strengthen our observations that the catalytic subunits of plant SnRK1 enzymes can act as active kinases in the absence of other regulatory subunits, in analogy e.g., to several animal AMPK-like kinases.

Furthermore, it is still a question whether AKIN β 3 is a genuine subunit of trimeric SnRK1 enzymes as interaction of AKIN β 3 with other SnRK1 subunits awaits confirmation *in vivo*.

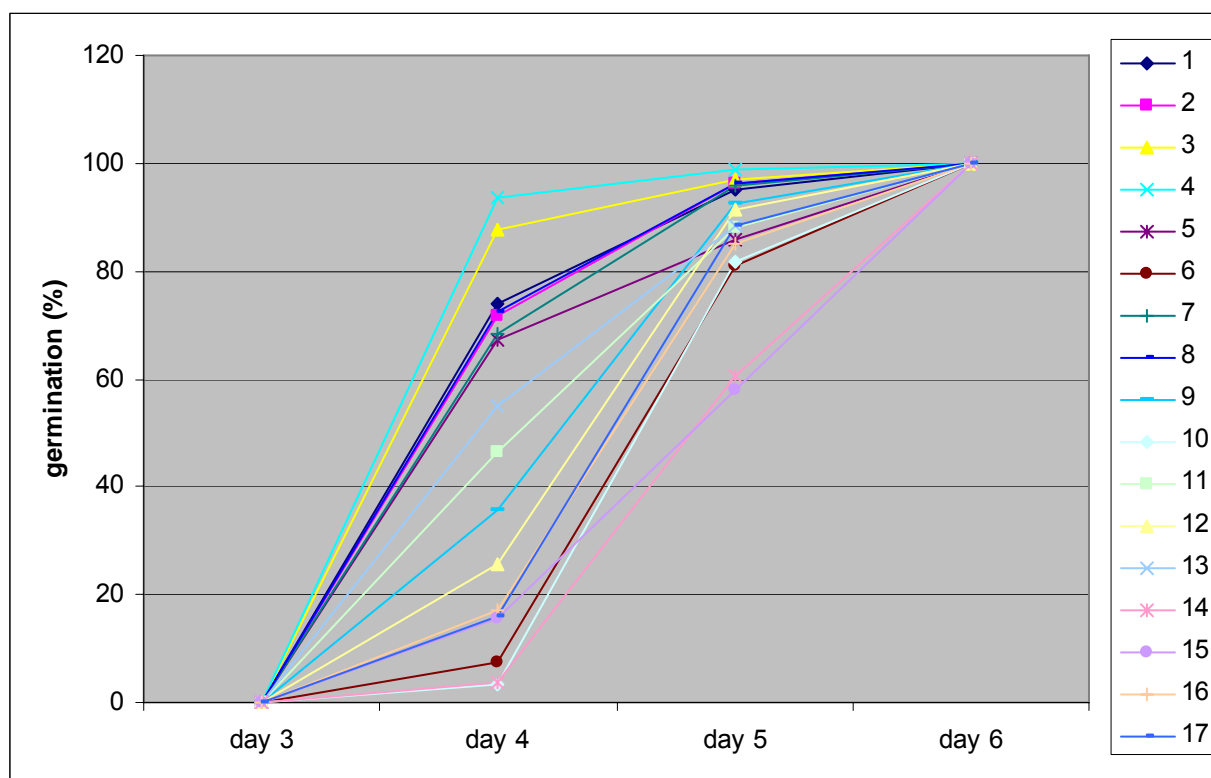
From the data described in this thesis it is apparent that there is a great need for additional studies for precise definition of temporal and spatial cellular localization, traffic and expression level of different SnRK1 subunits proteins during plant development and in response to sugar and stress stimuli. These studies can only be performed with native gene constructs in combination with the available knockout mutations. Our data clearly illustrate that artificial overexpression of various SnRK1 subunits is not suitable to address specific questions concerning the activation of SnRK1 kinases and mechanisms controlling their *in vivo* stability. Nonetheless, these previous studies using artificial overexpression of kinases subunits shed light onto one important regulatory aspect of SnRK1 functions by identifying important light and sugar-dependent post-translational control mechanisms. Along with other emerging data, these observations support the model that SnRK1 kinases play central regulatory roles in the coordination of light, sugar and stress signaling pathways in plants. At the same time, destabilization of SnRK1 subunits by sucrose and light treatments question some recently published data, which have derived from the analysis of transcriptional regulatory effects of SnRK1 catalytic α -subunits in an artificial protoplast system (i.e., maintained in the presence of 3% sucrose and 3% sorbitol, [159]). Furthermore, data derived from RNAi inhibition of AKIN kinases also remain to be confirmed by application of inducible, gene specific artificial microRNAs instead of using silencing constructs for targeting the conserved catalytic α -subunits of SnRK1 kinases. Finally, precise functional dissection of SnRK1 kinases, especially their roles in the regulation of transcription and proteolysis of transcription factors, requires precise resolution of subunits of various nuclear SnRK1 complexes, which will be impossible without a breakthrough in their purification and subsequent analysis using mass spectrometry.

5. APPENDIX

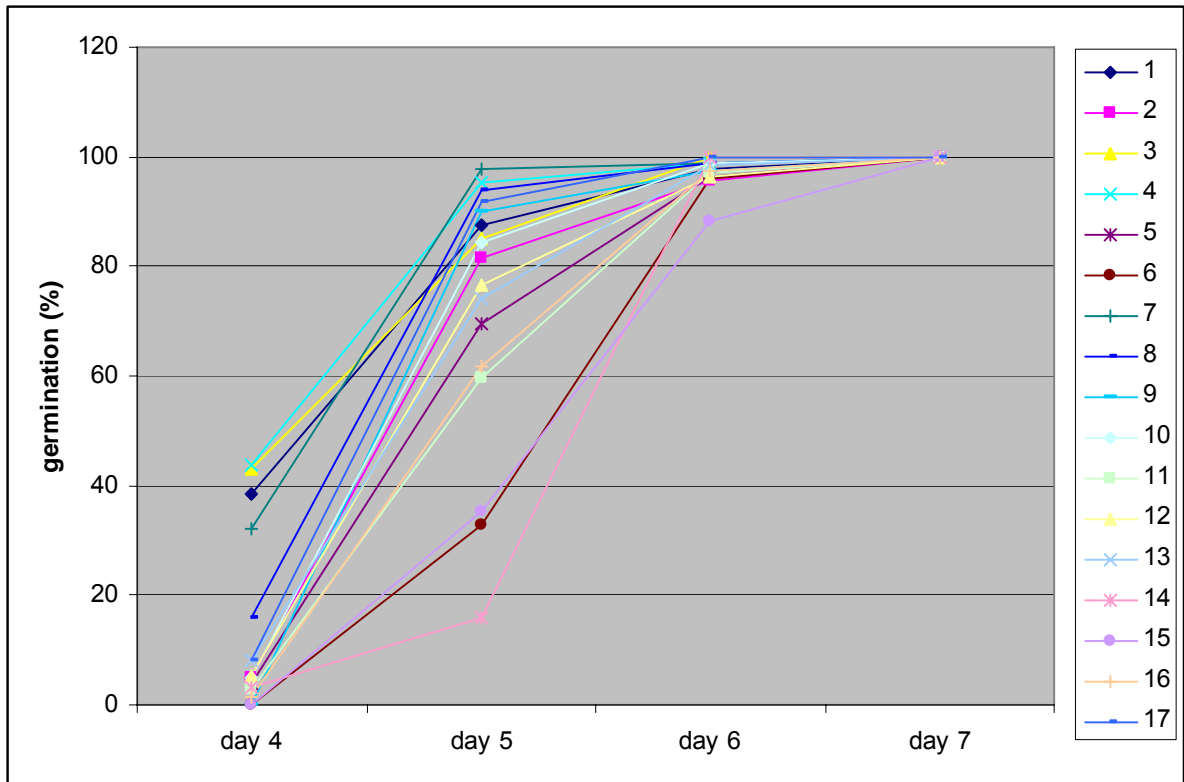
5.1. GERMINATION DATA OF T-DNA INSERTION MUTANTS IN SNRK1 SUBUNIT AND SNAK KINASE GENES

Supplementary data to the chapter 3.1.7.

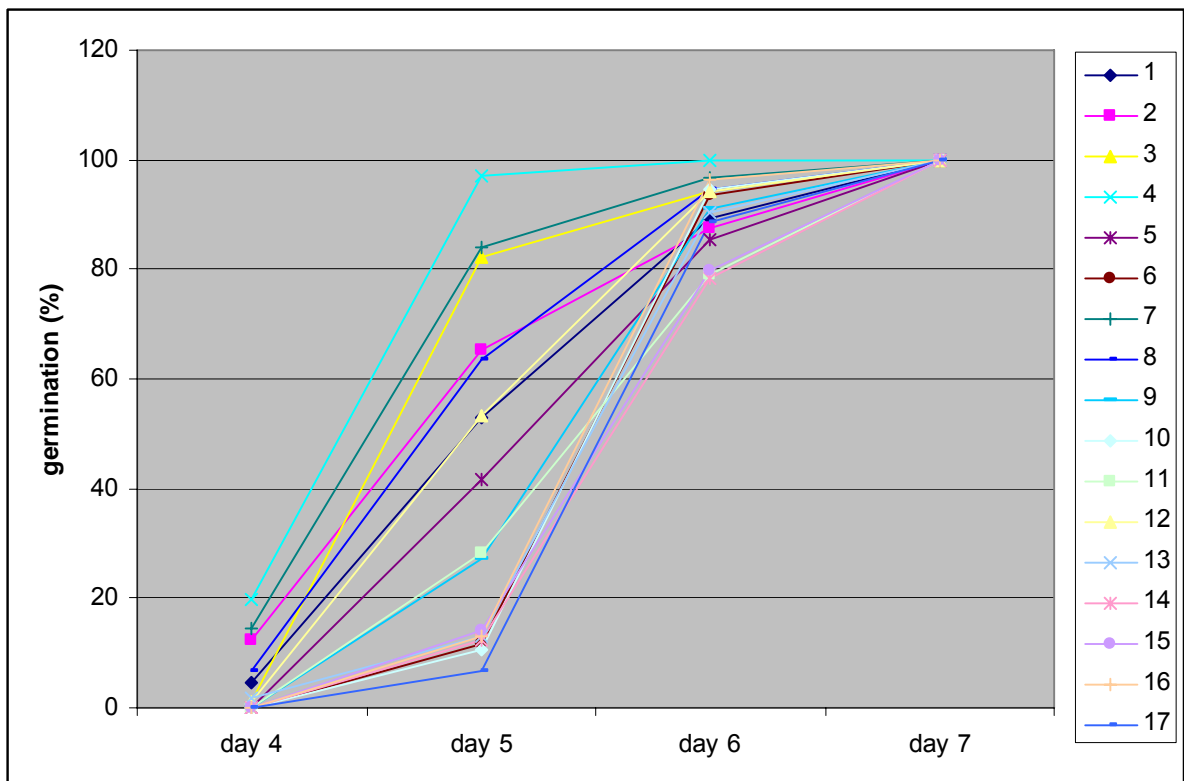
1. TLK1 Salk 000044 T2/1
2. TLK1 Salk 000044 T2/3
3. TLK1 Salk 015230 T2/1
4. TLK1 Salk 015230 T2/2
5. TLK2 Salk 142938 T2/1
6. TLK2 Salk 142938 T2/3
7. AKIN10 GABI 579E09 T2/3
8. AKIN10 GABI 579E09 T2/6
9. AKIN β 1 Koncz 14344 T3 from T2/13
10. AKIN β 1 GABI T3 from T2/2
11. AKIN β 1 Salk 008325 T3 from T2/2
12. AKIN β 2 Salk 037416 T3 from T2/10
13. AKIN β 2 Koncz 87453 T3 from T2/2
14. AKIN β 1 Salk x AKIN β 2 Koncz T2/9
15. AKIN β 1 Salk x AKIN β 2 Salk T2/11
16. AKIN β 1 Salk x AKIN β 2 Salk T2/15
17. Col-0 wt



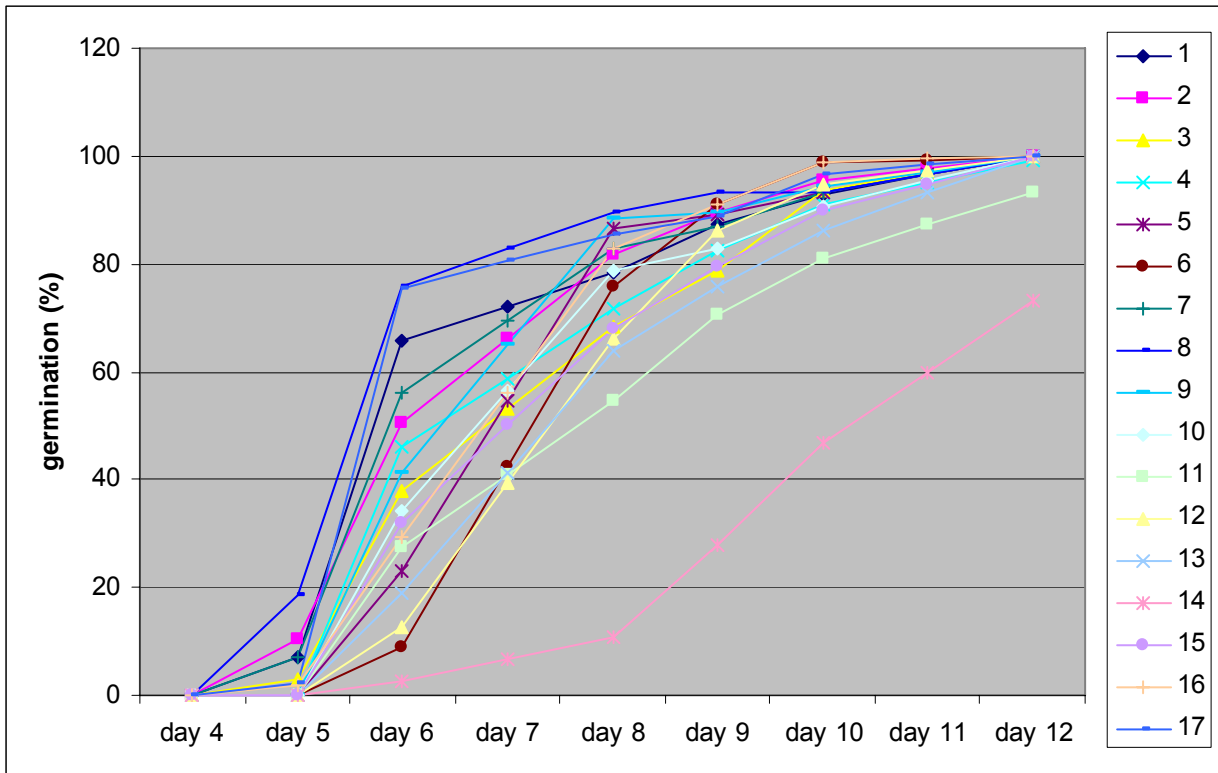
MSAR (normal medium)



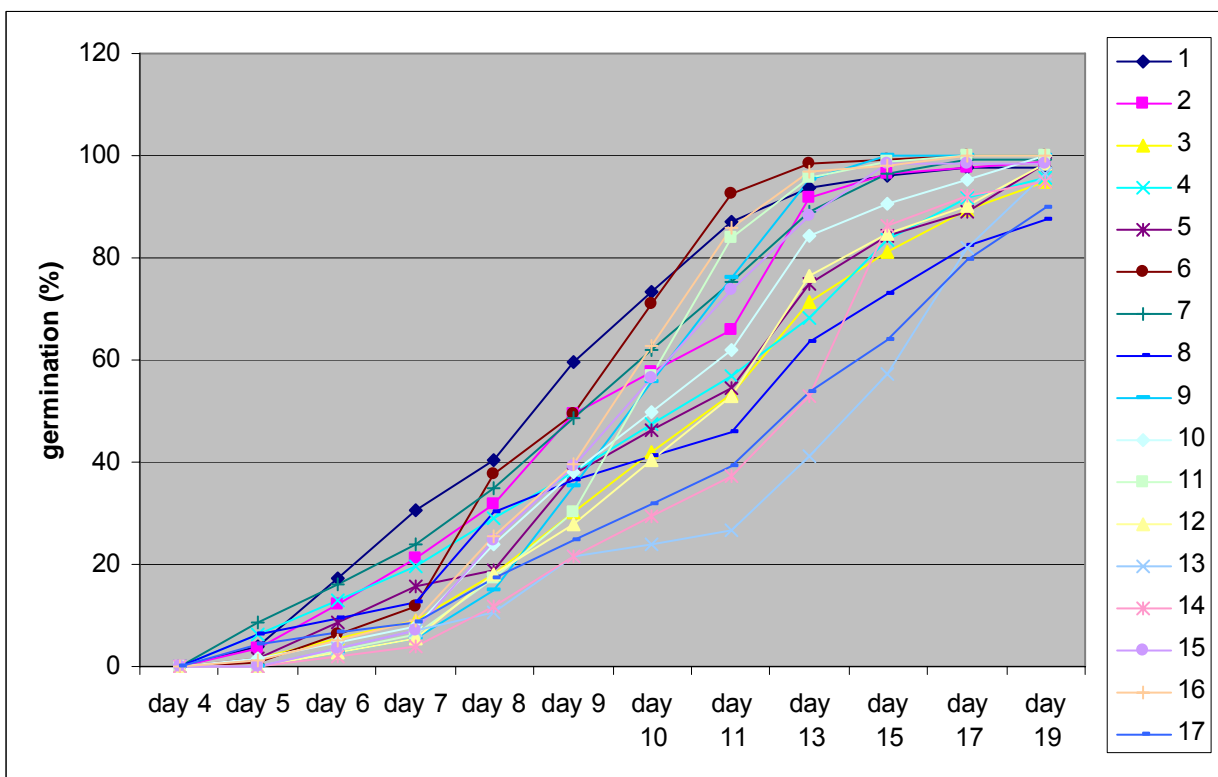
3% glucose in MSAR



5% sucrose in MSAR

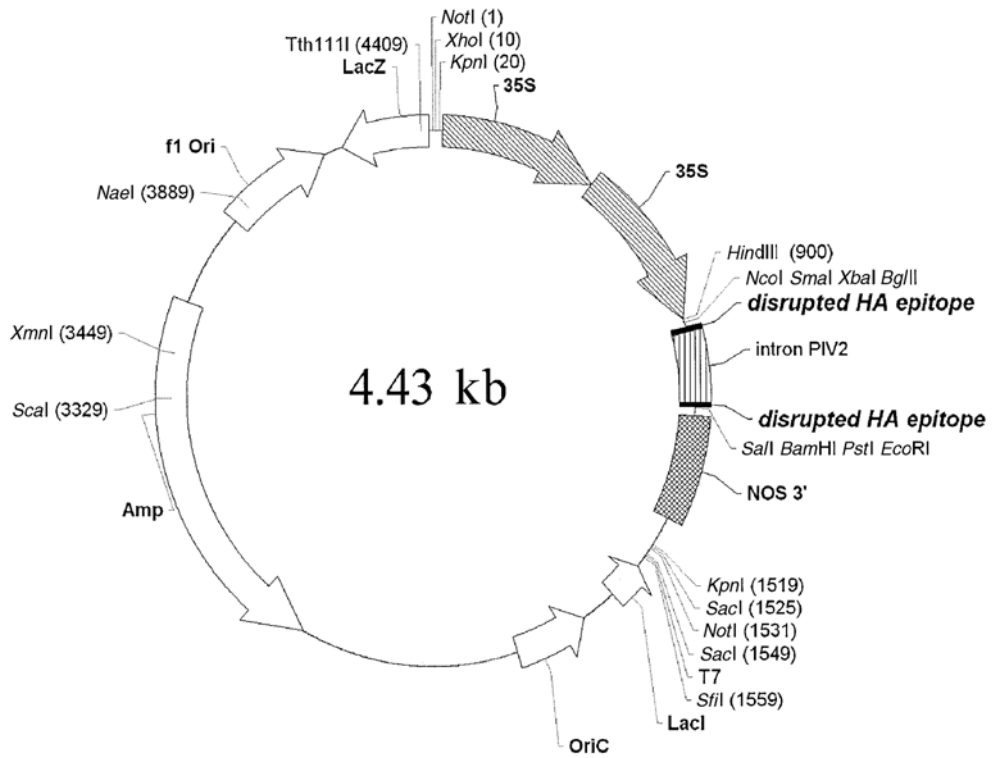


1 μM ABA in MSAR



2 μM ABA in MSAR

5.2. MAP OF pPILY VECTOR



pPILY

H::A
IV2
H::A

HindIII
NcoI
SmaI
XbaI
BglII
Y P Y D
intron
V P D Y A
SaI
BamHI
PstI
EcoRI

CAAGCTTCACC ATG GCG CCC GGG TCT AGA AGA TCT TAT CCA TAC GAT gt.....ag GTT CCA GAT TAT GCT GAG TCG ACG GAT CCA CTG CAG TGA ATT C

*

pMENCHU

H::A
IV2
H::A

HindIII
NcoI
SmaI
XbaI
BglII
Y P Y D
intron
V P D Y A
SaI
BamHI
PstI
EcoRI

CAAGCTTCACC ATG GCG CCC GGG TCT AGA AGA TCT TAT CCA TAC GAT gt.....ag GTT CCA GAT TAT GCT GGT CGA CGG ATC CAC TGC AGT GAA TTC

5.3. MASS SPECTROMETRIC IDENTIFICATION OF PHOSPHORYLATION SITES IN ABI5, DPBF4 AND IAA6 PROTEINS

Phosphorylated proteins were digested with trypsin or gultamyl endopeptidase. Isolated phosphopeptides were fragmented by electrotransfer decay (ETD) or collision induced decay (CID) before the second mass spectrometer unit. Mass of the expected fragment ions are listed below. In red bold the actually detected fragment ions are highlighted. Amino acid residues marked with asterisk are phosphorylated based on the molecular mass difference of neighboring peptides.

ABI5 V8 (Glu-C) ETD

#	c	c ⁺⁺	Seq.	y	y ⁺⁺	z+1	z+1 ⁺⁺	z+2	z+2 ⁺⁺	#
1	132.0768	66.5420	N							12
2	189.0982	95.0527	G	1309.4589	655.2331	1293.4401	647.2237	1294.4480	647.7276	11
3	317.1932	159.1002	K	1252.4374	626.7223	1236.4187	618.7130	1237.4265	619.2169	10
4	431.2361	216.1217	N	1124.3424	562.6749	1108.3237	554.6655	1109.3315	555.1694	9
5	578.3045	289.6559	F	1010.2995	505.6534	994.2808	497.6440	995.2886	498.1479	8
6	635.3260	318.1666	G	863.2311	432.1192	847.2124	424.1098	848.2202	424.6137	7
7	802.3243	401.6658	S*	806.2096	403.6085	790.1909	395.5991	791.1987	396.1030	6
8	933.3648	467.1860	M	639.2113	320.1093	623.1926	312.0999	624.2004	312.6038	5
9	1047.4077	524.2075	N	508.1708	254.5890	492.1521	246.5797	493.1599	247.0836	4
10	1178.4482	589.7278	M	394.1279	197.5676	378.1091	189.5582	379.1170	190.0621	3
11	1293.4752	647.2412	D	263.0874	132.0473	247.0687	124.0380	248.0765	124.5419	2
12			E	148.0604	74.5339	132.0417	66.5245	133.0495	67.0284	1

MS/MS Fragmentation of **NGKNFGSMNMDE**

Monoisotopic mass of neutral peptide Mr (calc): 1422.4945

S7: Phospho (ST), with neutral losses 0.0000 (shown in table), 97.9769

#	c	c ⁺⁺	Seq.	y	y ⁺⁺	z+1	z+1 ⁺⁺	z+2	z+2 ⁺⁺	#
1	132.0768	66.5420	N							12
2	189.0982	95.0527	G	1325.4538	663.2305	1309.4351	655.2212	1310.4429	655.7251	11
3	317.1932	159.1002	K	1268.4323	634.7198	1252.4136	626.7104	1253.4214	627.2143	10
4	431.2361	216.1217	N	1140.3374	570.6723	1124.3186	562.6630	1125.3265	563.1669	9
5	578.3045	289.6559	F	1026.2944	513.6508	1010.2757	505.6415	1011.2835	506.1454	8
6	635.3260	318.1666	G	879.2260	440.1166	863.2073	432.1073	864.2151	432.6112	7
7	802.3243	401.6658	S*	822.2045	411.6059	806.1858	403.5965	807.1936	404.1005	6
8	933.3648	467.1860	M	655.2062	328.1067	639.1875	320.0974	640.1953	320.6013	5
9	1047.4077	524.2075	N	524.1657	262.5865	508.1470	254.5771	509.1548	255.0810	4
10	1194.4432	597.7252	M	410.1228	205.5650	394.1041	197.5557	395.1119	198.0596	3
11	1309.4701	655.2387	D	263.0874	132.0473	247.0687	124.0380	248.0765	124.5419	2
12			E	148.0604	74.5339	132.0417	66.5245	133.0495	67.0284	1

MS/MS Fragmentation of **NGKNFGSMNMDE**

Monoisotopic mass of neutral peptide Mr (calc): 1438.4894

S7 : Phospho (ST), with neutral losses 0.0000 (shown in table), 97.9769

M10: Oxidation (M), with neutral losses 0.0000 (shown in table), 63.9983

#	c	c ⁺⁺	Seq.	y	y ⁺⁺	z+1	z+1 ⁺⁺	z+2	z+2 ⁺⁺	#
1	132.0768	66.5420	N							20
2	269.1357	135.0715	H	2231.0380	1116.0226	2215.0193	1108.0133	2216.0271	1108.5172	19
3	366.1884	183.5979	P	2093.9791	1047.4932	2077.9604	1039.4838	2078.9682	1039.9877	18
4	513.2568	257.1321	F	1996.9263	998.9668	1980.9076	990.9574	1981.9154	991.4613	17
5	614.3045	307.6559	T	1849.8579	925.4326	1833.8392	917.4232	1834.8470	917.9271	16
6	701.3365	351.1719	S	1748.8102	874.9088	1732.7915	866.8994	1733.7993	867.4033	15
7	814.4206	407.7139	L	1661.7782	831.3927	1645.7595	823.3834	1646.7673	823.8873	14
8	871.4421	436.2247	G	1548.6941	774.8507	1532.6754	766.8413	1533.6832	767.3453	13
9	1027.5432	514.2752	R	1491.6727	746.3400	1475.6539	738.3306	1476.6618	738.8345	12
10	1155.6018	578.3045	Q	1335.5716	668.2894	1319.5528	660.2801	1320.5607	660.7840	11
11	1242.6338	621.8205	S	1207.5130	604.2601	1191.4943	596.2508	1192.5021	596.7547	10
12	1409.6321	705.3197	S*	1120.4810	560.7441	1104.4622	552.7348	1105.4701	553.2387	9
13	1522.7162	761.8617	I	953.4826	477.2449	937.4639	469.2356	938.4717	469.7395	8
14	1685.7795	843.3934	Y	840.3985	420.7029	824.3798	412.6935	825.3876	413.1975	7
15	1772.8116	886.9094	S	677.3352	339.1712	661.3165	331.1619	662.3243	331.6658	6
16	1885.8956	943.4515	L	590.3032	295.6552	574.2845	287.6459	575.2923	288.1498	5
17	1986.9433	993.9753	T	477.2191	239.1132	461.2004	231.1038	462.2082	231.6077	4
18	2100.0274	1050.5173	L	376.1714	188.5894	360.1527	180.5800	361.1605	181.0839	3
19	2215.0543	1108.0308	D	263.0874	132.0473	247.0687	124.0380	248.0765	124.5419	2
20			E	148.0604	74.5339	132.0417	66.5245	133.0495	67.0284	1

MS/MS Fragmentation of **NHPFTSLGRQSSIYSLTLDE**

Monoisotopic mass of neutral peptide Mr (calc): 2344.0736

S12: Phospho (ST), with neutral losses 0.0000 (shown in table), 97.9769

ABI5 trypsin ETD

#	c	c ⁺⁺	Seq.	y	y ⁺⁺	z+1	z+1 ⁺⁺	z+2	z+2 ⁺⁺	#
1	146.0924	73.5498	Q							15
2	243.1452	122.0762	P	1706.7747	853.8910	1690.7560	845.8816	1691.7638	846.3855	14
3	424.1592	212.5832	T*	1609.7219	805.3646	1593.7032	797.3552	1594.7110	797.8592	13
4	571.2276	286.1174	F	1428.7079	714.8576	1412.6892	706.8482	1413.6970	707.3522	12
5	628.2490	314.6282	G	1281.6395	641.3234	1265.6208	633.3140	1266.6286	633.8179	11
6	757.2916	379.1495	E	1224.6181	612.8127	1208.5993	604.8033	1209.6072	605.3072	10
7	888.3321	444.6697	M	1095.5755	548.2914	1079.5567	540.2820	1080.5646	540.7859	9
8	989.3798	495.1935	T	964.5350	482.7711	948.5163	474.7618	949.5241	475.2657	8
9	1102.4639	551.7356	L	863.4873	432.2473	847.4686	424.2379	848.4764	424.7418	7
10	1231.5065	616.2569	E	750.4032	375.7053	734.3845	367.6959	735.3923	368.1998	6
11	1346.5334	673.7703	D	621.3606	311.1840	605.3419	303.1746	606.3497	303.6785	5
12	1493.6018	747.3045	F	506.3337	253.6705	490.3150	245.6611	491.3228	246.1650	4
13	1606.6859	803.8466	L	359.2653	180.1363	343.2466	172.1269	344.2544	172.6308	3
14	1705.7543	853.3808	V	246.1812	123.5942	230.1625	115.5849	231.1703	116.0888	2
15			K	147.1128	74.0600	131.0941	66.0507	132.1019	66.5546	1

MS/MS Fragmentation of **QPTFGEMTLEDFLVK**

Monoisotopic mass of neutral peptide Mr (calc): 1833.8260

T3: Phospho (ST), with neutral losses 0.0000 (shown in table), 97.9769

#	c	c ⁺⁺	Seq.	y	y ⁺⁺	z+1	z+1 ⁺⁺	z+2	z+2 ⁺⁺	#
1	146.0924	73.5498	Q							21
2	233.1244	117.0659	S	2392.0527	1196.5300	2376.0339	1188.5206	2377.0418	1189.0245	20
3	400.1228	200.5650	S*	2305.0206	1153.0140	2289.0019	1145.0046	2290.0097	1145.5085	19
4	513.2068	257.1071	I	2138.0223	1069.5148	2122.0036	1061.5054	2123.0114	1062.0093	18
5	676.2702	338.6387	Y	2024.9382	1012.9727	2008.9195	1004.9634	2009.9273	1005.4673	17
6	763.3022	382.1547	S	1861.8749	931.4411	1845.8562	923.4317	1846.8640	923.9356	16
7	876.3863	438.6968	L	1774.8429	887.9251	1758.8241	879.9157	1759.8320	880.4196	15
8	977.4339	489.2206	T	1661.7588	831.3830	1645.7401	823.3737	1646.7479	823.8776	14
9	1090.5180	545.7626	L	1560.7111	780.8592	1544.6924	772.8498	1545.7002	773.3537	13
10	1205.5450	603.2761	D	1447.6271	724.3172	1431.6083	716.3078	1432.6162	716.8117	12
11	1334.5875	667.7974	E	1332.6001	666.8037	1316.5814	658.7943	1317.5892	659.2982	11
12	1481.6560	741.3316	F	1203.5575	602.2824	1187.5388	594.2730	1188.5466	594.7769	10
13	1609.7145	805.3609	Q	1056.4891	528.7482	1040.4704	520.7388	1041.4782	521.2427	9
14	1746.7735	873.8904	H	928.4305	464.7189	912.4118	456.7095	913.4196	457.2135	8
15	1817.8106	909.4089	A	791.3716	396.1894	775.3529	388.1801	776.3607	388.6840	7
16	1930.8946	965.9510	L	720.3345	360.6709	704.3158	352.6615	705.3236	353.1654	6
17	2090.9253	1045.9663	C	607.2504	304.1289	591.2317	296.1195	592.2395	296.6234	5
18	2219.9679	1110.4876	E	447.2198	224.1135	431.2011	216.1042	432.2089	216.6081	4
19	2334.0108	1167.5090	N	318.1772	159.5922	302.1585	151.5829	303.1663	152.0868	3
20	2391.0323	1196.0198	G	204.1343	102.5708	188.1155	94.5614	189.1234	95.0653	2
21			K	147.1128	74.0600	131.0941	66.0507	132.1019	66.5546	1

MS/MS Fragmentation of **QSSIYSLTLDEFQHALCENGK****Monoisotopic mass of neutral peptide Mr (calc): 2519.1039****S3: Phospho (ST), with neutral losses 0.0000 (shown in table), 97.9769**

#	c	c ⁺⁺	Seq.	y	y ⁺⁺	z+1	z+1 ⁺⁺	z+2	z+2 ⁺⁺	#
1	146.0924	73.5498	Q							21
2	233.1244	117.0659	S	2392.0527	1196.5300	2376.0339	1188.5206	2377.0418	1189.0245	20
3	400.1228	200.5650	S*	2305.0206	1153.0140	2289.0019	1145.0046	2290.0097	1145.5085	19
4	513.2068	257.1071	I	2138.0223	1069.5148	2122.0036	1061.5054	2123.0114	1062.0093	18
5	676.2702	338.6387	Y	2024.9382	1012.9727	2008.9195	1004.9634	2009.9273	1005.4673	17
6	763.3022	382.1547	S	1861.8749	931.4411	1845.8562	923.4317	1846.8640	923.9356	16
7	876.3863	438.6968	L	1774.8429	887.9251	1758.8241	879.9157	1759.8320	880.4196	15
8	977.4339	489.2206	T	1661.7588	831.3830	1645.7401	823.3737	1646.7479	823.8776	14
9	1090.5180	545.7626	L	1560.7111	780.8592	1544.6924	772.8498	1545.7002	773.3537	13
10	1205.5450	603.2761	D	1447.6271	724.3172	1431.6083	716.3078	1432.6162	716.8117	12
11	1334.5875	667.7974	E	1332.6001	666.8037	1316.5814	658.7943	1317.5892	659.2982	11
12	1481.6560	741.3316	F	1203.5575	602.2824	1187.5388	594.2730	1188.5466	594.7769	10
13	1609.7145	805.3609	Q	1056.4891	528.7482	1040.4704	520.7388	1041.4782	521.2427	9
14	1746.7735	873.8904	H	928.4305	464.7189	912.4118	456.7095	913.4196	457.2135	8
15	1817.8106	909.4089	A	791.3716	396.1894	775.3529	388.1801	776.3607	388.6840	7
16	1930.8946	965.9510	L	720.3345	360.6709	704.3158	352.6615	705.3236	353.1654	6
17	2090.9253	1045.9663	C	607.2504	304.1289	591.2317	296.1195	592.2395	296.6234	5
18	2219.9679	1110.4876	E	447.2198	224.1135	431.2011	216.1042	432.2089	216.6081	4
19	2334.0108	1167.5090	N	318.1772	159.5922	302.1585	151.5829	303.1663	152.0868	3
20	2391.0323	1196.0198	G	204.1343	102.5708	188.1155	94.5614	189.1234	95.0653	2
21			K	147.1128	74.0600	131.0941	66.0507	132.1019	66.5546	1

MS/MS Fragmentation of **QSSIYSLTLDEFQHALCENGK****Monoisotopic mass of neutral peptide Mr (calc): 2519.1039****S3 : Phospho (ST), with neutral losses 0.0000 (shown in table), 97.9769**

N-term.	ion	b	b-17	b-18	b-Pi	y	y-17	y-18	y-Pi	C-term.	ion
1	N	115.050	98.024	0.000	0.000	147.113	130.086	0.000	0.000	9	K
2	P	212.103	195.076	0.000	0.000	262.140	245.113	244.129	0.000	8	D
3	S*	379.101	362.075	361.091	281.124	375.224	358.197	357.213	0.000	7	L
4	C	539.132	522.105	521.121	441.155	488.308	471.281	470.297	0.000	6	L
5	P	636.185	619.158	618.174	538.208	585.361	568.334	567.350	0.000	5	P
6	L	749.269	732.242	731.258	651.292	745.391	728.365	727.381	0.000	4	C
7	L	862.353	845.326	844.342	764.376	912.390	895.379	894.379	814.413	3	S*
8	D	977.380	960.353	959.369	879.403	1009.442	992.416	991.432	911.466	2	P
9	K	1105.475	1088.448	1087.464	1007.498	1123.485	1106.459	1105.475	1025.508	1	N

MS/MS fragmentation of **NPSCPLLDK**

S3: Phospho (ST)

DPBF4 trypsin ETD

#	c	c ⁺⁺	Seq.	y	y ⁺⁺	z+1	z+1 ⁺⁺	z+2	z+2 ⁺⁺	#
1	146.0924	73.5498	Q							8
2	203.1139	102.0606	G	823.4073	412.2073	807.3886	404.1979	808.3964	404.7019	7
3	370.1122	185.5597	S*	766.3859	383.6966	750.3672	375.6872	751.3750	376.1911	6
4	483.1963	242.1018	L	599.3875	300.1974	583.3688	292.1880	584.3766	292.6920	5
5	584.2440	292.6256	T	486.3035	243.6554	470.2847	235.6460	471.2926	236.1499	4
6	697.3280	349.1677	L	385.2558	193.1315	369.2371	185.1222	370.2449	185.6261	3
7	794.3808	397.6940	P	272.1717	136.5895	256.1530	128.5801	257.1608	129.0840	2
8			R	175.1190	88.0631	159.1002	80.0538	160.1081	80.5577	1

MS/MS Fragmentation of **QGSLTLPR**

Monoisotopic mass of neutral peptide Mr (calc): 950.4586

S3 : Phospho (ST), with neutral losses 0.0000 (shown in table), 97.9769

#	c	c ⁺⁺	Seq.	y	y ⁺⁺	z+1	z+1 ⁺⁺	z+2	z+2 ⁺⁺	#
1	146.0924	73.5498	Q							8
2	260.1353	130.5713	N	904.4176	452.7124	888.3988	444.7031	889.4067	445.2070	7
3	427.1337	214.0705	S*	790.3746	395.6910	774.3559	387.6816	775.3637	388.1855	6
4	540.2177	270.6125	L	623.3763	312.1918	607.3576	304.1824	608.3654	304.6863	5
5	703.2811	352.1442	Y	510.2922	255.6498	494.2735	247.6404	495.2813	248.1443	4
6	790.3131	395.6602	S	347.2289	174.1181	331.2102	166.1087	332.2180	166.6126	3
7	903.3972	452.2022	L	260.1969	130.6021	244.1781	122.5927	245.1860	123.0966	2
8			K	147.1128	74.0600	131.0941	66.0507	132.1019	66.5546	1

MS/MS Fragmentation of **QNSLYSLK**

Monoisotopic mass of neutral peptide Mr (calc): 1031.4688

S3 : Phospho (ST), with neutral losses 0.0000 (shown in table), 97.9769

#	c	c ⁺⁺	Seq.	y	y ⁺⁺	z+1	z+1 ⁺⁺	z+2	z+2 ⁺⁺	#
1	131.1179	66.0626	L							25
2	268.1768	134.5920	H	2670.2957	1335.6515	2654.2770	1327.6421	2655.2848	1328.1460	24
3	397.2194	199.1133	E	2533.2368	1267.1220	2517.2181	1259.1127	2518.2259	1259.6166	23
4	496.2878	248.6475	V	2404.1942	1202.6007	2388.1755	1194.5914	2389.1833	1195.0953	22
5	624.3464	312.6768	Q	2305.1258	1153.0665	2289.1070	1145.0572	2290.1149	1145.5611	21
6	725.3941	363.2007	T	2177.0672	1089.0372	2161.0485	1081.0279	2162.0563	1081.5318	20
7	862.4530	431.7301	H	2076.0195	1038.5134	2060.0008	1030.5040	2061.0086	1031.0079	19
8	975.5370	488.2722	L	1938.9606	969.9839	1922.9419	961.9746	1923.9497	962.4785	18

9	1032.5585	516.7829	G	1825.8765	913.4419	1809.8578	905.4325	1810.8656	905.9365	17
10	1119.5905	560.2989	S	1768.8551	884.9312	1752.8363	876.9218	1753.8442	877.4257	16
11	1206.6226	603.8149	S	1681.8230	841.4152	1665.8043	833.4058	1666.8121	833.9097	15
12	1263.6440	632.3257	G	1594.7910	797.8991	1578.7723	789.8898	1579.7801	790.3937	14
13	1391.7390	696.3731	K	1537.7696	769.3884	1521.7508	761.3791	1522.7587	761.8830	13
14	1488.7918	744.8995	P	1409.6746	705.3409	1393.6559	697.3316	1394.6637	697.8355	12
15	1601.8758	801.4415	L	1312.6218	656.8146	1296.6031	648.8052	1297.6109	649.3091	11
16	1658.8973	829.9523	G	1199.5378	600.2725	1183.5190	592.2632	1184.5269	592.7671	10
17	1825.8956	913.4515	S*	1142.5163	571.7618	1126.4976	563.7524	1127.5054	564.2563	9
18	1956.9361	978.9717	M	975.5179	488.2626	959.4992	480.2532	960.5070	480.7572	8
19	2070.9790	1035.9932	N	844.4775	422.7424	828.4587	414.7330	829.4666	415.2369	7
20	2184.0631	1092.5352	L	730.4345	365.7209	714.4158	357.7115	715.4236	358.2155	6
21	2299.0901	1150.0487	D	617.3505	309.1789	601.3317	301.1695	602.3396	301.6734	5
22	2428.1326	1214.5700	E	502.3235	251.6654	486.3048	243.6560	487.3126	244.1600	4
23	2541.2167	1271.1120	L	373.2809	187.1441	357.2622	179.1347	358.2700	179.6387	3
24	2654.3008	1327.6540	L	260.1969	130.6021	244.1781	122.5927	245.1860	123.0966	2
25			K	147.1128	74.0600	131.0941	66.0507	132.1019	66.5546	1

MS/MS Fragmentation of LHEVQTHLGSSGKPLGSMNLDLELLK

Monoisotopic mass of neutral peptide Mr (calc): 2782.3725

S17 : Phospho (ST), with neutral losses 0.0000(shown in table), 97.976

N-term.	ion	c	c-1	z	z+1	z+2	C-term.	ion
1	T	119.082	118.074	130.086	131.094	132.102	9	K
2	N	233.124	232.117	245.113	246.121	247.129	8	D
3	S*	400.123	399.115	344.182	345.159	346.197	7	V
4	A	471.160	470.152	457.266	458.273	459.281	6	L
5	S	558.192	557.184	544.298	545.306	546.313	5	S
6	L	671.276	670.268	615.335	616.343	617.350	4	A
7	V	770.344	769.337	782.333	783.341	784.349	3	S*
8	D	885.371	884.364	896.384	897.384	898.392	2	N
9	K	1013.466	1012.458	998.432	998.432	999.439	1	T

MS/MS fragmentation of TNSASLVDK

S3: Phospho (ST)

DPBF4 V8 (Glu-C) ETD

#	c	c ⁺⁺	Seq.	y	y ⁺⁺	z+1	z+1 ⁺⁺	z+2	z+2 ⁺⁺	#
1	117.1022	59.0548	V							19
2	245.1608	123.0840	Q	1966.8576	983.9324	1950.8389	975.9231	1951.8467	976.4270	18
3	346.2085	173.6079	T	1838.7990	919.9031	1822.7803	911.8938	1823.7881	912.3977	17
4	483.2674	242.1373	H	1737.7513	869.3793	1721.7326	861.3699	1722.7404	861.8739	16
5	596.3515	298.6794	L	1600.6924	800.8499	1584.6737	792.8405	1585.6815	793.3444	15
6	653.3729	327.1901	G	1487.6084	744.3078	1471.5896	736.2985	1472.5975	736.8024	14
7	740.4050	370.7061	S	1430.5869	715.7971	1414.5682	707.7877	1415.5760	708.2916	13
8	827.4370	414.2221	S	1343.5549	672.2811	1327.5361	664.2717	1328.5440	664.7756	12
9	884.4585	442.7329	G	1256.5228	628.7651	1240.5041	620.7557	1241.5119	621.2596	11
10	1012.5534	506.7803	K	1199.5014	600.2543	1183.4827	592.2450	1184.4905	592.7489	10
11	1109.6062	555.3067	P	1071.4064	536.2068	1055.3877	528.1975	1056.3955	528.7014	9
12	1222.6902	611.8488	L	974.3537	487.6805	958.3349	479.6711	959.3428	480.1750	8
13	1279.7117	640.3595	G	861.2696	431.1384	845.2509	423.1291	846.2587	423.6330	7
14	1446.7101	723.8587	S*	804.2481	402.6277	788.2294	394.6183	789.2372	395.1223	6

15	1593.7455	797.3764	M	637.2498	319.1285	621.2310	311.1192	622.2389	311.6231	5
16	1707.7884	854.3978	N	490.2144	245.6108	474.1956	237.6015	475.2035	238.1054	4
17	1820.8725	910.9399	L	376.1714	188.5894	360.1527	180.5800	361.1605	181.0839	3
18	1935.8994	968.4533	D	263.0874	132.0473	247.0687	124.0380	248.0765	124.5419	2
19			E	148.0604	74.5339	132.0417	66.5245	133.0495	67.0284	1

MS/MS Fragmentation of **VQTHLGSSGKPLGSMNLDE**

Monoisotopic mass of neutral peptide Mr (calc): 2064.9187

S14 : Phospho (ST), with neutral losses 0.0000 (shown in table), 97.9769**M15** : Oxidation (M), with neutral losses 0.0000 (shown in table), 63.9983

IAA6 Trypsin CID

#	b	b ⁺⁺	b*	b ^{*+}	b ⁰	b ⁰⁺	Seq.	y	y ⁺⁺	y*	y ^{*+}	y ⁰	y ⁰⁺	#
1	100.08	50.54					V							32
2	213.16	107.08					L	3294.52	1647.77	3277.50	1639.25	3276.51	1638.76	31
3	282.18	141.59			264.17	132.59	S*	3181.44	1591.22	3164.41	1582.71	3163.43	1582.22	30
4	397.21	199.11			379.20	190.10	D	3112.42	1556.71	3095.39	1548.20	3094.41	1547.71	29
5	528.25	264.63			510.24	255.62	M	2997.39	1499.20	2980.36	1490.69	2979.38	1490.19	28
6	659.29	330.15			641.28	321.14	M	2866.35	1433.68	2849.32	1425.17	2848.34	1424.67	27
7	760.34	380.67			742.33	371.67	T	2735.31	1368.16	2718.28	1359.65	2717.30	1359.15	26
8	847.37	424.19			829.36	415.18	S	2634.26	1317.64	2617.24	1309.12	2616.25	1308.63	25
9	934.40	467.70			916.39	458.70	S	2547.23	1274.12	2530.20	1265.61	2529.22	1265.11	24
10	1005.44	503.22			987.43	494.22	A	2460.20	1230.60	2443.17	1222.09	2442.19	1221.60	23
11	1118.52	559.76			1100.51	550.76	L	2389.16	1195.08	2372.14	1186.57	2371.15	1186.08	22
12	1233.55	617.28			1215.54	608.27	D	2276.08	1138.54	2259.05	1130.03	2258.07	1129.54	21
13	1334.60	667.80			1316.59	658.80	T	2161.05	1081.03	2144.02	1072.52	2143.04	1072.02	20
14	1463.64	732.32			1445.63	723.32	E	2060.00	1030.51	2042.98	1021.99	2041.99	1021.50	19
15	1577.68	789.34	1560.66	780.83	1559.67	780.34	N	1930.96	965.98	1913.93	957.47	1912.95	956.98	18
16	1706.72	853.87	1689.70	845.35	1688.71	844.86	E	1816.92	908.96	1799.89	900.45	1798.91	899.96	17
17	1820.77	910.89	1803.74	902.37	1802.76	901.88	N	1687.87	844.44	1670.85	835.93	1669.86	835.44	16
18	1907.80	954.40	1890.77	945.89	1889.79	945.40	S	1573.83	787.42	1556.81	778.91	1555.82	778.41	15
19	2006.87	1003.94	1989.84	995.42	1988.86	994.93	V	1486.80	743.90	1469.77	735.39	1468.79	734.90	14
20	2105.94	1053.47	2088.91	1044.96	2087.93	1044.47	V	1387.73	694.37	1370.70	685.86	1369.72	685.36	13
21	2192.97	1096.99	2175.94	1088.47	2174.96	1087.98	S	1288.66	644.84	1271.64	636.32	1270.65	635.83	12
22	2280.00	1140.50	2262.97	1131.99	2261.99	1131.50	S	1201.63	601.32	1184.60	592.81	1183.62	592.31	11
23	2379.07	1190.04	2362.04	1181.52	2361.06	1181.03	V	1114.60	557.80	1097.57	549.29	1096.59	548.80	10
24	2508.11	1254.56	2491.09	1246.05	2490.10	1245.55	E	1015.53	508.27	998.50	499.76	997.52	499.26	9
25	2623.14	1312.07	2606.11	1303.56	2605.13	1303.07	D	886.49	443.75	869.46	435.23	868.48	434.74	8
26	2752.18	1376.59	2735.15	1368.08	2734.17	1367.59	E	771.46	386.23	754.43	377.72	753.45	377.23	7
27	2839.21	1420.11	2822.19	1411.60	2821.20	1411.10	S	642.42	321.71	625.39	313.20	624.41	312.71	6
28	2952.30	1476.65	2935.27	1468.14	2934.29	1467.65	L	555.39	278.20	538.36	269.68			5
29	3049.35	1525.18	3032.32	1516.67	3031.34	1516.17	P	442.30	221.65	425.28	213.14			4
30	3148.42	1574.71	3131.39	1566.20	3130.41	1565.71	V	345.25	173.13	328.22	164.62			3
31	3247.49	1624.25	3230.46	1615.73	3229.48	1615.24	V	246.18	123.59	229.15	115.08			2
32							K	147.11	74.06	130.09	65.55			1

MS/MS Fragmentation of **VLSDMMTSSALDTENENSVSSVEDESLPVVK**

Monoisotopic mass of neutral peptide Mr (calc): 3490.56

S3 : Phospho (STY), with neutral losses 97.98 (shown in table), 0.00

6. REFERENCES

1. R.R. van der Ploeg, W Böhm, M B Kirkham (1999) History of soil science. On the origin of the theory of mineral nutrition of plants and the law of the minimum. *Soil Sci Soc Am J* 63:1055-1062
2. Van't Hof J (1966) Experimental control of cell division in higher plants. *Am J Bot* 53: 970-976
3. Van't Hof J. and Webster (1973) The regulation of cell division in higher plants. *Brook. Symp.* 25: 152-165
4. Rolland F, Winderickx J, Thevelein JM (2002) Glucose-sensing and -signalling mechanisms in yeast. *FEMS Yeast Res* 2, 183-201
5. Rolland F, Moore B, Sheen J (2002) Sugar sensing and signalling in plants. *Plant Cell* S185-S205 Supplement 2002
6. Rolland F, Baena-Gonzalez E, Sheen J (2006) Sugar sensing and signalling in plants: conserved and novel mechanisms. *Annu Rev Plant Biol* 57: 675-709
7. León P and Sheen J (2003) Sugar and hormone connections. *Trends in Plant Science* Vol.8 No.3 110-116
8. Rook F and Bevan MW (2003) Genetic approaches to understanding sugar-response pathways. *J Exp Bot* Vol.54 No.382, 495-501
9. Coruzzi G M and Zhou Li (2001) Carbon and nitrogen sensing and signaling in plants: emerging 'matrix effects'. *Curr Op Plant Biol* 4:247-253
10. Zakhleniuk OV, Raines CA, Lloyd JC (2001) *pho3*: a phosphorus-deficient mutant of *Arabidopsis thaliana* (L.) Heynh. *Planta*. 212: 529-534
11. Scheible WR, Gonzalez-Frontez A, Lauerer M, Muller-Rober B, Caboche M, Stitt M (1997) Nitrate acts as a signal to induce organic acid metabolism and repress starch metabolism in tobacco. *Plant cell* 9:783-798
12. Koprivova A, Suter M, den Camp RO, Brunold C, Kopriva S (2000) Regulation of sulphate assimilation by nitrogen in Arabidopsis. *Plant Physiol* 122 (3): 737-746
13. Hesse H, Trachsel N, Suter M, Kopriva S, von Ballmoos P, Rennenberg H, Brunold C (2003) Effect of glucose on assimilatory sulphate reduction in Arabidopsis thaliana roots. *J Exp Bot* 54(388):1701-1709
14. Santangelo GM (2006) Glucose signaling in *Saccharomyces cerevisiae*. *Microbiol Mol Biol Rev* 2006 March 253-282
15. Carlson M, Osmond BC and Botstein D (1981) Mutants of yeast defective in sucrose utilization. *Genetics* 98(1):25-40
16. Celenza JL and Carlson M (1984) Cloning and genetic mapping of SNF1, a gene required for expression of glucose-repressible genes in *Saccharomyces cerevisiae*. *Mol Cell Biol* 4(1):49-53
17. Celenza JL and Carlson M (1986) A yeast gene that is essential for release from glucose repression encodes a protein kinase. *Science* 233(4769):1175-80
18. Ferrer A, Caelles C, Massot N, Hegardt FG (1985) Activation of rat liver cytosolic 3-hydroxy-3-methylglutaryl coenzyme A reductase kinase by adenosine 5'-monophosphate. *Biochem Biophys Res Comm* 132(2):497-504
19. Munday MR, Carling D, Hardie DG (1998) Negative interactions between phosphorylation of acetyl-CoA carboxylase by the cyclic AMP-dependent and AMP-activated protein kinases. *FEBS Lett* 235(1-2):144-148
20. Davies SP, Carling D, Munday MR, Hardie DG (1992) Diurnal rhythm of phosphorylation of rat liver acetyl-CoA carboxylase by the Amp-activated protein kinase, demonstrated using freeze-clamping. Effects of high fat diets. *Eur J Biochem* 203(3):615-623
21. Clarke PR and Hardie DG (1990) Regulation of HMG-CoA reductase: identification of the site phosphorylated by the AMP-activated protein kinase in vitro and in intact rat liver. *EMBO J* 9(8):2439-2446
22. Fryer LG, Parbu-Patel A, Carling D (2002) The anti-diabetic drugs rosiglitazone and metformin stimulate AMP-activated protein kinase through distinct signaling pathways. *J Biol Chem* 277(28):25226-32

23. Hawley SA, Gadalla AE, Olsen GS, Hardie DG (2002) The anti-diabetic drug metformin activates the AMP-activated protein kinase cascade via an adenine-nucleotide independent mechanism. *Diabetes* 51(8):2420-2425
24. Sugden C, Donaghy PG, Halford NG, Hardie DG (1999) Two SNF1-related protein kinases from spinach leaf phosphorylate and inactivate 3-hydroxy-3-methylglutaryl-coenzyme A reductase, nitrate reductase, and sucrose phosphate synthase in vitro. *Plant Phys* Vol.120, 257-274
25. Provan F and Lillo C (1999) Photosynthetic post-translational modification of nitrate reductase. *J Plant Physiol* 154:605-609
26. Orlova M, Kanter E, Krakovich D, Kuchin S (2006) Nitrogen availability and TOR regulate the Snf1 protein kinase in *Saccharomyces cerevisiae*. *Eukaryot Cell* 5(11):1831-1837
27. Kopriva S, Muheim R, Koprivova A, Trachsel N, Catalano C, Suter M, Brunold C (1999) Light regulation of assimilatory sulphate reduction in *Arabidopsis thaliana*. *Plant J* 20(1):37-44
28. Hong S-P and Carlson M (2007) Regulation of Snf1 protein kinase in response to environmental stress. *J Biol Chem* Vol.282 No.23 16838-16845
29. Dubacq C, Chevalier A, Mann C. (2004) The protein kinase Snf1 is required for tolerance to the ribonucleotide reductase inhibitor hydroxyurea. *Mol Cell Biol* 24(6):2560-2572
30. Chen Z, Odstrcil EA, Tu BP and McKnight SL (2007) Restriction of DNA replication to the reductive phase of the metabolic cycle protects genome integrity. *Science* 316(5833):1916-9
31. Hrabak EM et al (2003) The *Arabidopsis* CDPK-SnRK superfamily of protein kinases. *Plant Physiol* Vol.132, 666-680
32. Halford NG and Hardie DG (1998) SNF-related protein kinases: global regulators of carbon metabolism in plants. *Plant Mol Biol* 37:735-748
33. Yang X, Jiang R, Carlson M (1994) A family of proteins containing a conserved domain that mediates interaction with the yeast SNF1 protein kinase complex. *EMBO J* Vol.13, No.24, 5878-5886
34. Celenza JL, Eng FJ, Carlson M (1989) Molecular analysis of the SNF4 gene of *Saccharomyces cerevisiae*: evidence for physical association of the SNF4 protein with the SNF1 protein kinase. *Mol Cell Biol* 9(11):5045-54
35. Polge C and Thomas M (2006) SNF1/AMPK/SnRK1 kinases, global regulators at the heart of energy control? *Trends in Plant Science* Vol.12, No.1, 20-28
36. Dyck JR, Gao G, Widmer J, Stapleton D, Fernandez CS, Kemp BE, Witters LA (1996) Regulation of 5'-AMP-activated protein kinase activity by the noncatalytic beta and gamma subunits. *J Biol Chem* 271(30):17798-803
37. Hunter T and Plowman GD (1997) The protein kinases of budding yeast: six score and more. *Trends in Biol Sci* 22. January
38. Wang D, Harper JF, Gribshkov M (2003) Systematic trans-genomic comparison of protein kinases between *Arabidopsis* and *Saccharomyces cerevisiae*. *Plant Physiol* Vol.132, 2152-2165
39. Manning G, Whyte DB, Martinez R, Hunter T, Sudarsanam S (2002) The protein kinase complement of the human genome. *Science* 298(5600):1912-34
40. Lizcano JM et al (2004) LKB1 is a master kinase that activates 13 kinase of the AMPK subfamily including MARK/PAR-1. *EMBO J* 23:833-843
41. Gong D, Guo Y, Schumaker KS, Zhu J-K (2004) The SOS3 family of Calcium Sensors and SOS2 family of protein kinases in *Arabidopsis*. *Plant Physiol* 134(3):919-26
42. Mizunuma M, Hirata D, Miyaoka R, Miyakawa T (2001) GSK-3 kinase Mck1 and calcineurin coordinately mediate Hsl1 down-regulation by Ca²⁺ in budding yeast. *EMBO J* 20(5):1074-85
43. Estruch F, Treitel MA, Yang X, Carlson M (1992) N-terminal mutations modulate yeast SNF1 protein kinase function. *Genetics* 132(3):639-50
44. Crute BE, Seefeld K, Gamble J, Kemp BE, Witters LA (1998) Functional domains on the alpha1 catalytic subunit of the AMP-activated protein kinase. *J Biol Chem* 273(52):35347-54

45. Stein SC, Woods A, Jones NA, Davison MD, Carling D (2000) The regulation of AMP-activated protein kinase by phosphorylation. *Biochem J* 345 Pt 3:437-43
46. Sugden C, Crawford RM, Halford NG, Hardie DG (1999) Regulation of spinach SNF1-related (SnRK1) kinases by protein kinases and phosphatases is associated with phosphorylation of the T-loop and is regulated by 5'-AMP. *Plant J* 19(4):433-439
47. Jeffrey PD, Russo AA, Polyak K, Gibbs E, Hurwitz J, Massagué J, Pavletich NP (1995) Mechanism of CDK activation revealed by the structure of cyclinA-CDK2 complex. *Nature* 376(6538):313-320
48. Siccheri F, Kuryan J (1997) Structures of Src-family tyrosine kinases. *Curr Opin Struc Biol* 7(6):777-785
49. Hong SP, Leiper FC, Woods A, Carling D, Carlson M (2003) Activation of yeast Snf1 and mammalian AMP-activated protein kinase by upstream kinases. *PNAS* 100(15):8839-43
50. Nath N, McCartney RR, Schmidt MC (2003) Yeast Pak1 kinase associates with and activates Snf1. *Mol Cell Biol* 23(11):3909-17
51. Sutherland CM, Hawley SA, McCartney RR, Leech A, Stark MJ, Schmidt MC, Hardie DG (2003) Elm1p is one of three upstream activating kinases for the *Saccharomyces cerevisiae* Snf1 complex. *Curr Biol* 13(15):1299-305
52. Elbing K, McCartney RR, Schmidt MC (2006) Purification and characterization of the three Snf1-activating kinases of *Saccharomyces cerevisiae*. *Biochem J* 393, 797-805
53. Hawley SA, Boudeau J, Reid JL, Mustard KJ, Udd L, Mäkelä TP, Alessi DR, Hardie DG (2003) Complexes between the LKB1 tumor suppressor, STRAD alpha/beta and MO25 alpha/beta are upstream kinases in the AMP-activated protein kinase cascade. *J Biol* 2(4):28
54. Woods A, Johnstone SR, Dickerson K, Leiper FC, Fryer LG, Neumann D, Schlattner U, Wallimann T, Carlson M, Carling D (2003) LKB is the upstream kinase in the AMP-activated protein kinase cascade. *Curr Biol* 13(22):2004-8
55. Hong S-P, Momcilovic M, Carlson M (2005) Function of mammalian LKB1 and Ca²⁺/calmodulin-dependent protein kinase kinase α as Snf1-activating kinases in yeast. *J Biol Chem* 280(23):21804-21809
56. Woods A, Dickerson K, Heath R, Hong S-P, Momcilovic M, Johnstone SR, Carlson M, Carling D (2005) Ca²⁺/calmodulin-dependent protein kinase kinase-beta acts upstream of AMP-activated protein kinase in mammalian cells. *Cell Metab* 2(1):21-33
57. Momcilovic M, Hong S-P, Carlson M (2006) Mammalian TAK1 activates Snf1 protein kinase in yeast and phosphorylates AMP-activated protein kinase in vitro. *J Biol Chem* 281(35):25336-43
58. Hey S, Mayerhofer H, Halford NG, Dickinson JR (2007) DNA sequences from *Arabidopsis*, which encode protein kinases and function as upstream regulators of Snf1 in yeast. *J Biol Chem* 282(14):10472-9
59. Neumann D, Woods A, Carling D, Wallimann T, Schlattner U (2003) Mammalian AMP-activated protein kinase: functional, heterotrimeric complexes by co-expression of subunits in *Escherichia coli*. *Protein Expr Purif* 30(2):230-7
60. Bhalerao RP, Salchert K, Bakó L, Ökrész L, Szabados L, Muranaka T, Machida Y, Schell J, Koncz C (1999) Regulatory interaction of PRL1 WD protein with *Arabidopsis* SNF1-like protein kinases. *PNAS* 96(9):5322-7
61. Rubenstein EM, McCartney RR, Schmidt MC (2006) Regulatory domains of Snf1-activating kinases determine pathway specificity. *Eukaryot Cell* 5(4):620-7
62. Woods A, Vertommen D, Neumann D, Turk R, Bayliss J, Schlattner U, Wallimann T, Carling D, Rider MH (2003) Identification of phosphorylation sites in AMP-activated protein kinase (AMPK) for upstream AMPK kinases and study of their roles by site-directed mutagenesis. *J Biol Chem* 278(31):28434-42
63. Ludin K, Jiang R and Carlson M (1998) Glucose-regulated interaction of a regulatory subunit of protein phosphatase 1 with the Snf1 protein kinase in *Saccharomyces cerevisiae*. *PNAS* 95(11):6245-50
64. McCartney RR and Schmidt MC (2001) Regulation of Snf1 kinase. Activation requires phosphorylation of threonine 210 by an upstream kinase as well as a distinct step mediated by the Snf4 subunit. *J Biol Chem* 276(39):36460-6

65. Sanz P, Alms GR, Haystead TA, Carlson M (2000) Regulatory interactions between the Reg1-Glc7 protein phosphatase and the Snf1 protein kinase. *Mol Cell Biol* 20(4):1321-8
66. Sanz P, Ludin K, Carlson M (2000) Sip5 interacts with both the Reg1/Glc7 protein phosphatase and the Snf1 protein kinase of *Saccharomyces cerevisiae*. *Genetics* 154(1):99-107
67. Treitel MA, Kuchin S, Carlson M (1998) Snf1 protein kinase regulates phosphorylation of the Mig1 repressor in *Saccharomyces cerevisiae*. *Mol Cell Biol* 18(11):6273-80
68. Randez-Gil F, Herrero P, Sanz P, Prieto JA, Moreno F (1998) Hexokinase PII has a double cytosolic-nuclear localisation in *Saccharomyces cerevisiae*. *FEBS Lett* 425(3):475-8
69. Herrero P, Martinez-Campa C, Moreno F (1998) The hexokinase 2 protein participates in regulatory DNA-protein complexes necessary for glucose repression of the SUC2 gene in *Saccharomyces cerevisiae*. *FEBS Lett* 434(1-2):71-6
70. Ahuatzzi D, Riera A, Peláez R, Herrero P, Moreno F (2007) Hxk2 regulates the phosphorylation state of Mig1 and therefore its nucleocytoplasmic distribution. *J Biol Chem* 282(7):4485-93
71. Tomas-Cobos L, Sanz P (2002) Active Snf1 protein kinase inhibits expression of the *Saccharomyces cerevisiae* HXT1 glucose transporter gene. *Biochem J* 368(2):657-63
72. Alms GR, Sanz P, Carlson M, Haystead TA (1999) Reg1p targets protein phosphatase 1 to dephosphorylate hexokinase II in *Saccharomyces cerevisiae*: characterizing the effects of a phosphatase subunit on the yeast proteome. *EMBO J* 18(15):4157-68
73. Jiang R, Carlson M (1996) Glucose regulates protein interactions within the yeast SNF1 protein kinase complex. *Genes & Dev* 10:3105-3115
74. Sugden C, Crawford RM, Halford NG, Hardie DG (1999) Regulation of spinach SNF1-related (SnRK1) kinases by protein kinases and phosphatases is associated with phosphorylation of the T-loop and is regulated by 5'-AMP. *Plant J* 19(4):433-439
75. Wilson WA, Hawley SA, Hardie DG (1996) Glucose repression/derepression in budding yeast: SNF1 protein kinase is activated by phosphorylation under derepressing conditions, and this correlates with a high AMP:ATP ratio. *Curr Biol* 6(11):1426-1434
76. Townley R, Shapiro L (2007) Crystal structures of the adenylate sensor from fission yeast AMP-activated protein kinase. *Science*. 315(5819):1726-9
77. Adams J, Chen Z-P, Van Denderen BJW, Morton CJ, Parker MW, Witters LA, Stapleton D, Kemp BE (2003) Intrasteric control of AMPK via the γ 1 subunit allosteric regulatory site. *Protein Sci* 13(1):155-165
78. Mitchelhill K, Stapleton D, Gao G, House C, Michell B, Katsis F, Witters LA, Kemp BE (1994) Mammalian AMP-activated protein kinase shares structural and functional homology with the catalytic domain of yeast Snf1 protein kinase. *J Biol Chem* 269(4):2361-4
79. Ludin K, Jiang R, Carlson M (1998) Glucose-regulated interaction of a regulatory subunit of protein phosphatase 1 with the Snf1 protein kinase in *Saccharomyces cerevisiae*. *PNAS* 95(11):6245-50
80. Crute BE, Seefeld K, Gamble J, Kemp BE, Witters LA (1998) Functional domains of the α 1 catalytic subunit of the AMP-activated protein kinase. *J Biol Chem* 273(52):35347-54
81. Pang T, Xiong B, Li JY, Qiu BY, Jin GZ, Shen JK, Li J (2006) Conserved alpha-helix acts as autoinhibitory sequence in AMP-activated protein kinase alpha subunits. *J Biol Chem* 282(1):495-506
82. Hofmann K, Bucher P (1996) The UBA domain: a sequence motif present in multiple enzyme classes of the ubiquitination pathway. *Trends Biochem Sci* 21(5):172-3.
83. Bertolaet BL, Clarke DJ, Wolff M, Watson MH, Henze M, Divita G, Reed SI, (2001) UBA domains of DNA damage-inducible proteins interact with ubiquitin. *Nat Struct Biol* 8(5):417-22.
84. Buchberger A (2002) From UBA to UBX: new words in the ubiquitin vocabulary. *Trends Cell Biol* 12(5):216-21
85. Ortolan TG, Tongaonkar P, Lambertson D, Chen L, Shauber C, Madura K (2000) The DNA repair protein rad23 is a negative regulator of multi-ubiquitin chain assembly. *Nat Cell Biol* 2(9):601-8

86. Kang Y, Vossler RA, Diaz-Martinez LA, Winter NS, Clarke DJ, Walters KJ, (2006) UBL/UBA ubiquitin receptor proteins bind a common tetraubiquitin chain. *J Mol Biol* 356(4):1027-35
87. Jaleel M, Villa F, Deak M, Toth R, Prescott AR, Van Aalten DM, Alessi DR (2006) The ubiquitin-associated domain of AMPK-related kinases regulates conformation and LKB1-mediated phosphorylation and activation. *Biochem J* 394(Pt 3):545-55
88. Farrás R, Ferrando A, Jásik J, Kleinow T, Ökrész L, Tiburcio A, Salchert K, del Pozo C, Schell J, Koncz C (2001) SKP1-SnRK protein kinase interactions mediate proteasomal binding of a plant SCF ubiquitin ligase. *EMBO J* 20(11):2742-56
89. Panneerselvam S, Marx A, Mandelkow EM, Mandelkow E (2006) Structure of the catalytic and ubiquitin-associated domains of the protein kinase MARK/Par-1. *Structure* 14(2):173-83
90. Beullens M, Vancauwenbergh S, Morrice N, Deura R, Ceulemans H, Waelkens E, Bollen M (2005) Substrate specificity and activity regulation of protein kinase MELK. *J Biol Chem* 280(48):40003-11
91. Marx A, Nugoor C, Müller J, Panneerselvam S, Timm T, Bilanz M, Mylonas E, Svergun DI, Mandelkow EM, Mandelkow E (2006) Structural variations in the catalytic and ubiquitin-associated domains of microtubule-associated protein/microtubule affinity regulating kinase (MARK) 1 and MARK2. *J Biol Chem* 281(37):27586-99
92. Murphy JM, Korzhnev DM, Ceccarelli DF, Briant DJ, Zarrine-Afsar A, Sicheri F, Kay LE, Pawson T (2007) Conformational instability of the MARK3 UBA domain compromises ubiquitin recognition and promotes interaction with the adjacent kinase domain. *PNAS* 104(36):14336-41
93. Jiang R, Carlson M (1997) The Snf1 protein kinase and its activating subunit, Snf4, interact with distinct domains of the Sip1/Sip2/Gal83 component in the kinase complex. *Mol Cell Biol* 17(4):2099-106
94. Iseli TJ, Walter M, van Denderen BJ, Katsis F, Witters LA, Kemp BE, Michell BJ, Stapleton D (2005) AMP-activated protein kinase beta subunit tethers alpha and gamma subunits via its C-terminal sequence (186-270) *J Biol Chem* 280(14):13395-400
95. Vincent O, Townley R, Kuchin S, Carlson M (2001) Subcellular localization of the Snf1 kinase is regulated by specific beta subunits and a novel glucose signaling mechanism. *Genes Dev* 15(9):1104-14
96. Ashrafi K, Lin SS, Manchester JK, Gordon JI (2000) Sip2p and its partner snf1p kinase affect aging in *S. cerevisiae*. *Genes Dev* 14(15):1872-85
97. Lin SS, Manchester JK, Gordon JI (2003) Sip2, an N-myristoylated beta subunit of Snf1 kinase, regulates aging in *Saccharomyces cerevisiae* by affecting cellular histone kinase activity, recombination at rDNA loci, and silencing. *J Biol Chem* 278(15):13390-7
98. Sarma NJ, Haley TM, Barbara KE, Buford TD, Willis KA, Santangelo GM (2007) Glucose-responsive regulators of gene expression in *Saccharomyces cerevisiae* function at the nuclear periphery via a reverse recruitment mechanism. *Genetics* 175(3):1127-35
99. Mitchelhill K, Michell BJ, House CM, Stapleton D, Dyck J, Gamble J, Ullrich C, Witters LA, Kemp BE (1997) Posttranslational modifications of the 5'-AMP-activated protein kinase beta1 subunit. *J Biol Chem* 272(39):24475-9
100. Warden SM, Richardson C, O'Donnell J, Stapleton D, Kemp BE, Witters LA (2001) Post-translational modifications of the beta-1 subunit of AMP-activated protein kinase affect enzyme activity and cellular localization. *Biochem J* 354(Pt 2):275-83
101. Hedbacker K, Carlson M (2006) Regulation of the nucleocytoplasmic distribution of Snf1-Gal83 protein kinase. *Eukaryot Cell* 5(12):1950-6
102. Hedbacker K, Townley R, Carlson M (2004) Cyclic AMP-dependent protein kinase regulates the subcellular localization of Snf1-Sip1 protein kinase. *Mol Cell Biol* 24(5):1836-43
103. Ashrafi K, Farazi TA, Gordon JI (1998) A role for *Saccharomyces cerevisiae* fatty acid activation protein 4 in regulating protein N-myristoylation during entry into stationary phase. *J Biol Chem* 273(40):25864-74
104. Pierre M, Traverso JA, Boisson B, Domenichini S, Bouchez D, Giglione C, Meinel T (2007) N-myristoylation regulates the SnRK1 pathway in *Arabidopsis*. *Plant Cell* 19(9):2804-21

105. Gissot L, Polge C, Jossier M, Girin T, Bouly JP, Kreis M, Thomas M (2006) AKINbetagama contributes to SnRK1 heterotrimeric complexes and interacts with two proteins implicated in plant pathogen resistance through its KIS/GBD sequence. *Plant Physiol* 142(3):931-44
106. Stapleton D, Gao G, Michell BJ, Widmer J, Mitchelhill K, Teh T, House CM, Witters LA, Kemp BE (1994) Mammalian 5'-AMP-activated protein kinase non-catalytic subunits are homologs of proteins that interact with yeast Snf1 protein kinase. *J Biol Chem* 269(47):29343-6
107. Nath N, McCartney RR, Schmidt MC (2002) Purification and characterization of Snf1 kinase complexes containing a defined Beta subunit composition. *J Biol Chem* 277(52):50403-8
108. Warden SM, Richardson C, O'Donnell J, Sapleton D, Kemp BE, Witters LA (2001) Post-translational modifications of the beta-1 subunit of AMP-activated protein kinase affect enzyme activity and cellular localization. *Biochem J* 354(Pt 2):275-83
109. Hedbacker K, Hong SP, Carlson M (2004) Pak1 protein kinase regulates activation and nuclear localization of Snf1-Gal83 protein kinase. *Mol Cell Biol* 24(18):8255-63
110. Hedbacker K, Townley R, Carlson M (2004) Cyclic AMP-dependent protein kinase regulates the subcellular localization of Snf1-Sip1 protein kinase. *Mol Cell Biol* 24(5):1836-43
111. Vincent O, Carlson M (1999) Gal83 mediates the interaction of the Snf1 kinase complex with the transcription activator Sip4. *EMBO J* 18(23):6672-81
112. Schmidt M, McCartney RR (2000) beta-subunits of Snf1 kinase are required for kinase function and substrate definition. *EMBO J* 19(18):4936-43
113. Polekhina G, Gupta A, Michell BJ, van Denderen B, Murthy S, Feil SC, Jennings IG, Campbell DJ, Witters LA, Parker MW, Kemp BE, Stapleton D (2003) AMPK beta subunit targets metabolic stress sensing to glycogen. *Curr Biol* 13;13(10):867-71
114. Katsuya Y, Mezaki Y, Kubota M, Matsuura Y (1998) Three-dimensional structure of Pseudomonas isoamylase at 2.2 Å resolution. *J Mol Biol* 281(5):885-97
115. Henrissat B (1998) Glycosidase families. *Biochem Soc Trans* 26(2):153-6
116. Arad M, Benson DW, Perez-Atayde AR, McKenna WJ, Sparks EA, Kanter RJ, McGarry K, Seidmann JG, Seidmann CE (2002) Constitutively active AMP kinase mutations cause glycogen storage disease mimicking hypertrophic cardiomyopathy. *J Clin Invest* 109(3):357-62
117. Carling D, Hardie DG (1989) The substrate and sequence specificity of the AMP-activated protein kinase. Phosphorylation of glycogen synthase and phosphorylase kinase. *Biochim Biophys Acta* 1012(1):81-6
118. Rolland F, Baena-Gonzalez E, Sheen J (2006) Sugar sensing and signaling in plants: conserved and novel mechanisms. *Annu Rev Plant Biol* 57:675-709
119. Randez-Gil F, Herrero P, Sanz P, Prieto JA, Moreno F (1998) Hexokinase PII has a double cytosolic-nuclear localisation in *Saccharomyces cerevisiae*. *FEBS Lett* 425(3):475-8
120. Colombo S, Ronchetti D, Thevelein JM, Winderickx J, Martegani E (2004) Activation state of the Ras2 protein and glucose-induced signaling in *Saccharomyces cerevisiae*. *J Biol Chem* 279(45):46715-22
121. Wang Y, Pierce M, Schnepfer L, Güldal CG, Zhang X, Tavazoie S, Broach JR (2004) Ras and Gpa2 mediate one branch of a redundant glucose signaling pathway in yeast. *PLoS Biol* 2(5):E128
122. Vojtek AB, Fraenkel DB (1990) Phosphorylation of yeast hexokinases. *Eur J Biochem* 190(2):371-5
123. Westergaard SL, Bro C, Olsson L, Nielsen J. (2004) Elucidation of the role of Grr1p in glucose sensing by *Saccharomyces cerevisiae* through genome-wide transcription analysis. *FEMS Yeast Res* 5(3):193-204
124. Hsiung Y, Chang HC, Pellequer JL, La Valle R, Lanker S, Wittenberg C (2001) F-box protein Grr1 interacts with phosphorylated targets via the cationic surface of its leucine-rich repeat. *Mol Cell Biol* 21(7):2506-20
125. La Rue J, Tokarz S, Lanker S (2005) SCFGrr1-mediated ubiquitination of Gis4 modulates glucose response in yeast. *J Mol Biol* 349(4):685-98

126. Balciunas D, Ronne H (1999) Yeast genes GIS1-4: multicopy suppressors of the Gal-phenotype of *snf1 mig1 srb8/10/11* cells. *Mol Gen Genet* 262(4-5):589-99
127. Ye T, Garcia-Salcedo R, Ramos J, Hohmann S (2006) Gis4, a new component of the ion homeostasis system in the yeast *Saccharomyces cerevisiae*. *Eukaryot Cell* 5(10):1611-21
128. Horak J, Wolf DH (2005) The ubiquitin ligase SCF(Grr1) is required for Gal2p degradation in the yeast *Saccharomyces cerevisiae*. *Biochem Biophys Res Commun* 335(4):1185-90
129. Liu Z, Spirek M, Thornton J, Butow RA (2005) A novel degron-mediated degradation of the RTG pathway regulator, Mks1p, by SCFGrr1. *Mol Biol Cell* 16(10):4893-904
130. Tomás-Cobos L, Viana R, Sanz P (2005) TOR kinase pathway and 14-3-3 proteins regulate glucose-induced expression of HXT1, a yeast low-affinity glucose transporter. *Yeast* 22(6):471-9.
131. Gavin AC et al (2002) Functional organization of the yeast proteome by systematic analysis of protein complexes. *Nature* 415(6868):141-7
132. Muslin AJ, Tanner JW, Allen PM, Shaw AS (1996) Interaction of 14-3-3 with signaling proteins is mediated by the recognition of phosphoserine. *Cell* 84(6):889-97.
133. Mayordomo I, Sanz P (2002) The *Saccharomyces cerevisiae* 14-3-3 protein Bmh2 is required for regulation of the phosphorylation status of Fin1, a novel intermediate filament protein. *Biochem J* 365(Pt 1):51-6.
134. Kakiuchi K, Yamauchi Y, Taoka M, Iwago M, Fujita T, Ito T, Song SJ, Sakai A, Isobe T, Ichimura T (2007) Proteomic analysis of in vivo 14-3-3 interactions in the yeast *Saccharomyces cerevisiae*. *Biochemistry* 46(26):7781-92
135. Mayordomo I, Regelmann J, Horak J, Sanz P (2003) *Saccharomyces cerevisiae* 14-3-3 proteins Bmh1 and Bmh2 participate in the process of catabolite inactivation of maltose permease. *FEBS Lett* 544(1-3):160-4.
136. Dombek KM, Kacherovsky N, Young ET (2004) The Reg1-interacting proteins, Bmh1, Bmh2, Ssb1, and Ssb2, have roles in maintaining glucose repression in *Saccharomyces cerevisiae*. *J Biol Chem* 279(37):39165-74
137. Bruckmann, A, Hensbergen PJ, Balog CI, Deelder AM, de Steensma HJ, van Heusden GP (2007) Post-transcriptional control of the *Saccharomyces cerevisiae* proteome by 14-3-3 proteins. *J Proteome Res* 6(5):1689-99
138. Gelperin D, Weigle J, Nelson K, Roseboom P, Irie K, Matsumoto K, Lemmon S (1995) 14-3-3 proteins: potential roles in vesicular transport and Ras signaling in *Saccharomyces cerevisiae*. *PNAS* 92(25):11539-43.
139. Usui T, Petrini JH (2007) The *Saccharomyces cerevisiae* 14-3-3 proteins Bmh1 and Bmh2 directly influence the DNA damage-dependent functions of Rad53. *PNAS* 104(8):2797-802.
140. Zeng Y, Piwnica-Worms H (1999) DNA damage and replication checkpoints in fission yeast require nuclear exclusion of the Cdc25 phosphatase via 14-3-3 binding. *Mol Cell Biol* 19(11):7410-9
141. van Heusden GP (2005) 14-3-3 proteins: regulators of numerous eukaryotic proteins. *IUBMB Life* 57(9):623-9.
142. Dombek KM, Voronkova V, Raney A, Young ET (1999) Functional analysis of the yeast Glc7-binding protein Reg1 identifies a protein phosphatase type 1-binding motif as essential for repression of ADH2 expression. *Mol Cell Biol* 19(9):6029-40
143. Al-Hakim AK, Göransson O, Deák M, Toth R, Capbell DG, Morrice NA, Prescott AR, Alessi DR (2005) 14-3-3 cooperates with LKB1 to regulate the activity and localization of QSK and SIK. *J Cell Sci* 118(Pt 23):5661-73
144. Göransson O, Deak M, Wullschleger S, Morrice NA, Prescott AR, Alessi DR (2006) Regulation of the polarity kinases PAR-1/MARK by 14-3-3 interaction and phosphorylation. *J Cell Sci* 119(Pt 19):4059-70
145. Le Guen L, Thomas M, Bianchi M, Halford NG, Kreis M (1992) Structure and expression of a gene from *Arabidopsis thaliana* encoding a protein related to SNF1 protein kinase. *Gene* 120(2):249-54
146. Gissot L, Polge C, Bouly JP, Lemaitre T, Kreis M, Thomas M (2005) AKINbeta3, a plant specific SnRK1 protein, is lacking domains present in yeast and mammals non-catalytic beta-subunits. *Plant Mol Biol* 56(5):747-59

147. Lumberras V, Alba MM, Kleinow T, Koncz C, Pagès M (2001) Domain fusion between SNF1-related kinase subunits during plant evolution. *EMBO Rep* 2(1):55-60
148. Bouly JP, Gissot L, Lessard P, Kreis M, Thomas M (1999) Arabidopsis thaliana proteins related to the yeast SIP and SNF4 interact with AKINalpha1, an SNF1-like protein kinase. *Plant J* 18(5):541-50
149. Thelander M, Olsson T, Ronne H (2004) Snf1-related protein kinase 1 is needed for growth in a normal day-night light cycle. *EMBO J* 23(8):1900-10
150. Wang W, Yang X, López de Silanes I, Carling D, Gorospe M (2003) Increased AMP:ATP ratio and AMP-activated protein kinase activity during cellular senescence linked to reduced HuR function. *J Biol Chem* 278(29):27016-23
151. Purcell PC, Smith AM, Halford NG (1998) Antisense expression of a sucrose non-fermenting-1-related protein kinase sequence in potato results in decreased expression of sucrose synthase in tubers and loss of sucrose-inducibility of sucrose synthase transcripts in leaves. *Plant J* 14(2):195-202
152. McGibbins RS, Muttucumaru N, Paul MJ, Powers SJ, Burrell MM, Coates S, Purcell PC, Tiessen A, Geigenberger P, Halford NG (2006) Production of high-starch, low-glucose potatoes through over-expression of the metabolic regulator SnRK1. *Plant Biotechnol J* 4(4):409-18.
153. Zhang Y, Shewry PR, Jones H, Barcelo P, Lazzeri PA, Halford NG (2001) Expression of Antisense SnRK1 protein kinase sequence causes abnormal pollen development and male sterility in transgenic barley. *Plant J* 28(4):431-41
154. Laurie S, McKibbin RS, Halford NG (2003) Antisense SNF1-related (SnRK1) protein kinase gene represses transient activity of an alpha-amylase (alpha-Amy2) gene promoter in cultured wheat embryos. *J Exp Bot* 54(383):739-47
155. Scwachtje J, Minchin PE, Jahnke S, van Dongen JT, Schittko U, Baldwin IT (2006) SNF1-related kinases allow plants to tolerate herbivory by allocating carbon to roots. *PNAS* 103(34):12935-40
156. Radchuk R, Radchuk V, Weschke W, Borisjuk L, Weber H (2006) Repressing the expression of the SUCROSE NONFERMENTING-1-RELATED PROTEIN KINASE gene in pea embryo causes pleiotropic defects of maturation similar to an abscisic acid-insensitive phenotype. *Plant Physiol* 140(1):263-78
157. Bradford KJ, Downie AB, Gee OH, Alvarado V, Yang H, Dahal B (2003) Abscisic acid and gibberellin differentially regulate expression of genes of the SNF1-related kinase complex in tomato seeds. *Plant Physiol* 132(3):1560-76
158. Rosnoblet C, Aubry C, Leprince O, Vu BL, Rogniaux H, Buitink J (2007) The regulatory gamma subunit SNF4b of the sucrose non-fermenting-related kinase complex is involved in longevity and stachyose accumulation during maturation of Medicago truncatula seeds. *Plant J* 51(1):47-59
159. Baena-González E, Rolland F, Thevelein JM, Sheen J (2007) A central integrator of transcription networks in plant stress and energy signalling. *Nature* 2007 Aug 1 (Epub ahead of print)
160. Halford NG, Hey S, Jhurreea D, Laurie S, McKibbin RS, Paul M, Zhang Y (2003) Metabolic signalling and carbon partitioning: role of Snf1-related (SnRK1) protein kinase. *J Exp Bot* 54(382):467-75
161. Sugden C, Donaghy PG, Halford NG, Hardie DG (1999) Two SNF1-related protein kinases from spinach leaf phosphorylate and inactivate 3-hydroxy-3-methylglutaryl-coenzyme A reductase, nitrate reductase, and sucrose phosphate synthase in vitro. *Plant Physiol* 120(1):257-74
162. Matthew Paul (2007) Trehalose 6-phosphate *Curr Opin Plant Biol* 10(3):3003-9
163. Ramon M, Rolland F (2007) Plant development: introducing trehalose metabolism. *Trends Plant Sci* 12(5):185-8
164. Cho YH, Yoo SD, Sheen J (2006) Regulatory functions of nuclear hexokinase1 complex in glucose signaling. *Cell* 127(3):579-89
165. Frommer WB, Schulze WX, Lalonde S (2003) Hexokinase, jack-of-all-trades *Science* 300(5617):261-3

166. Kim M, Lim JH, Ahn CS, Park K, Kim GT, Kim WT, Pai HS (2006) Mitochondria-associated hexokinases play a role in the control of programmed cell death in *Nicotiana benthamiana*. *Plant Cell* 18(9):2341-55
167. Moore B, Zhou L, Rolland F, Hall Q, Cheng WH, Liu YX, Hwang I, Jones T, Sheen J (2003) Role of the *Arabidopsis* glucose sensor HXK1 in nutrient, light, and hormonal signaling. *Science* 300(5617):261-3
168. Zhou L Yang JC, Jones TL, Sheen J (1998) Glucose and ethylene signal transduction crosstalk revealed by an *Arabidopsis* glucose-insensitive mutant. *PNAS* 95(17):10294-9.
169. Laby RJ, Kincaid MS, Kim D, Gibson SI (2000) The *Arabidopsis* sugar-insensitive mutants *sis4* and *sis5* are defective in abscisic acid synthesis and response. *Plant J* 23(5):587-96
170. Rook F, Corke F, Card R, Munz G, Smith C, Bevan MW (2001) Impaired sucrose-induction mutants reveal the modulation of sugar-induced starch biosynthetic gene expression by abscisic acid signalling. *Plant J* 26(4):421-33
171. Arenas-Huertero F, Arroyo A, Zhou L, Sheen J, León P (2000) Analysis of *Arabidopsis* glucose insensitive mutants, *gin5* and *gin6*, reveals a central role of the plant hormone ABA in the regulation of plant vegetative development by sugar. *Genes Dev* 14(16):2085-96
172. Finkelstein R, Zeevaert JA (1994) Gibberellin and abscisic acid biosynthesis and response. *Arabidopsis*, C. Somerville and E. Meyerowitz, eds (Cold Spring Harbor, NY: Cold Spring Harbor Laboratory Press), pp. 523–553.
173. Finkelstein RR, Wang ML, Lynch TJ, Rao S, Goodman HM (1998) The *Arabidopsis* abscisic acid response locus *ABI4* encodes an *APETALA 2* domain protein. *Plant Cell* 10(6):1043-54
174. Huijser C, Kortstee A, Pego J, Weisbeek P, Wisman E, Smeekens S (2000) The *Arabidopsis* *SUCROSE UNCOUPLED-6* gene is identical to *ABSCISIC ACID INSENSITIVE-4*: involvement of abscisic acid in sugar responses. *Plant J* 23(5):577-85
175. Quesada V, Ponce MR, Micol JL (2000) Genetic analysis of salt-tolerant mutants in *Arabidopsis thaliana*. *Genetics* 154(1):421-36
176. Penfield S, Li Y, Gilday AD, Graham S, Graham IA (2006) *Arabidopsis* *ABA INSENSITIVE4* regulates lipid mobilization in the embryo and reveals repression of seed germination by the endosperm. *Plant Cell* 18(8):1887-99
177. Ramon M, Rolland F, Thevelein JM, Van Dijck P, Leyman B (2006) *ABI4* mediates the effects of exogenous trehalose on *Arabidopsis* growth and starch breakdown. *Plant Mol Biol* 63(2):195-206
178. Finkelstein RR, Lynch TJ (2000) The *Arabidopsis* abscisic acid response gene *ABI5* encodes a basic leucine zipper transcription factor. *Plant Cell* 12(4):599-609
179. Lopez-Molina L, Mongrand S, Chua NH (2001) A postgermination developmental arrest checkpoint is mediated by abscisic acid and requires the *ABI5* transcription factor in *Arabidopsis*. *PNAS* 98(8):4782-7
180. Lopez-Molina L, Mongrand S, McLachlin DT, Chait BT, Chua NH (2002) *ABI5* acts downstream of *ABI3* to execute an ABA-dependent growth arrest during germination. *Plant J* 32(3):317-28
181. Pourtau N, Marès M, Purdy S, Quentin N, Ruël A, Wingler A (2004) Interactions of abscisic acid and sugar signalling in the regulation of leaf senescence. *Planta* 219(5):765-72
182. Finkelstein RR, Lynch TJ (2000) Abscisic acid inhibition of radicle emergence but not seedling growth is suppressed by sugars. *Plant Physiol* 122(4):1179-86
183. Cheng WH, Endo A, Zhou L, Penney J, Chen HC, Arroyo A, Leon P, Nambara E, Asami T, Seo M, Koshiba T, Sheen J (2002) A unique short-chain dehydrogenase/reductase in *Arabidopsis* glucose signaling and abscisic acid biosynthesis and functions. *Plant Cell* 14(11):2723-43
184. Sharp RE, LeNoble ME, Else MA, Thorne ET, Gherardi F (2000) Endogenous ABA maintains shoot growth in tomato independently of effects on plant water balance: evidence for an interaction with ethylene. *J Exp Bot* 51(350):1575-84
185. De Smet I, Zhang H, Inzé D, Beeckman T (2006) A novel role for abscisic acid emerges from underground. *Trends Plant Sci* 11(9):434-9

186. Beaudoin N, Serizet C, Gosti F, Giraudat J (2000) Interactions between abscisic acid and ethylene signaling cascades. *Plant Cell* 12(7):1103-15
187. Ghassemian M, Nambara E, Cutler S, Kawaide H, Kamiya Y, McCourt P (2000) Regulation of abscisic acid signaling by the ethylene response pathway in Arabidopsis. *Plant Cell* 12(7):1117-26
188. Zhou L, Jang JC, Jones TL, Sheen J (1998) Glucose and ethylene signal transduction crosstalk revealed by an Arabidopsis glucose-insensitive mutant. *PNAS* 95(17):10294-9.
189. Smalle J, Haegman M, Kurepa J, Van Montagu M, Straeten DV (1997) Ethylene can stimulate Arabidopsis hypocotyl elongation in the light. *PNAS* 94(6):2756-61
190. Gibson, S.I., Laby, R.J., Kim, D. (2001) The sugar-insensitive1 (sis1) mutant of Arabidopsis is allelic to ctr1. *Biochem Biophys Res Commun* 280(1):196-203
191. Wilson AK, Pickett FB, Turner JC, Estelle M (1990) A dominant mutation in Arabidopsis confers resistance to auxin, ethylene and abscisic acid. *Mol Gen Genet* 222(2-3):377-83
192. Reed JW (2001) Roles and activities of Aux/IAA proteins in Arabidopsis. *Trends Plant Sci* 6(9):420-5
193. Barnes SA, Quaggio RB, Chua NH (1996) Phytochrome signal-transduction: characterization of pathways and isolation of mutants. *Philos Trans R Soc Lond B Biol Sci.* 350(1331):67-74
194. Dijkwel PP, Huijser C, Weisbeek PJ, Chua NH, Smeeckens, S.C. (1997) Sucrose control of phytochrome A signaling in Arabidopsis. *Plant Cell* 9(4):583-95
195. Foo E, Ross JJ, Davies NW, Reid JB, Weller JL (2006) A role for ethylene in the phytochrome-mediated control of vegetative development. *Plant J* 46(6):911-21
196. Tsai CH, Miller A, Spalding M, Rodermeil S (1997) Source Strength Regulates an Early Phase Transition of Tobacco Shoot Morphogenesis. *Plant Physiol* 115(3):907-914
197. Corbesier L, Lejeune P, Bernier G (1998) The role of carbohydrates in the induction of flowering in Arabidopsis thaliana: comparison between the wild type and a starchless mutant. *Planta* 206(1):131-7
198. Roldán M, Gómez-Mena C, Ruiz-García L, Salinas J, Martínez-Zapater JM (1999) Sucrose availability on the aerial part of the plant promotes morphogenesis and flowering of Arabidopsis in the dark. *Plant J* 20(5):581-90
199. van Dijken AJ, Schluepmann H, Smeeckens SC (2004) Arabidopsis trehalose-6-phosphate synthase 1 is essential for normal vegetative growth and transition to flowering. *Plant Physiol* 135(2):969-77
200. Ohto M, Onai K, Furukawa Y, Aoki E, Araki T, Nakamura K (2001) Effects of sugar on vegetative development and floral transition in Arabidopsis. *Plant Physiol* 127(1):252-61
201. Corbesier L, Bernier G, Périlleux C (2002) C : N ratio increases in the phloem sap during floral transition of the long-day plants Sinapis alba and Arabidopsis thaliana. *Plant Cell Physiol* 43(6):684-8.
202. Zhang H, Forde BG (1998) An Arabidopsis MADS box gene that controls nutrient-induced changes in root architecture. *Science* 279(5349):407-9
203. Bläsing OE, Gibon Y, Günther M, Höhne M, Morcuende R, Osuna D, Thimm O, Usadel B, Scheible WR, Stitt M (2005) Sugars and circadian regulation make major contributions to the global regulation of diurnal gene expression in Arabidopsis. *Plant Cell* 17(12):3257-81
204. Gagne JM, Downes BP, Shiu SH, Durski AM, Vierstra RD (2002) The F-box subunit of the SCF E3 complex is encoded by a diverse superfamily of genes in Arabidopsis. *PNAS* 99(17):11519-24
205. Zhou P, Howley PM (1998) Ubiquitination and degradation of the substrate recognition subunits of SCF ubiquitin-protein ligases. *Mol Cell* 2(5):571-80
206. Ruedger M, Dewey E, Gray WM, Hobbie L, Turner J, Estelle M (1998) The TIR1 protein of Arabidopsis functions in auxin response and is related to human SKP2 and yeast grr1p. *Genes Dev* 12(2):198-207
207. Yanagisawa S, Yoo SD, Sheen J (2003) Differential regulation of EIN3 stability by glucose and ethylene signalling in plants. *Nature* 425(6957):521-5
208. Thelander M, Fredriksson D, Schouten J, Hoge JH, Ronne H (2002) Cloning by pathway activation in yeast: identification of an Arabidopsis thaliana F-box protein that can turn on glucose repression. *Plant Mol Biol* 49(1):69-79

209. Lorenz S, Tintelnot S, Reski R, Decker EL (2003) Cyclin D-knockout uncouples developmental progression from sugar availability. *Plant Mol Biol* 53(1-2):227-36
210. Riou-Khamlichi C, Menges M, Healy JM, Murray JA (2000) Sugar control of the plant cell cycle: differential regulation of Arabidopsis D-type cyclin gene expression. *Mol Cell Biol* 20(13):4513-21
211. Planchais S, Samland AK, Murray JA (2004) Differential stability of Arabidopsis D-type cyclins: CYCD3;1 is a highly unstable protein degraded by a proteasome-dependent mechanism. *Plant J* 38(4):616-25
212. Diehl JA, Zindy F, Sherr CJ (1997) Inhibition of cyclin D1 phosphorylation on threonine-286 prevents its rapid degradation via the ubiquitin-proteasome pathway. *Genes Dev* 11(8):957-72
213. Cotellet V, Meek SEM, Provan F, Milne FC, Morrice N, MacKintosh C (2000) 14-3-3s regulate global cleavage of their diverse binding partners in sugar-starved *Arabidopsis* cells. *EMBO J* 19(12):2869-2876
214. MacKintosh C, Meek SEM (2001) Regulation of plant NR activity by reversible phosphorylation, 14-3-3 proteins and proteolysis. *CMLS Cell Mol Life Sci* 58:205-214
215. Bachmann M, Huber JL, Liao PC, Gage DA, Huber SC. (1996) The inhibitor protein of phosphorylated nitrate reductase from spinach (*Spinacia oleracea*) leaves is a 14-3-3 protein. *FEBS Lett* 3;387(2-3):127-31.
216. Finnemann J, Schjoerring JK (2000) Post-translational regulation of cytosolic glutamine synthetase by reversible phosphorylation and 14-3-3 protein interaction. *Plant J* Oct;24(2):171-81.
217. Toroser D, Athwal GS, Huber SC (1998) Site-specific regulatory interaction between spinach leaf sucrose-phosphate synthase and 14-3-3 proteins. *FEBS Lett* Sep 11;435(1):110-4.
218. Harthill JE, Meek SE, Morrice N, Peggie MW, Borch J, Wong BH, Mackintosh C (2006) Phosphorylation and 14-3-3 binding of Arabidopsis trehalose-phosphate synthase 5 in response to 2-deoxyglucose. *Plant J* 47(2):211-23
219. Kulma A, Villadsen D, Campbell DG, Meek SE, Harthill JE, Nielsen TH, Mackintosh C (2004) Phosphorylation and 14-3-3 binding of Arabidopsis 6-phosphofructo-2-kinase/fructose-2,6-bisphosphatase. *Plant J* 37(5):654-67
220. Fuglsang AT, Guo Y, Cuin TA, Qiu Q, Song C, Kristiansen KA, Bych K, Schulz A, Shabala S, Schumaker KS, Palmgren MG, Zhu JK (2007) Arabidopsis protein kinase PKS5 inhibits the plasma membrane H⁺-ATP-ase by preventing interaction with 14-3-3 protein. *Plant cell* 19(5):1617-34
221. Koncz C, Schell J. (1986) The promoter of TL-DNA gene 5 controls the tissue specific expression of chimaeric genes carried by a novel type of Agrobacterium binary vector. *Mol Gen Genet* 204:383-396
222. Zuo J, Niu, QW, Chua NH. (2000) Technical advance: An estrogen receptor-based transactivation XVE mediates highly inducible gene expression in transgenic plants. *Plant J* 24(2):265-73
223. Koncz C, Martini N, Szabados L, Hroudá M, Bachmair A, Schell J. (1994) Specialized vectors for gene tagging and expression studies. *Plant Mol Biol Manual* B2: 1-22
224. Ferrando A, Farrás R, Jásik J, Schell J, Koncz C. (2000) Intron-tagged epitope: a tool for facile detection and purification of proteins expressed in Agrobacterium-transformed plant cells. *Plant J* 22(6): 553-60
225. Németh K, Salchert K, Putnoky P, Bhalerao R, Koncz-Kálmán Z, Stankovic-Stangeland B, Bakó L, Mathur J, Okresz L, Stabel S, Geigenberger P, Stitt M, Rédei G P, Schell J, Koncz C. (1998) Pleiotropic control of glucose and hormone responses by PRL1, a nuclear WD protein, in Arabidopsis. *Genes Dev* 12(19): 3059-73
226. Maniatis T, Fritsch EF, Sambrook J. (1982) Molecular cloning. A Laboratory Manual. Cold Spring Harbor Laboratory ISBN 3540526889
227. Deng WP, Nickoloff JA. (1992) Site-directed mutagenesis of virtually any plasmid by eliminating a unique site. *Anal Biochem* 200:81
228. Walker JM. (2002) The Protein Protocols Handbook. Humana Press. ISBN 0896039412
229. Clough SJ, Bent AF (1998) Floral dip. A simplified method for Agrobacterium-mediated transformation of Arabidopsis thaliana. *Plant J* 16(6):735-743

230. Rogers SO, Bendich AJ. (1985) Extraction of DNA from milligram amounts of fresh, herbarium and mummified plant tissues. *Plant Mol Biol* 5:69-76
231. Furihata T, Maruyama K, Fujita Y, Umezawa T, Yoshida R, Shinozaki K, Yamaguchi-Shinozaki K. (2006) Abscisic acid-dependent multisite phosphorylation regulates the activity of a transcription activator AREB1. *Proc Natl Acad Sci USA* 103(6):1988-93
232. Bachmair A, Becker F, Schell J. (1993) Use of a reporter transgene to generate arabidopsis mutants in ubiquitin-dependent protein degradation. *Proc Natl Acad Sci USA* 90(2):418-21
233. Lu CA, Lin CC, Lee KW, Chen JL, Huang LF, Ho SL, Liu HJ, Hsing YI, Yu SM. (2007) The SnRK1A protein kinase plays a key role in sugar signaling during germination and seedling growth of rice. *Plant Cell* 19(8):2484-99
234. Lopez-Molina L, Mongrand S, McLachlin DT, Chait BT, Chua NH. (2002) ABI5 acts downstream of ABI3 to execute an ABA-dependent growth arrest during germination. *Plant J* 32: 317-328
235. Colón-Carmona A, Chen DL, Yeh KC, Abel S. (2000) Aux/IAA proteins are phosphorylated by phytochrome in vitro. *Plant Physiol* 124(4):1728-38
236. Dreher KA, Brown J, Saw RE, Callis J. (2006) The Arabidopsis Aux/IAA protein family has diversified in degradation and auxin responsiveness. *Plant Cell* 18(3): 699-714

7. ACKNOWLEDGEMENTS

I am grateful to my supervisor Prof. Dr. Csaba Koncz for the great support during my studies. I could always rely on his professional knowledge and help.

I am indebted to Zsuzsanna Koncz for being an excellent colleague and friend. Her presence provided a nice atmosphere.

I would like to thank to Prof. Dr. George Coupland for his support and providing the necessities for my studies

I would like to thank to Gergely Molnar to supervise me during my PhD studies. I appreciated also his friendship.

I am grateful to Marta Bitrian for her collaboration in the RT-PCR analysis of mutant plants

I would like to thank all the previous and current lab members who supported my work during four years. Special thanks to Sabine Schäfer for her help in the mutant screens and for her care in support if the lab.

I greatly appreciated the professional help of Jürgen Schmidt, Thomas Colby, Anne Bräutigam and Ursula Wieneke at the proteomics group

I would like to acknowledge Prof. Dr. Elmon Scmelzer for his patient help with laser scanning microscopy

Erklärung

Ich versichere, daß ich die von mir vorgelegte Dissertation selbständig angefertigt, die benutzten Quellen und Hilfsmittel vollständig angegeben und die Stellen der Arbeit - einschließlich Tabellen, Karten und Abbildungen -, die anderen Werken im Wortlaut oder dem Sinn nach entnommen sind, in jedem Einzelfall als Entlehnung kenntlich gemacht habe; daß diese Dissertation noch keiner anderen Fakultät oder Universität zur Prüfung vorgelegen hat; daß sie - abgesehen von unten angegebenen Teilpublikationen - noch nicht veröffentlicht worden ist sowie, daß ich eine solche Veröffentlichung vor Abschluß des Promotionsverfahrens nicht vornehmen werde.

Die Bestimmungen der Promotionsordnung sind mir bekannt. Die von mir vorgelegte Dissertation ist von Prof. Dr. George Coupland betreut worden.

Köln den 23. November 2007

Mihály Horváth

Lebenslauf

Name: Mihály Horváth
Geburtsdatum: 16. November 1977
Geburtsort: Komárom, Ungarn
Staatsangehörigkeit: Ungarisch
Familienstand: ledig

Gymnasium: Berzsényi Dániel Gymnasium, Budapest (1992-1996)
(mathematische Fakultät)

Universitätsstudien: ELTE Universität, Biologie-Chemie Lehrer Fach (1996-1997)

Universitätsdiplom: ELTE Universität, Budapest, Ungarn (1997-2002)
Biologie, MSc
Supervisor: Dr László Tamás
Titel der Diplomarbeit: Development of an alternative wheat transformation method by microinjection of egg cells with *in vitro* assembled T-DNA complex

2002-2003: Für 8 Monate wissenschaftlicher Mitarbeiter im Biologischen Forschungszentrum (Biological Research Centre) in Szeged, Ungarn

seit März 2003 Promotionsarbeit am Max Planck Institut für Züchtungsforschung, Köln.
Supervisor: Prof. Ulf Ingo Flügge, Prof George Coupland
Betreuer: Dr Csaba Koncz
Titel der Promotionsarbeit: *Arabidopsis* AMP-activated protein kinases in proteasomal complexes and their role in cell signalling

13. November 2007 Zulassung zur Promotion